

INFORMATION TO USERS

This manuscript has been reproduced from the microfilm master. UMI films the text directly from the original or copy submitted. Thus, some thesis and dissertation copies are in typewriter face, while others may be from any type of computer printer.

The quality of this reproduction is dependent upon the quality of the copy submitted. Broken or indistinct print, colored or poor quality illustrations and photographs, print bleedthrough, substandard margins, and improper alignment can adversely affect reproduction.

In the unlikely event that the author did not send UMI a complete manuscript and there are missing pages, these will be noted. Also, if unauthorized copyright material had to be removed, a note will indicate the deletion.

Oversize materials (e.g., maps, drawings, charts) are reproduced by sectioning the original, beginning at the upper left-hand corner and continuing from left to right in equal sections with small overlaps.

Photographs included in the original manuscript have been reproduced xerographically in this copy. Higher quality 6" x 9" black and white photographic prints are available for any photographs or illustrations appearing in this copy for an additional charge. Contact UMI directly to order.

**Bell & Howell Information and Learning
300 North Zeeb Road, Ann Arbor, MI 48106-1346 USA
800-521-0600**

UMI[®]

Simple Acid-Base Hydrolytic Chemistry Approach to Molecular Self-Assembly

by

Chi Ming Yam

*A thesis submitted to the Faculty of Graduate Studies and Research of
McGill University in partial fulfillment of the requirements for
the degree of Doctor of Philosophy.*

January 1999
Department of Chemistry
McGill University
Montreal, Quebec
Canada

© Chi Ming Yam



**National Library
of Canada**

**Acquisitions and
Bibliographic Services**

**395 Wellington Street
Ottawa ON K1A 0N4
Canada**

**Bibliothèque nationale
du Canada**

**Acquisitions et
services bibliographiques**

**395, rue Wellington
Ottawa ON K1A 0N4
Canada**

Your file Votre référence

Our file Notre référence

The author has granted a non-exclusive licence allowing the National Library of Canada to reproduce, loan, distribute or sell copies of this thesis in microform, paper or electronic formats.

The author retains ownership of the copyright in this thesis. Neither the thesis nor substantial extracts from it may be printed or otherwise reproduced without the author's permission.

L'auteur a accordé une licence non exclusive permettant à la Bibliothèque nationale du Canada de reproduire, prêter, distribuer ou vendre des copies de cette thèse sous la forme de microfiche/film, de reproduction sur papier ou sur format électronique.

L'auteur conserve la propriété du droit d'auteur qui protège cette thèse. Ni la thèse ni des extraits substantiels de celle-ci ne doivent être imprimés ou autrement reproduits sans son autorisation.

0-612-50283-X

Canada

*This thesis is dedicated to my parents, Wah Yam and Yuet Yee Tam
for their infinite love and support.*

Acknowledgments

I would like to deeply thank my research supervisor Prof. Ashok K. Kakkar for his kind guidance and helpful suggestions throughout my study at McGill University.

I would also like to thank all my lab-mates, especially Hongwei Jiang, Maria G. L. Petrucci and Samuel S. Y. Tong for creating an enjoyable environment to work in.

I would like to express my gratitude to:

Y.-K. I. Leung and Adam Dickie for proof-reading my thesis.

Frederic Chaumel for translation of the abstract to French.

Mr. Nadim Saadeh for running the mass spectra.

Mr. Michel Boulay for his assistance with the infrared spectrometers.

Dr. F. Sauriol for technical assistance in NMR spectrometry.

Dr. Georges Veilleux at INRS-Energie Varenne and Ms. Suzie Poulin at École Polytechnique (Université de Montréal) for the use of their X-ray photoelectron spectrometers.

All members of the support staff in the Department of Chemistry, especially Ms. Renée Charron for her help throughout my stay at McGill.

All my friends in the Otto Maass building and Montreal.

Financial support from the Department of Chemistry, McGill University in the form of a teaching assistantship.

Finally, I would like to thank my parents, my sisters and my best friend, Sau Ling Cheung for their love and encouragement.

Foreword

In accordance with guideline I-C of the “Guidelines for Thesis Preparation” (Faculty of Graduate Studies and Research), the following text is cited:

“Candidates have the option of including, as part of the thesis, the text of one or more papers submitted, or to be submitted, for publication, or the clearly-duplicated text of one or more published papers. These texts must conform to the “guidelines for Thesis Preparation” with respect to font size, line spacing and margin sizes and must be bound together as an integral part of the thesis. The thesis must be more than a mere collection of manuscripts. All components must be integrated into a cohesive unit with a logical progression from one chapter to the next. In order to ensure that the thesis has continuity, connecting texts that provide logical bridges between the different papers are usually desirable in the interest of cohesion. The thesis must include the following: a table of contents, an abstract in English and French, an introduction which states the objectives of the research, a review of the literature (in addition to that covered in the introduction to each paper), a final conclusion and summary. Where appropriate, additional material must be provided (e.g. in appendices) in sufficient detail to allow a clear and precise judgment to be made of the importance and originality of the research reported in the thesis. When co-authored papers are included in the thesis the candidate must have made a substantial contribution to all papers included in the thesis. The candidate is required to make an explicit statement in the thesis as to who contributed to such work and to what extent.”

Chapters 5, 6 and 7 are published papers and manuscripts written by the author and were used in preparation of this thesis. Following normal procedure, all the papers have been published, accepted for publication or submitted for publication in scientific journals. A list of papers is given below.

Chapter 5: Simple Acid-Base Hydrolytic Chemistry Approach to Molecular Self-Assembly: Thin Films of Long Chain Alcohols Terminated with Alkyl, Phenyl, and Acetylene Groups on Inorganic Oxide Surfaces.
Yam, C. M.; Tong, S. S. Y.; Kakkar, A. K. *Langmuir* **1998**, *14*, 6941-6947.

Chapter 6: Molecular Self-Assembly of Dihydroxy Terminated Molecules via Acid-Base Hydrolytic Chemistry on Silica Surfaces: Step-by-Step Multilayered Thin Film Construction.

Yam, C. M.; Kakkar, A. K. *Langmuir* 1999, in press.

Chapter 7: Molecular Self-Assembly of Dialkynyl Terminated Chromophores via Acid-Base Hydrolytic Chemistry on Inorganic Oxide Surfaces: Step-by-Step Multilayered Thin Film Construction.

Yam, C. M.; Kakkar, A. K. *Langmuir* 1999, submitted.

All the papers include the research director, Dr. Ashok K. Kakkar, as co-author. The manuscript in chapter 4 includes Samuel S. Y. Tong (McGill University) who co-authored this paper, and assisted in the study of the three-step deposition process. Other than the supervision, advice and direction of Dr. Ashok K. Kakkar, all of the work presented in this thesis was performed by the author.

Abstract

A new route to molecular self-assembly using a simple acid-base hydrolytic approach on silica based surfaces, is reported in this thesis. Based on this methodology, a number of compounds containing terminal groups with acidic protons, such as alcohols, thiols, carboxylic acids, and terminal alkynes, can be easily deposited on silica surfaces. The quality of the thin films was monitored by contact angle goniometry, ellipsometry, XPS, FTIR-ATR and UV-Vis absorption spectroscopies. The deposition conditions were optimized to produce ordered and densely packed mono- and multilayers. Using the two-step process, self-assembled monolayers (SAMs) of a variety of long chain alcohols containing terminal alkyl, phenyl and acetylene groups on silica surfaces were successfully prepared. The newly formed monolayers were found to be relatively ordered and densely packed. They showed comparable stabilities to OTS/SiO₂ at ambient and high temperatures, and upon treatment with acids and bases. A layer-by-layer construction methodology, based on acid-base hydrolysis of aminosilanes and dihydroxy terminated molecules containing rigid-rod type and alkyldiacetylene backbones, led to multilayers with higher stability under various conditions compared to monolayers. The thin film assemblies were subjected to topochemical polymerization, and upon UV-Vis exposure, the formation of a blue film was observed.

Using the acid-base hydrolytic chemistry approach, silica surfaces functionalized with Sn-NEt₂ groups can be easily modified using a number of terminal alkyne molecules with varied backbones. SAMs of a variety of rigid-rod alkynes on silica surfaces were successfully prepared. The π - π interactions in the molecules lead to ordered and densely packed thin film structures with a surface coverage of 2-7 molecules/100 Å². The thin film assembly with diacetylene backbone was also subjected to topochemical polymerization, and upon UV-Vis exposure, the formation of a blue film was observed. Furthermore, a

layer-by-layer construction methodology using aminostannanes and dialkyne terminated molecules containing alkyl or aromatic type backbone led to multilayered structures on silica surfaces without increasing disorder in the thin films with the increase in number of layers. The acetylene groups in the thin film assemblies were found to coordinate with cobalt carbonyl, corroborated by the observation of λ_{max} at 277 nm.

Résumé

Une nouvelle méthodologie pour l'auto-assemblage moléculaire utilisant une simple hydrolyse acide-base sur des surfaces de silice, est rapportée dans cette thèse. Basée sur cette technologie, un nombre de composés contenant des groupements terminaux avec des protons acides, tel que des alcools, thiols, acides carboxyliques et alcynes terminaux, peuvent être aisément déposés sur des surfaces de silice. La qualité des films minces a été contrôlée par goniométrie à angle de contact, éllipsométrie, XPS, FTIR-ATR et spectroscopie d'absorption UV-Vis. Les conditions de déposition ont été optimisées pour produire de simples et multicouches ordonnées et densément entassées. Utilisant le procédé à deux étapes, une variété de monocouches auto-assemblées (SAMs) d'alcool à longue chaîne contenant des groupements alcyls, phényls et acétylènes sur des surfaces de silice ont été préparées avec succès. Ces nouvelles monocouches ont démontré une grande densité et organisation. Elles ont démontré des stabilités comparables à OTS/SiO₂ à température ambiante et élevée et aux traitements aux acides et aux bases. Une méthodologie de construction couche par couche, basée sur l'hydrolyse acide-base des aminosilanes, de molécules de type barre rigide terminées par un groupement dihydroxy et sur une chaîne alkyldiacétylène, résulta en des multicouches de stabilité supérieure, sous différentes conditions, comparativement aux monocouches. Les réactifs des films minces ont été soumis à la polymérisation topochimique, et après exposition à des rayons UV-Vis, la formation d'un film bleu a été observée.

Utilisant l'approche de l'hydrolyse acide-base, les surfaces fonctionnalisées de silice avec des groupes Sn-NEt_2 , peuvent être facilement modifiées utilisant des alcynes terminaux avec différentes chaînes. Une grande variété de SAMs comprenant des barres rigides d'alcynes ont été successivement préparées. Les interactions π - π entre les molécules ont permis la formation de films minces ordonnés et denses avec une couverture de 2-7 molécules/100 Å². Le film mince assemblé avec une chaîne de diacétylène a aussi été

soumis à la polymérisation topochimique, et sous exposition UV-Vis, la formation d'un film bleu a été observée. De plus, une méthodologie de construction de couche par couche utilisant des aminostannates et des molécules terminées par des groupements dialcynes et contenant une chaîne de type alkyl ou aromatique ont mené à des structures multicouches sur des surfaces de silice sans augmenter le désordre dans le film mince avec l'augmentation du nombre de couches. Il a été observé que les groupements acétylènes dans les réactifs des films minces pouvaient coordonner avec le cobalt carbonyl, corroboré par l'observation du λ_{max} à 277 nm.

Table of Contents

Acknowledgments	Page iii
Foreword	iv
Abstract	vi
Résumé	viii
Table of Contents	x
List of Schemes	xvi
List of Tables	xvii
List of Figures	xix
List of Abbreviations	xxii
List of Publications Originated from Research at McGill University	xxiii
Chapter 1 General Review of Molecular Self-Assembly and Scope of Thesis	
1.1 Organic Thin Films	1
1.2 Langmuir-Blodgett (LB) Films	2
1.3 Self-Assembled Monolayers (SAMs)	4
1.4 SAMs of Alkanoic Acids on Metal Oxide Surfaces	5
1.4.1 SAMs of Alkanoic Acids on Silver, Copper and Aluminum Oxide	6
1.4.2 SAMs of Alkanoic Acids with Aromatic Chromophores	9
1.4.3 Stability Tests	9
1.4.4 SAMs of Hydroxamic Acids	9
1.4.5 SAMs of Dioic Acids	10
1.5 SAMs of Organosulfur Compounds on Metal Surfaces	11
1.5.1 SAMs of Thiols on Gold	11
1.5.1.1 Deposition Process	12
1.5.1.2 Monolayer Structures	13
1.5.1.3 Thermal and Chemical Stabilities	14
1.5.2 SAMs of ω -Substituted Thiols on Gold	15
1.5.3 SAMs of Aryl Thiols on Gold	16
1.5.4 SAMs of Chelating Aromatic Dithiols on Gold	17

1.5.5	SAMs of Conjugated α,ω -Dithiols and Acetylthiols on Gold	18
1.5.6	SAMs of Dialkyl Sulfides on Gold	19
1.5.7	SAMs of Dialkyl Disulfides on Gold	20
1.5.8	SAMs of Branched Thiols and Disulfides on Gold	21
1.5.9	SAMs of Thiols on Copper and Silver	23
1.6	SAMs of Organosilicon Derivatives on Hydroxylated Surfaces	23
1.6.1	Deposition Process	24
1.6.2	Reproducibility	26
1.6.3	Monolayer Structures	26
1.6.4	Chemical and Thermal Stabilities	27
1.6.5	SAMs with Aromatic Chromophores	28
1.6.6	SAMs with Second Order Nonlinear Optical Properties	29
1.6.7	Surface Modification	30
1.6.8	Multilayer Formation	30
1.6.8.1	Hydroboration-Oxidation of a Terminal Vinyl Group	31
1.6.8.2	LiAlH_4 Reduction of a Surface Ester Group	31
1.6.8.3	Photolysis of a Nitrate-Bearing Group	32
1.6.8.4	Hydrolysis of a Boronate-Protecting Group	32
1.7	Alkyl Monolayers on Silicon	33
1.8	SAMs with Alternate "Inorganic/Organic" Systems	34
1.8.1	Layered Phosphonate Thin Films	35
1.8.2	Cobalt-Diisocyanide Thin Films	35
1.9	Monomeric and Polymerized Diacetylene LB and Self-Assembled Thin Films	36
1.10	Limitation of Traditional Approaches to Molecular Self-Assembly	38
1.11	Acid-Pase Hydrolytic Chemistry	39
1.11.1	Synthesis of Aminosilanes	39
1.11.2	Chemistry of Aminosilanes	40
1.11.2.1	Reaction with Water	40
1.11.2.2	Reactions with Alcohols, Phenols and Silanols	40
1.11.2.3	Reactions with Thiols and Carboxylic Acids	40
1.11.2.4	Reaction with Acetylene Compounds	41
1.11.3	Synthesis of Aminostannanes	41
1.11.4	Chemistry of Aminostannanes	42
1.11.4.1	Reactions with Water and Air	42

1.11.4.2 Reactions with Protic Species	42
1.12 Acid-Base Hydrolytic Chemistry Approach to Molecular Self-Assembly on Inorganic Oxide Surfaces	43
1.13 Scope of Thesis	44
1.14 References	46
Chapter 2 Methods for Surface Characterization	
2.1 Contact Angle Goniometry	61
2.2 Fourier Transform Infrared Spectroscopy in the Attenuated Total Reflection Mode (FTIR-ATR)	63
2.3 Ellipsometry	64
2.4 X-ray Photoelectron Spectroscopy (XPS)	66
2.5 UV-Visible Spectroscopy	67
2.6 References	68
Chapter 3 A Novel Route to Efficient Inorganic Oxide Surface Modification <i>via</i> Simple Acid-Base Hydrolytic Chemistry	
3.1 Introduction	69
3.2 Acid-Base Hydrolysis	70
3.3 Surface Functionalization	72
3.3.1 Si-NEt ₂ Approach	72
3.3.2 Sn-NEt ₂ Approach	73
3.4 Optimization of Deposition Conditions	73
3.5 Surface Properties of Thin Films	78
3.6 Conclusion	80
3.7 Experimental Section	81
3.7.1 Materials	81
3.7.2 Substrate Preparation	82
3.7.3 Si-NEt ₂ Approach to Surface Functionalization	82
3.7.3.1 Two-Step Deposition Process	82
3.7.3.2 Three-Step Deposition Process	83
3.7.4 Sn-NEt ₂ Approach to Surface Functionalization	83
3.7.5 Contact Angle Measurements	83
3.7.6 Ellipsometry	84
3.8 References	89

Chapter 4 Links between Material Presented in Chapters Five to Seven 92

Chapter 5 Simple Acid-Base Hydrolytic Chemistry Approach to Molecular Self-Assembly: Thin Films of Long Chain Alcohols Terminated with Alkyl, Phenyl and Acetylene Groups on Inorganic Oxide Surfaces

5.1	Introduction	93
5.2	Acid-Base Hydrolysis	94
5.3	Surface Functionalization	95
5.4	Three-Step vs Two-Step Deposition Process	106
5.5	Stability of SAMs	107
5.6	Conclusion	111
5.7	Experimental Section	111
5.7.1	Materials	111
5.7.2	Substrate Preparation	112
5.7.3	Two-Step Deposition Process	113
5.7.4	Three-Step Deposition Process	113
5.7.5	Contact Angle Measurements	113
5.7.6	Fourier Transform Infrared Spectroscopy in the Attenuated Total Reflection Mode	113
5.7.7	Ellipsometry	114
5.7.8	X-ray Photoelectron Spectroscopy	114
5.8	References	115

Chapter 6 Molecular Self-Assembly of Dihydroxy Terminated Molecules *via* Acid-Base Hydrolytic Chemistry on Inorganic Oxide Surfaces: Step-by-Step Multilayered Thin Film Construction

6.1	Introduction	118
6.2	Acid-Base Hydrolysis	120
6.3	Monolayers of Diols	120
6.4	Multilayered Thin Film Assemblies of 2,4-Hexadiyne-1,6-diol and 5,7-Dodecadiyne-1,12-diol	126
6.5	Stability of Mono- and Multilayers	136
6.6	UV-Vis Exposure of Mono- and Multilayers	140

6.7	Conclusion	143
6.8	Experimental Section	144
6.8.1	Materials	144
6.8.2	Substrate Preparation	147
6.8.3	Preparation of SAMs	148
6.8.4	Preparation of Multilayers	148
6.8.5	Contact Angle Measurements	148
6.8.6	Fourier Transform Infrared Spectroscopy in the Attenuated Total Reflection Mode	149
6.8.7	Ellipsometry	149
6.8.8	X-ray Photoelectron Spectroscopy	150
6.8.9	UV-Polymerization	150
6.9	References	150

**Chapter 7 Molecular Self-Assembly of Alkynyl Terminated Chromophores
on Inorganic Oxide Surfaces *via* Acid-Base Hydrolytic
Chemistry: Monolayer and Step-by-Step Multilayered Thin Film
Construction**

7.1	Introduction	154
7.2	Acid-Base Hydrolysis	156
7.3	Monolayers of Alkynes	156
7.4	Estimation of Surface Coverage of Rigid-Rod Alkyne Chromophores	167
7.5	UV-Vis Exposure of a SAM of <i>p</i> -Bis(butadiynyl)benzene	170
7.6	Multilayer Thin Film Assemblies of 1,9-Decadiyne and <i>p</i> -Diethynylbenzene	172
7.7	Cobalt Carbonyl Adsorption on Monolayers and Multilayers of 1,9-Decadiyne and <i>p</i> -Diethynylbenzene	177
7.8	Conclusion	180
7.9	Experimental Section	181
7.9.1	Materials	181
7.9.2	Substrate Preparation	181
7.9.3	Preparation of SAMs	181
7.9.4	Preparation of Multilayers	182
7.9.5	Cobalt Carbonyl Adsorption	182
7.9.6	Contact Angle Measurements	182

7.9.7 Fourier Transform Infrared Spectroscopy in the Attenuated Total Reflection Mode	182
7.9.8 Ellipsometry	183
7.9.9 X-ray Photoelectron Spectroscopy	183
7.9.10 UV-Polymerization	184
7.10 References	184

Chapter 8 Conclusions, Contribution to Original Knowledge and Suggestions for Future Work

8.1 Conclusions	188
8.2 Contribution to Original Knowledge	190
8.3 Suggestions for Future Work	192
8.4 References	193

List of Schemes

All the schemes shown in the thesis depict a 'cartoon representation' of the various steps involved in the thin-film construction process.

Scheme 3.1	Si-NEt ₂ approach to surface functionalization	72
Scheme 3.2	Sn-NEt ₂ approach to surface functionalization	73
Scheme 5.1	Surface functionalization using two different reaction methodologies: two-step and three-step processes	95
Scheme 5.2	Molecular self-assembly of a series of short-to-long chain length alcohols terminated with alkyl, phenyl and acetylene groups on glass, quartz and single crystal silicon	97
Scheme 6.1	Molecular self-assembly of a series of dihydroxy molecules on glass, quartz and single crystal silicon	121
Scheme 6.2	A step-by-step reaction methodology for fabrication of multilayers of dihydroxy molecules on glass, quartz and single crystal silicon	129
Scheme 7.1	Molecular self-assembly of a series of alkynyl chromophores on glass, quartz and single crystal silicon	157
Scheme 7.2	A step-by-step reaction methodology for fabrication of multilayers of dialkynes on glass, quartz and single crystal silicon	158

List of Tables

Table 1.1	Peak positions for $\text{CH}_3(\text{CH}_2)_n\text{SH}$ CH_2 stretching modes in crystalline and liquid states and adsorbed on gold	14
Table 1.2	Advancing contact angles of water ($\text{CA}_{\text{H}_2\text{O}}$) and HD (CA_{HD}) on thiol monolayers adsorbed on gold	16
Table 1.3	Physical properties of monolayers on silicon, oxidized silicon and gold	34
Table 1.4	Acid strength of some protic species	43
Table 3.1	The effect of silanation time on surface properties ($\text{CA}_{\text{H}_2\text{O}}$ and T_e) of octadecanol thin films using a two-step process	75
Table 3.2	Static contact angles of water ($\text{CA}_{\text{H}_2\text{O}}$), ellipsometric (T_e) and theoretical thicknesses (T_i) for monolayers on Si(100) substrates	80
Table 5.1	Static contact angles of water ($\text{CA}_{\text{H}_2\text{O}}$), theoretical (T_i) and ellipsometric thicknesses (T_e), and FTIR-ATR data of alcohol thin films self-assembled on Si(100) by the two-step process	99
Table 5.2	Static contact angles of water ($\text{CA}_{\text{H}_2\text{O}}$), theoretical (T_i) and ellipsometric thicknesses (T_e), and FTIR-ATR data of alcohol thin films self-assembled on Si(100) by the three-step process	107
Table 5.3	Results of the stability tests on the octadecanol thin film on a Si(100) substrate	108
Table 6.1	Static contact angles of water ($\text{CA}_{\text{H}_2\text{O}}$), theoretical (T_i) and ellipsometric thicknesses (T_e), and XPS data for SAMs prepared from dihydroxy terminated molecules on Si(100) substrates	123
Table 6.2	FTIR-ATR data for SAMs prepared from dihydroxy terminated molecules on Si(100) substrates	124
Table 6.3	Static contact angles of water ($\text{CA}_{\text{H}_2\text{O}}$), ellipsometric thicknesses (T_e), and FTIR-ATR data for the multilayers prepared from 2,4-hexadiyne-1,6-diol on Si(100) substrates	132
Table 6.4	Static contact angles of water ($\text{CA}_{\text{H}_2\text{O}}$), ellipsometric thicknesses (T_e), and FTIR-ATR data for the multilayers prepared from 5,7-dodecadiyne-1,12-diol on Si(100) substrates	134

Table 6.5	(a) Results of the stability studies on SAMs of 2,4-hexadiyne-1,6-diol and 5,7-dodecadiyne-1,12-diol	137
	(b) Results of the stability studies on a SAM of octadecanol and a thin film of 2,4-hexadiyne-1,6-diol capped with OTS	138
	(c) Results of the stability studies on multilayers of 2,4-hexadiyne-1,6-diol capped with OTS	139
	(d) Results of the stability studies on multilayers of 5,7-dodecadiyne-1,12-diol capped with OTS	140
Table 7.1	Static contact angles of water and HD, theoretical (T_e) and ellipsometric thicknesses (T_e), and XPS data for SAMs of alkynes on Si(100) substrates	159
Table 7.2	FTIR-ATR data for SAMs of alkynes on Si(100) substrates	160
Table 7.3	λ_{\max} (nm), absorption (A), absorption coefficient (ϵ) and surface coverage (θ) of rigid-rod alkyne thin films on quartz	168
Table 7.4	Static contact angle of water (CA_{H_2O}), ellipsometric thickness (T_e), and FTIR-ATR data of a SAM of <i>p</i> -bis(butadiynyl)benzene on a Si(100) substrate upon exposure to UV-lamp for 30 min	171
Table 7.5	Static contact angles of water (CA_{H_2O}) and HD (CA_{HD}), ellipsometric thicknesses (T_e) and FTIR-ATR data for the multilayers of 1,9-decadiyne on Si(100) substrates	176
Table 7.6	Static contact angles of water (CA_{H_2O}) and HD (CA_{HD}), ellipsometric thicknesses (T_e) and FTIR-ATR data for the multilayers of <i>p</i> -diethynylbenzene on Si(100) substrates	177
Table 7.7	Static contact angles of water (CA_{H_2O}), ellipsometric thicknesses (T_e) and FTIR-ATR data for the thin films of <i>p</i> -diethynylbenzene and 1,9-decadiyne on Si(100) substrates after reaction with cobalt carbonyl	180

List of Figures

Figure 1.1	Schematic diagram of a Langmuir-Blodgett trough for deposition of monolayers	3
Figure 1.2	A schematic view of the forces in a self-assembled monolayer	4
Figure 1.3	A SAM of octadecanoic acid on silver	7
Figure 1.4	A SAM of octadecanoic acid on copper and aluminum oxide	8
Figure 1.5	A SAM of octadecanethiol on gold	12
Figure 1.6	A SAM of 1,2-bis(mercaptomethyl)-4,5-di(tetradecyl)benzene on gold	18
Figure 1.7	A SAM of dioctadecyl sulfide on gold	20
Figure 1.8	A SAM of dioctadecyl disulfide on gold	21
Figure 1.9	A SAM of a branched thiol on gold	22
Figure 1.10	A SAM of a branched disulfide on gold	22
Figure 1.11	A SAM of octadecyltrichlorosilane on Si/SiO ₂	24
Figure 2.1	(a) A typical water contact angle on a methyl surface (b) A typical hexadecane contact angle on a methyl surface	63
Figure 2.2	A schematic description of an optical setup for ATR measurements	64
Figure 2.3	A schematic description of an ellipsometer	66
Figure 3.1	The effect of silanation time on contact angles of water of octadecanol thin films using a two-step process	76
Figure 3.2	The effect of silanation time on ellipsometric thickness of octadecanol thin films using a two-step process	77
Figure 5.1	Static contact angles of water for monolayers of octadecyltrichlorosilane, octadecanol, hexadecanol, tetradecanol, decanol and hexanol on Si(100) substrates	100
Figure 5.2	Static contact angles of water for monolayers of propynol, butynol, pentynol, hexynol and undecynol on Si(100) substrates	103
Figure 5.3	FTIR-ATR (nonpolarized) spectra for monolayers of undecynol, hexynol, pentynol, butynol and propynol on Si(100) substrates in the region 2800 - 3000 cm ⁻¹	105

Figure 5.4	FTIR-ATR (nonpolarized) spectra for monolayers of $-O-(CH_2)_{17}-CH_3$ on Si(100) substrates in the region $2800-3000\text{ cm}^{-1}$: A, before any treatment; B, after heating at $150\text{ }^\circ\text{C}$ for 1 h; C, treatment with aq. 2.5 M H_2SO_4 , $25\text{ }^\circ\text{C}$, 1 h; D, boiling $CHCl_3$, 2 h; E, boiling methanol, 2 h; F, aq. 1 M NH_4OH , $25\text{ }^\circ\text{C}$, 1 h	109
Figure 6.1	Ellipsometric thickness of the 1 to 10 layered thin films of 2,4-hexadiyne-1,6-diol	130
Figure 6.2	Ellipsometric thickness of the 1 to 10 layered thin films of 5,7-dodecadiyne-1,12-diol	131
Figure 6.3	FTIR-ATR (nonpolarized) spectra for the 1 to 10 layered (top to bottom) thin films of 2,4-hexadiyne-1,6-diol on Si(100) substrates in the region $2800-3000\text{ cm}^{-1}$	133
Figure 6.4	FTIR-ATR (nonpolarized) spectra for the 1 to 10 layered (top to bottom) thin films of 5,7-dodecadiyne-1,12-diol on Si(100) substrates in the region $2800-3000\text{ cm}^{-1}$	135
Figure 6.5	UV-Vis spectra of the 1 to 10 layered thin films of 2,4-hexadiyne-1,6-diol on quartz. The inset shows the UV-Vis spectra of the 1 and 2 layered thin films	141
Figure 6.6	UV-Vis spectra of a 10-layered thin film of 2,4-hexadiyne-1,6-diol upon exposure to UV-lamp for a period of 0, 5, 15, 30, 60 and 120 min (top to bottom)	142
Figure 7.1	Static contact angles of water for monolayers of hexadiyne, octadiyne, nonadiyne and decadiyne on Si(100) substrate	162
Figure 7.2	Ellipsometric thickness for monolayers of hexadiyne, octadiyne, nonadiyne and decadiyne on Si(100) substrate	164
Figure 7.3	FTIR-ATR (nonpolarized) spectra for monolayers of hexadiyne, octadiyne, nonadiyne and decadiyne on Si(100) substrates in the region $2800-3000\text{ cm}^{-1}$	166
Figure 7.4	UV-Vis spectrum of a monolayer of <i>p</i> -diethynylanthracene on quartz	169
Figure 7.5	UV-Vis absorption of a monolayer of <i>p</i> -bis(butadiynyl)benzene upon exposure to UV-lamp for a period of 0, 5, 15, 30 and 60 min	171
Figure 7.6	Ellipsometric thickness of the 1 to 5 layered thin films of 1,9-decadiyne	173
Figure 7.7	Ellipsometric thickness of the 1 to 5 layered thin films of	

	<i>p</i> -diethynylbenzene	174
Figure 7.8	UV-Vis absorption of the 1 to 5 layered thin films of 1,9-decadiyne	175
Figure 7.9	UV-Vis spectrum of a thin film on quartz of <i>p</i> -diethynylbenzene with adsorbed cobalt carbonyl	179

List of Abbreviations

A	Absorbance
ATR	Attenuated total reflection
br	Broad
CA _{H₂O}	Contact angle of water
CA _{HD}	Contact angle of hexadecane
d	Doublet
Et	Ethyl group
FTIR	Fourier transform infrared spectroscopy
h	Hour
HD	Hexadecane
J	Coupling constant
LB	Langmuir-Blodgett
m	Multiplet
min	Minute
Me	Methyl group
MS	Mass spectrometry
NMR	Nuclear magnetic resonance
OTS	Octadecyltrichlorosilane
Ph	Phenyl group
R, R', R	Alkyl group
s	Singlet
SA	Self-assembly/self-assembled
SAM	Self-assembled monolayer
t	Triplet
T _e	Ellipsometric thickness
T _i	Theoretical Thickness
THF	Tetrahydrofuran
UV-Vis	Ultra violet and visible
XPS	X-ray photoelectron spectroscopy
λ_{\max}	Position of maximum peaks on UV-Vis spectra
ν_a	Asymmetric stretching
ν_s	Symmetric stretching

**List of Publications Originated from Research at
McGill University**

- (1) Yam, C. M.; Kakkar, A. K. *J. Chem. Soc., Chem. Commun.* **1995**, 907.
- (2) Yam, C. M.; Tong, S. S. Y.; Kakkar, A. K. *Langmuir* **1998**, *14*, 6941.
- (3) Yam, C. M.; Dickie, A.; Malkhasian, A.; Kakkar, A. K.; Whitehead, M. A. *Can. J. Chem.* **1998**, *76*, 1766.
- (4) Yam, C. M.; Kakkar, A. K. *Langmuir* **1999**, in press.
- (5) Yam, C. M.; Kakkar, A. K. *Langmuir* **1999**, submitted.

Chapter One

General Review of Molecular Self-Assembly and Scope of Thesis

1.1 Organic Thin Films

Optoelectronics and molecular electronics have recently emerged as an important area in material science.¹ Due to the limitations of inorganic materials in both areas, ordered organic materials are becoming increasingly significant. This may be the main reason¹ for the growing interest in both Langmuir-Blodgett (LB), and self-assembled (SA) thin films. Both SA and LB films are formed from molecular assemblies, the former from solution and the latter at the air/water interface. They allow the chemist to construct thin films with desirable properties by incorporating suitably oriented chromophores with different functional groups. These thin films offer significant potential in technology²⁻³ including, for example, thin-film optics,⁴ sensors and transducers,⁵ protective⁶ and patternable materials,⁷ surface preparation and modification,⁸ chemically modified electrodes,⁹ and biological thin films of proteins.¹⁰

Although the advance in thin film technology seems exciting and promising, there are still many unsolved problems.³ Organic thin films suffer from fragility, impurities, and defects, resulting in difficulties in producing films with good mechanical, thermal, and chemical stability. In order to improve the latter properties, films can be polymerized and cross-linked. Interchain interactions, such as van der Waals forces, π - π interactions and covalent bonding (such as Si-O-Si cross linkages in alkyltrichlorosilane monolayers on silica), are important factors in the molecular engineering of thin film construction. Although there are many ways to construct thin films, assemblies with chromophores

containing desired backbones and the optimization of the overall properties of the organized structures in the targeted domain still await further investigation.³

1.2 Langmuir-Blodgett (LB) Films

Much effort has been devoted for the construction of thin films by the LB technique (Figure 1.1).¹¹⁻¹² Blodgett first reported the preparation of ultrathin organic films using this deposition method in 1935.¹³ During the process of LB film deposition, amphiphilic compounds spread at the air-water interface to produce monolayers. Usually an amphiphile consists of two parts, a hydrophilic headgroup and a long-chain hydrophobic tail. The molecules are oriented at the interface upon compression. The monolayer can then be transferred onto the substrate by dipping the substrate perpendicularly through the interface. Several layers can be built on the substrate by repeating the dipping process. By controlling the number of dipping cycles, highly ordered ultrathin films with appropriate thickness can be obtained. LB films with different molecular orientations, such as X- (tail-to-head), Y- (tail-to-tail and head-to-head) or Z- (head-to-tail) structures are prepared by allowing the deposition to occur either during the down- and upstroke, or only during the downstroke or the upstroke. In addition, "mixed" (two or more amphiphiles per layer) and "alternate" films (two or more amphiphiles in successive layers) can also be easily prepared using a specially designed "alternate layer" trough.¹⁴

In recent years, molecules of completely different structure such as porphyrins,¹⁵ phthalocyanines,¹⁶ oligothiophenes,¹⁷ and polycyclic aromatic quinones,¹⁸ have also been used to form stable LB films. They have gained increasing importance due to their improved mechanical, thermal, and chemical stabilities. Many of the recent activities on LB films are focused on photochemical¹⁹ and thermal reactivity,²⁰ electrical conductivity,²¹ pyroelectric activity,²² and nonlinear optical properties.²³ These films can be adopted to electronic applications,^{1c} such as infrared sensors, frequency converters and information storage.

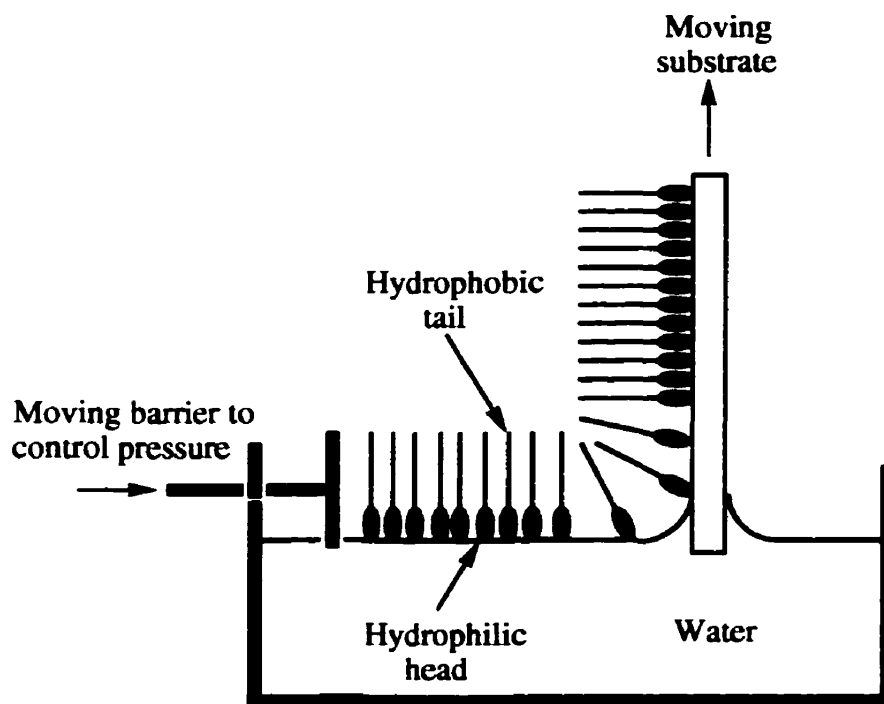


Figure 1.1 Schematic diagram of a Langmuir-Blodgett trough for deposition of monolayers.

Although the LB technique is effective in film formation, it has some drawbacks.²⁴⁻²⁵ LB films are usually unstable under a variety of chemical or physical conditions because the interactions between the films and the substrate surface are weak. As a consequence, these surface layers can easily rearrange. Under large compressive or tensile stress, surface reorganization of the films occurs. It becomes highly difficult to control domain structures in the films since film quality depends on mechanical manipulation. Furthermore, planar substrates are required for thin film deposition. These limitations prevent the extension of the technique to more sophisticated systems such as three-dimensional molecular structures and multilayer assemblies.²⁴ Therefore, it is necessary to develop other molecular assembly methods, although the chemistry involved may often not be straightforward.²⁵

1.3 Self-Assembled Monolayers (SAMs)

The field of self-assembled monolayers (SAMs) has attracted growing attention over the past 15 years or so.^{12,26,27} In 1946 Zisman first published the preparation of monolayers by adsorption of a surfactant onto a clean metal surface,²⁸ but the potential of self-assembly was not recognized until Nuzzo and Allara successfully prepared SAMs of dialkyl disulfides on gold more recently.²⁹

A self-assembling molecule can be divided into three parts,¹² the head group, alkyl chain and the terminal functional group (Figure 1.2). The head group provides chemisorption on the substrate surface, and results in the formation of a covalent Si–O bond for alkyltrichlorosilanes on hydroxylated surfaces; a covalent, but slightly polar, Au–S bond for alkanethiols on gold; or an ionic CO_2^-Ag^+ bond for carboxylic acids on AgO/Ag. The alkyl chains provide interchain van der Waals interactions which help in the formation of an ordered and closely packed assembly. When a polar bulky group is substituted in the alkyl chain, stronger long-range electrostatic interactions are introduced in the assembly. The terminal functional group may be modified to allow adsorption of another layer. The SA monolayer is chemically bonded to the surface, while the LB monolayer is only physically adsorbed. Thus, the SAMs are expected to be stronger and more resistant than the LB thin films.³⁰

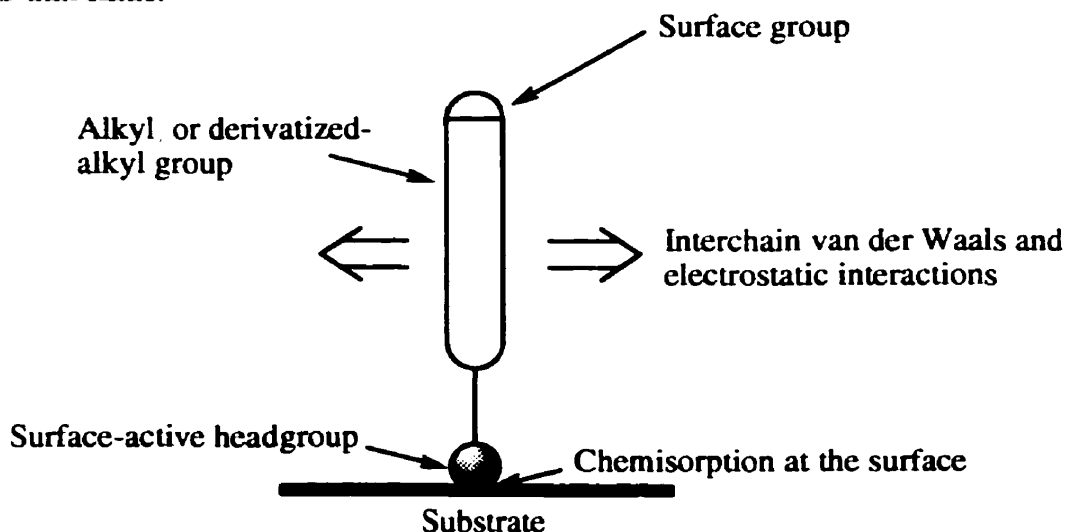


Figure 1.2 A schematic view of the forces in a self-assembled monolayer.¹²

Moreover, the SA technique allows the preparation of highly ordered and stable monolayers on various surfaces.^{12,31-36} By tailoring both head and tail groups of the molecules, SAMs provide excellent systems for a more fundamental understanding of such phenomena as ordering and growth, wetting, adhesion, lubrication, and corrosion.²⁶ These studies may be important in designing assemblies of three-dimensional structures. In addition, the densely packed, highly stable and ordered SAMs offer great potential in the areas of corrosion prevention, wear protection and the preparation of electrooptic devices and sensor arrays.³⁷

There has been extensive investigation on many self-assembling systems, including organosilicon compounds on hydroxylated surfaces (e.g., SiO₂ on Si and Al₂O₃ on Al)^{25, 38-54} alkanethiols on gold,^{31,34,55-63} silver³⁶ and copper,³⁵ dialkyl sulfides on gold,⁶⁴ dialkyl disulfides on gold,^{29,65} carboxylic acids on silver,⁶⁶ copper⁶⁷ and aluminum oxide,⁶⁸⁻⁶⁹ 1-alkenes on hydrogen-terminated silicon,⁷⁰⁻⁷¹ and films with alternate “inorganic/organic” systems⁷²⁻⁷⁶ (including layered phosphonate films on silica and gold⁷⁷⁻⁷⁹). In all these cases, the molecules attach to the surface of the substrates via strong chemical bonds.

1.4 SAMs of Alkanoic Acids on Metal Oxide Surfaces

The molecular self-assembly of long-chain n-alkanoic acids on metallic oxides, such as silver, copper and aluminum oxides, has been studied in the past 10 years. The driving force for these thin films is the formation of a surface salt between the carboxylate anion and a surface metal cation based on acid-base reactions. Allara and Nuzzo⁶⁸ and Ogawa et al.⁶⁹ have studied the adsorption of n-alkanoic acids on aluminum oxide, and reported that under appropriate conditions, long-chain alkanoic acids adsorb on oxidized aluminum surfaces to form closely packed and ordered monolayers, displaying advancing contact angles of water and hexadecane (HD) of ~110° and ~50°, respectively.

Besides thin films on aluminum oxide, Schlotter et al.⁶⁶ have also studied the adsorption of arachidic acids on silver. The latter SAM exhibits an ellipsometric thickness of $27.6 \pm 0.8 \text{ \AA}$, which is comparable to the calculated thickness of 28.0 \AA for a fully extended chain. From the FT-IR spectra, they observed that the acid head group dissociatively chemisorbs on the surface with a *trans* zigzag conformation with a tilt angle of $\sim 10^\circ$ to the surface normal. On the other hand, Samant et al.⁸⁰ reported similar results, that an ordered SAM of docosanoic acid was formed on silver with a tilt angle of $\sim 27^\circ$ to the surface normal.

1.4.1 SAMs of Alkanoic Acids on Silver, Copper and Aluminum Oxide

It has been found that there are differences in the chemisorption of alkanoic acids on different metal oxide surfaces, such as Ag, Cu, and Al.⁶⁷ On the surface of Ag, the n-alkanoic acid dissociatively adsorbs in a very ordered way and fully occupies all the available sites, and the two oxygen atoms of the carboxylate sit nearly symmetrical on the surface (Figure 1.3). This binding geometry is not significantly affected by the chain-chain interactions. A similar packing density with a *trans* zigzag conformation and a similar chain tilt was observed for both long and short chain acids. The “odd-even” effect observed in contact angle and FT-IR data is closely tied to the orientation of the terminal methyl group. For even numbered carbon chains, the symmetric vibration mode for the methyl group is stronger, and the asymmetric vibration mode is weaker because the terminal methyl group points closer to the surface normal, resulting in a higher contact angle, especially for HD, on such a “methyl” surface. For odd numbered carbon chains, the symmetric vibration mode is weaker and the asymmetric vibration mode is stronger because the terminal methyl group points away from the surface normal, resulting in an exposure of the methylene unit next to the methyl group to the surface and exhibiting a lower contact angle. For acids of sufficient length ($n > 11$), all the even chain acids give an identical structures but all the odd chain acids display slightly different structures.

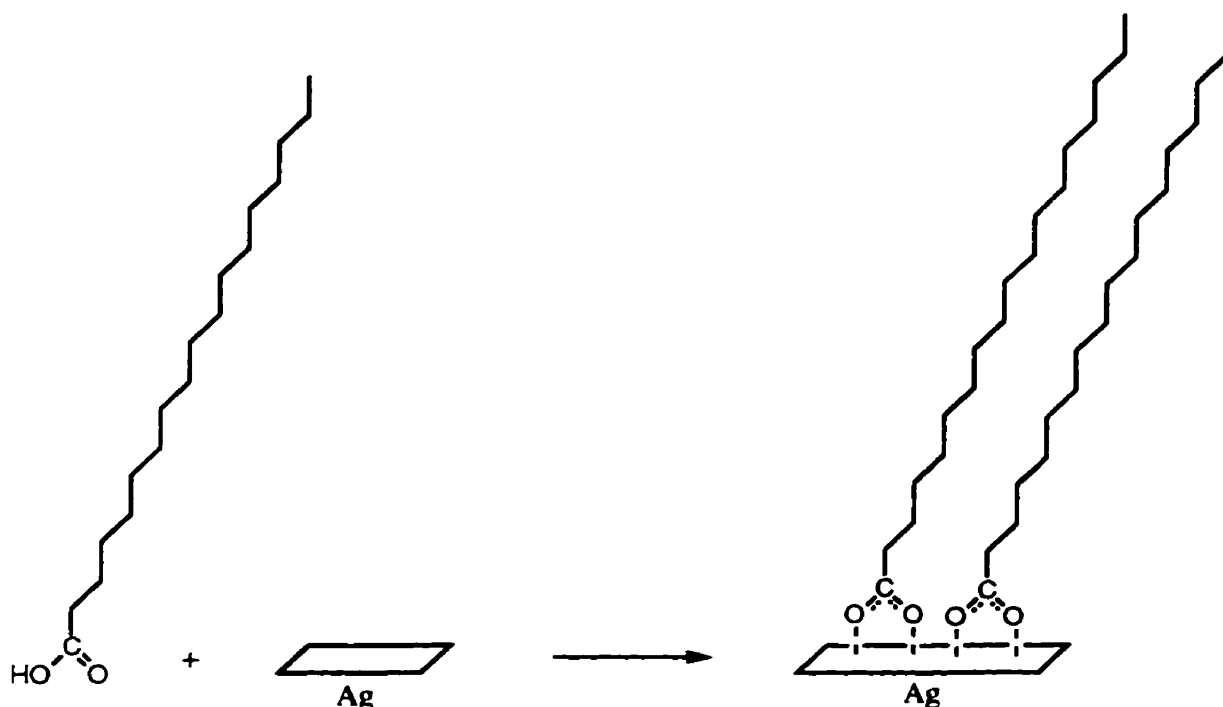


Figure 1.3 A SAM of octadecanoic acid on silver.⁶⁷

On the surface of Cu and Al, n-alkanoic acid also completely dissociates, but the head group carboxylate coordinates to the surface with a tilt (Figure 1.4). For shorter chain acids, the film is disordered due to insufficient cohesive interactions which result in a less dense film. As the chain length increases, the cohesive force becomes strong enough to pull the molecular chains into a "normal" orientation for optimal interaction energy.⁵⁶ Moreover, some twisting or strain of the chains has to develop to achieve the ultimate perpendicular orientation. Consequently, acids with odd or even chains have the same "outer surface structure". Only those methylene units near the head group contribute to most of the absorption intensity of the methylene modes. The rest of the groups have only little contribution because of the perpendicular orientation. For the chains that are beyond a certain threshold length, they stand up straight.

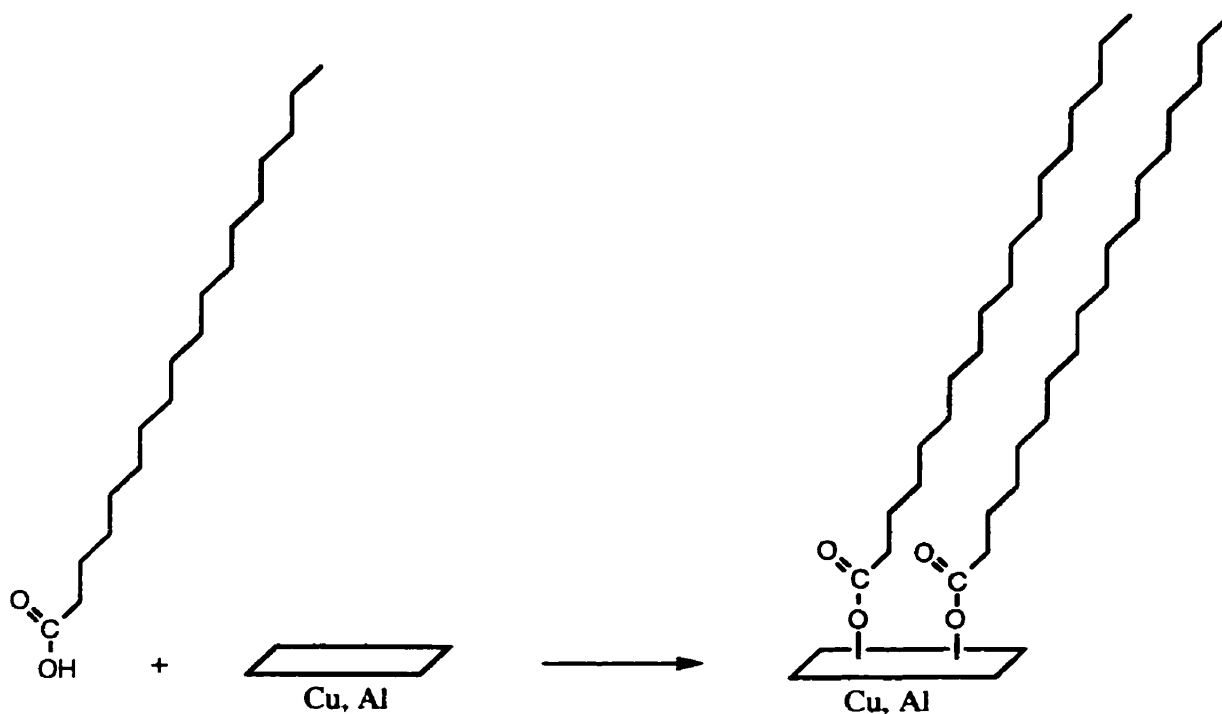


Figure 1.4 A SAM of octadecanoic acid on copper and aluminum oxide.⁶⁷

Although it has been suggested that long alkane chain acids are aligned normal on both Cu and Al surfaces, there are still some differences in the band shape for the methylene stretches, $\nu_a(\text{CH}_2)$ and $\nu_s(\text{CH}_2)$. On copper, the $\nu_a(\text{CH}_2)$ band around 2917 cm^{-1} and the $\nu_s(\text{CH}_2)$ band at 2849 cm^{-1} are more or less symmetrically shaped. On aluminum, the $\nu_a(\text{CH}_2)$ band has broad multiple peaks, and the $\nu_s(\text{CH}_2)$ band is shifted to a slightly higher frequency. It was suggested that the strain or twist of the molecular chains is more serious on aluminum than on copper, leading to a more ordered system for the latter. It is attributable to a difference in the binding geometry/strength of the carboxylate on each metal as well as the surface lattice of the metal oxides.

Upon exposure to air, all three metal surfaces form oxides with different basicities. The peak frequency for symmetric carboxylate of the SAM on the metal oxide increases in the order: 1402 cm^{-1} on silver < 1440 cm^{-1} on copper < 1478 cm^{-1} on aluminum. The shift is parallel to the stability of the monolayer on metal in the order of Al < Cu < Ag. However,

Allara and Nuzzo,⁶⁸ Smith and Porter,⁸¹ and Soundag et al.⁸² concluded that the monolayer of stearic acid on AgO surface is less ordered than that on Al₂O₃. Differences between the results in the two groups may be due to the differences in the preparation conditions.²⁶

1.4.2 SAMs of Alkanoic Acids with Aromatic Chromophores

In their study of the effect of introducing aromatic chromophores along the alkyl chain of alkanolic acid films on the monolayer structure, Tao et al.⁸³ reported that a variety of aromatic chromophores, except for large molecules, can be incorporated in a monolayer assembly, resulting in a well-ordered SAM on the surface of silver. These large chromophores, such as 1,4-substituted naphthyl and 9,10-substituted anthracenyl groups, require a more expanded lattice for packing, resulting in a wider separation between the alkyl chains above the chromophores. Thus they need to tilt further in a less ordered and *trans* zigzag way to make molecular contact with neighboring chains. However, it is still uncertain as to whether the disorder of alkyl chains is due to a disorder in the arrangement of the chromophores or whether it is a mere result of the larger spacings between the chains.

1.4.3 Stability Tests

In a study of the stability of the alkanolic acid films,⁸⁰ it was found that the SAMs of alkanolic acid dissolved in chloroform, resulting in a significant decrease in contact angles for both HD and water. It is attributable to a weak bonding of carboxylate to the metal surface. The low stability of the acid films limits their applications in thin film technology.

1.4.4 SAMs of Hydroxamic Acids

In order to improve the stability of the above films on metallic oxides, monolayers of hydroxamic acids (R(CH₂)_nCONHOH) on native oxides of metals were examined.⁸⁴ Hydroxamic acids form more stable monolayers on basic metal oxides such as silver and

copper; but form less stable monolayers on acidic metal oxides such as aluminum, iron, titanium and zirconium. Furthermore, hydroxamic acids form more stable monolayers than carboxylic acids or phosphonic acids on these substrates. There are two advantages of using hydroxamic acids compared to thiols on copper and silver.⁸⁴ First, the thiols will etch the surface of copper oxide during thin film formation, but the hydroxamic acids do not. Second, hydroxamic acids are more inert to oxidation, and are thus more stable in air for a longer time.⁸⁵ Monolayers of thiolates photooxidize on the surface resulting in the formation of metal-sulfonates.⁸⁵ Therefore, hydroxamic acids can be used as an alternative to thiols as protective coatings. Other potential uses of these monolayers comprise lithography, corrosion resistance, and tribology.^{6a,33}

On the native oxides of aluminum, zirconium, and iron, hydroxamic acids also form more stable monolayers than carboxylic acids or phosphonic acids. Owing to the smaller size of the hydroxamic acid than the phosphonic acid, more ordered monolayers of hydroxamic acids on zirconium oxide can be formed.⁷⁷⁻⁷⁹ They may have similar technical applications as the SAMs of the phosphonic acids on zirconium oxide. Finally, Folkers et al.⁸⁴ found that phosphonic acids form more stable monolayers than hydroxamic and carboxylic acids on titanium oxide.

1.4.5 SAMs of Dioic Acids

We now turn to research on the thin films of α,ω -alkanedioic acids on Ag which may be used to build multilayers of carboxylic acids on metallic oxides. Allara and Atre⁸⁶ reported the first example of a SAM of a folded dioic acid, 1,32-dotriacontanedioic acid, on silver. The monolayer structure consists of folded chains of loop shape bound by the carboxyl groups on the substrate, resulting in a theoretical thickness of ~ 22 Å which is consistent with the measured value of 20 ± 2 Å. Exposure of CH_2 groups to the surface was confirmed by the wetting measurements on the monolayer and clean polyethylene. A lower water contact angle of 103° was obtained in both cases. The similarity of these thin

films to the polyethylene surfaces was further supported by having a contact angle for HD of $\sim 0^\circ$. Besides the symmetric and asymmetric CH_2 stretching frequencies at ~ 2850 and $\sim 2920 \text{ cm}^{-1}$, a shoulder at the higher frequency side of the 2928 cm^{-1} band, representing a component with a low degree of conformational disorder,⁸⁷ appears in the FT-IR spectra. Furthermore, the intense peak centered at 1400 cm^{-1} and the weaker bands at 1537 cm^{-1} are attributed to the symmetric and asymmetric stretching modes, respectively, of a carboxylate group.⁶⁶ Thus, the looped structure of dioic acid makes it impossible for fabrication of multilayered thin film assemblies.

1.5 SAMs of Organosulfurs Compounds on Metal Surfaces

In 1983, Nuzzo and Allara²⁹ first reported that dialkyl disulfides (RS-SR) can form ordered monolayers on gold surfaces. Later, it was found that sulfur compounds coordinate very strongly to gold,^{31,34,55-63} silver,³⁶ copper,³⁵ and platinum surfaces.⁶⁴ Since gold does not form a stable oxide, it can be handled in ambient conditions. Thus, most of the work has been done on gold surfaces. SAMs on gold have potential applications in industrial technologies, such as electrode modification,⁸⁸ corrosion resistance,⁸⁹ biomaterial coatings,⁹⁰ and biosensor technology.⁹¹ This is due to a strong interaction of sulfur with the gold surface ($\sim 40\text{--}45 \text{ kcal mol}^{-1}$), and thiols on gold can form highly ordered SAMs with the thickness in angstroms scale.¹² However, SAMs of alkanethiols on gold are relatively fragile⁹² and decompose on moderate heating³⁴ (e.g., 80°C in hexadecane). Hence, the thiol thin films have limited applications in adhesion, lubrication, and optoelectronic device fabrication.³

1.5.1 SAMs of Thiols on Gold

SAMs of organosulfur compounds including dialkyl sulfide,⁶⁴ dialkyl disulfides,²⁹ thiophenols,⁹³ mercaptopyridines,⁹⁴ mercaptoanilines,⁹⁵ thiophenes,⁹⁶ cysteines,⁹⁷ xanthates,⁹⁸ thiocarbaminates,⁹⁹ thiocarbamates,¹⁰⁰ thioureas,¹⁰¹ and mercaptoimidazoles¹⁰²

on gold have been reported in recent years. However, the SAMs of alkanethiols on gold are the most well-studied ones (Figure 1.5). Among the thiols, octadecanethiol monolayer has been shown to form a protecting coating of the metal surface against oxidation.^{6a}

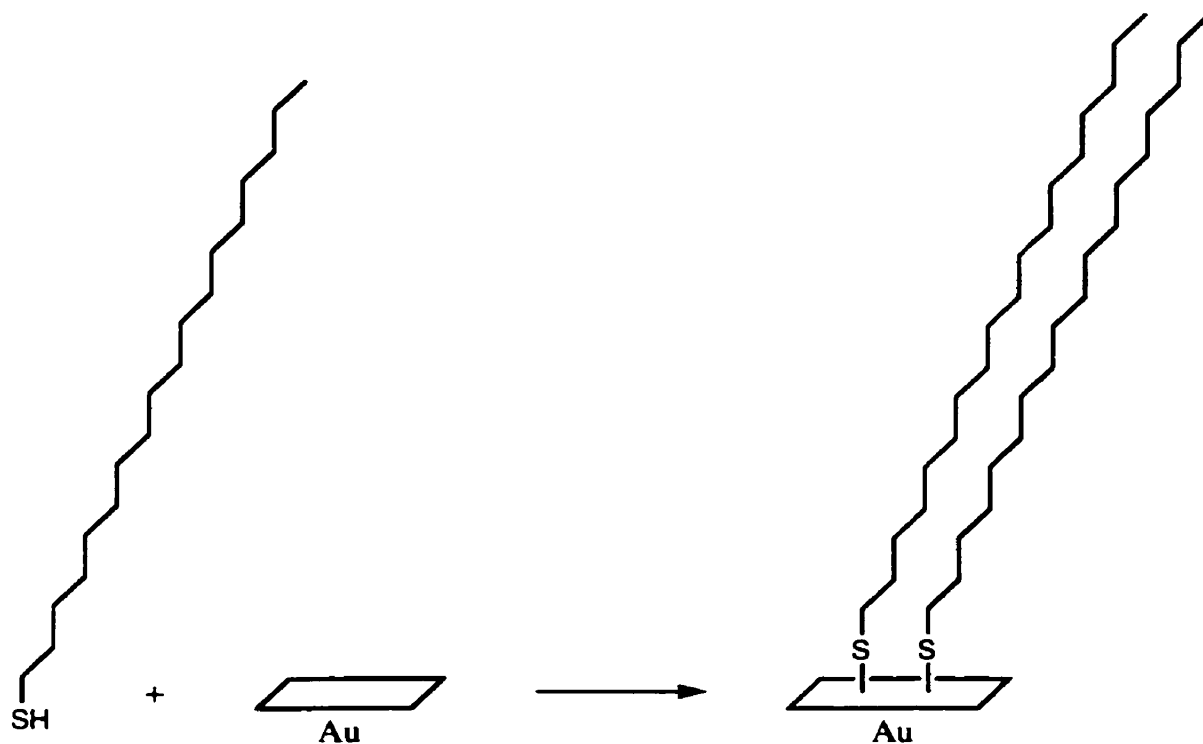


Figure 1.5 A SAM of octadecanethiol on gold.

1.5.1.1 Deposition Process

It has been reported that even with very dilute solution (e.g. 5 μM) of long-chain alkanethiols (e.g. C22) the main process of film formation is quite fast (~ 1 min).¹⁰³ During the adsorption process, small and disordered clusters grow, followed by an ordered domain formation.³⁴ From kinetic studies, a very fast step takes a few minutes to reach 80-90% of the limiting values of the contact angles and thickness, followed by a slow step which lasts several hours before they reach their final values of thickness and contact angles.³⁴

1.5.1.2 Monolayer Structures

The presence of a closely packed, methyl-terminated monolayer is often indicated by an advancing water contact angle of $\sim 110^\circ$, and an advancing HD contact angle of $\sim 45^\circ$.^{25,29,31,34-36,44,67-68,104-105} A lower value of the contact angle, relative to a well-characterized system such as alkanethiols on gold, indicates disorder and/or lower surface coverage in the monolayer. However, a value comparable to that of the ordered system does not necessarily indicate the same structure or a corresponding degree of order.

Porter et al.³¹ observed that there was a significant drop in the ellipsometric thickness for short chains of alkanethiols on gold. Together with the FT-IR data, they indicate increasing disorder with loose packing. Bain et al.³⁴ also saw a similar trend in the contact-angle data. For $n > 10$, advancing contact angles, $CA_{\text{H}_2\text{O}}$ and CA_{HD} were found to be $111-114^\circ$ and $45-48^\circ$, respectively. The contact angles became lower for shorter chains. This trend could have been caused by the probe liquid sensing the underlying gold³⁴ or increasing disorder in short-chain monolayers. For the partially formed monolayers, and monolayers where disorder has been introduced intentionally, lower contact angles were observed.¹⁰⁶ The odd-even effect, as mentioned before in the case of the alkanolic acids on silver, is less prominent for short ($n < 11$) chains of thiols on gold.

As the length of the alkyl chains increases, the frequency for the $\nu_{\text{a}}(\text{CH}_2)$ and $\nu_{\text{s}}(\text{CH}_2)$ modes decreases.³¹ From Table 1.1,³¹ it was observed that the frequencies of $\nu_{\text{a}}(\text{CH}_2)$ and $\nu_{\text{s}}(\text{CH}_2)$ decreased from 2921 cm^{-1} to 2918 cm^{-1} , and 2852 cm^{-1} to 2850 cm^{-1} , respectively, as the length of the alkyl chain increased from $n = 5$ to $n = 21$. This suggests that for shorter chains, the thin films are more disordered and liquid-like; while for longer chains, the thin films become more ordered and crystalline-like.

In addition, the measured intensities of the methylene stretches can be used to calculate average tilt of the chain axis from the surface normal. The details for this type of

calculation have been reported elsewhere,^{68b} and involve the comparison between the measured intensities and those which are calculated for a hypothetical isotropic monolayer. It was found that for $n = 15-21$, the monolayers of alkanethiols have a tilt angle of $20-30^\circ$ from the surface normal and $50-55^\circ$ rotation about the molecular axis.²⁶

Table 1.1 Peak positions for $\text{CH}_3(\text{CH}_2)_n\text{SH}$ CH_2 stretching modes in crystalline and liquid states and adsorbed on gold³¹

CH_2	Peak positions for crystalline and liquid states, cm^{-1}		Peak positions for $\text{CH}_3(\text{CH}_2)_n\text{SH}$ adsorbed on gold, cm^{-1}						
	crystalline	liquid	$n = 21$	$n = 17$	$n = 15$	$n = 11$	$n = 9$	$n = 7$	$n = 5$
ν_a	2918	2924	2918	2917	2918	2919	2920	2921	2921
ν_s	2851	2855	2850	2850	2850	2851	2851	2852	2852

1.5.1.3 Thermal and Chemical Stabilities

SAMs of alkanethiols on gold have been found to be inert to air, water and ethanol at room temperature, consistent with the results that there is no change in contact angle or thickness under such conditions for several months.³⁴ The monolayers desorbed upon heating to temperatures above 70° . Qualitatively, desorption was the slowest in air, faster in ethanol and the fastest in a hydrocarbon solvent. As compared to amine monolayers on Cr^{107} and carboxylic acid monolayers on silver,⁸⁰ thiol monolayers on gold are more stable; however, they are less stable than silane monolayers on silica. Furthermore, monolayers of the long-chain thiols are thermally more stable than those of the short-chain thiols.

From the contact angle and ellipsometry data, monolayers of octadecanethiol on gold were resistant toward 1 M HCl or 1 M NaOH at room temperature for 1 day, but were

attacked after a month.³⁴ Over this period, the water contact angle was lowered by 3° in a base, and 8° in an acid. In addition, the surface of the gold was visibly pitted in the latter case. The deterioration became more severe in boiling acid and base. Other chemicals that attack either the gold surface, such as aqua regia, mercury and I_3^- , or the thiol monolayers themselves such as halogens (I_2 , Br_2), strong oxidizing agents (peroxide, ozone), and ethereal solutions of borane and phosphorus pentachloride, must be avoided.³⁴

1.5.2 SAMs of ω -Substituted Thiols on Gold

SAMs of functionalized alkanethiols are important for surface modification. A number of functional groups can be introduced in the chromophore structure provided that (i) they do not react with thiols; (ii) they do not compete strongly with the thiol to adsorb onto the gold; and (iii) they are not too large to prevent close packing of the hydrocarbon chains. As the length of the hydrocarbon chain becomes shorter, the perturbations of the structure of the monolayer by interactions between the tail groups increase.⁵⁵

Table 1.2⁵⁵ summarizes the contact angles of water and HD on various monolayers, from $HS(CH_2)_{15}COOH$ having CA_{H_2O} of 0° to $HS(CH_2)(CF_2)_5CF_3$ having CA_{H_2O} of 118°. A comparison of the nitrile and methyl ester surfaces provides an example of the length scales determining the wetting interaction.¹⁰⁸ Both surfaces have comparable CA_{H_2O} of ~65°, but hexadecane only wets the nitrile surface. On the methyl ester surface, hexadecane interacts with the exposed methyl group mainly by a London force, whereas water interacts with the underlying polar ester group by long-range dipole-dipole interactions.¹⁰⁹ The contact angle data for the thiol monolayers suggest that they are closely packed to expose the tail group on the surface.

On the other hand, functionalized alkanethiol SAMs are essential tools for surface engineering. The OH and COOH groups are very useful terminal groups for surface modification. A carboxylic acid-terminated thiol can react with the acid chloride to produce the corresponding thioester. Based on this reaction, Kim et al.¹¹⁰ synthesized polymeric

self-assembled monolayers and multilayers from the diacetylene $\text{HS}(\text{CH}_2)_{10}\text{C}\equiv\text{CC}\equiv\text{C}(\text{CH}_2)_{10}\text{COOH}$, which are discussed in Section 1.9. SAMs of OH-terminated alkanethiols have been used in many surface modification reactions, for example, a second monolayer of OTS can be chemisorbed on the monolayers of 11-hydroxyundecane-1-thiol (HUT) on gold surfaces,¹¹¹ resulting in a highly ordered and closely packed bilayer. Thus, a combination of these two technologies seems to be promising to construct stable multilayers on gold surfaces.

Table 1.2 Advancing contact angles of water ($\text{CA}_{\text{H}_2\text{O}}$) and HD (CA_{HD}) on thiol monolayers adsorbed on gold⁵⁵

RSH	$\text{CA}_{\text{H}_2\text{O}}$	CA_{HD}	RSH	$\text{CA}_{\text{H}_2\text{O}}$	CA_{HD}
$\text{HS}(\text{CH}_2)_2(\text{CF}_2)_5\text{CF}_3$	118	71	$\text{HS}(\text{CH}_2)_{11}\text{OCH}_3$	74	35
$\text{HS}(\text{CH}_2)_{21}\text{CH}_3$	112	47	$\text{HS}(\text{CH}_2)_{12}\text{SCOCH}_3$	70	0
$\text{HS}(\text{CH}_2)_{17}\text{CH}=\text{CH}_2$	107	39	$\text{HS}(\text{CH}_2)_{10}\text{CO}_2\text{CH}_3$	67	28
$\text{HS}(\text{CH}_2)_{11}\text{OSi}(\text{CH}_3)_2\text{-(C(CH}_3)_3)$	104	30	$\text{HS}(\text{CH}_2)_8\text{CN}$	64	0
$\text{HS}(\text{CH}_2)_{11}\text{Br}$	83	0	$\text{HS}(\text{CH}_2)_{11}\text{OH}$	0	0
$\text{HS}(\text{CH}_2)_{11}\text{Cl}$	83	0	$\text{HS}(\text{CH}_2)_{15}\text{CO}_2\text{H}$	0	0

1.5.3 SAMs of Aryl Thiols on Gold

Besides the alkanethiol SAMs, organosulfur monolayers containing aromatic moieties in the backbone on gold have also been studied.¹¹²⁻¹¹⁹ The thiolate headgroup of alkanethiol SAMs may be susceptible to oxidation under ambient conditions, resulting in the formation of sulfonates.^{85,120} These oxidized monolayers become highly unstable.¹²¹⁻¹²² It has been suggested that the thiolate is less subject to oxidation under ambient conditions when the mercapto group is directly attached to an aryl.¹¹³ Sabatani et al.⁹³ prepared SAMs of the

aromatic compounds thiophenol (TP), *p*-biphenyl mercaptan (BPM), and *p*-terphenyl mercaptan (TPM) on gold. BPM/Au and TPM/Au have either higher contact angles of water (BPM) or have a smaller hysteresis (difference between advancing and receding contact angles) (TPM) than TP/Au, suggesting a better packing or different orientation of the former monolayers. The ellipsometric thickness of a TP monolayer is significantly smaller than the theoretical value, possibly due to a nonperpendicular orientation of the phenyl ring with respect to the surface¹²³ and/or poorer packing of the molecules in the monolayer. However, the ellipsometric thicknesses of BPM and TPM monolayers are comparable to the theoretical values. Furthermore, BPM and TPM films are comparatively more stable than TP layers under a variety of conditions.⁹³ In addition, Kolega and Schlenoff¹²⁴ reported that well-ordered SAMs can be produced by linearly attaching more phenyl groups to the thiophenol. On the other hand, Tao et al.^{114,119} have studied the surface properties of the SAMs generated from various aromatic-containing thiols on gold, silver and copper, indicating that these thiols produce densely packed and well-ordered films without introducing steric influence in the monolayer assemblies. Cygan et al.¹²⁵ reported that SAMs of 4-(2'-ethyl-4'-(phenylethynyl)phenylethynyl)-1-phenylthiolate, a representative of a family of linear conjugated oligomers having a phenylene ethynylene backbone, on Au, have a potential to act as molecular wires.

1.5.4 SAMs of Chelating Aromatic Dithiols on Gold

In order to increase the thermal stability of thiol films, Gary et al.¹²⁶ prepared SAMs of chelating aromatic dithiols, derivatives of 1,2-bis(mercaptomethyl)-4,5-dialkylbenzene, on gold (Figure 1.6). The advancing contact angles of water and HD were found to be $114 \pm 2^\circ$ and $48 \pm 2^\circ$, respectively, on the SAMs of the long-chain chelates. The wettabilities of the chelating SAMs do not reflect the “odd-even” effect as observed for the normal thiol SAMs.¹²⁷ The data suggest that the thin films of the long-chain chelating aromatic dithiols

are densely packed and highly oriented, exposing terminal methyl rather than methylene groups.³⁴ In contrast, SAMs of the shorter chain analogues exhibited lower contact angles for both water and HD. Preliminary thermal stabilities of the films suggested that the chelating aromatic SAMs are more thermally stable than their normal alkanethiol analogues.

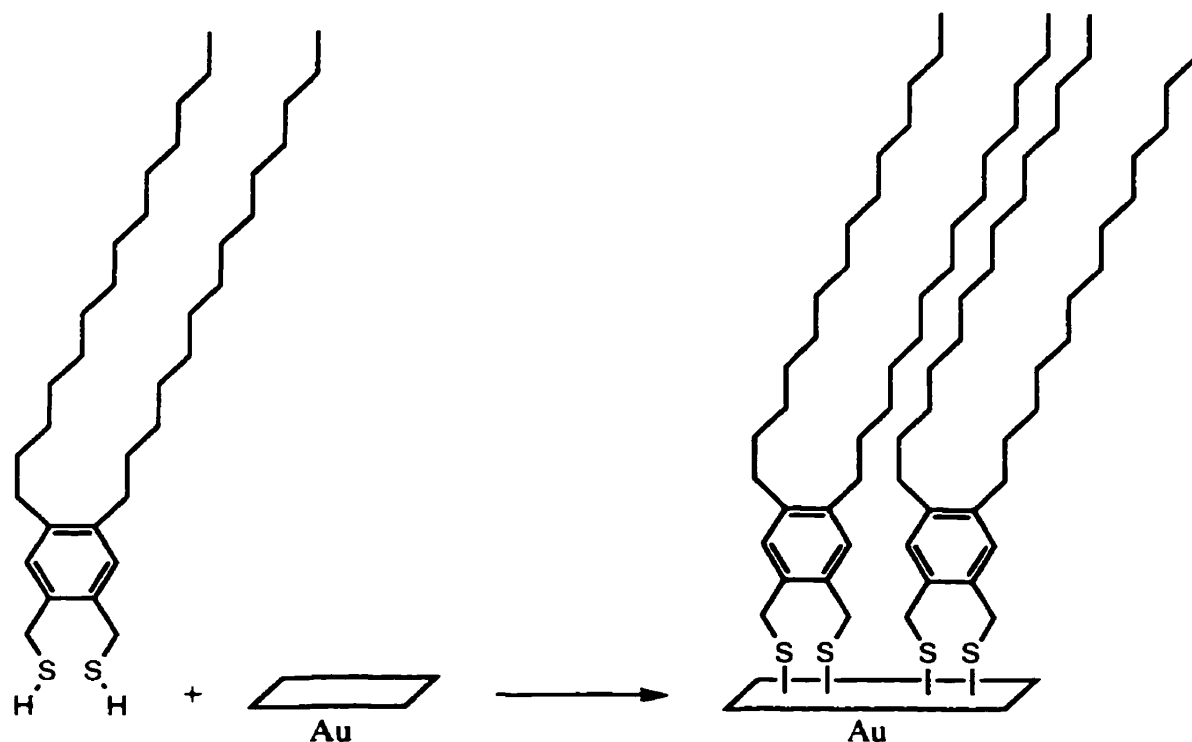


Figure 1.6 A SAM of 1,2-bis(mercaptomethyl)4,5-di(tetradecyl)benzene on gold.¹²⁶

1.5.5 SAMs of Conjugated α,ω -Dithiols and Acetylthiols on Gold

Flexible α,ω -dithiols have been shown to form either multilayers via disulfide linkages or looped structures with both ends of the molecule attaching to the surface.³⁴ For rigid α,ω -dithiols, for example, 1,4-phenyldithiol and 4,4'-biphenyldithiol, there was no indication towards looped structures. Multilayer thin films were constructed by adsorbing

one thiol end to the surface while freeing the other end for oxidative S-S coupling,^{75,110} resulting in densely packed structures.¹¹⁵ The use of acetyl-protected thiols, for example, 1,4-phenyldithiolacetyl and 4,4'-biphenyldithiolacetyl, is a convenient method for the in situ, base-promoted liberation of the thiol. Moreover, the acetyl-protected thiols can adsorb directly on gold without the use of exogenous base. There are difficulties in oxygen-promoted multilayer formation with the aromatic dithiols but they can be overcome by the direct adsorption of the acetyl thiols. These aromatic α,ω -dithiol monolayers may be useful in the design of molecular wires which are capable of bridging proximate gold surfaces.

1.5.6 SAMs of Dialkyl Sulfides on Gold

Systems based on dialkyl sulfides (such as $R(\text{CH}_2)_m\text{S}(\text{CH}_2)_n\text{R}'$, where R and R' represent different functional groups such as CH_3 or COOH) on gold⁶⁴ (Figure 1.7) are attractive because the structures of the two alkyl groups connected to sulfur can be varied independently by straightforward synthetic methods. This variation allows a degree of control of the local structure of the adsorbed monolayer that is not easily possible with other organosulfur compounds or simple fatty acid derivatives.⁶⁴ SAMs of dialkyl sulfides were shown to be resistant to air, water, dilute acid and ethanol, but highly non-resistant to strong base. Furthermore, they are not stable at high temperature ($\sim 80^\circ\text{C}$) and to some reagents including 30% hydrogen peroxide and ethereal solutions of diborane and phosphorous pentachloride. It was found that the methyl-terminated dialkyl sulfides exhibited slightly lower contact angles with water than the methyl-terminated thiols. The carboxylic acid terminated dialkyl sulfides showed much higher contact angles with water than the carboxylic acid terminated thiols due to the fact that the dialkyl sulfides films are less tightly packed and ordered on gold than those of the analogous alkanethiols.

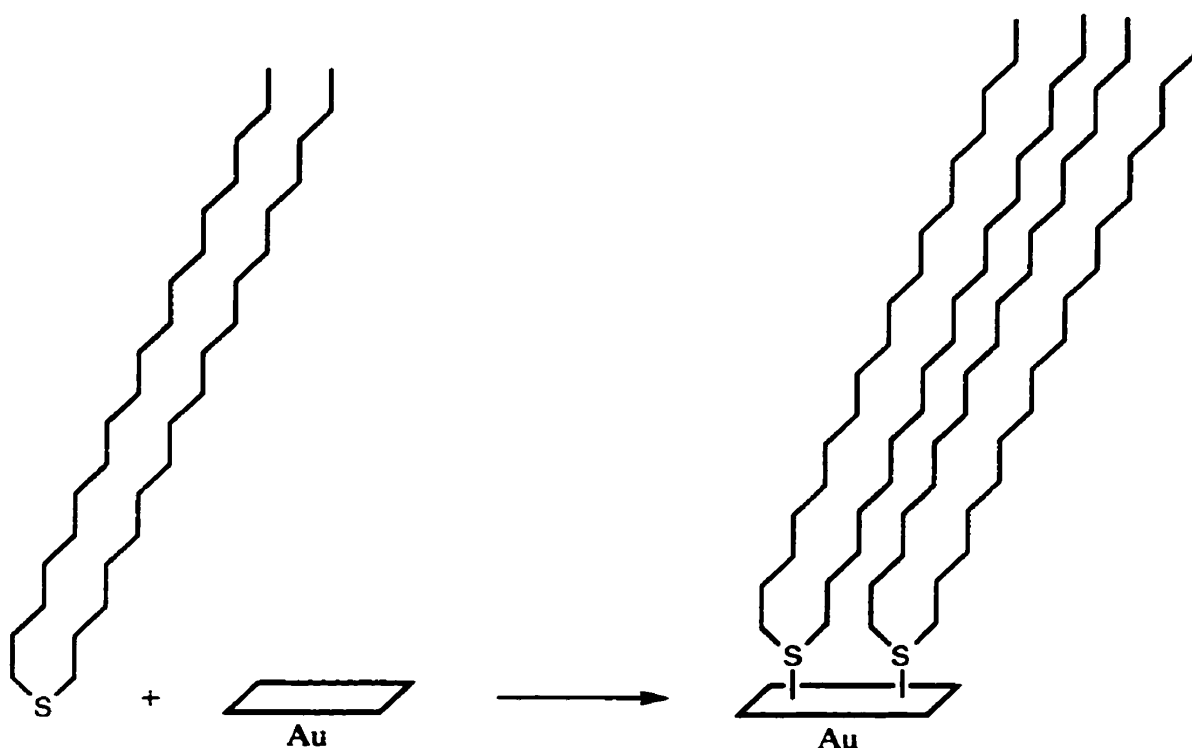


Figure 1.7 A SAM of dioctadecyl sulfide on gold.⁶⁴

1.5.7 SAMs of Dialkyl Disulfides on Gold

Nuzzo et al.^{29,65} reported that monolayers prepared from a variety of substituted dialkyl disulfide molecules (such as $(X(CH_2)_nS)_2$, where $X = CH_3$, $COOH$, or NH_2) on gold surfaces are stable and densely packed (Figure 1.8). The surface properties, as well as the stabilities of these SAMs have been shown to be similar to SAMs of thiols. Enhanced stabilities have also been observed in SAMs prepared from polydisulfides.¹²⁸ The detailed structures of the assemblies involve intra- and intermolecular interactions similar to those of the bulk crystalline phases. The SAMs of dialkyl disulfides provide a lot of significant applications in electrochemistry, adhesion and wetting, biology, microelectronics, and material science.⁶⁵

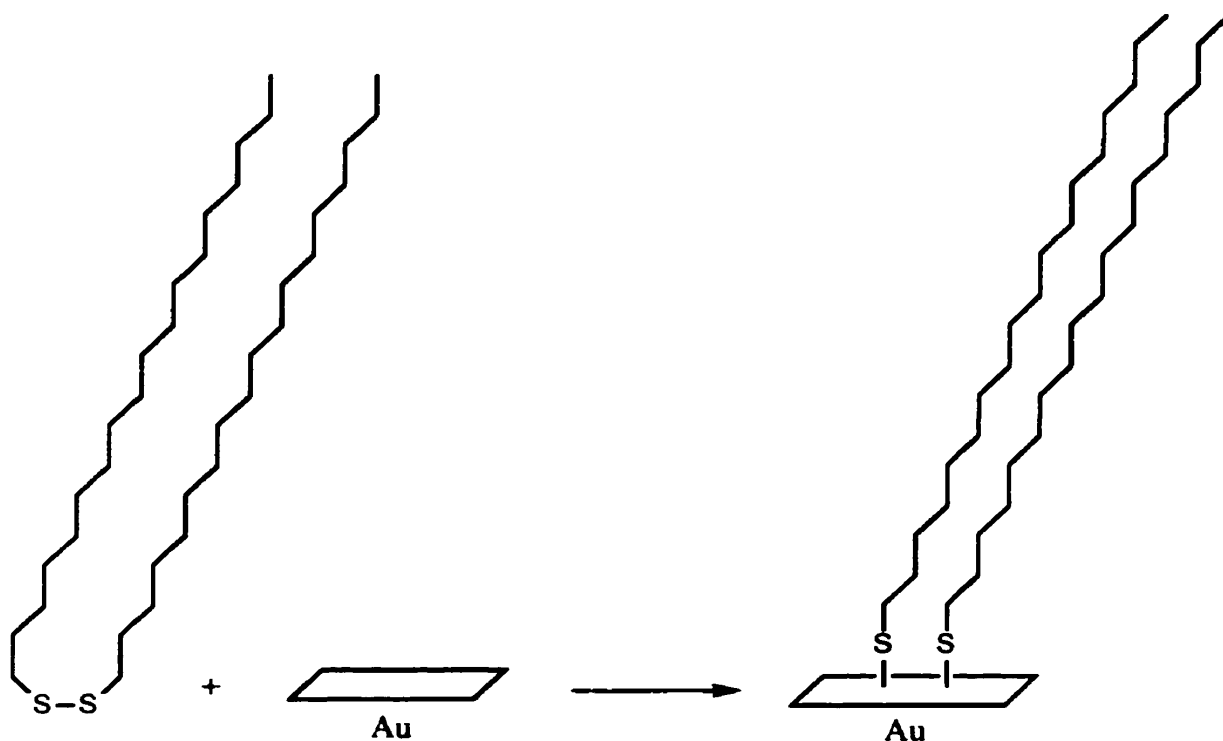


Figure 1.8 A SAM of dioctadecyl disulfide on gold.⁶⁵

1.5.8 SAMs of Branched Thiols and Disulfides on Au

Besides SAMs of non-branched thiols and disulfides, SAMs of branched thiols, $[\text{CH}_3(\text{CH}_2)_{11}\text{CH}_2]_2\text{-CH}(\text{SH})$ (Figure 1.9), and disulfides, $([\text{CH}_3(\text{CH}_2)_{11}\text{CH}_2]_2\text{-CH-S})_2$ (Figure 1.10), can also be deposited on gold.¹²⁹ The sulfur atoms in the disulfide groups are still available for interaction with the gold surface, resulting in a tilt angle of $\sim 15^\circ$ to the surface normal. This is significantly smaller than the tilt in alkanethiol monolayers ($\sim 30^\circ$) because the total area occupied by two alkane chains in SAMs of branched thiols is larger than that occupied by a sulfur attaching onto the gold surface. The SAMs of branched disulfides have been shown to be less well-packed than the corresponding thiol monolayers; but SAMs with polar functional groups were more closely packed. These branched disulfide monolayers have a lower surface coverage than SAMs of linear disulfides because when a branched disulfide molecule self-assembles on the gold surface, two Au-S bonds form but four alkane chains become immobilized.

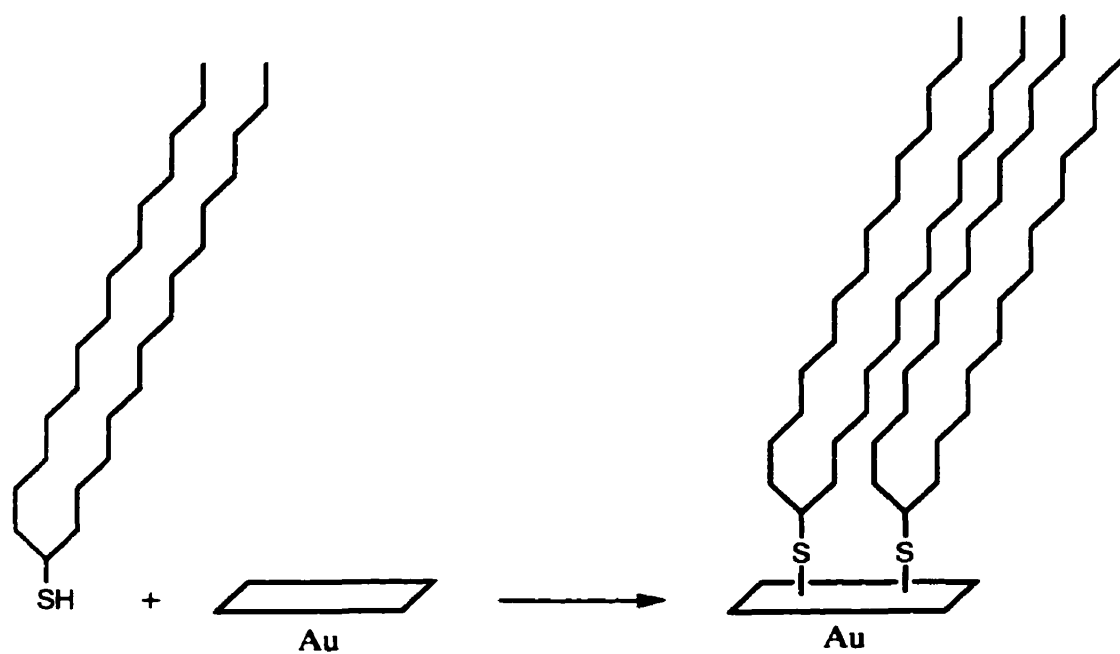


Figure 1.9 A SAM of a branched thiol on gold.¹²⁹

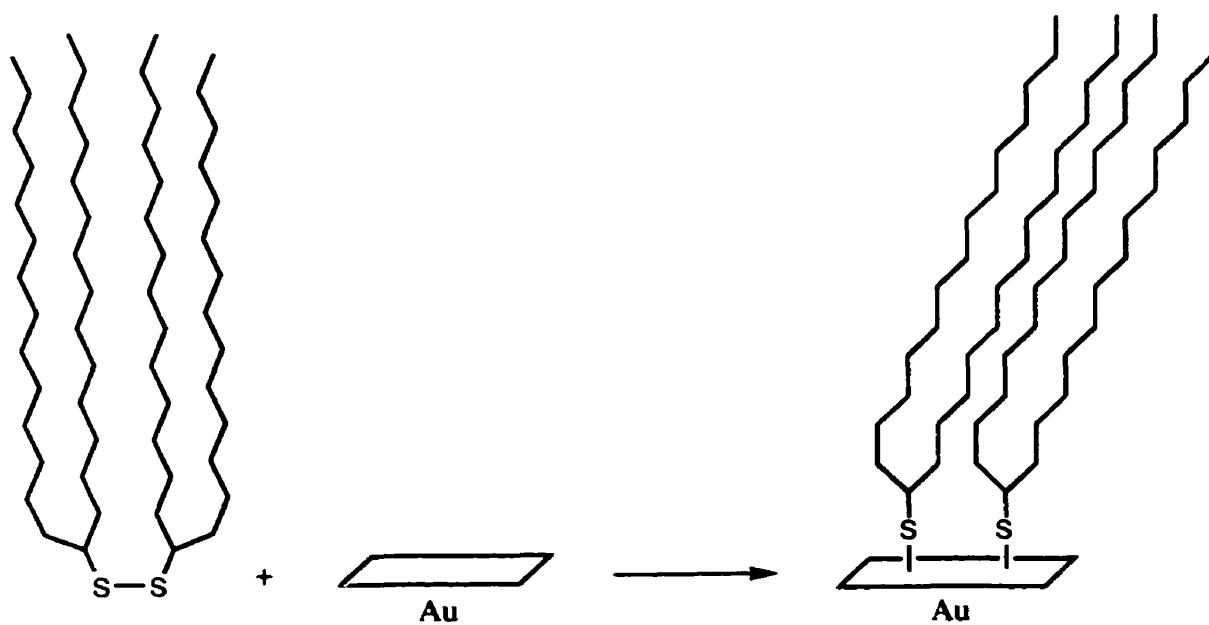


Figure 1.10 A SAM of a branched disulfide on gold.¹²⁹

1.5.9 SAMs of Thiols on Copper and Silver

n-Alkanethiols can also self-assemble on surfaces of copper and silver.³⁵⁻³⁶ Contact angle measurements of long-chain ($n \geq 12$) monolayers indicate that they are also densely packed and well-ordered. The structure of the thin films on silver and copper are different from that on gold in the following ways: (i) the hydrocarbon chain tilts more closely to the surface normal; (ii) thin films have a lower population of gauche conformations at room temperature; and (iii) the “odd-even” effect is offset by one methylene group, compared to monolayers on gold. The structural differences between a thiol monolayer on Ag/Cu and that on Au are due to a difference in the bonding between the head group and the metal. As compared to thiols on Au, the thin films on Ag/Cu are more densely packed. However, since Ag/Cu are more reactive than Au, it is more difficult to prepare reproducible thiol monolayers on Ag/Cu than on Au. Thus, it requires more effort to prepare high-quality thin films of thiols on Ag/Cu. Nevertheless, they offer the opportunity to explore how the structural differences affect properties, such as wetting, intercalation, and capacitance.

1.6 SAMs of Organosilicon Derivatives on Hydroxylated Surfaces

SAMs of long-chain organosilane compounds ($R-SiCl_3$, $R-Si(OCH_3)_3$, R = alkyl group with > 10 carbon atoms) on hydroxylated surfaces³⁸⁻⁵⁴ (Figure 1.11) have attracted growing attention since their discovery by Sagiv et al.²⁵ in 1980, although this reaction of silanization was devised more than 40 years ago for chromatographic applications.¹³⁰ These SAMs have been successfully prepared on substrates of silicon oxide,^{25,30,39,44} aluminum oxide,^{38,42} quartz,¹³¹⁻¹³² glass,¹³³ mica,^{45,134} zinc selenide,^{38,133} germanium oxide,¹³³ and oxidized gold.^{40,135} SAMs of trichlorosilane on silica appeared to be very attractive because of the availability of large silica-like substrates, such as glass and silicon wafers.¹³⁶ Amongst the silanes, octadecyltrichlorosilane (OTS) is the most popular one for generating SAMs on different substrates. These SAMs can be widely employed in the preparation of reverse phase HPLC columns for the chromatographic separation/analysis of a range of

organic/bio-organic molecules.¹³⁷ Furthermore, the SAMs of OTS on inorganic oxide surfaces offer significant applications in environmental analysis,¹³⁸ biomedical studies,¹³⁹ the formation of antithrombogenic biomaterials,¹⁴⁰ lubricants,¹⁴¹ glass-reinforced composites,¹⁴² the investigation of polymer interfacial properties,¹⁴³ chemical sensors/biosensors,¹⁴⁴ as well as electrochemical studies.¹⁴⁵

1.6.1 Deposition Process

Substrates with hydroxylated surfaces are required for the formation of SAMs of alkylchloro- and alkylalkoxysilanes. The SAMs of the silanes adsorb on these substrate surfaces via strong Si-O-Si bonds to the surface silanol groups (-Si-OH).²⁶ Alkoxysilanes are more stable to hydrolysis than chlorosilanes¹⁴⁶ because (i) the byproduct from the hydrolysis of chlorosilanes (acid), catalyzes further reactions and quickly leads to gel formation; and (ii) the hydrolysis of chlorosilanes is more exothermic than that of alkoxysilanes.¹⁴⁷

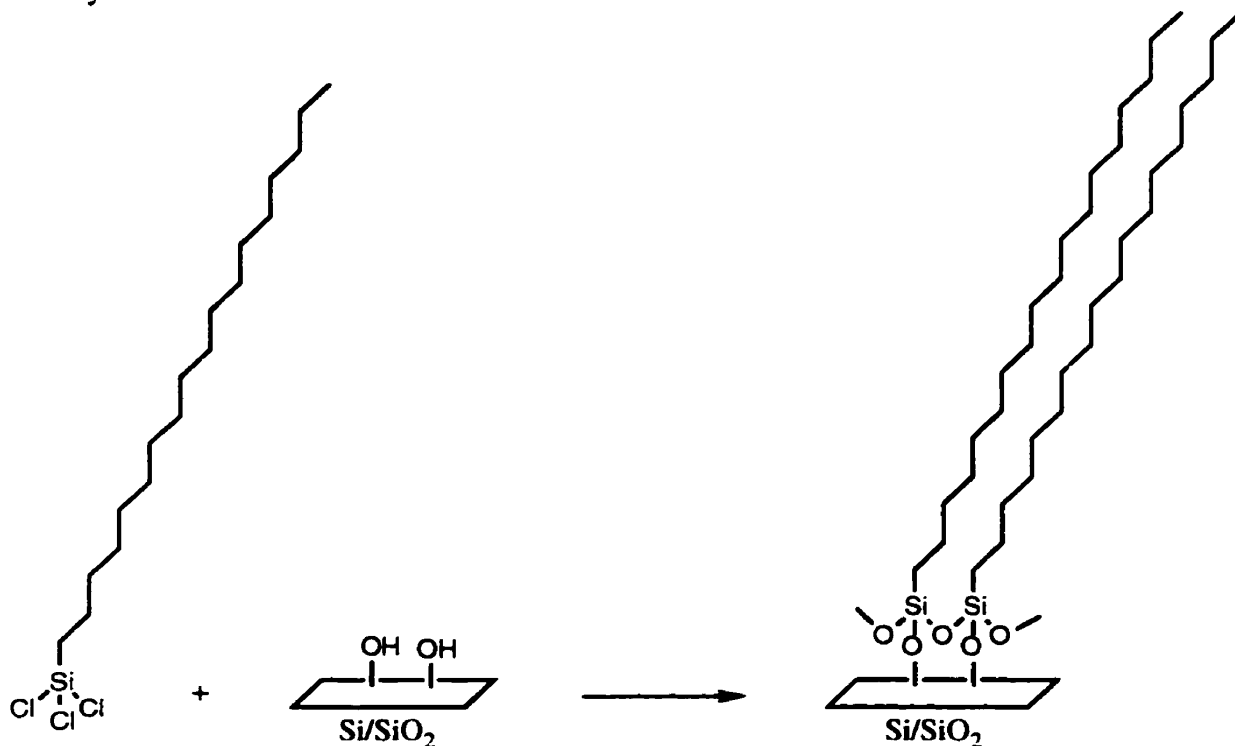


Figure 1.11 A SAM of octadecyltrichlorosilane on Si/SiO₂.

The deposition mechanism is assumed to divide into three parts:²⁵ (i) the trichlorosilane molecules approach the clean silica surface by polar-polar interactions; (ii) since the silica surface is hydrated¹⁴⁸, the trichlorosilane groups of the silane molecules are hydrolyzed when they get close enough to the surface, followed by (iii) water elimination with the surface silanols and their close neighbors via strong, covalent Si-O bonds. It has been reported¹⁴⁹ that only some of the OTS chains, about one in five, form bonds to the surface. Thus, a completely hydrated surface is not necessary for complete surface coverage. But trifunctionality of the silane molecules is necessary to form densely packed monolayers. In addition, curing at 150 °C¹⁵⁰ promotes cross-linking of organosilane molecules and covalent bond formation to the silica surface, resulting in highly stable and well-ordered layers.¹⁵¹

However, it is difficult to produce high-quality SAMs of trichlorosilanes because the alkyltrichlorosilanes are highly moisture sensitive.^{30,150,152} While incomplete monolayers are formed in the absence of water,^{44,149} excess water results in facile polymerization in solution and deposition of polysiloxane on the surface.¹³¹ Angst et al.¹⁵⁰ reported that the SAMs of OTS on hydrated thermal oxide are ordered and densely packed, whereas they are disordered and loosely packed on dry oxide. McGonern et al.¹⁵³ suggested a moisture quantity of 0.15 mg/100 ml of solvent to be optimal for the formation of closely packed monolayers. Under such condition, XPS studies confirm the complete surface reaction of the -SiCl₃ groups.¹⁵⁴ Recently, Tripp and Hair¹⁵⁵ demonstrated that methylchlorosilanes were completely hydrolyzed to methylsilanols at the solid-gas interface by surface water on a hydrated silica.

Temperature is another important parameter in the monolayer formation. It was found that the threshold temperature below which an ordered monolayer is formed increases with the chain length. For example 18 °C and 10 °C is preferred for the deposition of octadecyl and tetradecyl chain, respectively.³⁰ There is competition between the polymerization of the hydrolyzed silanes in solution and the reaction of such groups with surface Si-OH groups

to form a SAM. As temperature decreases, surface reaction is preferred and reaction kinetics decrease, resulting in an ordered system. This is confirmed by recent solid-state ^{13}C NMR studies of OTS monolayers deposited on fumed silica particles.¹⁵⁶

1.6.2 Reproducibility

A problem arises in the reproducibility of alkyltrichlorosilane monolayers because the quality of the monolayers is very sensitive to reaction conditions. For example, Silberzan et al.³⁰ argued that 2 minutes is enough for the formation of a monolayer, while Banga et al.⁵¹ suggested 90 minutes, and Wasserman et al.⁴⁴ 24 hours. Sagiv et al.¹⁵⁷ reported that partial OTS monolayers have heterogeneous island structure, which is confirmed by recent AFM studies. However, Ohtake et al.,⁴⁷ Mathauser and Frank,¹³² Wasserman et al.^{154,158} and Ulman¹² all reported that the monolayers are homogeneous and disordered. These conflicting results might have simply come from different substrate properties and/or different experimental conditions for the film preparation.¹⁵⁹ Furthermore, the competition between polymerization and surface anchoring is a major source of the reproducibility problems because small differences in water content and in surface Si-OH group concentration may cause significant differences in monolayer quality.²⁶ Nevertheless, owing to high stability of the alkylsilane monolayers, they are still considered as ideal materials for surface modification and functionalization applications, such as adhesion promoters¹⁶⁰ and boundary lubricants.¹⁶¹

1.6.3 Monolayer Structures

Wasserman et al.⁴⁴ reported that monolayers prepared from a homologous series of methyl-terminated alkyltrichlorosilanes display $\text{CA}_{\text{H}_2\text{O}}$ of $\sim 110^\circ$, consistent with that reported by Sagiv et al.;³⁹ and CA_{HD} of $\sim 40^\circ$, consistent with the values of Ulman et al.⁴² However, values of CA_{HD} were $3\text{--}6^\circ$ lower than the corresponding values of SAMs of n-

alkanethiols on gold,³⁴ and an “odd-even” effect of CA_{HD} was not observed. The thicknesses measured by ellipsometry and by low-angle X-ray reflection share a high correspondence with each other, suggesting that the alkyl chains are in the all-*trans* conformation and orient nearly normal to the surface.⁴²

In the FT-IR study of a homologous series of alkyltrichlorosilanes,^{39,42} the frequency of the asymmetric methylene stretch, $\nu_s(\text{CH}_2)$ was found to decrease as the chain length is increased. For example, $\nu_s(\text{CH}_2)$ decreases from 2922 cm^{-1} to 2918 cm^{-1} as the chain length increases from tetradecyltrichlorosilane (TTS) to octadecyltrichlorosilane (OTS). Furthermore, the peak at 2920 cm^{-1} is much broader in the TTS monolayer (band width = 21 cm^{-1}) than in the OTS monolayer (band width = 16 cm^{-1}). Both frequency shift and peak broadening suggest that the monolayer becomes more disordered and liquid-like as the chain length decreases.

Allara et al.⁵³ found that the tilt angles of the alkyl chains in OTS monolayers on SiO_2 and oxidized gold are $10 \pm 2^\circ$ from the surface normal with a monolayer coverage of $\sim 96 \pm 4\%$. Biernbaum et al.¹⁶² used near-edge X-ray absorption fine structure spectroscopy and X-ray photoelectron spectroscopy to study SAMs of OTS, octadecyltrimethoxysilane (OTMS), and (17-aminoheptadecyl)trimethoxysilane (AHTMS). They found that (i) the tilt angles of the chains in OTS SAMs are $5 \pm 5^\circ$; (ii) SAMs of OTMS exhibit a higher tilt angle of $20 \pm 5^\circ$ because of the difference in the adsorption mechanisms of trichlorosilane and trimethoxysilane groups; and (iii) the introduction of a polar amino group at the chain terminus results in a more disordered monolayer.

1.6.4 Chemical and Thermal Stabilities

Monolayers with high stability bear significant contributions to molecular electronics.¹⁶³ Wasserman et al.⁴⁴ reported that monolayers of methyl-terminated siloxanes were resistant to a variety of conditions such as air, 1% detergent solution, hot water and

hot organic solvents. Moreover, the wettability or thickness of the monolayer was unaffected by rubbing the surface vigorously with a tissue or cotton swab. However, when the monolayers were exposed to aqueous base at room temperature for 80 min, approximately 50% of the monolayer had been removed. After 160 min, their surfaces were visibly etched because the Si-O bonds hydrolyze under basic conditions.¹⁶⁴ The high stability of these monolayers is due to the formation of the covalent Si-O bond, as well as the maximization of van der Waals interactions between adjacent alkyl chains.

The thermal stability of OTS monolayers on aluminum was studied by Cohen et al.¹⁵⁷ They heated the monolayer to ~125 °C and then cooled it back to room temperature. A partial (60%) SA monolayer of OTS on aluminum, a SAM of arachidic acid (AA) on aluminum, a LB monolayer of cadmium arachidate (CA), and a trilayer having a LB bilayer of cadmium arachidate on OTS/Al were employed for comparison. From the contact angles and FT-IR data, the OTS/Al monolayer was shown to be more stable than the other systems. For example, all the systems, except the OTS/Al monolayer, showed a decrease in both CA_{H_2O} and CA_{HD} under such conditions. In the FT-IR spectra, they observed apparent randomization between 100 °C and 130 °C, in both the C-H and the C=O stretching regions for the CA bilayer on OTS (van der Waals interaction between monolayer and substrate). For the SA monolayer of AA and LB monolayers of CA (ionic monolayer-substrate interaction), there were changes only in the C-H, but not in the C=O stretching region.¹⁶⁴ For the OTS/Al system, there were only slight changes, suggesting that it is the most stable system. Therefore, it could be concluded that the polysiloxane backbone in the SAM of OTS/Al provides extra stability to the system.

1.6.5 SAMs with Aromatic Chromophores

Thin films with useful aromatic and other functional groups have growing prominence in industry because of their optical and electronic uses.⁴² Incorporation of aromatic or heteroaromatic rings into the alkyl chain might introduce disorder into the

monolayer because such groups possess symmetries different from cylindrical, long-chain alkyl groups. Tillman et al.⁴² found that the construction of SAMs of trichlorosilanes containing aromatic groups, $\text{CH}_3-(\text{CH}_2)_m-\text{C}_6\text{H}_4-\text{O}-(\text{CH}_2)_n-\text{SiCl}_3$, requires alkyl chain lengths greater than at least 13 carbons, unless forces other than van der Waals attractions of alkyl chains (such as dipole-dipole interactions) have been introduced into the systems to produce ordered thin films. For example, monolayers prepared from 1-(trichlorosilyl)-11-(*p*-n-nonylphenoxy)undecane showed that the phenoxy group can be introduced into such monolayers without losing order and close packing, as compared with OTS. These systems become more disordered and liquid-like as the alkyl lengths decrease.

1.6.6 SAMs with Second Order Nonlinear Optical Properties

Based on the above alkyltrichlorosilane chemistry, SAMs of compounds with second order nonlinear optical properties can be easily deposited on silica surfaces. Synthesis of molecular materials with large second-order optical nonlinearities have extensive uses in second harmonic generation, electrooptic, and photorefractive devices.⁴ Poled polymer^{3,165} and LB film transfer approaches¹⁶⁶ have been employed in the fabrication of noncentrosymmetric assemblies in recent years. There are, however, certain difficulties which persist in the synthesis.^{3,165-166} An attractive alternative approach is to build the SAMs with second order nonlinear optical (NLO) materials via molecular self-assembly,¹⁶⁷ resulting in photochemically and thermally stable multilayers.¹⁶⁸

Marks et al.¹⁶⁹ have developed a SA strategy by attaching the $-\text{SiCl}_3$ group to small molecules, and introducing a monolayer of NLO-active dyes via an $\text{S}_{\text{N}}2$ reaction with the SAM. For example, SAMs of 2-(*p*-chloromethylphenyl)ethynylsilane were allowed to react with [2-[4-[N,N-bis(3-hydroxypropyl)amino]phenyl]ethynyl]-4'-pyridine which possesses second order NLO properties. They constructed highly ordered SAMs from a dilute solution of [[4-[N,N-bis(3-hydroxypropyl)amino]phenyl]azo]-4'-pyridine on a

benzyl chloride SAM surface, followed by annealing at 110 °C. By repeating this process, they could prepare multilayered thin films with significant second order NLO properties.^{169d}

1.6.7 Surface Modification

Surface modification can be achieved by using SAMs of alkyltrichlorosilanes with terminal functional groups, for example, halogen,¹⁷⁰⁻¹⁷¹ cyanide,¹⁷² thiocyanides,¹⁷² methyl ether,¹⁷⁰ acetate,¹⁷⁰ thioacetate,¹⁷³ α -haloacetate,¹⁷⁴ vinyl,^{24b,41} (trimethylsilyl)ethynyl,¹⁷⁵ methyl ester,^{43,176} and *p*-chloromethylphenyl.¹⁶⁹ Surface modification reactions are important for providing active surfaces for the attachment of molecules with different properties. For example, pyridine surfaces can be produced by reacting bromo-terminated alkylsilane monolayers with the lithium salt of 4-methylpyridine.^{171,176} Such surfaces react with palladium,¹⁷⁷ rhenium,¹⁷⁶ and osmium complexes¹⁷¹ to provide immobilization of organometallic moieties.

1.6.8 Multilayer Formation

In order to transform thin films into practical devices with technological uses, multilayers of appropriate thickness should be reproducibly constructed with minimum disorder.⁴³ However, most recently published reports suggest that the quality of trichlorosilane films rapidly degrades as the thickness of the films increases.^{104,178-179}

In multilayer construction, the monolayer surface is first modified to a hydroxylated one by a chemical reaction, for example, the hydroboration-oxidation of a terminal vinyl group,^{25,107,178} the LiAlH_4 reduction of a surface ester group,^{43,179} the photolysis of a nitrate-bearing group,¹⁸⁰ and the hydrolysis of a boronate-protecting group.¹⁸¹ The hydroxylated surface then allows another monolayer to adsorb on top of it. Upon the repetition of this process, multilayered films may be constructed.

1.6.8.1 Hydroboration-Oxidation of a Terminal Vinyl Group

Sagiv et al.^{25,104,178} reported that an olefin-terminated SAM can be converted into an alcohol-bearing surface on which self-assembled multilayer assemblies can be built. However, olefin hydroboration did not satisfy the quantitative yields required to optimize such a strategy. Hence, the water contact angle of the alcohol surface was higher than expected. Nevertheless, the OH-bearing surface was a suitable base for the construction of multilayer assemblies of average-quality.

1.6.8.2 LiAlH₄ Reduction of a Surface Ester Group

An improvement in multilayer construction based on the LiAlH₄ reduction of methyl esters to alcohols was reported by Tillman et al.⁴³ They created the construction of multilayer films of methyl 23-(trichlorosilyl)tricosanoate (MTST) of ~0.1 μm thickness on oxidized silicon substrates. The advancing water contact angle on the hydroxylated surfaces was found to increase as the number of layers increased. For example, the contact angle for water on the reduced 20th layer had increased to ~50° from the initial value of ~30°, suggesting that there is an exposure of CH₂ groups to the surface. The reasons for this disorder may include (i) the imperfect packing of the ester group; (ii) the introduction of disorder by the chemical reaction of the ester group with LiAlH₄, or by the polysiloxane network; and (iii) the surface reorganization^{43,182} by burying the OH groups as much as possible, to expose more CH₂ groups to the surface. In a similar way, contact angles for HD, on the third layer of the unreduced ester surface, decreased to 12° from the initial value of 28°, reflecting a tendency towards increasing disorder of the films with increasing layer number. FT-IR data indicated that the alkyl chains in the multilayer samples are more tilted and disordered, and a small amount of ester groups remained unreacted. The primary disadvantage of this method is the requirement of a very aggressive and air/moisture sensitive reagent for LiAlH₄ reduction, leaving some inorganic residues on the substrate

surface after each reduction cycle. Nevertheless, it is possible to prepare a multilayer film with a thickness of $\sim 0.1 \mu\text{m}$.²⁶

1.6.8.3 Photolysis of a Nitrate-Bearing Group

Analogous to previously reported phototransformations of SAMs,¹⁸³ a new approach to multilayer formation by the photolysis of a nitrate-bearing SAM was reported by Collins et al.¹⁸⁰ The success of this methodology was supported by (i) the decrease of the water contact angle from 81° to 31° , (ii) the lack of substantial change in the methylene stretching region of the FT-IR spectrum ($2900\text{--}3000 \text{ cm}^{-1}$), and (iii) the small decrease in ellipsometric thickness (1.5 \AA), upon photolysis.

1.6.8.4 Hydrolysis of a Boronate-Protecting Group

Another approach to multilayered thin film construction, based on the hydrolysis of a boronate-protecting group, has been developed by Kato et al.¹⁸¹ They prepared a SAM of 5-(2-methyl-1,3,2-dioxaborinan-5-yl)pentyltrichlorosilane (MBPS) on aluminized silicon, with an ellipsometric thickness (T_e) of $15 \pm 3 \text{ \AA}$, which is comparable to the theoretical thickness. Upon hydrolysis by water/ethanol, the boronate protecting group of the SAM converted to the diol-terminated group which further reacted with another MBPS to result in a two-layered film with a thickness of $29 \pm 3 \text{ \AA}$. By repeating the process, a three-layered film of MBPS with a thickness of $42 \pm 4 \text{ \AA}$ was constructed. If the hydrolyzed two-layered film was treated with OTS, a three-layered assembly with a reasonable thickness of $54 \pm 5 \text{ \AA}$ was formed. This method provides a route to construct multilayers with high molecular density and effective surface coverage. Furthermore, the surface of the multilayers can be functionalized with designed silane compounds.

1.7 Alkyl Monolayers on Silicon

The surface of silicon has been comprehensively studied for many years because of its importance in modern technology.⁷⁰ A stable and densely-packed SAM covalently bonded directly to the silicon surface can lead to a new area in film technology.

Linford and Chidsey⁷⁰ recently reported that diacyl monolayers can be covalently bonded directly to the hydrogen-terminated silicon surface upon pyrolysis of neat diacyl peroxides. They have comparable monolayer thickness, chain packing, and wetting properties to the monolayers of long-chain alkyl thiols on gold or trichloroalkylsilanes on oxidized silicon. However, FT-IR spectra suggested the presence of some carbonyl groups which indicated that these monolayers did not solely comprise alkyl chains.

The physical properties, in term of $\nu_s(\text{CH}_2)$, $\text{CA}_{\text{H}_2\text{O}}$, CA_{HD} and T_c , of the three monolayer systems, diacyl peroxides on silicon, alkyltrichlorosilanes on oxidized silicon and alkanethiols on gold, are shown in Table 1.3.⁷⁰ It was found that the properties of the monolayers containing 17 and 18 carbons are nearly identical, suggesting that all are closely-packed and highly ordered. For shorter-chain species, $[\text{CH}_3(\text{CH}_2)_{10}\text{C}(\text{O})\text{O}]_2/\text{H-Si}(111)$ and $\text{CH}_3(\text{CH}_2)_{11}\text{SiCl}_3/\text{oxidized Si}$ are shown to be less ordered than $\text{CH}_3(\text{CH}_2)_{11}\text{SH}/\text{Au}$. A lower surface coverage of 10-25% was observed in the case of stearic acid and octanoyl chloride on silicon. The films prepared from the longer-chain acyl peroxide showed comparable stabilities with those from the longer trichlorosilane. For example, after 2 h in boiling chloroform and 1 h in boiling water, the frequency of the asymmetric CH_2 stretch had shifted from 2917.5 cm^{-1} to 2919.9 cm^{-1} for $[\text{CH}_3(\text{CH}_2)_{16}\text{C}(\text{O})\text{O}]_2/\text{H-Si}(111)$; and from 2917.3 cm^{-1} to 2919.9 cm^{-1} for $\text{CH}_3(\text{CH}_2)_{17}\text{SiCl}_3/\text{oxidized Si}$. On the other hand, for $\text{CH}_3(\text{CH}_2)_{17}\text{SH}/\text{Au}$, the asymmetric stretching frequency of CH_2 increased from 2917.9 cm^{-1} to 2920.9 cm^{-1} , and the thickness decreased by 30%, after only 30 min in boiling chloroform.

Table 1.3 Physical properties of monolayers on silicon, oxidized silicon, and gold⁷⁰

System	$\nu_s(\text{CH}_2)$, cm^{-1}	$\text{CA}_{\text{H}_2\text{O}}$, °	CA_{HD} , °	T_s , Å
$[\text{CH}_3(\text{CH}_2)_{16}\text{COO}]_2/\text{H-Si}(111)$	2917.5	112	46	25
$\text{CH}_3(\text{CH}_2)_{17}\text{SH}/\text{Au}$	2917.9	114	50	28
$\text{CH}_3(\text{CH}_2)_{17}\text{SiCl}_3/\text{oxidized Si}$	2917.3	112	46.5	25
$[\text{CH}_3(\text{CH}_2)_{10}\text{COO}]_2/\text{H-Si}(111)$	2921.0	112	40.5	17
$\text{CH}_3(\text{CH}_2)_{11}\text{SH}/\text{Au}$	2919.2	113.5	47	17
$\text{CH}_3(\text{CH}_2)_{11}\text{SiCl}_3/\text{oxidized Si}$	2921.7	114	42	17
$\text{CH}_3(\text{CH}_2)_{16}\text{COOH}/\text{H-Si}(111)$	2923.3	---	---	---
$\text{CH}_3(\text{CH}_2)_{16}\text{COCl}/\text{H-Si}(111)$	2925.8	---	---	---

In order to improve the quality of the newly formed monolayers, alkyl monolayers on silicon have been prepared from 1-alkene and hydrogen-terminated Si(111), upon free-radical initiation with diacyl peroxides.⁷¹ They have been shown to be densely packed and highly ordered, exhibiting $\text{CA}_{\text{H}_2\text{O}}$ of 113°, CA_{HD} of 45°, and $\nu_s(\text{CH}_2)$ at 2921 cm^{-1} , similar to those for the SAMs of trichloroalkylsilanes on oxidized silicon and alkanethiols on gold.^{31,34} The monolayers were highly resistant to boiling chloroform, boiling water, boiling acid and boiling base.

1.8 SAMs with Alternate "Inorganic/Organic" Systems

Alternate "inorganic/organic" systems, based on transition-metal coordination chemistry, have been developed for preparing self-assembled multilayers with potential uses as active components in charge-separated assemblies,¹⁸⁴ and materials with selective chemical responses for sensor applications.⁵⁷ Metal-ligand coordination chemistry, including pyrazines with Ru,⁷² dithiols with Cu,⁷³ diamines with Ru,⁷⁴ and diamines with Ni-Pt(CN)₄,⁷⁵ have been involved in multilayer deposition. Moreover, Mallouk et al.⁷⁷⁻⁷⁹

developed layered phosphonate films and Ansell et al.⁷⁶ a new self-assembly system based on the cobalt-diisocyanide system.

1.8.1 Layered Phosphonate Thin Films

Yamanaka et al.¹⁸⁵ and Alberti et al.¹⁸⁶ initiated the study of the chemistry of γ -metal (IV) phosphonates in the mid-1970s. These phosphonates¹⁸⁷ are good for the molecular design of structures with specific properties because a number of organic groups can be attached to the γ -layers. Moreover, almost any organic molecule can be converted into a phosphonic acid derivative, and crystallized as a highly ordered and stable layered metal phosphonate.⁷⁷ These layered materials have a wide range of applications,¹⁸⁸ including chemical sensing, nonlinear optics, catalysis, dielectric coatings, and ion exchangers.

Highly ordered and stable multilayers of metal-bis(phosphonate) (MBP) are relatively easy to make. Mallouk et al.⁷⁷⁻⁷⁹ first demonstrated that this could be achieved by adsorbing the appropriate metal salt (e.g. ZrOCl_2) and α,ω -bis(phosphonic acid) alternately onto a suitably prepared surface, such as silicon and gold substrates. Usually, an “anchoring” molecule (thiol, e.g. $[\text{S}(\text{CH}_2)_4\text{PO}_3\text{H}_2]_2$, or silanol, e.g. $\text{HO}(\text{CH}_3)_2\text{Si}(\text{CH}_2)_3\text{PO}_3\text{H}_2$), which possesses a surface active group at one end and a phosphonate group at the other, is first adsorbed, followed by binding a layer of metal ions through metal-phosphonate bonds. A monolayer of α,ω -bis(phosphonic acid) then attaches one end to the adsorbed metal ion layer, freeing the other end to attach another layer of metal salt. Multilayers can be prepared by repeating these adsorption steps. For example, the Mallouk group⁷⁷⁻⁷⁹ has successfully prepared a 12-layered thin film of zirconium 1,10-decanebisphosphonate.

1.8.2 Cobalt-Diisocyanide Thin Films

Cobalt-1,4-diisocyanobenzene (Co-DiCNB) multilayer films can be prepared on an amine-functionalized surface. Ansell et al.⁷⁶ have previously found that Co^{2+} ions could bind strongly to the amine-terminal surfaces. However, it is difficult to bind another amine

molecule to the surface-anchored cobalt. As shown from the FT-IR and ellipsometry data for the Co-DiCNB system, isocyanide ligands bind strongly to the surface-bound cobalt ions. Multilayers of Co-DiCNB can be constructed by repeated alternate deposition of cobalt and diisocyanobenzene on an amine-functionalized substrate. This system provides an alternative to MBP chemistry for multilayered self-assembly. In addition, when we combine both MBP and Co-DiCNB systems together, "hybrid" structures with alternating metal-bisphosphonate and cobalt-isocyanide layers can be fabricated.⁷⁶

1.9 Monomeric and Polymerized Diacetylene Langmuir-Blodgett and Self-Assembled Thin Films

The major disadvantage of Langmuir-Blodgett films is their limited stability towards various chemical or physical conditions. The stability problem can be solved by the two-dimensional polymerization of the LB films. Since diacetylenes are monomeric amphiphiles with two triple bonds in the hydrocarbon tails of the molecules, they can undergo topochemical polymerization upon UV-irradiation to form extended polymers both on solid supports and at the air-water interface.¹⁸⁹⁻¹⁹¹ Polymerization of the monolayer helps to increase its mechanical strength. Thus, a highly stable film of polydiacetylene (PDA) can be used as a protective surface coating for biomedical or optoelectronic applications.^{24a} Furthermore, the PDA films have potential use as stabilizers of lipid membranes,¹⁹² supporting matrices for biosensing molecules,¹⁹³ liposomes for drug-delivery,¹⁹² and optical components in nonlinear optical devices.¹⁹⁴

Wegner first reported polymerization of diacetylenes in the solid state.¹⁹¹ Sheth and Leckband^{24a} found that the polymerization of 10,12-pentacosadiyonic acid (PCA) monolayers helps to improve the chemical and mechanical stability, and the aging behavior of the film. However, in the preparation of the two dimensional polymer from PCA and its derivatives, unpolymerized domains and defects are introduced in the polymer films.^{24a}

These constraints on fabrication must be overcome before high quality, homogeneous films can be prepared.

Although the factors affecting the stability of a SAM are not well understood, its stability may be related to the interactions between individual molecules and various types of molecular defects,¹⁹⁵ and defects between ordered domains.¹⁹⁶⁻¹⁹⁷ SAMs are fairly stable under ambient conditions, but they become fragile at extreme pHs,⁷¹ in many nonaqueous solvents,¹⁹⁸ in the presence of Cl^- , CN^- , and thiols,¹⁹⁹ at high temperatures,^{196,200} and at extreme electrode potentials.²⁰¹ Thus, they are not applicable in corrosion passivation and inhibition,^{6c} lubrication,^{8a} nor adhesion.^{8b} In order to improve the durability of SAMs, Kim et al.²⁰² have prepared diacetylenic SAMs ($\text{HS}(\text{CH}_2)_{10}\text{C}\equiv\text{CC}\equiv\text{C}(\text{CH}_2)_{10}\text{COOH}$, DA-COOH) that can be polymerized in a plane parallel to the substrate upon UV exposure. They compared the stability of unpolymers (hexadecanethiol, HDT) and polymerized SAMs (PDA-COOH), by exposing them to an especially aggressive solvent, a 1:1 mixture of ethanol and 1.0 M aqueous KOH at 100 °C. The entire SAM of HDT desorbs while there is only a little change in the FT-IR spectrum of the SAM of PDA-COOH after solvent exposure, thereby attesting the improvement in the stability of the PDA SAM.

From the FT-IR data of the $\text{HS}(\text{CH}_2)_{10}\text{C}\equiv\text{CC}\equiv\text{C}(\text{CH}_2)_{10}\text{COOH}$,¹¹⁰ it was found that the absorbance in the hydrocarbon region increased with the increase in number of layers. However, upon UV-polymerization the magnitude of these peaks decreased significantly, suggesting that the methylene bonds are oriented more parallel to the substrate after polymerization.²⁰³ The UV-Vis data indicate that polymerization is complete within 5 min; afterward the intensity or position of the absorption maximum (620 nm), does not change further. Yet, two absorption maxima are usually observed in studies of polydiacetylene LB films,²⁰⁴ one is found between 600 and 640 nm, which corresponds to the “blue polymer”, and the other is between 500 and 550 nm, which corresponds to the “red polymer”. The result suggests that the self-assembly approach only gives rise to the more highly

conjugated “blue polymer”. These materials have potential uses in such areas as ultrathin photoresists, and rugged adhesion layers for grafting of bilayers, and multilayers.^{110,202,205}

1.10 Limitation of Traditional Approaches to Molecular Self-Assembly

Although the above described approaches to molecular self-assembly have their own advantages, they have their individual limitations also. The self-assembly of organosulfur compounds on gold depends on the specific interaction between the sulfur head group and the gold surface. Moreover, these compounds do not adsorb on the surfaces of many other metal oxides.⁸⁴ Carboxylic acids and phosphonic acids do adsorb on various metal surfaces, but the adsorption is weak.^{66-68,78-80} It is impossible to selectively adsorb a carboxylic acid in the presence of a terminal phosphonic acid group on metal oxide surfaces.²⁶ These systems can neither be used to incorporate polar groups into a monolayer,²⁰⁶ introducing difficulty in layer-by-layer construction of multilayers with complicated polar and interesting planar bulky π -systems.¹ Moreover, phosphonic acids have large head groups which are more inconvenient to synthesize.⁸⁴ In the case of alkyltrichlorosilane monolayers, although (i) they are physically and chemically robust because of the presence of 3-dimensional polymer network;¹⁵¹ and (ii) they can self-assemble on a large number of silica-like substrates,¹³⁶ it is difficult to synthesize a number of silane coupling agents with designed surface functional groups because most of them are highly moisture sensitive. There is also a difficulty in depositing alkyl monolayers with desired functional groups on silicon via free-radical initiation with diacyl peroxides. Multilayer formation using long chain alkanes on silicon is also a significant issue.

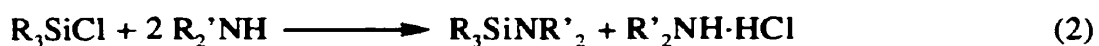
An ideal thin film construction methodology should be able to fulfill the following requirements: (i) it should involve easily accessible reagents to construct self-assembled monolayers and multilayers on industrially important substrates; (ii) be versatile in incorporating a variety of compounds with different surface functional groups; and (iii) in the resulting monolayers or multilayers it should be feasible to carry out topochemical

polymerization of suitably oriented diacetylene groups. We have developed an alternative approach to molecular self-assembly on inorganic oxide surfaces using acid-base hydrolytic chemistry of amino-silanes and -stannanes with molecules containing terminal acidic moieties. It addresses some of the issues mentioned above in constructing self-assembled thin films.

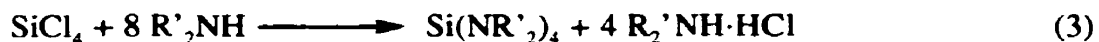
1.11 Acid-Base Hydrolytic Chemistry

1.11.1 Synthesis of Aminosilanes

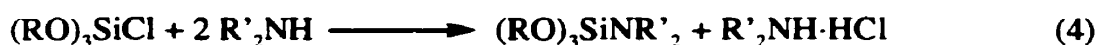
The reaction of ammonia or an amine with a halosilane results in the formation of a silicon-nitrogen bond.²⁰⁷ The bromo- and iodosilanes appear more reactive toward a given amine than the chlorosilanes. Owing to their availability, however, the chlorosilanes are most frequently employed. The halides released during the course of the reaction are precipitated as the ammonium or amine salts.²⁰⁷



Similarly, amines react with tetrachlorosilanes via stepwise substitution of chlorines to give $\text{Si}(\text{NR}'_2)_4$.²⁰⁷



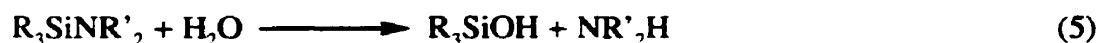
Trialkoxychlorosilanes react with amines in the same way as trialkylchlorosilanes and the alkoxy groups are inert under these conditions.²⁰⁷



1.11.2 Chemistry of Aminosilanes

1.11.2.1 Reaction with Water

Aminosilanes react with water, resulting in the cleavage of the silicon-nitrogen bond. The first step of the hydrolysis is the formation of a silanol. Depending upon its stability and the reaction conditions, the silanol may either be isolated or undergo condensation with another silanol or aminosilane to yield the disiloxane.²⁰⁷



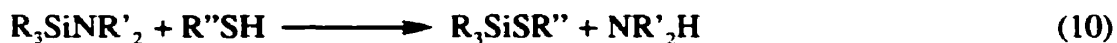
1.11.2.2 Reactions with Alcohols, Phenols and Silanols

Aminosilanes react with alcohols, phenols, and silanols to form alkoxysilanes, phenoxysilanes, and disiloxanes, respectively.²⁰⁷ The extent and rate of reaction are dependent on (i) hindrance around both the Si-N bond and the hydroxyl group of the alcohol or silanol and (ii) the acidity of the attacking alcohol.



1.11.2.3 Reactions with Thiols and Carboxylic Acids

With thiols and carboxylic acids, aminosilanes react to yield silylthiols and silylcarboxylates, respectively.²⁰⁷



1.11.2.4 Reaction with Acetylene Compounds

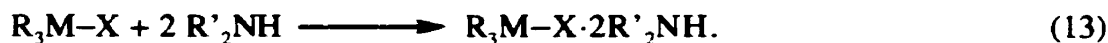
However, aminosilanes do not react with protic species with lower acidity, such as acetylene compounds.²⁰⁷ Because of its lower metal-to-nitrogen bond strength, and the higher basicity of nitrogen in aminostannanes than the corresponding aminosilanes, the Sn-N bond can be easily cleaved by such protic species.²⁰⁸ Acid-base hydrolytic chemistry of aminostannanes is discussed below.

1.11.3 Synthesis of Aminostannanes

The simple aminostannanes were not synthesized until about 1961.²⁰⁹ In a comparative study of the behavior of group IV halides towards amines,²⁰⁸ Si and Ge were found to react as:



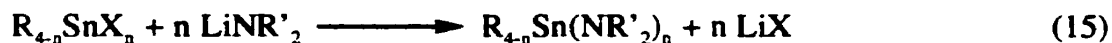
whereas Sn and Pb as:



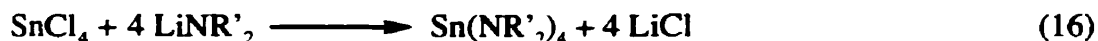
However, if a protic reagent (HA) is present together with an amine, the following reaction can occur.²⁰⁸



In order to make aminostannanes directly and more efficiently, lithium salts of secondary amines are used to react with organotin halides.²⁰⁸⁻²⁰⁹



For example, tin(IV) chlorides react with lithium salts of secondary amines to give tetraaminostannanes.²⁰⁸



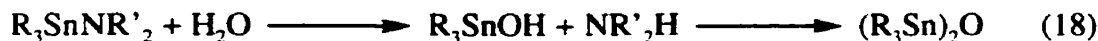
1.11.4 Chemistry of Aminostannanes

1.11.4.1 Reactions with Water and Air

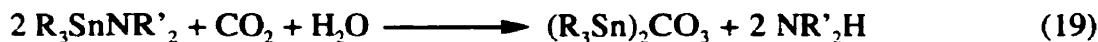
In general, the aminostannanes are very sensitive to moisture and carbon dioxide and must be protected from the atmosphere.²¹⁰ Water is only one of a wide range of protic species (HA) which attack the aminostannanes as indicated by the general equation.^{208,210}



For example, aminostannanes are easily hydrolyzed to the hydroxide or oxide.



Exposure of aminostannanes to the atmosphere actually affords the carbonates.



1.11.4.2 Reactions with Protic Species

The reactions of aminostannanes with protic species, appear to require that HA should have a pK_a value of ≤ 25 (Table 1.4).²⁰⁸ Among the more interesting examples are those where HA is an alcohol, carboxylic acid, thiol, indene, cyclopentadiene, phosphine, and acetylene (Eq. 17). The reaction of aminostannanes with protic species becomes the

basis of many preparative procedures and can be applied to the preparation of stannosiloxanes.²¹⁰

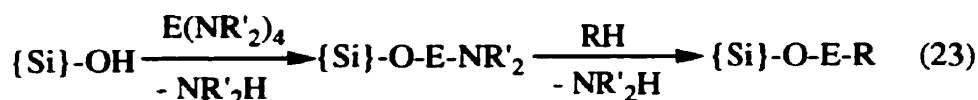
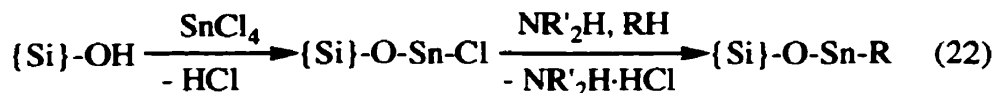
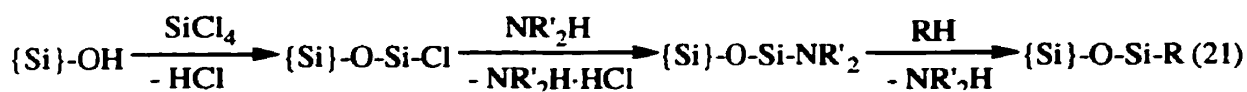


Table 1.4. Acid strength of some protic species²⁰⁸

Protic Species	pK_a
PH_3	26
$\text{RC}\equiv\text{CH}$	25
Indene	20
Cyclopentadiene	16
ROH	16-19
RSH	10-11
ArOH	10
ArSH	8
RCOOH	4-5

1.12 Acid-Base Hydrolytic Chemistry Approach to Molecular Self-Assembly on Inorganic Oxides Surfaces

The surfaces of inorganic oxides such as silica, glass and quartz are acidic in nature, and contain surface hydroxyl groups.²¹¹ Thus, the acid-base hydrolytic chemistry described above can be easily applied to these surfaces to give a versatile chemisorption method for a variety of organic microstructures (RH), according to following equations, where E = Si, Sn.



1.13 Scope of Thesis

Using acid-base hydrolytic chemistry described above for amino-silanes and -stannanes, a new approach to molecular self-assembly has been developed. Treatment of surface hydroxyl groups on glass, quartz and single crystal silicon with commercially available group (IV) chlorides, ECl_4 ($\text{E} = \text{Si}, \text{Sn}$), and then NEt_2H or directly with $\text{Si}(\text{NEt}_2)_4$ or $\text{Sn}(\text{NEt}_2)_4$ yields surface-anchored NEt_2 moieties, which react with several organic molecules containing terminal acidic protons, such as alcohol, carboxylic acid, thiol, phosphine, cyclopentadiene, indene, and alkynes, via acid-base hydrolysis, leading to molecularly self-assembled monolayers. This new approach is elaborated in Chapter 3 and optimal conditions for thin film construction are discussed.

Using the simple acid-base hydrolysis route, silica surfaces functionalized with aminosilanes can be easily modified with a variety of long alkane chain alcohols terminating with different functionalities. In Chapter 5, the generality of the new acid-base hydrolytic approach to self-assembly of a series of thin films containing short-to-long chain alcohols terminated with alkyl, phenyl and acetylene groups on Si/SiO_2 surfaces and a comparison of a two-step thin film construction process involving the reaction of $\text{Si}(\text{NEt}_2)_4$ with surface hydroxyl groups followed by the reaction with ROH , with the three-step sequence using SiCl_4 , NEt_2H and ROH , are discussed.

The traditional preparation methodologies for building multilayered structures have limitations associated with controlling film thickness and individual layer compositions of the resulting thin film assemblies. Based on the hydrolysis of surface-anchored aminosilanes with molecules containing terminal bifunctional groups, silica surfaces can be modified with a variety of multilayered films. In Chapter 6, the possibility of building multilayered assemblies in a layer-by-layer fashion using bifunctional chromophores, is explored. The multilayered thin films are constructed via the reaction of $\text{Si}(\text{NEt}_2)_4$ with hydroxyl groups of the inorganic oxide surfaces, followed by the reaction with dihydroxy chromophores incorporating acetylene, diacetylene and aromatic moieties in the backbone. Upon repetitive reactions with $\text{Si}(\text{NEt}_2)_4$ followed by $\text{R}(\text{OH})_2$, multilayered thin film assemblies can be fabricated on Si/SiO_2 . The possibility of topochemical polymerization of the diacetylenic moieties in the mono- and multilayered assemblies upon UV-Vis exposure is also investigated.

There have been a number of attempts made to introduce other useful moieties into the alkanes while retaining the basic long chain structure that leads to self-organization via van der Waals forces of attraction. Investigations of the organic microstructures with extensive conjugation in the backbone which will involve purely intermolecular π - π interactions for molecular self-assembly, have just begun. Because of its lower metal-to-nitrogen bond strength, and the higher basicity of nitrogen in aminostannanes than the corresponding aminosilanes, the Sn-N bond can be easily cleaved by protic species. Owing to the lower acidity of acetylene than alcohol, SAMs of chromophores with terminating acetylenic hydrogen on SiO_2/Si can only be constructed via aminostannane approach rather than aminosilane approach. In Chapter 7, molecular self-assembly of a number of rigid-rod alkynyl chromophores on inorganic oxide surfaces anchored with aminostannanes as well as the possibility of topochemical polymerization of the diacetylene moieties in the thin films upon UV-Vis exposure are discussed. Using this methodology, step-by-step multilayered thin film construction by the reaction of surface-anchored aminostannanes with

dialkynyl terminated chromophores becomes possible. Thus, a two-step thin film construction process involving the reaction of $\text{Sn}(\text{NEt}_2)_4$ with hydroxyl groups of the inorganic oxide surfaces, followed by the reaction with dialkyne chromophores incorporating alkyl and aromatic moieties in the backbone is also discussed in Chapter 7. By repetitive reactions with $\text{Sn}(\text{NEt}_2)_4$ followed by $\text{H}-\text{C}\equiv\text{C}-\text{R}-\text{C}\equiv\text{C}-\text{H}$, multilayered thin film assemblies were fabricated on Si/SiO_2 .

The evolution of thin film structures was routinely monitored by surface wettability measurements, FTIR-ATR, ellipsometry, X-ray photoelectron spectroscopy and UV-Vis spectroscopy. These surface characterization techniques probe the structure of the newly formed thin films by different physical processes, and can provide complementary and definitive information. A summary of these surface characterization techniques is provided in Chapter 2. The links between material presented in Chapters 5 to 7 are provided in Chapter 4. Finally, conclusions, contributions to original knowledge, and suggestions for future work are discussed in Chapter 8.

1.14 References

- (1) Ulman, A. *Adv. Mater.* **1990**, 2, 573.
- (2) (a) Williams, D.J. *Angew. Chem., Int. Ed. Engl.* **1984**, 23, 690. (b) Marks, T. J.; Ratner, M. A. *Angew. Chem. Int. Ed. Engl.* **1995**, 34, 155. (c) Tieke, B. *Adv. Mater.* **1990**, 2, 222. (d) Yitzchaik, S.; Marks, T.J. *Acc. Chem. Res.* **1996**, 29, 197. (e) Kaino, T.; Tomarus, S. *Adv. Mater.* **1993**, 5, 172. (f) Tachibana, H.; Matsumoto, M. *Adv. Mater.* **1993**, 5, 796.
- (3) Swalen, J. D.; Allara, D. L.; Andrade, J. D.; Chandross, E.A.; Garoff, S.; Israelachvili, J.; McCarthy, T. J.; Murray, R.; Pease, R. F.; Rabolt, J. F.; Wynne, K. J.; Yu, H. *Langmuir* **1987**, 3, 932.
- (4) (a) Moerner, W. E.; Silence, S. M. *Chem. Rev.* **1994**, 94, 127. (b) Dalton, L. R.;

- Harper, A. W.; Ghosn, R.; Steier, W. H.; Ziari, M.; Fetterman, H.; Shi, Y.; Mustacich, R. V.; Jen, A. K.; Shea, K. J. *Chem. Mater.* **1995**, *7*, 1060. (c) Dalton, L. R.; Harper, A. W.; Wu, B.; Ghosn, R.; Laquindanum, J.; Liang, Z.; Hubbel, A.; Xu, C. *Adv. Mater.* **1995**, *7*, 519.
- (5) (a) Zhong, C.; Porter, M. D. *Anal. Chem.* **1995**, *67*, 709A. (b) Cornell, B. A.; Braach-Makvytis, V. L. B.; King, L. G.; Osman, P. D. J.; Raguse, B.; Wieczorek, L.; Pace, R. J. *Nature* **1997**, *387*, 580.
- (6) (a) Laibinis, D. E.; Whitesides, G. M. *J. Am. Chem. Soc.* **1992**, *114*, 9022. (b) Ohno, N.; Uehara, J.; Aramaki, K. *J. Electrochem. Soc.* **1993**, *140*, 2512. (c) Li, Y.; Chailapakul, O.; Crooks, R. M. *J. Vac. Sci. Technol. B* **1995**, *13*, 1300.
- (7) Srinivasan, R.; Braren, B.; Dreyfus, R. W.; Hadel, L.; Seeger, D. E. *J. Opt. Soc. Am. B* **1986**, *3*, 785.
- (8) (a) Tangyungyong, P.; Thomas, R. C.; Houston, J. E.; Michalske, T. A.; Crooks, R.M.; Howard, A. J. *Phys. Rev. Lett.* **1993**, *71*, 3319. (b) Thomas, R. C.; Kim, T.; Crooks, R.M.; Houston, J. E.; Michalske, T.A. *J. Am. Chem. Soc.* **1995**, *117*, 3830.
- (9) (a) Murray, R. W. *Annu. Rev. Mater. Sci.* **1984**, *14*, 145. (b) Chidsey, C. E. D.; Murray, R. W. *Science* **1986**, *231*, 25. (c) Wrighton, M. S. *Science* **1986**, *231*, 32. (d) Murray, R. W. *Molecular Design of Electrode Surface*; Wiley: New York, 1992.
- (10) (a) MacRitchie, F. *Adv. Protein Chem.* **1978**, *32*, 283. (b) Norde, W. *Adv. Colloid Interface Sci.* **1986**, *25*, 267.
- (11) (a) Roberts, G. G. *Adv. Phys.* **1985**, *34*, 475. (b) Proc. 5th Int. Conf. on Langmuir-Blodgett Films: *Thin Solid Films* **1992**, 210. (c) Roberts, G. *Langmuir-Blodgett Films*; Plenum: New York, 1990. (d) Barraud, A.; Vandevyver, M. *Thin Solid Films* **1983**, *99*, 221.
- (12) Ulman, A. *An Introduction to Ultrathin Organic Films from Langmuir-Blodgett to Self-Assembly*; Academic Press: Boston, 1991.

- (13) Blodgett, K. B. *J. Am. Chem. Soc.* **1935**, 57, 1007.
- (14) (a) Puterman, M.; Fort, T. Jr.; Lando, J. B. *J. Colloid Interface Sci.* **1974**, 47, 105.
(b) Holcroft, B.; Petty, M. C.; Roberts, G. G.; Russel, G. J. *Thin Solid Films* **1985**, 134, 83.
- (15) Jones, R.; Tredgold, R. H.; Hoorfar, A.; Hodge, P. *Thin Solid Films* **1984**, 113, 115.
- (16) Snow, A. W.; Barger, W. A.; Klusty, M.; Wohltjen, H.; Jarvis, N. L. *Langmuir* **1986**, 2, 513.
- (17) Nakahara, H.; Nakayama, J.; Hoshino, M.; Fukuda, K. *Thin Solid Films* **1988**, 160, 87.
- (18) Kenny, P. W.; Miller, L. L.; Rak, S. F.; Jozefiak, T. H.; Christopfel, W. C.; Kim, J. H.; Uphans, R. A. *J. Am. Chem. Soc.* **1988**, 110, 4445.
- (19) Tieke, B. *Adv. Polym. Sci.* **1985**, 71, 79.
- (20) Sugi, M.; Saito, M.; Fukui, T.; Iizima, S. *Thin Solid Films* **1985**, 129, 15.
- (21) (a) Wegmann, A.; Hunziker, M.; Tieke, B. *J. Chem. Soc., Chem. Commun.* **1989**, 1179. (b) Nakamura, T.; Kojima, K.; Matsumoto, M.; Tachibana, H.; Tanaka, M.; Manda, E.; Kawabata, Y. *Chem. Lett.* **1989**, 369. (c) Richard, J.; Vandevyver, M.; Barraud, A.; Morand, J. P.; Lapoujade, R.; Delhaes, P.; Jacquinet, J. F.; Rouillay, M. *J. Chem. Soc., Chem. Commun.* **1988**, 754.
- (22) Smith, G. W.; Daniel, M. F.; Barton, J. W.; Ratcliffe, N. *Thin Solid Films* **1985**, 132, 125.
- (23) Ledoux, I.; Josse, D.; Fremaux, P.; Piel, J. P.; Post, G.; Zyss, J.; Mclean, T.; Hann, R. A.; Gordon, P. F.; Allen, S. *Thin Solid Films* **1988**, 160, 217.
- (24) (a) Sheth, S. R.; Leckband, D. E. *Langmuir* **1997**, 13, 5652. (b) Ogawa, K.; Mino, N.; Tamura, H.; Hatada, M. *Langmuir* **1990**, 6, 851.
- (25) Sagiv, J. *J. Am. Chem. Soc.* **1980**, 102, 92.
- (26) Ulman, A. *Chem. Rev.* **1996**, 96, 1533.

- (27) (a) Dubois, L. H.; Nuzzo, R. G. *Annu. Rev. Phys. Chem.* **1992**, *43*, 437. (b) Delamarche, E.; Michel, B.; Biebuyck, H. A.; Gerber, C. *Adv. Mater.* **1996**, *8*, 719.
- (28) Bigelow, W.C.; Pickett, D. L.; Zisman, W. A. *J. Colloid Interface Sci.* **1946**, *1*, 513.
- (29) Nuzzo, R. G.; Allara, D. L. *J. Am. Chem. Soc.* **1983**, *105*, 4481.
- (30) Silberzan, P.; Leger, L.; Ausserre, D.; Benattar, J. J. *Langmuir* **1991**, *7*, 1647.
- (31) Porter, M. D.; Bright, T. B.; Allara, D. L.; Chidsey, C. E. D. *J. Am. Chem. Soc.* **1987**, *109*, 3559.
- (32) Finklea, H. O.; Avery, S.; Lynch, M.; Furtch, T. *Langmuir* **1987**, *3*, 409.
- (33) Nuzzo, R. G.; Zegarski, B. R.; Dubois, L. H. *J. Am. Chem. Soc.* **1987**, *109*, 733.
- (34) (a) Bain, C.D.; Troughton, E. B.; Tao, Y.; Evall, J.; Whitesides, G. M.; Nuzzo, R. *G.J. Am. Chem. Soc.* **1989**, *111*, 321. (b) Badia, A.; Demers, L.; Dickinson, L.; Morin, F. G.; Lennox, R. B.; Reven, L. *J. Am. Chem. Soc.* **1997**, *119*, 11104. (c) Badia, A.; Cuccia, L.; Demers, L.; Morin, F.; Lennox, R. B. *J. Am. Chem. Soc.* **1997**, *119*, 2682.
- (35) Laibinis, P.; Whitesides, G. M.; Parikh, A. N.; Tao, Y.; Allara, D. L.; Nuzzo, R. G. *J. Am. Chem. Soc.* **1991**, *113*, 7152.
- (36) Walczak, M. M.; Chung, C.; Stole, S. M.; Widrig, C. A.; Porter, M. D. *J. Am. Chem. Soc.* **1991**, *113*, 2370.
- (37) Kumar, A.; Biebuyck, H. A.; Whitesides, G. M. *Langmuir* **1994**, *10*, 1498.
- (38) Gun, J.; Iscovici, R.; Sagiv, J. *J. Colloid Interface Sci.* **1984**, *101*, 201.
- (39) Maoz, R.; Sagiv, J. *J. Colloid Interface Sci.* **1984**, *100*, 465. (b) Maoz, R.; Sagiv, J. *Thin Solid Films* **1985**, *132*, 135.
- (40) Finklea, H.O.; Robinson, L. R.; Blackburn, A.; Richter, B.; Allara, D. L.; Bright, T. *Langmuir* **1986**, *2*, 239.
- (41) Maoz, R.; Sagiv, J. *Langmuir* **1987**, *3*, 1045.

- (42) Tillman, N.; Ulman, A.; Schildkraut, J. S.; Penner, T. L. *J. Am. Chem. Soc.* **1988**, *110*, 6136.
- (43) Tillman, N.; Ulman, A.; Penner, T.L. *Langmuir* **1989**, *5*, 101.
- (44) Wasserman, S. R.; Tao, Y.; Whitesides, G. M. *Langmuir* **1989**, *5*, 1074.
- (45) Kessel, C. R.; Granick, S. *Langmuir* **1991**, *7*, 532.
- (46) Cheng, S. S.; Scherson, D. A.; Sukenik, C. N. *J. Am. Chem. Soc.* **1992**, *114*, 5436.
- (47) Ohtake, T.; Mino, N.; gawa, K. *Langmuir* **1992**, *8*, 2081.
- (48) Parikh, A. N.; Allara, D. L.; Azouz, I.B.; Rondolez, F. *J. Phys. Chem.* **1994**, *98*, 7577.
- (49) Hoffmann, H.; Mayer, U.; Krischanitz, A. *Langmuir* **1995**, *11*, 1304.
- (50) Peanasky, J.; Schneider, H. M.; Granick, S.; Kessel, C. R. *Langmuir* **1995**, *11*, 953.
- (51) Banga, R.; Yarwood, J.; Morgan, A. M.; Evans, B.; Kells, J. *Langmuir* **1995**, *11*, 4393.
- (52) Thompson, W. R.; Pemberton, J. E. *Langmuir* **1995**, *11*, 1720.
- (53) Allara, D. L.; Parikh, A. N.; Rondolez, F. *Langmuir* **1995**, *11*, 2357.
- (54) Jeon, N. L.; Finnie, K.; Branshaw, K.; Nuzzo, R. G. *Langmuir* **1997**, *13*, 3382.
- (55) Bain, C. D.; Whitesides, G. M. *J. Am. Chem. Soc.* **1988**, *110*, 3665.
- (56) Ulma, A.; Eilers, J.; Tillman, N. *Langmuir* **1989**, *5*, 1147.
- (57) Rubinstein, I.; Steinberg, S.; Tor, Y.; Shanzer, A.; Sagiv, J. *Nature* **1988**, *332*, 426.
- (58) Strong, L.; Whitesides, G. M. *Langmuir* **1988**, *4*, 546.
- (59) Chidsey, C. E. D.; Liu, G.; Rowntree, P.; Scoles, G. *J. Chem. Phys.* **1989**, *91*, 4421.
- (60) Bain, C.D.; Whitesides, G. M. *J. Am. Chem. Soc.* **1989**, *111*, 7164.
- (61) Nuzzo, R. G.; Dubois, L. H.; Allara, D. L. *J. Am. Chem. Soc.* **1990**, *112*, 558.

- (62) Whitesides, G. M.; Laibinis, P. E. *Langmuir* **1990**, *6*, 87.
- (63) Chidsey, C. E. D.; Loiacono, D. N. *Langmuir* **1990**, *6*, 709.
- (64) Troughton, E. B.; Bain, C. D.; Whitesides, G. M.; Nuzzo, R. G.; Allara, D. L.; Porter, M. D. *Langmuir* **1988**, *4*, 365.
- (65) Nuzzo, R. G.; Fusco, F. A.; Allara, D. L. *J. Am. Chem. Soc.* **1987**, *109*, 2358.
- (66) Schlotter, N. E.; Porter, M. D.; Bright, T. B.; Allara, D. L. *Chem. Phys. Lett.* **1986**, *132*, 93.
- (67) Tao, Y. *J. Am. Chem. Soc.* **1993**, *115*, 4350.
- (68) (a) Allara, D. L.; Nuzzo, R. G. *Langmuir* **1985**, *1*, 45. (b) Allara, D. L.; Nuzzo, R. G. *Langmuir* **1985**, *1*, 52.
- (69) Ogawa, H.; Chihera, T.; Taya, K. *J. Am. Chem. Soc.* **1985**, *107*, 1365.
- (70) Linford, M. R.; Chidsey, C. E. D. *J. Am. Chem. Soc.* **1993**, *115*, 12631.
- (71) Linford, M. R.; Fenter, P.; Eisenberger, P. M.; Chidsey, C. E. D. *J. Am. Chem. Soc.* **1995**, *117*, 3145.
- (72) Li, D.; Smith, D. C.; Swanson, B. I.; Barr, J. D.; Paffett, M. T.; Hawley, M. E. *Chem. Mater.* **1992**, *4*, 1047.
- (73) Evans, S. D.; Ulman, A.; Goppert-Berarducci, K. E.; Gerenser, L. J. *J. Am. Chem. Soc.* **1991**, *113*, 5866.
- (74) Bell, C. M.; Keller, S. W.; Lynch, V. M.; Mallouk, T. E. *Mater. Chem. Phys.* **1993**, *35*, 225.
- (75) Bell, C. M.; Arendt, M. F.; Gomez, L.; Schmehl, R. H.; Mallouk, T. E. *J. Am. Chem. Soc.* **1994**, *116*, 8374.
- (76) Ansell, M. A.; Zeppenfeld, A. C.; Yoshimoto, K.; Cogan, E. B.; Page, C. J. *Chem. Mater.* **1996**, *8*, 591.
- (77) (a) Cao, G.; Hong, H.; Mallouk, T. E. *Acc. Chem. Res.* **1992**, *25*, 420. (b) Gao, W.; Dickinson, L.; Grozinger, C.; Morin, F. G.; Reven, L. *Langmuir* **1996**, *12*, 6429. (c) Gao, W.; Dickinson, L.; Morin, F. G.; Reven, L. *Chem. Mater.* **1997**, *9*,

3113.

- (78) Lee, H.; Kepley, L. J.; Hong, H.; Mallouk, T. E. *J. Am. Chem. Soc.* **1988**, *110*, 618.
- (79) Lee, H.; Kepley, L. J.; Hong, H.; Akhter, S.; Mallouk, T. E. *J. Phys. Chem.* **1988**, *92*, 2597.
- (80) Samant, M. G.; Brown, C. A.; Gordon, J.G. II *Langmuir* **1993**, *9*, 1082.
- (81) Smith, E. L.; Porter, M. D. *J. Phys. Chem.* **1993**, *97*, 4421.
- (82) Soundag, A. H. M.; Tol, A. J. W.; Touwslager, F. J. *Langmuir* **1992**, *8*, 1127.
- (83) Tao, Y.; Chang, S.; Ma, L. *J. Chin. Chem. Soc.* **1995**, *42*, 659.
- (84) Folkers, J. P.; Gorman, C. B.; Laibinis, P. E.; Buchholz, S.; Whitesides, G. M.; Nuzzo, R. G. *Langmuir* **1995**, *11*, 813.
- (85) (a) Tarlov, M. J.; Newman, J. G. *Langmuir* **1992**, *7*, 1398. (b) Huang, J.; Hemminger, J. C. *J. Am. Chem. Soc.* **1993**, *115*, 3342.
- (86) Allara, D. L.; Atre, S. V. *J. Am. Chem. Soc.* **1991**, *113*, 1852.
- (87) Snyder, R. G.; Strauss, H. L.; Elliger, C. A. *J. Phys. Chem.* **1982**, *86*, 5145.
- (88) (a) Ju, H.; Leech, D. *Langmuir* **1998**, *14*, 300. (b) Doron, A.; Portnoy, M.; Lion-Dagan, M.; Katz, E.; Willner, I. *J. Am. Chem. Soc.* **1996**, *118*, 8937. (c) Sayre, C. N.; Collard, D. M. *Langmuir* **1995**, *11*, 302. (d) Yip, C. M.; Bard, M. D. *Langmuir* **1994**, *10*, 549. (e) Tarlov, M. J.; Bowden, E. F. *J. Am. Chem. Soc.* **1991**, *113*, 1846.
- (89) (a) Jennings, G.K.; Laibinis, P. E. *J. Am. Chem. Soc.* **1997**, *119*, 5208. (b) Zamborini, F. P.; Campbell, J. K.; Crooks, R. M. *Langmuir* **1998**, *14*, 640.
- (90) (a) Singhvi, R.; Kumar, A.; Lopez, G. P.; Stephanopoulos, G. N.; Wong, D. I. C.; Whitesides, G. M.; Inber, D. E. *Science* **1994**, *264*, 696. (b) DiMilla, P. A.; Folkers, J. P.; Biebuyck, H. A.; Harter, R.; Lopez, G. P.; Whitesides, G. M. *J. Am. Chem. Soc.* **1994**, *116*, 2225. (c) Lopez, G. P.; Albers, M. W.; Schreiber, S. L.; Carroll, R.; Peralta, E.; Whitesides, G. M. *J. Am. Chem. Soc.* **1993**, *115*,

5877.

- (91) (a) Hausling, L.; Ringsdorf, H.; Schmitt, F.; Knoll, W. *Langmuir* **1991**, *7*, 1837.
 (b) Rubin, S.; Chow, J. T.; Ferraris, J. P.; Zawodzinski, T. A. Jr. *Langmuir* **1996**, *12*, 363.
- (92) Delamarche, E.; Michel, B.; Kang, H.; Gerber, Ch. *Langmuir* **1994**, *10*, 4103.
- (93) Sabatani, E.; Cohen-Boulakia, J.; Bruening, M.; Rubinstein, I. *Langmuir* **1993**, *9*, 2974.
- (94) Bryant, M. A.; Joa, S. L.; Pemberton, J.E. *Langmuir* **1992**, *9*, 753.
- (95) Hill, W.; Wehling, B. *J. Phys. Chem.* **1993**, *97*, 9451.
- (96) Li, T. T.; Liu, H. Y.; Weaver, M. J. *J. Am. Chem. Soc.* **1984**, *106*, 1233.
- (97) (a) Cooper, J. M.; Greenough, K. R.; McNeil, C. J. *J. Electroanal. Chem.* **1993**, *347*, 267. (b) Uvdal, K.; Boda, P.; Liedberg, B. *J. Colloid Interface Sci.* **1992**, *149*, 162.
- (98) Ihs, A.; Uvdal, K.; Liedberg, B. *Langmuir* **1993**, *9*, 733.
- (99) Arndt, Th.; Schupp, H.; Schepp, W. *Thin Solid Films* **1989**, *178*, 319.
- (100) Mielczarski, J. A.; Yoon, R. H. *Langmuir* **1991**, *7*, 101.
- (101) Edwards, T. R. G.; Cunnane, V. J.; Parsons, R.; Gani, D. *J. Chem. Soc., Chem. Commun.* **1989**, 1041.
- (102) (a) Arduengo, A. j.; Moran, J. R.; Rodriguez-Paradu, J.; Ward, M. D. *J. Am. Chem. Soc.* **1990**, *112*, 6153. (b) Bharathi, S.; Yegnaraman, V.; Rao, G. D. *Langmuir* **1993**, *9*, 1614.
- (103) Bensebaa, F.; Voicu, R.; Huron, L.; Ellis, T. H. *Langmuir* **1997**, *13*, 5335.
- (104) Netzer, L.; Sagiv, J. *J. Am. Chem. Soc.* **1983**, *105*, 674.
- (105) Chen, S. H.; Frank, C. W. *Langmuir* **1989**, *5*, 978.
- (106) Turro, N. J.; Aikawa, M.; Butcher, J. A. Jr. *J. Am. Chem. Soc.* **1980**, *102*, 5127.
- (107) (a) Bartell, L. S.; Ruch, R. J. *J. Phys. Chem.* **1956**, *60*, 1231. (b) Bartell, L. S.;

- Ruch, R. J. *J. Phys. Chem.* **1959**, *63*, 1045.
- (108) Neumann, A. W.; Good, R. J.; Hope, C. J.; Sejpal, M. *J. Colloid Interface Sci.* **1974**, *49*, 291.
- (109) Shafrin, E. G.; Zisman, W. A. *J. Phys. Chem.* **1962**, *66*, 740.
- (110) Kim, T.; Crooks, R. M.; Tsen, M.; Sun, L. *J. Am. Chem. Soc.* **1995**, *117*, 3963.
- (111) Ulama, A.; Tillman, N. *Langmuir* **1989**, *5*, 1418.
- (112) Mebrahtu, T.; Berry, G. M.; Bravo, B. G.; Michelhaugh, S. L.; Soriaga, M. P. *Langmuir* **1988**, *4*, 1147.
- (113) Chadwick, J. E.; Myles, D. C.; Garrell, R. L. *J. Am. Chem. Soc.* **1993**, *115*, 10364.
- (114) Chang, S.; Chao, I.; Tao, Y. *J. Am. Chem. Soc.* **1994**, *116*, 6792.
- (115) Tour, J. M.; Jone, L. II; Pearson, D. L.; Lamba, J. J. S.; Burgin, T. P.; Whitesides, G. M.; Allara, D. L.; Parikh, A. N.; Atre, S. V. *J. Am. Chem. Soc.* **1995**, *117*, 9529.
- (116) Wells, M.; Dermody, D. L.; Yang, H. C.; Kim, T.; Crooks, R. M.; Ricco, A. J. *Langmuir* **1996**, *12*, 1989.
- (117) Dhirani, A.; Zehner, R. W.; Hsung, R. P.; Guyot-Sionnest, P.; Sita, L. R. *J. Am. Chem. Soc.* **1996**, *118*, 3319.
- (118) Zehner, R. W.; Siata, L. R. *Langmuir* **1997**, *13*, 2973..
- (119) Tao, Y.; Wu, C.; Eu, J.; Lin, W.; Wu, K.; Chen, C. *Langmuir* **1997**, *13*, 4018.
- (120) Li, Y.; Huang, J.; McIver, R. T.; Hemminger, J. C. *J. Am. Chem. Soc.* **1992**, *114*, 2428.
- (121) Tarlov, M. J.; Burgess, D. R. F.; Gillen, G. *J. Am. Chem. Soc.* **1993**, *115*, 5305.
- (122) Huang, J.; Dahlgren, D. A.; Hemminger, J. C. *Langmuir* **1994**, *10*, 626.
- (123) Gui, J. Y.; Stern, D. A.; Frank, D. G.; Lu, F.; Zapien, D. C.; Hubbard, A. T. *Langmuir* **1991**, *7*, 955.

- (124) Kolega, R. R.; Schlenoff, J. B. *Langmuir* **1998**, *14*, 5469.
- (125) Cygan, M. T.; Dunbar, T. D.; Arnold, J. J.; Bumm, L. A.; Shedlock, N. F.; Burgin, T. P.; Jones, L. II; Allara, D. L.; Tour, J. M.; Weiss, P. S. *J. Am. Chem. Soc.* **1998**, *120*, 2721.
- (126) Garg, N.; Lee, T. R. *Langmuir* **1998**, *14*, 3815.
- (127) Sellers, H.; Ulman, A.; Schnidman, Y.; Eilers, J. E. *J. Am. Chem. Soc.* **1993**, *115*, 9389.
- (128) Sun, F.; Castner, D. G.; Grainger, D. W. *Langmuir* **1993**, *9*, 3200.
- (129) Chechik, V.; Schonherr, H.; Vancso, G. J.; Stirling, C. J. M. *Langmuir* **1998**, *14*, 3003.
- (130) Bigelow, W. C.; Pickett, D. L.; Zisman, W. A. *J. Colloid Sci.* **1946**, *1*, 513.
- (131) Brandriss, S.; Margel, S. *Langmuir* **1993**, *9*, 1232.
- (132) (a) Mathauser, K.; Frank, C. W. *Langmuir* **1993**, *9*, 3002. (b) Mathauser, K.; Frank, C. W. *Langmuir* **1993**, *9*, 3446.
- (133) Gun, J.; Sagiv, J. *J. Colloid Interface Sci.* **1984**, *101*, 201.
- (134) Schwartz, D. K.; Steinberg, S.; Israelachvili, J.; Zasadzinski, Z. A. N. *Phys. Rev. Lett.* **1992**, *69*, 3354.
- (135) Rubinstein, I.; Sabatani, E.; Maoz, R.; Sagiv, J. *Electroanal. Chem.* **1987**, *219*, 365.
- (136) Kumar, A.; Abbott, N. L.; Kim, E.; Biebuyck, H. A.; Whitesides, G. M. *Acc. Chem. Res.* **1995**, *28*, 219.
- (137) (a) Regnier, F. E.; Unger, K. K.; Majors, R. E. *J. Chromatogr.* **1991**, 544. (b) Nanrocki, J.; Buszewski, B. *J. Chromatogr. Rev.* **1988**, *449*, 1.
- (138) Ballschmiter, K.; Bacher, R.; Mennel, A.; Fischer, R.; Riehle, U.; Swerev, M. J. *High Resolut. Chromatogr.* **1992**, *15*, 260.
- (139) Ziumermann, R. M.; Schmidt, C. F.; Gaub, H. E. *J. Colloid Interface Sci.* **1990**, *139*, 268.

- (140) Pitt, W. G.; Grasel, T. G.; Cooper, S. L. *Biomaterials* **1988**, 9, 36.
- (141) De Palma, V.; Tillman, N. *Langmuir* **1989**, 5, 868.
- (142) Cave, N. G.; Kinloch, A. J. *Polymer* **1992**, 33, 1162.
- (143) Migler, K. B.; Hervet, H.; Leger, L. *Phys. Rev. Lett.* **1993**, 70, 287.
- (144) Kim, J. H.; Cotton, T. M.; Uphaus, R. A. *J. Phys. Chem.* **1988**, 92, 5575.
- (145) Charych, D. H.; Landau, E. M.; Majda, M. *J. Am. Chem. Soc.* **1991**, 113, 3340.
- (146) Voorhoeve, R. J. H. *Organohalosilanes*; Elsevier: Amsterdam, 1967.
- (147) Hammond, G. S. *J. Am. Chem. Soc.* **1955**, 77, 334.
- (148) Plueddemann, E. P. *Silane Coupling Agents*; Plenum Press: New York, 1991.
- (149) Le Grange, J. D.; Markham, J. L.; Kurkjian, C. R. *Langmuir* **1993**, 9, 1749.
- (150) Angst, D. L.; Simmons, G. W. *Langmuir* **1991**, 7, 2236.
- (151) De Palma, V.; Tillman, N. *Langmuir* **1989**, 5, 970.
- (152) Tripp, C. P.; Hair, M. L. *Langmuir* **1992**, 8, 1120.
- (153) McGovern, M. E.; Kallury, K. M. R.; Thompson, M. *Langmuir* **1994**, 10, 3607.
- (154) Wasserman, S. R.; Whitesides, G. M.; Tidswell, I. M.; Ocko, B. M.; Pershan, P. S.; Axe, J. D. *J. Am. Chem. Soc.* **1989**, 111, 5852.
- (155) Tripp, C. P.; Hair, M. L. *Langmuir* **1995**, 11, 149.
- (156) Gao, W.; Reven, L. *Langmuir* **1995**, 11, 1860.
- (157) Cohen, S. R.; Noaman, R.; Sagiv, J. *J. Phys. Chem.* **1986**, 90, 3054.
- (158) Tidswell, S. R.; Ocko, B. M.; Pershan, P. S.; Wasserman, S. R.; Whitesides, G. M.; Axe, J. D. *Phys. Rev. B* **1990**, 141, 1111.
- (159) Vallant, T.; Brunner, H.; Mayer, U.; Hoffmann, H.; Leitner, T.; Resch, R.; Friedbacher, G. *J. Phys. Chem. B* **1998**, 102, 7190.
- (160) (a) Kurth, D. G.; Bein, T. *Langmuir* **1993**, 9, 2965. (b) Kurth, D. G.; Bein, T. *Langmuir* **1995**, 11, 3061.
- (161) (a) Xiao, X.; Liu, G.; Charych, D. H.; Salmeron, M. *Langmuir* **1995**, 11, 1600. (b) Xiao, X.; Hue, J.; Charych, D. H.; Salmeron, M. *Langmuir* **1996**, 12, 235.

- (162) Bierbaum, K.; Kinzler, M.; Woll, CH.; Grunze, M.; Hahner, G.; Heid, S.; Effeberger, F. *Langmuir* **1995**, *11*, 512.
- (163) Cotton, F. A.; Wilkinson, G. *Advanced Inorganic Chemistry*, 3rd ed.; Wiley: New York, 1972; p.321.
- (164) Zisman, W. A. *Adv. Chem. Ser.* **1964**, *43*, 1.
- (165) Burland, D. M.; Miller, R. D.; Walsh, C. A. *Chem. Rev.* **1994**, *94*, 31.
- (166) (a) Ashwell, G. J.; Jackson, P. D.; Crossland, W. A. *Nature* **1994**, *368*, 438. (b) Penner, T. L.; Matschmann, H. R.; Armstrong, N. J.; Ezenyilimba, M. C.; Williams, D. J. *Nature* **1994**, *367*, 49.
- (167) (a) Li, D.; Ratner, M. A.; Marks, T. J.; Zhang, C.; Yang, J.; Wong, G. K. *J. Am. Chem. Soc.* **1990**, *112*, 7389. (b) Katz, H. E.; Scheller, G.; Putvinski, T. M.; Schilling, M. L.; Wilson, W. L.; Chidsey, C. E. D. *Science* **1991**, *254*, 1485. (c) Katz, H. E.; Wilson, W. L.; Scheller, G. *J. Am. Chem. Soc.* **1994**, *116*, 6636.
- (168) (a) Lin, W.; Lin, W.; Wong, G. K.; Marks, T. J. *J. Am. Chem. Soc.* **1996**, *118*, 8034. (b) Gao, L. H.; Wang, K. Z.; Huang, C. H.; Zhao, X. S.; Xia, X. H.; Li, T. K.; Xu, J. M. *Chem. Mater.* **1995**, *7*, 1047.
- (169) (a) Kakkar, A. K.; Yitzchaik, S.; Roscoe, S. B.; Kubota, F.; Allan, D. S.; Marks, T. J.; Xu, Z.; Lin, W.; Wong, G. K. *Langmuir* **1993**, *9*, 388. (b) Yitzchaik, S.; Roscoe, S. B.; Kakkar, A. K.; Allan, D. S.; Marks, T. J.; Xu, Z.; Zhang, T.; Lin, W.; Wong, G. K. *J. Phys. Chem.* **1993**, *97*, 6958. (c) Roscoe, S. B.; Yitzchaik, S.; Kakkar, A. K.; Marks, T. J.; Lin, W.; Wong, G. K. *Langmuir* **1994**, *10*, 1337.
- (170) Chaudhury, M. K.; Whitesides, G. M. *Science* **1992**, *255*, 1230.
- (171) Chupa, J. A.; Xu, S.; Fishchetti, R. F.; Strongin, R. M.; McCauley, J. P.; Smith, A. B.; Blasie, J. K. *J. Am. Chem. Soc.* **1993**, *115*, 4383.
- (172) Balachander, N.; Sukenik, C. N. *Langmuir* **1990**, *6*, 1621.
- (173) Wasserman, S. R.; Biebuyck, H.; Whitesides, G. M. *J. Mater. Res.* **1989**, *4*, 886.

- (174) Lee, Y. W.; Reed-Mundell, J.; Sukenik, C. N.; Zull, J. E. *Langmuir* **1993**, *9*, 3009.
- (175) Ogawa, K.; Mino, N.; Tamura, H.; Hatada, M. *Langmuir* **1990**, *6*, 1807.
- (176) Paulson, S.; Morris, K.; Sullivan, B. P. *J. Chem. Soc., Chem. Commun.* **1992**, 1615.
- (177) Dressick, W. J.; Dulcey, C. S.; Georger, J. H.; Calvert, J. M. *Chem. Mater.* **1993**, *5*, 148.
- (178) Netzer, L.; Iscovichi, R.; Sagiv, J. *Thin Solid Films* **1983**, *100*, 67.
- (179) Pomerantz, M.; Segmuller, A.; Netzer, L.; Sagiv, J. *Thin Solid Films* **1985**, *132*, 153.
- (180) Collins, R. J.; Bae, I. T.; Sxherson, D. A.; Sukenik, C. N. *Langmuir* **1996**, *12*, 5509.
- (181) Kato, S.; Pac, C. *Langmuir* **1998**, *14*, 2372.
- (182) Evans, S. D.; Sharma, R.; Ulman, A. *Langmuir* **1991**, *7*, 156.
- (183) (a) Dulcey, C. S.; Georger, J. H.; Chen, M. S.; McElvany, S. W.; O'Ferrall, C. E.; Benezra, V. I.; Calvert, J. M. *Langmuir* **1996**, *12*, 1638. (b) Delamarche, E.; Sundarababu, G.; Biebuyck, H.; Michel, B.; Gerber, Ch.; Sigirist, H.; Wolf, H.; Ringsdorf, H.; Xanthopoulos, N.; Mathieu, H. J. *Langmuir* **1996**, *12*, 1997.
- (184) (a) Vermeulen, L. A.; Thompson, M. E. *Nature* **1992**, *358*, 656. (b) Vermeulen, L. A.; Snover, J. L.; Sapochak, L. S.; Thompson, M. E. *J. Am. Chem. Soc.* **1994**, *115*, 11767.
- (185) Yamanaka, S. *Inorg. Chem.* **1976**, *15*, 2811.
- (186) Alberti, G.; Costantino, U.; Allulli, S.; Tomassini, N. J. *Inorg. Nucl. Chem.* **1978**, *40*, 1113.
- (187) (a) Alberti, G. *Solid-State Supramolecular Chemistry: Two- and Three-Dimensional Inorganic Networks*; Alberti, G.; Bein, T.; Eds.; (Vol. 7 of Comprehensive Supramolecular Chemistry; Lehn, J. M., Chairman Ed.); Pergamon Elsevier

- Science: Oxford, 1996. (b) Clearfield, A. *Progr. Inorg. Chem.* **1998**, *47*, 373.
- (188) (a) Alberti, G. *Acc. Chem. Res.* **1978**, *11*, 163. (b) Clearfield, A. *Chem. Rev.* **1988**, *88*, 125. (c) Centi, G.; Trifiro, F.; Ebner, J. R.; Franchetti, V. M. *Chem. Rev.* **1988**, *88*, 55. (d) Rong, D.; Kim, Y. I.; Hong, H. G.; Krueger, J. S.; Mayer, J. E.; Mallouk, T. E. *Coord. Chem. Rev.* **1990**, *97*, 237. (e) Thompson, M. E. *Chem. Mater.* **1994**, *6*, 1168. (f) Vermeulen, L. A.; Thompson, M. E. *Nature* **1992**, *358*, 656. (g) Vermeulen, L. A.; Snover, J. L.; Sapochak, L. S.; Thompson, M. E. *J. Am. Chem. Soc.* **1994**, *115*, 11767.
- (189) Day, D.; Ringsdorf, H. *J. Polym. Sci., Polym. Lett. Ed.* **1978**, *16*, 205.
- (190) Tieke, B.; Lieser, G.; Wegner, G. *J. Polym. Sci.; Polym. Chem. Ed.* **1979**, *17*, 1631.
- (191) Wegner, G. *Z. Naturforsch.* **1969**, *24b*, 824.
- (192) (a) Sells, T.; O'Brien, D. F. *Macromolecules* **1994**, *27*, 226. (b) Lamparski, H.; O'Brien, D. F. *Macromolecules* **1995**, *28*, 1786.
- (193) (a) Charych, D. H.; Nagy, J. O.; Spevak, W.; Bednarski, M. D. *Science* **1993**, *261*, 585. (b) Reichert, A.; Nagy, J. O.; Spevak, W.; Charyck, D. H. *J. Am. Chem. Soc.* **1995**, *117*, 829.
- (194) Wenzel, M.; Atkinson, G. H. *J. Am. Chem. Soc.* **1989**, *111*, 6123.
- (195) (a) Chailapakul, O.; Crooks, R. M. *Langmuir* **1993**, *9*, 884. (b) Sabatani, E.; Rubinstein, I. *J. Phys. Chem.* **1987**, *91*, 6663. (c) Bilewicz, R.; Majda, M. *J. Am. Chem. Soc.* **1991**, *113*, 5464.
- (196) Poirier, G. E.; Tarlov, M. J. *Langmuir* **1994**, *10*, 2853.
- (197) Poirier, G. E.; Tarlov, M. J.; Rushmeier, H. E. *Langmuir* **1994**, *10*, 3383.
- (198) Schneider, T. W.; Buttry, D. A. *J. Am. Chem. Soc.* **1993**, *115*, 12391.
- (199) (a) Chidsey, C. E. D.; Bertozzi, C. R.; Putvinski, T. M.; Majsce, A. M. *J. Am. Chem. Soc.* **1990**, *112*, 4301. (b) Schoer, J. K.; Ross, C. B.; Crooks, R. M.; Corbitt, T. S.; Hampden-Smith, M. J. *Langmuir* **1994**, *10*, 615.

- (200) (a) Li, J.; Liang, K.; Camillone, N.; Leung, T.; Scoles, G. *J. Chem. Phys.* **1995**, *102*, 5012. (b) McCarley, R. L.; Dunaway, D. J.; Willicut, R. J. *Langmuir* **1993**, *9*, 2775.
- (201) Walczak, M. M.; Popenoe, D. D.; Deinhammer, R. S.; Lamp, B. D.; Chung, C.; Porter, M. D. *Langmuir* **1991**, *7*, 2687.
- (202) Kim, T.; Chan, K. C.; Crooks, R. M. *J. Am. Chem. Soc.* **1997**, *119*, 189.
- (203) Porter, M. D. *Anal. Chem.* **1988**, *6*, 1143A.
- (204) Bloor, D.; Chance, R. R. *Polydiacetylenes*; Martinus Nijhogg: Pordrecht, 1985, p363.
- (205) Chan, K. C.; Kim, T.; Schoer, J. K.; Crooks, R. M. *J. Am. Chem. Soc.* **1995**, *117*, 5875.
- (206) Allara, D.L.; Atre, S. V.; Elliger, C. A.; Snyder, R. G. *J. Am. Chem. Soc.* **1991**, *113*, 1852.
- (207) Fessenden, R.; Fessenden, J. S. *Chem. Rev.* **1961**, *61*, 361.
- (208) Jones, K.; Lappert, M. F. *Organotin Compounds, Vol. 2*. Sawyer, A. K., Ed.; Marcel Dekker, Inc.: New York, 1971, p510.
- (209) Van Der Kelen, C. D.; Van Der Berghe, E. V.; Verdonck, L. *Organotin Compounds, Vol. 1*, Sawyer, A. K., Ed.; Marcel Dekker, Inc.: New York, 1971, p96.
- (210) Poller, R. C. *The Chemistry of Organotin Compounds*; Academic Press: New York, 1970, p94.
- (211) (a) Iler, R. K. *The Chemistry of Silicon*; Wiley: New York, 1979. (b) Pintchovski, F.; Pricew, J. B.; Tobin, P. L.; Peavy, J.; Kobold, K. *J. Electrochem. Soc.* **1979**, *126*, 1428.

Chapter Two

Methods for Surface Characterization

In the study of thin films, we are interested in both their surface and bulk properties. The evolution of thin film structures¹⁻³ can be monitored by contact angle goniometry, ellipsometry, FTIR-ATR, X-ray photoelectron and UV-Vis spectroscopies. Contact angles with different liquids, such as water and hexadecane, are measured to evaluate wetting properties, surface energy, and uniformity, and to obtain information on surface order.⁴ Fourier transform infrared (FT-IR) spectroscopy, in the attenuated total reflection (ATR) mode,⁵ is used to determine the identity, molecular packing and orientation of chromophores. Ellipsometry⁶⁻⁷ is used to measure the thickness and uniformity of freshly prepared films. X-ray photoelectron spectroscopy (XPS)⁸ is used to study surface composition and monolayer structure, and UV-Vis spectroscopy⁹ for chromophore identification and estimation of surface coverage. A combination of these techniques provides a useful indication of the quality of the thin films. A brief introduction to these techniques is given below.

2.1 Contact Angle Goniometry

The quality of monolayer and multilayer films can be estimated from contact angle measurements. The shape of a liquid drop on a plane, homogeneous surface is highly dependent on the free energy of both the liquid drop and the surface.⁴ The contact angle is the angle at the contact point on the surface. The contact angle of a liquid is the result of the mechanical equilibrium of a drop on a solid surface under the action of surface tensions, γ_{SV} , γ_{LV} , and γ_{SL} , according to Young's equation:¹⁰

$$\gamma_{LV} \cos\theta = \gamma_{SV} - \gamma_{SL}$$

where, γ is the surface interfacial tension, and LV, SV, and SL refer to liquid-vapor, solid-vapor, and solid-liquid interfaces, respectively.

If there is no interaction between the solid and the liquid (ideal case), the contact angle will be 180° .¹ As the interaction between the solid and liquid increases, the liquid spreads until $\theta = 0^\circ$. Since real surfaces seldom display a true, unique, thermodynamic equilibrium contact angle, a different contact angle is measured when the drop has advanced (θ_a) or receded (θ_r) on the surface prior to measurement.¹ An advancing contact angle is measured using the following steps: while the needle is still in the drop (captive drop), a small volume of liquid is added to the drop, and the contact angle is measured before the boundary of the drop has moved. A similar procedure is employed for measuring receding contact angle: while the needle is in the drop, a fixed volume of liquid is withdrawn, and the contact angle is measured before the boundary of the drop has moved. For easier and more convenient operation, contact angle measurements of a free-standing (sessile) drop are established. However, if the drop is allowed to fall from the needle to the surface, smaller contact angles are usually obtained because of mechanical vibrations.¹ Normally, the contact angles are measured on both sides of the droplet, and a number of readings are collected at different places on the surface, to provide a statistical meaning to the value.

Contact angle goniometry is also dependent on the relative hydrophilicity or hydrophobicity of the thin film surface and the wetting liquid. For example, a clean and unfunctionalized glass surface produces a contact angle of $\sim 18^\circ$ with water. When a non-polar liquid such as hexadecane is deposited onto a hydrophilic surface such as unfunctionalized glass slide, an increase in the forces of repulsion at the solid-liquid interface results in a higher contact angle. Conversely, when hexadecane is deposited onto an organic monolayer, an increase in the forces of attraction results in the lowering of the contact angle. Typical water and hexadecane contact angles on a methyl surface are 110 - 115° and 40 - 45° respectively (Figure 2.1).¹¹ Thus, contact angle goniometry is a sensitive tool to examine surface composition and the structure of organic thin films.

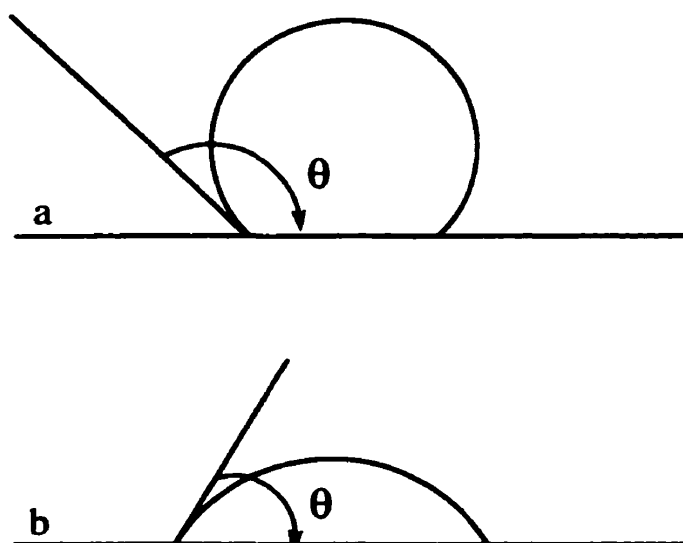


Figure 2.1 (a) A typical water contact angle on a methyl surface, where $\theta = 110 - 115^\circ$, and (b) a typical hexadecane contact angle on a methyl surface, where $\theta = 40 - 45^\circ$.¹

2.2 Fourier Transform Infrared Spectroscopy in the Attenuated Total Reflection Mode (FTIR-ATR)

FT-IR spectroscopy is a common tool for the study of molecular packing and orientation in organic films.⁵ However, a number of problems arise in the case of self-assembled thin films. The intensity of the signal is too weak for measurement since the film is only monomolecularly thick. Thus, FTIR-ATR, has been employed to increase the sensitivity for surface analysis. The intensity of the signal will also be dependent on the coverage, thickness and density of the film. A typical setup for an FTIR-ATR experiment is shown in Figure 2.2.¹ This method makes use of a prism that allows the incoming beam to hit the internal surfaces and then reflect, which occur a number of times before exiting. Such multiple reflections intensify the signal to a reasonable detectable level. The prisms employed are generally made up of silicon, germanium, KRS-5 or ZnSe. Under conditions

of total internal reflection, a decaying evanescent wave appears outside the sides of the prism.² When a thin film of sample is pressed against the crystal with a firm contact, the evanescent wave will penetrate the film approximately a micrometer before reflecting and infrared spectra of the surface region can be obtained. It offers an advantage by limiting the depth region of the surface studied, and not the entire bulk of material. Furthermore, when a polarized light is employed, the orientation of molecular chain in the surface region can be determined.²

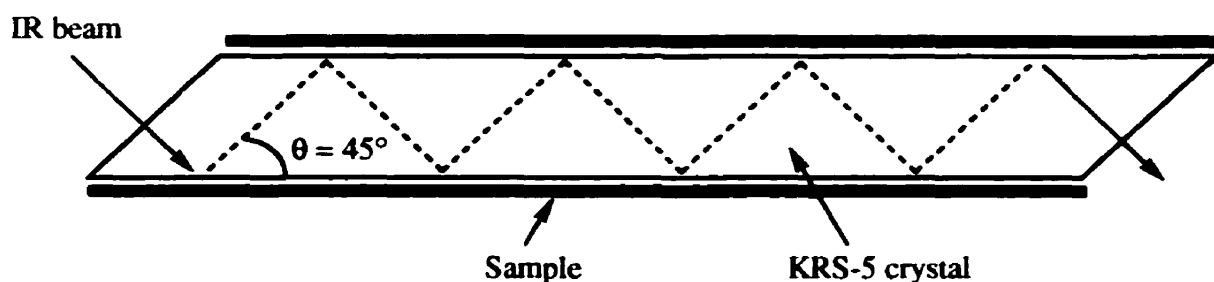


Figure 2.2 A schematic description of an optical setup for ATR measurements.

ATR is a useful tool for the determination of the packing and the crystallinity of organic thin film.¹ The detection of the IR bands depends on the orientation of the molecular chain itself. Vibrations that are parallel to the surface of the crystals are most readily detected due to the polarization of the IR beam. Those perpendicular to the surface are difficult to detect. For example, for alkyl groups that are *trans* molecularly-oriented and perpendicular to the surface, methylene C-H vibrations associated with them will be parallel to the surface. On the other hand, for disordered, *cis* oriented alkyl groups, it is difficult to detect the C-H vibrations which are perpendicular to the surface.

2.3 Ellipsometry

Film thickness can be determined from the ellipsometric parameters using standard classical electromagnetic theory¹² together with a parallel layer model consisting of an air/film/substrate structure. In this model, we assume the system to be reasonably described

as a flat sample consisting of an infinite substrate with a parallel overlayer of thickness (d). All phases are considered to be of homogeneous composition and isotropic, with the optical behavior of each phase being accurately described by a single dielectric function. A more complete description of this approach is given elsewhere,¹³ but specific relevant details are given below. The measured analyzer and polarized angles, A and P , respectively, are related to the complex electric fields of incident and reflected light via the following equations:

$$(E^-/E^+)_p/(E^-/E^+)_s = r_p/r_s \quad (1)$$

$$r_p/r_s = \tan \psi e^{i\Delta} \quad (2)$$

$$\psi = A (\geq 0) \quad (3)$$

$$\Delta = 2P + (\pi/2) \quad (4)$$

The E 's denote the complex electric fields of the incident (+) and reflected (-) light beams of p (parallel to the plane of incidence) and s (perpendicular to the plane of incidence) polarization. The terms r_p and r_s stand for the standard Fresnel coefficients (reflection coefficients) and are functions of both the parameters of $\tan \psi$ (the amplitude ratio) and Δ (the optical phase shift), which are calculated directly from the raw ellipsometry data, and r_p/r_s can be related to the optical properties of the sample.¹⁴ With this approach, it is possible to determine the refractive index of a film. The refractive index of a "clean" substrate acts as a reference value. For the same substrate, but with an overlayer of refractive index (n_f), thickness (d) and n_f can be calculated by numerical iteration techniques. However, errors exist in calculating n_f for monolayer samples which concern the impossibility to routinely obtain reliable values of both n_f and d ; moreover, the actual value of n_f for a close packed monolayer differs only slightly from the bulk material. In principle, ellipsometry can determine both the thickness and the refractive index if the film has a thickness greater than 50 Å.

In a typical ellipsometer (Figure 2.3),¹ monochromatic light (He-Ne laser) is plane polarized, hits the surface, and is then reflected. A compensator changes the latter elliptically polarized reflected beam to plane-polarized. The analyzer then determines the angle of polarization by which the compensator polarized the beam. Practically, one has to estimate the refractive index of the organic film. Usually a value of $n_f = 1.45 - 1.50$ ¹⁵ is used for monolayers of simple alkyl chains of, for example, alkanethiols on gold and alkyltrichlorosilanes on silica.

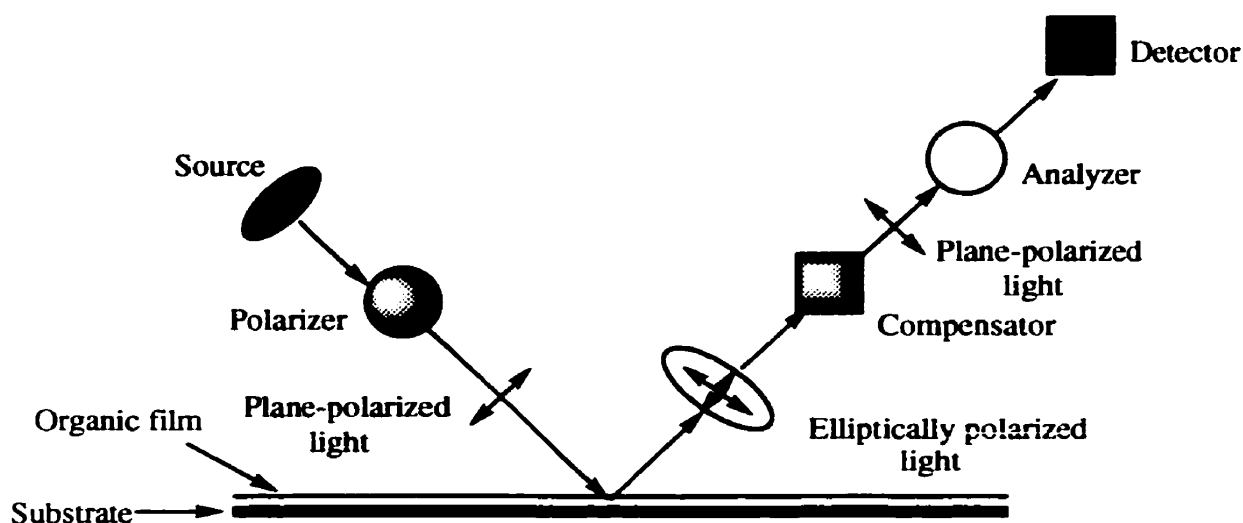


Figure 2.3 A schematic description of an ellipsometer.¹

2.4 X-ray Photoelectron Spectroscopy (XPS)

XPS has been intensively employed for studying chemical composition of organic surfaces. It offers chemists an opportunity to study such interfacial phenomena as wetting, adhesion and friction, and how they relate to the physiochemical parameters of functional groups.⁸ Furthermore, XPS is an essential tool to study the stability of an organic film on a surface by following the surface composition of the film as a function of time.

In an XPS experiment,⁸ a sample is exposed to X-ray radiation and the properties of inner-shell electrons are probed. If E_0 is the energy of the X-ray, and E_j is that of a core electron in the atom (s, p, etc.), $E_0 - E_j$ will be the energy of the ejected electron. Since the

value of E_j is characteristic of an electron in a particular atom, the determination of E_j provides atomic identification. Surface composition can also be determined quantitatively because the number of electrons ejected is proportional to the number of atoms present. Chemical state information can often be determined by measuring the small shifts ("chemical shifts") in E_j . Special techniques are employed, owing to the small depths of photoelectrons, in order to stress on the contribution from atoms in different depth positions in a film. For example, a grazing electron takeoff geometry emphasizes the contribution from surface atoms, and a study of photoelectron spectroscopy as a function of the takeoff angle provides an excellent way to study compositional depth distribution in a film.¹⁶

2.5 UV-Vis Spectroscopy

Chromophores (with π electron delocalization) give high optical absorption in the UV-Vis region. Using the Beer-Lambert law $A = \epsilon \cdot l \cdot c$, (where A stands for the absorbance, ϵ , l , and c the extinction coefficient, the thickness of film, and the concentration of the chromophores within the film, respectively), we can calculate the surface coverage, $d_{\text{surf}} = A \cdot \epsilon^{-1}$ (mol/cm^2).⁹ Assuming that the extinction coefficient of the chromophore in solution is the same as that of the film, it provides an estimation of the surface coverage. The UV-Vis spectra are collected from a quartz slide functionalized on both sides. Therefore, to calculate surface coverage, absorbance is divided by 2 to obtain the value for each individual monolayer. Quartz slides are chosen as the substrate because it does not absorb in the UV region as glass does.

2.6 References

- (1) Ulman, A. *An Introduction to Ultrathin Organic Films from Langmuir-Blodgett to Self-Assembly*; Academic Press: Boston, 1991.
- (2) Ulman, A. *Characterization of Organic Thin Films*; Butterworth-Heinemann: Boston, 1995.
- (3) Barraud, A.; Vandevyver, M. *Growth and Characterization of Organic Thin Films (Langmuir-Blodgett Films) in Nonlinear Optical Properties of Organic Molecules and Crystals, Vol. 1*; Chemla, D. S.; Zyss, J., Ed.; Academic Press: Orlando, 1987.
- (4) Fowkes, F. M. *Contact Angle, Wettability and Adhesion*, Advances in Chemistry Series 43; American Chemical Society: Washington, D. C., 1964.
- (5) Bubeck, C.; Holtkamp, D. *Adv. Mater.* **1991**, 3, 32.
- (6) McMarr, P. J.; Vedam, K. *J. Appl. Phys.* **1986**, 59, 694.
- (7) Flory, F. R. *Thin Films for Optical Systems*; M. Mekker: New York, 1995.
- (8) Nefedov, V. I. *X-ray Photoelectron Spectroscopy of Solid Surfaces*; VSP: Utrecht, 1988.
- (9) Li, D.; Swanson, B. I.; Robinson, J. M.; Hoffbauer, M. A. *J. Am. Chem. Soc.* **1993**, 115, 6975.
- (10) Young, T. *Miscellaneous Works*; Peacock, G., Ed.; Murray: London, 1855, Vol. 1.
- (11) Sagiv, J. *J. Am. Chem. Soc.* **1980**, 102, 92.
- (12) Azzam, R. M. A.; Bashara, N. M. *Ellipsometry and Polarized Light*; North-Holland: Amsterdam, 1977.
- (13) Allara, D. L.; Nuzzo, R. G. *Langmuir* **1985**, 1, 52.
- (14) Aspnes, D. E. *Optical Properties of Solids*; Seraphin, B. O., Ed.; North-Holland: Amsterdam, 1975.
- (15) Wasserman, S. R.; Whitesides, G. M.; Tidswell, I. M.; Ocko, B. M.; Pershan, P. S.; Axe, J. D. *J. Am. Chem. Soc.* **1989**, 111, 5852.
- (16) Tillman, N.; Ulman, A.; Elman, J. *Langmuir* **1990**, 6, 1512.

Chapter Three

A Novel Route to Efficient Inorganic Oxide Surface Modifications *via* Simple Acid-Base Hydrolytic Chemistry

3.1 Introduction

Robust and highly ordered two-dimensional thin film assemblies, incorporating organic molecules of a diverse nature, represent materials with potential applications in areas such as photonics, sensors and heterogenized homogeneous catalysis.¹ Manipulating the cooperative forces which cause molecular self-assembly and dictate the spatial and energetic aspects in the resulting thin films is a challenging task. Fabrication of ultrathin films on solid substrates via molecular self-assembly requires molecules with suitable end groups to effect surface anchoring by covalent bond formation.^{1a} Traditional molecular self-assembly routes include alkyltrichlorosilanes on Si/SiO₂,² alkanethiols on gold³, silver,⁴ and copper⁵ and carboxylic acids⁶ on silver, copper and aluminum oxides. These methodologies are end-group/substrate dependent. For example, thiols adsorb onto gold;⁷ the adsorption of carboxylic acids on metal oxide surfaces is weak;⁸ and although alkyltrichlorosilanes adsorb strongly on inorganic oxide surfaces, it is difficult to synthesize a number of silane coupling agents with desired backbone structures. We have developed an alternative approach to molecular assembly on inorganic oxides using simple acid-base hydrolytic chemistry.⁹⁻¹⁰ This new approach employs commercially available or easily synthesized reagents, leading to the formation of surface-anchored-NEt₂ moieties, which can react with a variety of organic compounds with terminal acidic groups. Using this simple acid-base hydrolysis route, the surfaces of inorganic oxides such as glass, quartz and single-crystal silicon containing hydroxyl groups that are acidic in nature,¹¹ can easily

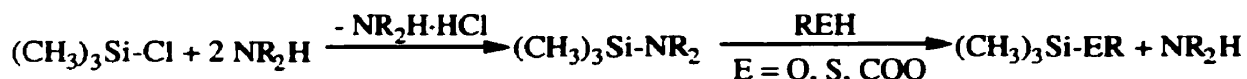
be converted into surface-anchored- NEt_2 moieties upon reacting with $\text{Si}(\text{NEt}_2)_4$ or $\text{Sn}(\text{NEt}_2)_4$. Treatment of the surface-anchored- NEt_2 moieties with several organic molecules containing terminal acidic protons, including rigid-rod alkynes, via acid-base hydrolysis, can lead to densely packed molecularly self-assembled monolayers.

3.2 Acid-Base Hydrolysis

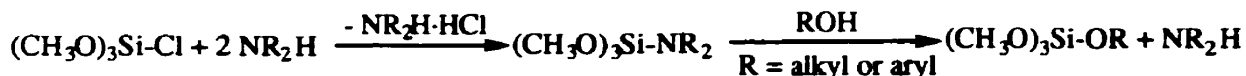
The chemistry of organosilicon-¹² and organotin-nitrogen¹³ ($\text{Me}_3\text{E}-\text{NR}'_2$, $\text{E} = \text{Si}, \text{Sn}$; $\text{R}' = \text{CH}_3, \text{C}_2\text{H}_5$) compounds towards various protic species including alcohols, thiols, carboxylic acids, cyclopentadiene, indene, phosphines and terminal alkynes, has been well documented. Because of the lower metal-to-nitrogen bond strength, and higher basicity of nitrogen in stannylamines than the corresponding aminosilanes, the $\text{Sn}-\text{N}$ bond in the former complexes can be more easily cleaved by a variety of protic species.¹³

The formation of $\text{Si}-\text{N}$ bond is extremely facile. When we treated a solution of $\text{Me}_3\text{Si}-\text{Cl}$ in diethylether with excess diethylamine, a white solid ($\text{NEt}_2\text{H}\cdot\text{HCl}$) was precipitated upon contact, at room temperature. The resulting $\text{Me}_3\text{Si}-\text{NEt}_2$ compound reacted with one mole equivalent of REH ($\text{R} = \text{alkyl or aryl}$; $\text{EH} = \text{OH}, \text{SH}, \text{COOH}$) yielding the corresponding $\text{Me}_3\text{Si}-\text{ER}$ compounds almost quantitatively (Equation 3.1).¹² According to the pK_a values of various protic species as shown in Table 1.4, $-\text{OH}$ is more acidic than $-\text{C}\equiv\text{CH}$. Thus, $\text{Me}_3\text{Si}-\text{NEt}_2$ reacts with one mole of equivalent of $\text{HC}\equiv\text{C}-(\text{CH}_2)_n-\text{OH}$ (e.g., $n = 1, 2, 3, 4$) to give $\text{Me}_3\text{Si}-\text{O}-(\text{CH}_2)_n-\text{C}\equiv\text{CH}$ quantitatively. In a similar way, $(\text{CH}_3\text{O})_3\text{Si}-\text{NEt}_2$, which was prepared by reacting $(\text{CH}_3\text{O})_3\text{Si}-\text{Cl}$ with diethylamine, reacted with one mole equivalent of ROH (e.g., $\text{ROH} = \text{CH}_3(\text{CH}_2)_{15}-\text{OH}$, $\text{HC}\equiv\text{C}-(\text{CH}_2)_2-\text{OH}$, $\text{HC}\equiv\text{C}-(\text{CH}_2)_4-\text{OH}$ and $\text{C}_6\text{H}_5-\text{C}\equiv\text{C}-\text{C}_6\text{H}_4-\text{OH}$) to give the corresponding $(\text{CH}_3\text{O})_3\text{Si}-\text{OR}$ (Equation 3.2).¹²

Equation 3.1



Equation 3.2

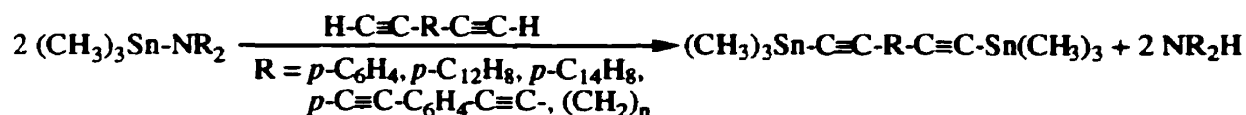


The $\text{Me}_3\text{Sn-NR}'_2$ ($\text{R}' = \text{CH}_3, \text{C}_2\text{H}_5$) compounds are conveniently prepared from $\text{Me}_3\text{Sn-Cl}$ with LiNR'_2 ($\text{R}' = \text{CH}_3, \text{C}_2\text{H}_5$) and easily react with ROH , RSH , RCOOH ($\text{R} =$ alkyl or aryl group), cyclopentadiene ($\text{C}_5\text{H}_5\text{H}$), indene ($\text{C}_9\text{H}_7\text{H}$), Ph_2PH , and alkynes (e.g., $\text{C}_6\text{H}_5\text{-C}\equiv\text{CH}$, $\text{CH}_3(\text{CH}_2)_{15}\text{-C}\equiv\text{CH}$) via acid-base hydrolysis to give $(\text{CH}_3)_3\text{Sn-OR}$, -SR , -OC(O)R , $\text{-C}_5\text{H}_5$, $\text{-C}_9\text{H}_7$, Ph_2P , $\text{-C}\equiv\text{C-C}_6\text{H}_5$ and $\text{-C}\equiv\text{C-(CH}_2)_{15}\text{CH}_3$ respectively in quantitative yields (Equation 3.3).¹³ Similarly, the reaction of two equivalents of $(\text{CH}_3)_3\text{Sn-NR}_2$ with $\text{H-C}\equiv\text{C-R-C}\equiv\text{C-H}$ ($\text{R} = p\text{-C}_6\text{H}_4$, $p\text{-C}_6\text{H}_4\text{-C}_6\text{H}_4$, $p\text{-C}_{14}\text{H}_8$, $\text{-C}\equiv\text{C-C}_6\text{H}_4\text{-C}\equiv\text{C-}$ and $(\text{CH}_2)_n$, $n = 2, 4, 5$ and 6), yields the corresponding trimethyltin substituted alkynes with the elimination of diethylamine (Equation 3.4).¹³

Equation 3.3



Equation 3.4



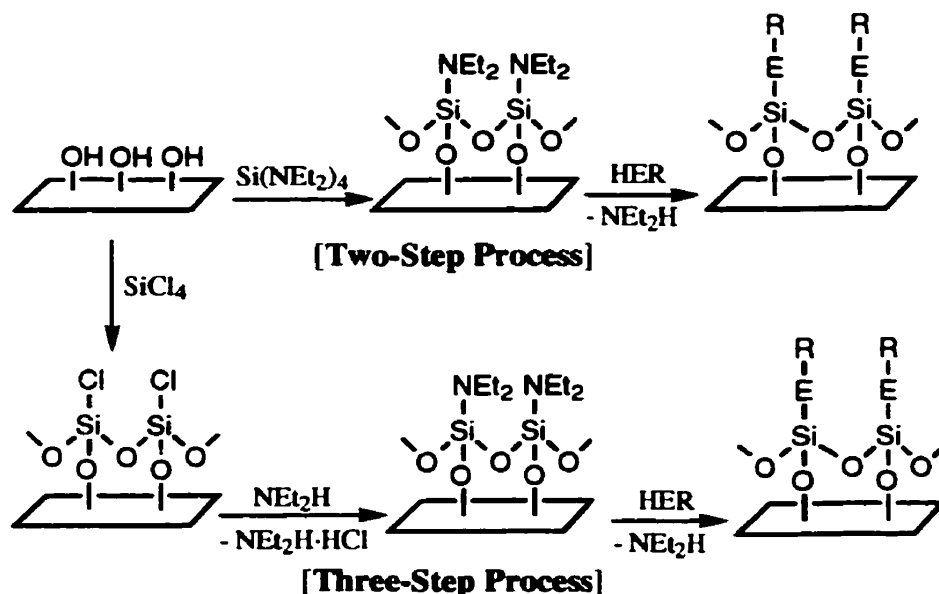
3.3 Surface Functionalization

As discussed above, the surfaces of inorganic oxides such as silica, glass and quartz are acidic in nature, and contain surface hydroxyl groups.¹¹ Thus the acid-base hydrolytic chemistry described above can be easily applied to these surfaces to construct SAMs for a variety of organic molecules with terminal acidic protons.

3.3.1 Si-NEt₂ Approach

The surface functionalization was carried out by two different strategies (Scheme 3.1): one is called “two-step process”; and the other a “three-step process”. In the two-step process, Si(NEt₂)₄, prepared¹⁴ and isolated by reacting SiCl₄ with NEt₂H, was reacted with clean substrates and then with the desired protic species (REH). In the three-step process, clean substrates were first functionalized with SiCl₄ followed by NEt₂H to prepare surface anchored-NEt₂ moieties which then reacted with the desired REH.

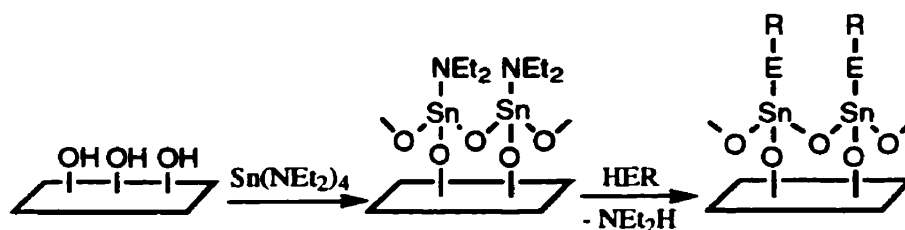
Scheme 3.1 Si-NEt₂ approach to surface functionalization



3.3.2 Sn-NEt₂ Approach

The reaction of SnCl₄ directly with amines does not lead to the formation of aminostannanes.¹⁵ However, the reaction of R'₃SnCl with REH in the presence of amines (NR''₂H) does lead to the formation of R'₃SnR with the elimination of NR''₂H·HCl.¹⁵ In this study, only a two-step Sn-NEt₂ approach is applied for the surface functionalization (Scheme 3.2). Sn(NEt₂)₄, prepared¹⁵ and isolated from the reaction between SnCl₄ and LiNEt₂, was used to functionalize the surface of clean substrates with a SnNEt₂ layer, and then reacted with the desired protic species (REH).

Scheme 3.2 Sn-NEt₂ approach to surface functionalization



3.4 Optimization of Deposition Conditions

The deposition of E(NEt₂)₄ (E = Si, Sn) on silica leading to a monolayer of [Si]-O-E-NEt₂ depends on the chemical reactions between E(NEt₂)₄ and the hydroxyl groups on the silica surface. The physical factors including water content in the system, temperature, nature of solvent, concentration of adsorbates, and reaction time which affect these reactions, had to be optimized in order to produce high-quality and densely packed thin films.

Due to the high reactivity of E(NEt₂)₄ towards water, the NEt₂-functionalized surface of Si/SiO₂ is also expected to be highly sensitive to moisture. However, a molar amount of water is required to form a polymeric network on the surface. Excess physisorbed water in the system was removed by (i) putting the clean substrates in an oven at ~150 °C before deposition, (ii) using dry solvent, and (iii) performing thin film deposition under nitrogen

in a self-assembly apparatus. When either a wet solvent or a wet substrate was employed, a thick white film on the surface was observed, since too much water gives rise to multilayered polymerized siloxane ($-\text{Si}-\text{O}-\text{Si}-$) or stannoxane ($-\text{Sn}-\text{O}-\text{Sn}-$) structures. This is consistent with the earlier studies¹⁶⁻¹⁷ of OTS deposition on Si/SiO_2 in which excess water results in facile polymerization in solution and polysiloxane deposition of the surface.

Temperature is another important parameter¹⁷ because it can affect the rate of deposition as well as the rate of polymerization of $\text{E}(\text{NEt}_2)_4$ in solution. It was found that a high temperature favors polymerization of ECl_4 and $\text{E}(\text{NEt}_2)_4$, and gives rise to turbidity in solution and a thick layer of siloxane or stannoxane on surface. Therefore, room temperature is sufficient for the silanation/stannation process. However, 70-80 °C is preferred for amination of Cl-functionalized surfaces to give surface-anchored- NEt_2 moieties and to remove the byproduct of $\text{NEt}_2\text{H}\cdot\text{HCl}$ from surface, which is soluble in hot toluene (three-step process: Schemes 3.1). Owing to the difference in reactivity of a variety of protic species towards NEt_2 -functionalized surfaces, and the fact that reaction on the surface is more retarded than that in solution due to steric effects, an optimized temperature of 70-80 °C was found to be ideal for alkynyl thin film deposition, and 40-60 °C for alcohol, thiol and acid film deposition.

As mentioned above, a wide range of temperatures is preferred for deposition of various protic species. Since toluene has a comparatively high boiling point, it satisfies the temperature requirement. In addition, since $\text{E}(\text{NEt}_2)_4$ and a number of alkyl and aromatic protic species are soluble in it, dry toluene was chosen as the solvent for thin film deposition. In the case of more polar protic species such as diols, dry THF was preferred since they are highly soluble in THF.

Concentration of adsorbates is another parameter to be considered since too much $\text{E}(\text{NEt}_2)_4$ can result in polymerization leading to thick layers of siloxane or stannoxane on the surface. According to published reports,¹⁸ a 2" diameter surface of standard Si/SiO_2 substrate contains $\sim 10^{16}$ OH groups. The concentration of ECl_4 , $\text{E}(\text{NEt}_2)_4$, or RH (protic

species) we employed was 0.1-0.5 % solution by volume (or weight), which is comparable to the concentration²⁻⁵ for OTS (or thiol) deposition, and is in excess for complete monolayer conversion.

Finally, reaction time can also affect the quality of thin films in such a way that insufficient time would lead to an incomplete monolayer, detected by surface wettability measurements and ellipsometry. However, excessive time could result in polymerization in the solvent and introduce a thick film of siloxane or stannoxane at the surface. Using octadecanol and $\text{Si}(\text{NEt}_2)_4$ as a model, the time effect on two-step silanation was examined. The data is presented in Table 3.1 and Figures 3.1 and 3.2.

Table 3.1. The effect of silanation time on surface properties ($\text{CA}_{\text{H}_2\text{O}}$ and T_e) of octadecanol thin films using a two-step process^a

Silanation Time, min	$\text{CA}_{\text{H}_2\text{O}}, ^\circ$	$T_e, \text{\AA}$
2	80	10
10	80	12
30	90	14
60 (1 h)	100	18
120 (2 h)	105	20
240 (4 h)	110	23
480 (8 h)	110	25
1080 (18 h)	110	50
2160 (36 h)	115	>100

^a Parameters for thin film deposition: concentration of $\text{Si}(\text{NEt}_2)_4$, 0.5% by volume; concentration of octadecanol, 0.1% by weight; temperature for silanation, rt.; temperature and reaction time for octadecanol deposition, 50 °C and 24 h, respectively. $\text{CA}_{\text{H}_2\text{O}}$ = contact angle with water in degrees; T_e = ellipsometric thickness in Å.

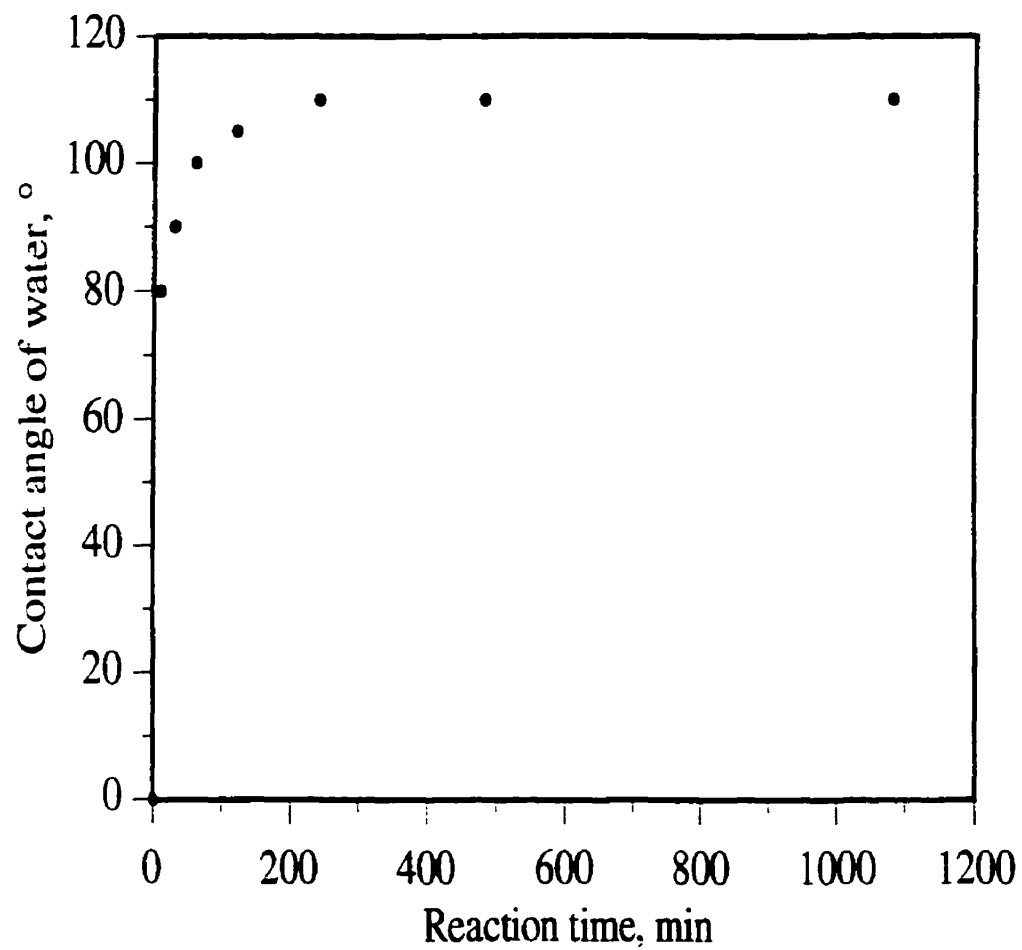


Figure 3.1. The effect of silanation time on contact angles of water of octadecanol thin films using a two-step process.

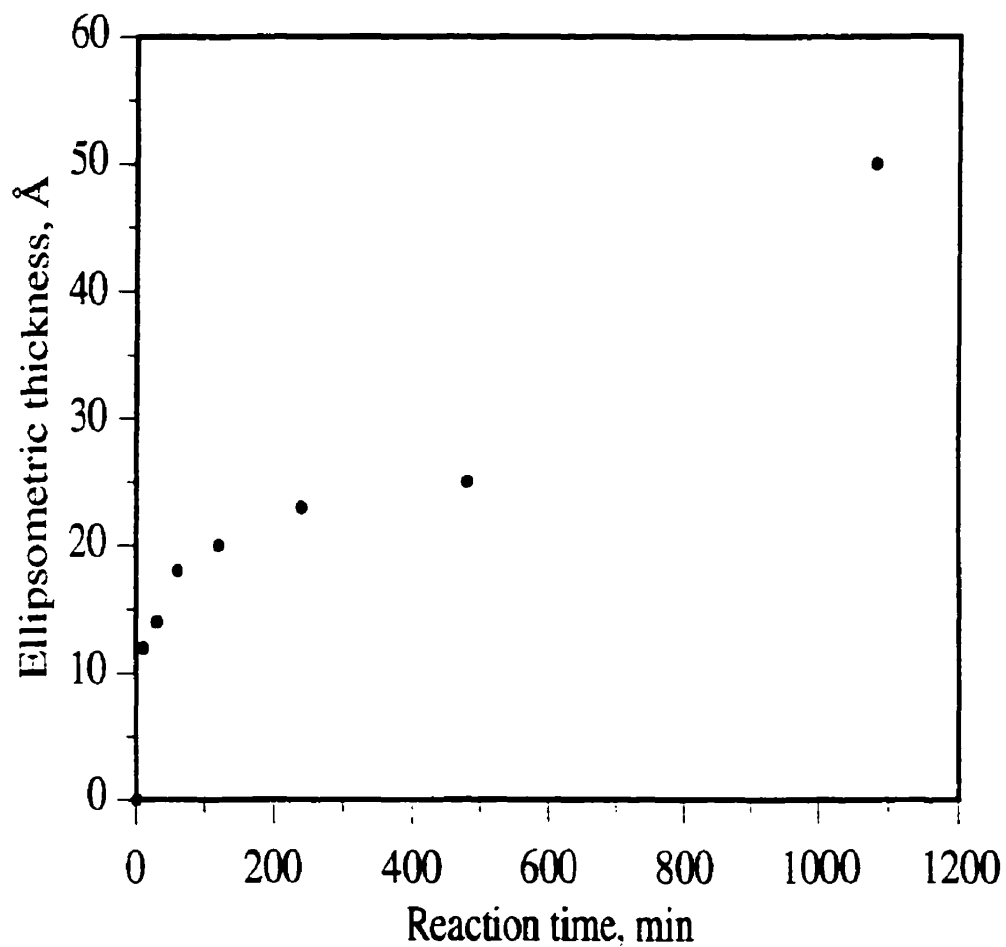


Figure 3.2. The effect of silanation time on ellipsometric thickness of octadecanol thin films using a two-step process.

The formation of a good-quality and densely packed monolayer of octadecanol on Si/SiO₂ should result in a water contact angle of $\sim 110^\circ$ and thickness of 27 Å.¹⁹ Both data for contact angle of water and ellipsometry indicated that incomplete monolayer formation resulted below 4 h and polymerization occurred above 8 h. Therefore, 8 h is optimal for silanation process, resulting in a thin film of octadecanol on Si/SiO₂ with water contact angle of 110° and ellipsometric thickness of ~ 25 Å. In the same way, the optimum time for deposition of Sn(NEt₂)₄ on Si/SiO₂, and its further reaction with the protic species was found to be 8 h and 24 h, respectively. In the latter case, incomplete monolayer formation was observed below 18 h, while any increase in time period beyond 24 h did not result in improved quality of the thin films.

3.5 Surface Properties of Thin Films

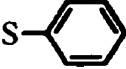
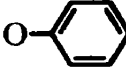
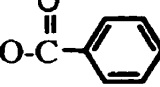
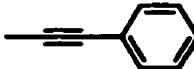


The generality of the new simple acid-base hydrolytic chemistry approach to molecular self-assembly under optimal conditions was examined using surface wettability and ellipsometric thicknesses of the thin films of a variety of chromophores on Si/SiO₂. Contact angle goniometry and ellipsometry were used to determine the hydrophobicity and the thickness of the thin films, respectively. These two methods together provide a complementary means of comparing the surface coverage in the newly formed thin films.

An investigation of the wetting characteristics of thin films was carried out by measuring static contact angles of deionized water on monolayer surfaces. The data presented in Table 3.2 is consistent with wetting characteristics of thin films:^{1a} clean Si(100) (Si/SiO₂) surface, 15° ; and E-R, $80-85^\circ$ (E = Si or Sn) for R = aryl or alkynyl, and $100-110^\circ$ for R = alkyl. The lower contact angles of water on the acetylene terminated surfaces ($80-82^\circ$) than the corresponding long alkyl chains (paraffins, $\sim 110^\circ$) may be caused by the fact that CH groups (sp character) adhere more strongly to water than CH₃ (sp³) groups.¹⁰ Similarly, potential factors responsible for the lower contact angles of water

on the phenyl terminated surfaces include (i) interactions between water and the π -clouds of the benzene rings,²⁰ and (ii) disorder in the aromatic monolayer assembly.²¹ The long alkyl chains also help to shield the water molecules from the polar surface of Si/SiO₂.²² When a long chain of alkyl groups (e.g. -(CH₂)₁₇-CH₃) is inserted into the backbone, the type of bonding at the surface: Si-S, Si-O, and Si-O-C(O) groups, also effects the wetting behavior of these thin films. On Si-NEt₂ functionalized surface, a thin film of octadecanol gave a higher contact angle of water (110°) than those of octadecanethiol and octadecanoic acid (100°), suggesting that the thin film of octadecanol is more ordered, and/or it has a higher coverage on surface than those of octadecanethiol and octadecanoic acid. It is probably attributable to the difference in binding geometry and/or binding strength of hydroxylate, thiolate and carboxylate on the surface of silica.²³ Similarly, on Sn-NEt₂ functionalized surface, a thin film of octadecanol gave a higher water contact angle (105°) than those of octadecanethiol and octadecanoic acid (95°).

Measurement of the thickness of thin films by ellipsometry was made by assuming a refractive index of the organic film of 1.46 which is comparable to literature values²⁴ of OTS film on silica (1.45-1.50). A detailed calculation of film thickness by ellipsometry has been reported elsewhere.²⁴⁻²⁵ The thickness of both functionalized and non-functionalized substrates were measured to determine the monolayer thickness. Calculation of the theoretical thicknesses was based on typical values²⁶ of bond lengths between elements projected on the surface. As shown in Table 3.2, the measured thicknesses, which are comparable to the theoretical values, suggest the formation of a densely packed monolayer for each sample with a tilt to normal. However, for thiols and carboxylic acids, they have a much smaller measured thickness than the theoretical value, suggesting that they are more tilted and/or they have a lower coverage on surface. A full characterization of the surface properties of SAMs of alcohols and alkynes on silica surfaces is presented in the following chapters.

Table 3.2. Static contact angles of water (CA_{H_2O}), ellipsometric (T_e) and theoretical thicknesses (T_t) for monolayers (Schemes 3.1 and 3.2) on Si(100) substrates

R Group on the Substrate	E = Si		E = Sn	
	$CA_{H_2O}, ^\circ$	$T_e (T_t), \text{\AA}$	$CA_{H_2O}, ^\circ$	$T_e (T_t), \text{\AA}$
	85	7 (10)	85	7 (11)
	85	7 (9)	83	7 (10)
	83	7 (10)	83	6 (11)
$S-(CH_2)_{17}-CH_3$	100	23 (28)	95	23 (29)
$O-(CH_2)_{17}-CH_3$	110	25 (27)	105	25 (28)
$O-C(O)-(CH_2)_{16}-CH_3$	100	20 (27)	95	21 (28)
			80	10 (11)
			80	12 (13)
			82	17 (18)

3.6 Conclusion

The acid-base hydrolysis of surface bound silyl- or stannylamines, obtained using commercially available or easily synthesized $E(NEt_2)_4$ ($E = Si, Sn$), is a general and promising approach to the functionalization of inorganic oxide surfaces, leading to the formation of densely packed thin films of a number of compounds with terminal acidic

protons. Using a two-step route, $\text{E}(\text{NEt}_2)_4$ was allowed to first react with hydroxyl groups of the inorganic oxide surfaces to produce surface-anchored NEt_2 moieties which further react with a variety of organic chromophores with terminal acidic protons. The reaction conditions were optimized for the formation of a relatively densely packed thin film via the two-step process: (1) for silanation/stannation reaction, an ideal concentration of amino-silane or -stannane solution was 0.5% by volume; reaction time, 8 h at room temperature; and (2) for the deposition of compounds with terminal acidic protons, the best concentration of reagents was found to be 0.1% by volume or weight; reaction time, 24 h at 40-60 °C for alcohols, thiols and carboxylic acids, and 70-80 °C for alkynes. A detailed investigation of the structural and physical properties of the alcohols and alkynes on Si/SiO_2 , and further synthetic elaboration to multilayered structures, will be discussed in Chapters 4-6.

3.7 Experimental Section

3.7.1 Materials

Silicon tetrachloride, tin(IV) chloride, *p*-methylthiophenol, thiophenol, phenol, benzoic acid, 1-octadecanethiol, 1-hexadecanol, 1-octadecanol, octadecanoic acid, cyclopentadiene, indene, diphenylphosphine, phenylacetylene, 1,8-nonadiyne, 2-propyn-1-ol, 3-butyne-1-ol and 5-hexyn-1-ol were purchased from Aldrich and used as received. 4-Pentyn-1-ol, 1,5-hexadiyne, 1,7-octadiyne, 1,9-decadiyne and octadec-1-yne were purchased from ChemSamp and used as received. $\text{Si}(\text{NEt}_2)_4$ was prepared¹⁴ from SiCl_4 and excess NEt_2H . $\text{Sn}(\text{NEt}_2)_4$ was prepared¹⁵ from SnCl_4 and LiNEt_2 . Other rigid-rod alkynes, $\text{H}-\text{C}\equiv\text{C}-\text{R}-\text{C}\equiv\text{C}-\text{H}$ ($\text{R} = p\text{-C}_6\text{H}_4$, $p\text{-C}_6\text{H}_4\text{-C}_6\text{H}_4$, $p\text{-C}_{14}\text{H}_8$ and $p\text{-C}\equiv\text{C}-\text{C}_6\text{H}_4\text{-C}\equiv\text{C}-$), employed in this study were conveniently prepared using literature procedures.²⁷ $\text{HOC}_6\text{H}_4\text{C}\equiv\text{CC}_6\text{H}_5$ was synthesized by modifications of published procedures.²⁸ Toluene was distilled over sodium. Diethylamine was distilled over KOH. The substrates were placed in a plastic carousel fitted with a magnetic stir-bar at the bottom. Thin film

depositions were performed under nitrogen in a self-assembly apparatus similar in design to a Schlenk flask but with a flat bottom.

3.7.2 Substrate Preparation

The glass, quartz or Si wafers were cleaned by (i) soaking in soap solution and sonicating for 1 h; (ii) repeated washings with deionized water; (iii) treatment with a solution mixture containing 70% conc. H_2SO_4 and 30% H_2O_2 (piranha solution) at 100 °C for 1 h. *Caution:* Piranha solution is highly explosive, and care should be taken while using this mixture; (iv) repeated washing with deionized water; and (v) finally heating in oven at 150 °C for 5 min and vacuum drying for 5 min to removed physisorbed water before taking into a nitrogen dry box.

3.7.3 Si- NEt_2 Approach to Surface Functionalization

Clean silica surfaces can be functionalized with protic species by following either two-step or three-step process.

3.7.3.1 Two-Step Deposition Process

The clean substrates were treated with (i) 0.5% solution by volume of $\text{Si}(\text{NEt}_2)_4$, which can be conveniently prepared¹⁴ by the reaction of SiCl_4 and excess dry NEt_2H , in dry toluene for 8 h at room temperature, followed by (ii) REH in dry toluene at 40-60 °C for 24 h after sonicating in dry toluene for 5 min to remove excess $\text{Si}(\text{NEt}_2)_4$ physisorbed on the surface. After thorough washing with toluene, the substrates were dried at 120 °C for 5 min.

3.7.3.2 Three-Step Deposition Process

The clean substrates were treated with (i) 0.5% solution by volume of SiCl_4 in dry toluene for 18 h at room temperature followed by sonicating in dry toluene for 5 min to remove excess SiCl_4 physisorbed on the surface, (ii) 0.5% solution by volume of dry NEt_2H in dry toluene for 18 h at 70 °C, followed by (iii) REH in dry toluene at 40-60 °C for 24 h after sonicating in dry toluene for 5 min to remove excess NEt_2H physisorbed on the surface. After thorough washing with toluene, the substrates were dried at 120 °C for 5 min.

3.7.4 Sn- NEt_2 Approach to Surface Functionalization

Similarly, clean silica surfaces can be functionalized with protic species by the following two-step process. The clean substrates were treated with (i) 0.5% solution by volume of $\text{Sn}(\text{NEt}_2)_4$, which can be conveniently prepared¹⁵ by the reaction of SnCl_4 and LiNEt_2 , in dry toluene for 8 h at room temperature, followed by (ii) REH in dry toluene at 70-80 °C for 24 h after sonicating in dry toluene for 5 min to remove excess $\text{Sn}(\text{NEt}_2)_4$ on the surface. After thorough washing with toluene, the substrates were dried at 120 °C for 5 min.

3.7.5 Contact-Angle ($\text{CA}_{\text{H}_2\text{O}}$) Measurements

The static and advancing contact angles were measured with a Rame-Hart NRL 100 goniometer. On average, 8 drops of water were measured on different areas of the polished side of a silicon wafer for each sample, and the values reported are the mean values with a maximum range of $\pm 2^\circ$. The advancing contact angles of captive drops were found to be roughly 5° above the static values of sessile (free-standing) drops. If the drop was allowed to fall from the needle of the syringe to the surface, smaller contact angles were usually obtained because of the mechanical vibrations.^{1a}

3.7.6 Ellipsometry

A Gaertner Scientific ellipsometer operating with a 633 nm He-Ne laser ($\lambda = 6328 \text{ \AA}$) was employed. The angle of incidence was 70° , and the compensator was set at 45° . All reported values with a maximum range of $\pm 2 \text{ \AA}$ are the average of at least six measurements taken at different locations on the sample. The thickness was calculated by comparing data from the same substrate before and after functionalization, and using a value of 1.46 for the refractive index. This value is based on the assumption that the monolayer is similar to bulk paraffins with a refractive index of 1.45.²⁴ If the monolayer is more crystalline-like, similar to polyethylene, the refractive index thus should be within 1.49-1.55.^{1a} It was found that an increase of 0.1 in the refractive index from 1.45 to 1.55 resulted in a decrease in the measured thickness by $\sim 2 \text{ \AA}$.

$\text{N}(\text{CH}_2\text{CH}_3)_2\text{H}\cdot\text{HCl}$: ^1H NMR (270 MHz, CDCl_3) δ 1.41 (t, $J = 7.3 \text{ Hz}$, 6H, CH_3), 2.97 (q, $J = 7.3 \text{ Hz}$, 4H, CH_2), 9.44 (b, s, $\text{H}\cdot\text{HCl}$); Mass Spec. (EI): 110.

$\text{Si}(\text{NEt}_2)_4$: ^1H NMR (200 MHz, C_6D_6) δ 0.95 (t, $J = 7.0 \text{ Hz}$, 24H, CH_3), 2.90 (q, $J = 7.0 \text{ Hz}$, 16H, CH_2); Mass Spec. (EI) 316.

$\text{Sn}(\text{NEt}_2)_4$: ^1H NMR (200 MHz, C_6D_6) δ 1.16 (t, $J = 7.0 \text{ Hz}$, 24H, CH_3), 3.16 (q, $J = 7.0 \text{ Hz}$, 16H, CH_2); Mass Spec. (EI) 407.

$(\text{CH}_3)_3\text{Si}\cdot\text{N}(\text{CH}_2\text{CH}_3)_2$: ^1H NMR (270 MHz, C_6D_6) δ 0.11 (s, 9H, $(\text{CH}_3)_3\text{Si}$), 0.96 (t, $J = 7.0 \text{ Hz}$, 6H, CH_3), 2.76 (q, $J = 7.0 \text{ Hz}$, 4H, CH_2); Mass Spec. (EI): 145.

$\text{C}_6\text{H}_5\cdot\text{O}\cdot\text{Si}(\text{CH}_3)_3$: ^1H NMR (270 MHz, CDCl_3) δ 0.30 (s, 9H, CH_3), 7.17, 7.54 (m, 5H, C_6H_5); Mass Spec. (EI) 166.

$\text{C}_6\text{H}_5\text{-C(O)O-Si(CH}_3)_3$: $^1\text{H NMR}$ (270 MHz, CDCl_3) δ 0.32 (s, 9H, CH_3), 7.33, 8.01 (m, 5H, C_6H_5); Mass Spec. (EI) 194.

$\text{CH}_3\text{-C}_6\text{H}_4\text{-S-Si(CH}_3)_3$: $^1\text{H NMR}$ (270 MHz, CDCl_3) δ 0.18 (s, 9H, $(\text{CH}_3)_3\text{Si}$), 2.23 (s, 3H, CH_3), 7.00, 7.29 (m, 4H, C_6H_4); Mass Spec. (EI) 196.

$\text{CH}_3(\text{CH}_2)_{17}\text{-O-Si(CH}_3)_3$: $^1\text{H NMR}$ (200 MHz, C_6D_6) δ 0.15 (s, 9H, $(\text{CH}_3)_3\text{Si}$), 0.94 (t, $J = 6.1$ Hz, 3H, CH_3), 1.35 (m, 30H, CH_2), 1.60 (m, 2H, CH_2), 3.57 (t, $J = 6.3$ Hz, 2H, CH_2); Mass Spec. (EI) 342.

$\text{CH}_3(\text{CH}_2)_{17}\text{-S-Si(CH}_3)_3$: $^1\text{H NMR}$ (200 MHz, C_6D_6) δ 0.16 (s, 9H, $(\text{CH}_3)_3\text{Si}$), 0.92 (t, $J = 6.2$ Hz, 3H, CH_3), 1.25 (m, 30H, CH_2), 1.61 (m, 2H, CH_2), 2.46 (t, $J = 6.2$ Hz, 2H, CH_2); Mass Spec (EI) 358.

$\text{CH}_3(\text{CH}_2)_{16}\text{-C(O)O-Si(CH}_3)_3$: $^1\text{H NMR}$ (200 MHz, C_6D_6) δ 0.14 (s, 9H, $(\text{CH}_3)_3\text{Si}$), 0.94 (t, $J = 6.0$ Hz, 3H, CH_3), 1.34 (m, 28H, CH_2), 1.87 (m, 2H, CH_2), 2.50 (t, $J = 6.3$ Hz, 2H, CH_2); Mass Spec. (EI) 356.

$(\text{CH}_3)_3\text{Si-O-(CH}_2)_4\text{-C}\equiv\text{CH}$: $^1\text{H NMR}$ (200 MHz, C_6D_6) δ 0.11 (s, 9H, CH_3), 1.79 (t, $J = 2.6$ Hz, 1H, $\text{C}\equiv\text{CH}$), 1.51 (m, 4H, CH_2), 1.98 (m, 2H, CH_2), 3.42 (t, $J = 6.0$ Hz, 2H, CH_2); Mass Spec. (EI) 170.

$(\text{CH}_3)_3\text{Si-O-(CH}_2)_3\text{-C}\equiv\text{CH}$: $^1\text{H NMR}$ (200 MHz, C_6D_6) δ 0.11 (s, 9H, CH_3), 1.78 (t, $J = 2.6$ Hz, 1H, $\text{C}\equiv\text{CH}$), 1.58 (m, 2H, CH_2), 2.15 (m, 2H, CH_2), 3.51 (t, $J = 6.0$ Hz, 2H, CH_2); Mass Spec. (EI) 156.

$(\text{CH}_3)_3\text{Si-O-(CH}_2)_2\text{-C}\equiv\text{CH}$: $^1\text{H NMR}$ (200 MHz, C_6D_6) δ 0.11 (s, 9H, CH_3), 1.77 (t, $J = 2.5$ Hz, 1H, $\text{C}\equiv\text{CH}$), 2.27 (m, 2H, CH_2), 3.55 (t, $J = 7.0$ Hz, 2H, CH_2); Mass Spec. (EI) 142.

$(\text{CH}_3)_3\text{Si-O-CH}_2\text{-C}\equiv\text{CH}$: ^1H NMR (200 MHz, C_6D_6) δ 0.10 (s, 9H, CH_3), 2.04 (t, J = 2.2 Hz, 1H, $\text{C}\equiv\text{CH}$), 4.07 (d, J = 2.4 Hz, 2H, CH_2); Mass Spec. (EI) 128.

$(\text{CH}_3\text{O})_3\text{Si-O-(CH}_2)_{15}\text{CH}_3$: ^1H NMR (200 MHz, C_6D_6) δ 3.54 (s, 9H, OCH_3), 1.01 (t, J = 7.2 Hz, 3H, CH_3), 1.34 (m, 26H, CH_2), 1.65 (m, 2H, CH_2), 3.89 (t, J = 6.4 Hz, 2H, CH_2); Mass Spec. (EI) 362.

$(\text{CH}_3)_3\text{Sn-N(CH}_3)_2$: ^1H NMR (270 MHz, C_6D_6) δ 0.09 (s, 9H, $(\text{CH}_3)_3\text{Sn}$), 2.74 (s, 6H, CH_3); Mass Spec. (EI) 208.

$\text{CH}_3(\text{CH}_2)_{17}\text{-O-Sn(CH}_3)_3$: ^1H NMR (200 MHz, C_6D_6) δ 0.25 (s, 9H, $(\text{CH}_3)_3\text{Sn}$), 0.93 (t, J = 6.4 Hz, 3H, CH_3), 1.35 (m, 32H, CH_2), 3.38 (t, J = 6.4 Hz, 2H, CH_2); Mass Spec. (EI) 433.

$\text{CH}_3(\text{CH}_2)_{17}\text{-S-Sn(CH}_3)_3$: ^1H NMR (200 MHz, C_6D_6) δ 0.28 (s, 9H, $(\text{CH}_3)_3\text{Sn}$), 0.91 (t, J = 6.6 Hz, 3H, CH_3), 1.34 (m, 32H, CH_2), 2.18 (t, J = 6.9 Hz, 2H, CH_2); Mass Spec. (EI) 449.

$(\text{CH}_3)_3\text{Sn-C}_5\text{H}_4\text{H}$: ^1H NMR (270 MHz, C_6D_6) δ 0.24 (s, 9H, CH_3), 2.22 (s, 1H, H), 5.50, 6.07 (m, 4H, C_5H_4); Mass Spec. (EI) 229.

$(\text{CH}_3)_3\text{Sn-C}_9\text{H}_6\text{H}$: ^1H NMR (270 MHz, C_6D_6) δ 0.24 (s, 9H, CH_3), 3.05 (s, 1H, H), 6.26, 6.75, 7.17, 7.31 (m, 6H, C_9H_6); Mass Spec. (EI) 279.

$\text{C}_6\text{H}_5\text{-C}\equiv\text{C-Sn(CH}_3)_3$: ^1H NMR (270 MHz, C_6D_6) δ 0.22 (s, 9H, CH_3), 6.78, 7.28 (m, 5H, C_6H_5); Mass Spec. (EI) 265.

$\text{CH}_3(\text{CH}_2)_{15}\text{-C}\equiv\text{C-Sn(CH}_3)_3$: ^1H NMR (200 MHz, C_6D_6) δ 0.25 (s, 9H, $(\text{CH}_3)_3\text{Sn}$), 0.93 (t, J = 6.3 Hz, 3H, CH_3), 1.34 (m, 28H, CH_2), 2.20 (t, J = 6.4 Hz, 2H, CH_2); Mass Spec. (EI) 413.

$(\text{CH}_3)_3\text{Sn}-\text{C}\equiv\text{C}-(\text{CH}_2)_2-\text{C}\equiv\text{C}-\text{Sn}(\text{CH}_3)_3$: ^1H NMR (200 MHz, C_6D_6) δ 0.16 (s, 18H, CH_3), 2.41 (s, 4H, CH_2); Mass Spec. (EI) 403.

$(\text{CH}_3)_3\text{Sn}-\text{C}\equiv\text{C}-(\text{CH}_2)_4-\text{C}\equiv\text{C}-\text{Sn}(\text{CH}_3)_3$: ^1H NMR (200 MHz, C_6D_6) δ 0.17 (s, 18H, CH_3), 1.58 (t, $J = 6.0$ Hz, 4H, CH_2), 2.13 (t, $J = 5.6$ Hz, 4H, CH_2); Mass Spec. (EI) 431.

$(\text{CH}_3)_3\text{Sn}-\text{C}\equiv\text{C}-(\text{CH}_2)_5-\text{C}\equiv\text{C}-\text{Sn}(\text{CH}_3)_3$: ^1H NMR (200 MHz, C_6D_6) δ 0.19 (s, 18H, CH_3), 1.40 (m, 6H, CH_2), 2.12 (t, $J = 5.5$ Hz, 4H, CH_2); Mass Spec. (EI) 445.

$(\text{CH}_3)_3\text{Sn}-\text{C}\equiv\text{C}-(\text{CH}_2)_6-\text{C}\equiv\text{C}-\text{Sn}(\text{CH}_3)_3$: ^1H NMR (200 MHz, C_6D_6) δ 0.19 (s, 18H, CH_3), 1.25 (t, $J = 4.6$ Hz, 4H, CH_2), 1.40 (m, 4H, CH_2), 2.14 (t, $J = 4.8$ Hz, 4H, CH_2); Mass Spec. (EI) 459.

$\text{HC}\equiv\text{C}-\text{C}_6\text{H}_4-\text{C}\equiv\text{CH}$: ^1H NMR (200 MHz, CDCl_3) δ 3.17 (s, 2H, $\text{C}\equiv\text{CH}$), 7.45 (s, 4H, C_6H_4); Mass Spec. (EI) 126; IR (KBr) ν_{ph} : 3040, 1494, $\nu_{\text{C}\equiv\text{CH}}$: 3263, $\nu_{\text{C}\equiv\text{C}}$: 2103.

$\text{HC}\equiv\text{C}-\text{C}_{12}\text{H}_9-\text{C}\equiv\text{CH}$: ^1H NMR (200 MHz, CDCl_3) δ 3.14 (s, 2H, $\text{C}\equiv\text{CH}$), 7.55 (s, 8H, C_{12}H_9); Mass Spec. (EI) 202; IR (KBr) ν_{ph} : 3034, 1488, $\nu_{\text{C}\equiv\text{CH}}$: 3272, $\nu_{\text{C}\equiv\text{C}}$: 2105.

$\text{HC}\equiv\text{C}-\text{C}_{14}\text{H}_9-\text{C}\equiv\text{CH}$: ^1H NMR (200 MHz, CDCl_3) δ 3.56 (s, 2H, $\text{C}\equiv\text{CH}$), 7.62, 8.62 (m, 8H, C_{14}H_9); Mass Spec. (EI) 226; IR (KBr) ν_{ph} : 3058, 1593, $\nu_{\text{C}\equiv\text{CH}}$: 3281, $\nu_{\text{C}\equiv\text{C}}$: 2093.

$\text{HC}\equiv\text{C}-\text{C}\equiv\text{C}-\text{C}_6\text{H}_4-\text{C}\equiv\text{C}-\text{C}\equiv\text{CH}$: ^1H NMR (200 MHz, CDCl_3) δ 2.48 (s, 2H, $\text{C}\equiv\text{CH}$), 7.39 (s, 4H, C_6H_4); Mass Spec. (EI) 174; IR (KBr) ν_{ph} : 3063, 3041, 1493, $\nu_{\text{C}\equiv\text{CH}}$: 3275, $\nu_{\text{C}\equiv\text{C}}$: 2191.

$\text{C}_6\text{H}_5\text{-C}\equiv\text{C-C}_6\text{H}_4\text{-OH}$: ^1H NMR (200 MHz, CDCl_3) δ 6.82, 7.34 (m, 5H, C_6H_5), 7.44, 7.51 (m, 4H, C_6H_4), 1.90 (s, br, OH); Mass Spec. (EI) 194; IR (KBr) ν_{ph} : 3076, 3053, 3018, 1512, ν_{OH} : 3419, $\nu_{\text{C}\equiv\text{C}}$: 2221.

$(\text{CH}_3)_3\text{-Sn-C}\equiv\text{C-C}_6\text{H}_4\text{-C}\equiv\text{C-Sn}(\text{CH}_3)_3$: ^1H NMR (200 MHz, CDCl_3) δ 0.36 (s, 18H, CH_3), 7.37 (s, 4H, C_6H_4); Mass Spec. (EI) 451; IR (KBr) ν_{ph} : 3042, 1490, $\nu_{\text{C-H}}$: 2963, 2920, $\nu_{\text{C}\equiv\text{C}}$: 2130.

$(\text{CH}_3)_3\text{-Sn-C}\equiv\text{C-C}_{12}\text{H}_8\text{-C}\equiv\text{C-Sn}(\text{CH}_3)_3$: ^1H NMR (200 MHz, C_6D_6) δ 0.28 (s, 18H, CH_3), 7.07, 7.43 (d, $J = 8.5$ Hz, 8H, C_{12}H_8); Mass Spec. (EI) 527; IR (KBr) ν_{ph} : 3034, 1488, $\nu_{\text{C-H}}$: 2985, 2916, $\nu_{\text{C}\equiv\text{C}}$: 2135.

$(\text{CH}_3)_3\text{-Sn-C}\equiv\text{C-C}_{14}\text{H}_8\text{-C}\equiv\text{C-Sn}(\text{CH}_3)_3$: ^1H NMR (200 MHz, C_6D_6) δ 0.32 (s, 18H, CH_3), 7.32, 8.98 (m, 8H, C_{14}H_8); Mass Spec. (EI) 551; IR (KBr) ν_{ph} : 3076, 3060, 3040, 1518, $\nu_{\text{C-H}}$: 2961, 2899, $\nu_{\text{C}\equiv\text{C}}$: 2147.

$(\text{CH}_3)_3\text{-Sn-C}\equiv\text{C-C}\equiv\text{C-C}_6\text{H}_4\text{-C}\equiv\text{C-C}\equiv\text{C-Sn}(\text{CH}_3)_3$: ^1H NMR (200 MHz, C_6D_6) δ 0.42 (s, 18H, CH_3), 7.35 (s, 4H, C_6H_4); Mass Spec. (EI) 499; IR (KBr) ν_{ph} : 3079, 1549, $\nu_{\text{C-H}}$: 2963, 2923, 2855, $\nu_{\text{C}\equiv\text{C}}$: 2203.

$(\text{CH}_3\text{O})_3\text{Si-N}(\text{CH}_2\text{CH}_3)_2$: ^1H NMR (200 MHz, C_6D_6) δ 1.01 (t, $J = 7.2$ Hz, 6H, CH_3), 2.46 (q, $J = 7.2$ Hz, 4H, CH_2), 3.49 (s, 9H, OCH_3); Mass Spec. (EI): 193; IR (CCl_4) $\nu_{\text{C-H}}$: 2967, 2942, 2868, 2841 cm^{-1} , $\nu_{\text{Si-O}}$: 1080 cm^{-1} .

$(\text{CH}_3\text{O})_3\text{Si-O-(CH}_2)_4\text{-C}\equiv\text{CH}$: ^1H NMR (200 MHz, CDCl_3) δ 3.59 (s, 9H, OCH_3), 1.95 (t, $J = 2.0$ Hz, 1H, $\text{C}\equiv\text{CH}$), 1.65 (m, 4H, CH_2), 2.23 (m, 2H, CH_2), 3.82 (t, $J = 5.5$

Hz, 2H, CH₂); Mass Spec. (EI) 218; IR (CCl₄) $\nu_{\text{C-H}}$: 2964, 2944, 2869, 2843 cm⁻¹, $\nu_{\text{C=C}}$: 2119, $\nu_{\text{Si-O}}$: 1086 cm⁻¹.

(CH₃O)₃Si-O-(CH₂)₂-C≡CH: ¹H NMR (200 MHz, CDCl₃) δ 3.60 (s, 9H, OCH₃), 1.98 (t, J = 2.7 Hz, 1H, C≡CH), 2.48 (m, 2H, CH₂), 3.90 (t, J = 6.9 Hz, 2H, CH₂); Mass Spec. (EI) 190; IR (CCl₄) $\nu_{\text{C-H}}$: 2965, 2945, 2844 cm⁻¹, $\nu_{\text{C=C}}$: 2124, $\nu_{\text{Si-O}}$: 1088 cm⁻¹.

(CH₃O)₃-Si-O-C₆H₄-C≡C-C₆H₅: ¹H NMR (200 MHz, CDCl₃) δ 3.49 (s, 9H, OCH₃), 6.88, 7.31 (m, 5H, C₆H₅), 7.39, 7.47 (m, 4H, C₆H₄); Mass Spec. (EI) 314; IR (KBr) ν_{ph} : 3037, 1512 cm⁻¹, $\nu_{\text{C-H}}$: 2947, 2846 cm⁻¹, $\nu_{\text{C=C}}$: 2218, $\nu_{\text{Si-O}}$: 1098 cm⁻¹.

3.8 References

- (1) (a) Ulman, A. *An Introduction to Ultrathin Organic Films. from Langmuir-Blodgett to Self-Assembly*; Academic Press: Boston, 1991. (b) Jackman, R. J.; Wilbur, J. L.; Whitesides, G. M. *Science* **1995**, 269, 664. (c) Chidsey, C. E. D. *Science* **1991**, 251, 919.
- (2) Sagiv, J. *J. Am. Chem. Soc.* **1980**, 102, 92.
- (3) Bain, C. D.; Troughton, E. B.; Tao, Y.; Evall, J.; Whitesides, G. M.; Nuzzo, R. G. *J. Am. Chem. Soc.* **1989**, 111, 321.
- (4) Walczak, M. M.; Chung, C.; Stole, S. M.; Widrig, C. A.; Porter, M. D. *J. Am. Chem. Soc.* **1991**, 113, 2370.
- (5) Laibinis, P. E.; Whitesides, G. M.; Allara, D. L.; Tao, Y.; Parikh, A. N.; Nuzzo, R. G. *J. Am. Chem. Soc.* **1991**, 113, 7152.
- (6) Tao, Y. *J. Am. Chem. Soc.* **1993**, 115, 4350.
- (7) Folkers, J. P.; Gorman, C. B.; Laibinis, P. E.; Buchholz, S.; Whitesides, G. M.; Nuzzo, R. G. *Langmuir* **1995**, 11, 813.

- (8) (a) Allara, D. L.; Nuzzo, R. G. *Langmuir* **1985**, *1*, 45. (b) Allara, D. L.; Nuzzo, R. G. *Langmuir* **1985**, *1*, 52.
- (9) (a) Yam, C. M.; Tong, S. S. Y.; Kakkar, A. K. *Langmuir* **1998**, *14*, 6941. (b) Yam, C. M.; Kakkar, A. K. *Langmuir* **1999**, in press.
- (10) (a) Yam, C. M.; Dickie, A.; Malkhasian, A.; Kakkar, A. K.; Whitehead, M. A. *Can. J. Chem.* **1998**, *76*, 1766. (b) Yam, C. M.; Kakkar, A. K. *J. Chem. Soc., Chem. Commun.* **1995**, 907.
- (11) (a) Iler, R. K. *The Chemistry of Silica*; Wiley: New York, 1979. (b) Pintchovski, F.; Pricew, J. B.; Tobin, P. L.; Peavy, J.; Kobold, K. *J. Electrochem. Soc.* **1979**, *126*, 1428.
- (12) Fessenden, R.; Fessenden, J. S. *Chem. Rev.* **1961**, *61*, 361.
- (13) Jones, K.; Lappert, M. F. In *Organotin Compounds*, Vol. 2, Sawyer, A. K. Ed.; Marcell Dekker: New York, 1977, 510.
- (14) Anderson, H. H. *J. Am. Chem. Soc.* **1952**, *74*, 1421.
- (15) Thomas, I. M. *Can. J. Chem.* **1961**, *39*, 1386.
- (16) (a) Brandriss, S.; Margel, S. *Langmuir* **1993**, *9*, 1232. (b) Tripp, C. P.; Hair, M. L. *Langmuir* **1995**, *11*, 149.
- (17) Silberzan, P.; Leger, L.; Ausserre, D.; Benattar, J. J. *Langmuir* **1991**, *7*, 1647.
- (18) Porter, M. D.; Bright, T. B.; Allara, D. L.; Chidsey, C. E. D. *J. Am. Chem. Soc.* **1987**, *109*, 3559.
- (19) Tillman, N.; Ulman, A.; Schildkraut, J. S.; Penner, T. L. *J. Am. Chem. Soc.* **1988**, *110*, 6136.
- (20) Fowkes, F. M. *Adv. Chem. Ser.* **1964**, *43*, 99.
- (21) Miller, W. J.; Abbott, N. L. *Langmuir* **1997**, *13*, 7114.
- (22) Adam, N. K. *Contact Angle, Wettability and Adhesion*, Advances in Chemistry Series, ACS, 1964, vol. 43, p.52.
- (23) Tao, Y. *J. Am. Chem. Soc.* **1993**, *115*, 4350.

- (24) Wasserman, S. R.; Whitesides, G. M.; Tidswell, I. M.; Ocko, B. M.; Pershan, P. S.; Axe, J. D. *J. Am. Chem. Soc.* **1989**, *111*, 5852.
- (25) Azzam, R. M. A.; Bashara, N. M. *Ellipsometry and Polarized Light*; North-Holland: Amsterdam, 1977.
- (26) Dean, J. A. *Lange's Handbook of Chemistry*; McGraw-Hill: New York, 1992.
- (27) (a) Lewis, J.; Khan, M. S.; Kakkar, A. K.; Johnson, B. F. G.; Marder, T. B.; Fyfe, H. B.; Wittmann, F.; Friend, R. H.; Dray, A. E. *J. Organomet. Chem.* **1992**, *425*, 165. (b) Jiang, J.; Kobayashi, E.; Aoshima, S. *Polym. J.* **1990**, *22*, 274. (c) Takahashi, S.; Kuroyama, Y.; Sonogashira, K.; Hagihara, N. *Synthesis Commun.*, **1980**, 627.
- (28) Wityak, J.; Chan, J. B. *Synthetic Commun.* **1991**, *21*, 977.

Chapter Four

Links between Material Presented in Chapters Five to Seven

Chapters **5-7** are written based on the following manuscripts.

Chapter **5**: Yam, C. M.; Tong, S. S. Y.; Kakkar, A. K. *Langmuir* **1998**, *14*, 6941-6947.

Chapter **6**: Yam, C. M.; Kakkar, A. K. *Langmuir* **1999**, in press.

Chapter **7**: Yam, C. M.; Kakkar, A. K. *Langmuir* **1999**, submitted.

Chapter **5** describes the molecular self-assembly of a series of alcohol compounds terminated with alkyl, phenyl and acetylene groups on Si/SiO₂ surfaces using the acid-base hydrolytic chemistry approach which was discussed in Chapter **4**. The two-step process based on the reaction of Si(NEt₂)₄ with surface hydroxyl groups followed by the reaction with ROH is compared with the three-step methodology involving the reaction of surface hydroxyl groups with SiCl₄, NEt₂H and ROH, in sequence. The former is found to be more efficient than the three-step process. The two-step thin film construction method, is then elaborated using dihydroxy chromophores containing acetylene, diacetylene and aromatic backbone structures to fabricate mono- and multilayered interfaces, as discussed in Chapter **6**.

Thin films containing chromophores with exclusive π -conjugation in the backbone offer significant potential in the fabrication of electronic and photonic based devices. In Chapter **7**, construction of mono- and multilayered thin films on Si/SiO₂ based on the reaction of surface anchored Sn-NEt₂ groups, which are much more basic than Si-NEt₂, with acetylenes, is reported. Such thin films help to examine the role of intermolecular π - π interactions exclusively in molecular self-assembly.

Chapter Five

Simple Acid-Base Hydrolytic Chemistry Approach to Molecular Self-Assembly: Thin Films of Long Chain Alcohols Terminated with Alkyl, Phenyl, and Acetylene Groups on Inorganic Oxide Surfaces

5.1 Introduction

“Molecular self-assembly” constitutes a prominent area of research due to its potential applications in the fabrication of materials with novel properties.¹ Self-assembled monolayers (SAMs) can provide the desired molecular level control, and offer an attractive route to molecular engineering of solid state devices.²⁻³ Much of the current emphasis has been placed on the preparation and characterization of the long alkane chain assemblies, since these studies are fundamental to the understanding of the self-organization phenomenon. Some of the common methodologies employed in the preparation of the “first-generation” self-organized thin films include chlorosilanes on silica surfaces,⁴ alkanethiols on gold,⁵⁻⁶ silver⁷ and copper,⁸ dialkyl sulfides on gold,⁹ dialkyl disulfides on gold,¹⁰ carboxylic acids on aluminum oxide and silver,¹¹ and 1-alkenes on hydrogen terminated Si(111).¹² The combination of spontaneous adsorption, strong molecule-substrate and van der Waals interactions, leads to highly ordered and densely packed monolayers using the above mentioned routes.

Hydroxylated silica based surfaces such as glass, quartz and single crystal silicon are of great technological importance.¹³ However, fabrication of thin film assemblies incorporating chromophores with desired functional groups via traditional molecular self-

assembly routes requires molecules with suitable end-groups to affect surface anchoring by covalent bond formation. Difficulties exist in synthesizing chromophores with appropriate end-group functionalities. We have developed a new and versatile approach to molecular self-assembly based on the hydrolysis of surface-anchored aminosilanes with organic chromophores containing acidic end-groups.¹⁴ Using this simple acid-base hydrolysis route, silica surfaces such as glass, quartz and single crystal Si can be easily modified. In addition, the advantage of using acid-base hydrolytic chemistry for molecular self-assembly is the ability to incorporate a variety of functionalities on a single substrate. In this chapter, we discuss molecular self-assembly of long alkane chain alcohols containing terminal alkyl, phenyl and acetylene moieties on inorganic oxide surfaces, and compare a two-step thin film construction process involving the reaction of $\text{Si}(\text{NEt}_2)_4$ with surface hydroxyl groups followed by the reaction with ROH, with the three-step sequence using SiCl_4 , NEt_2H and ROH. A detailed characterization of the resulting SAMs using surface wettability measurements, FTIR-ATR, ellipsometry and X-ray photoelectron spectroscopy (XPS) etc., indicates that the two-step process produces monolayers that are more densely packed and ordered than the three-step process. The long chain alkane SAMs prepared using our new two-step acid-base hydrolytic approach are of similar quality as those prepared from traditional surface functionalization routes.

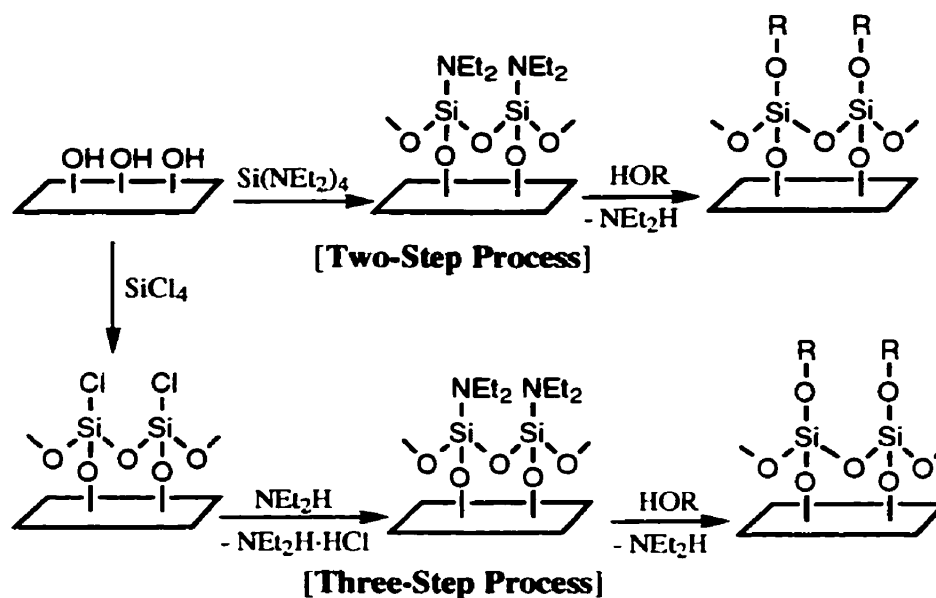
5.2 Acid-Base Hydrolysis

The chemistry of organosilicon-amines ($\text{R}'_3\text{Si-NR}''_2$, $\text{R}' = \text{Me, OMe}$, $\text{R}'' = \text{Me, Et}$) towards hydrolysis has been well documented.¹⁵ The formation of Si-N bond is extremely facile. For example, the reaction of $\text{R}'_3\text{Si-Cl}$ in diethylether with excess diethylamine at room temperature gives $\text{R}'_3\text{Si-NEt}_2$ in a quantitative yield. The resulting aminosilane, $\text{R}'_3\text{Si-NEt}_2$, reacts with 1 mol equiv. of ROH to give the corresponding silylated alcohol, $\text{R}'_3\text{Si-OR}$. We were intrigued by the behavior of the surface-immobilized NEt_2 moiety towards R-OH leading to surface modifications based on this simple acid-base hydrolysis.

5.3 Surface Functionalization

The surface functionalization was carried out using two different reaction methodologies. In a two-step process (Scheme 5.1), the aminosilane, $\text{Si}(\text{NEt}_2)_4$, was prepared¹⁶ and isolated by reacting SiCl_4 with NEt_2H . It was then used to react with clean substrates, followed by the reaction with the desired chromophore. In a three-step process (Scheme 5.1), surface anchored amino groups were prepared by reacting clean substrates first with SiCl_4 followed by NEt_2H . Substrates functionalized with amino groups were then reacted with the desired alcohol.

Scheme 5.1 Surface functionalization using two different reaction methodologies: two-step and three-step processes



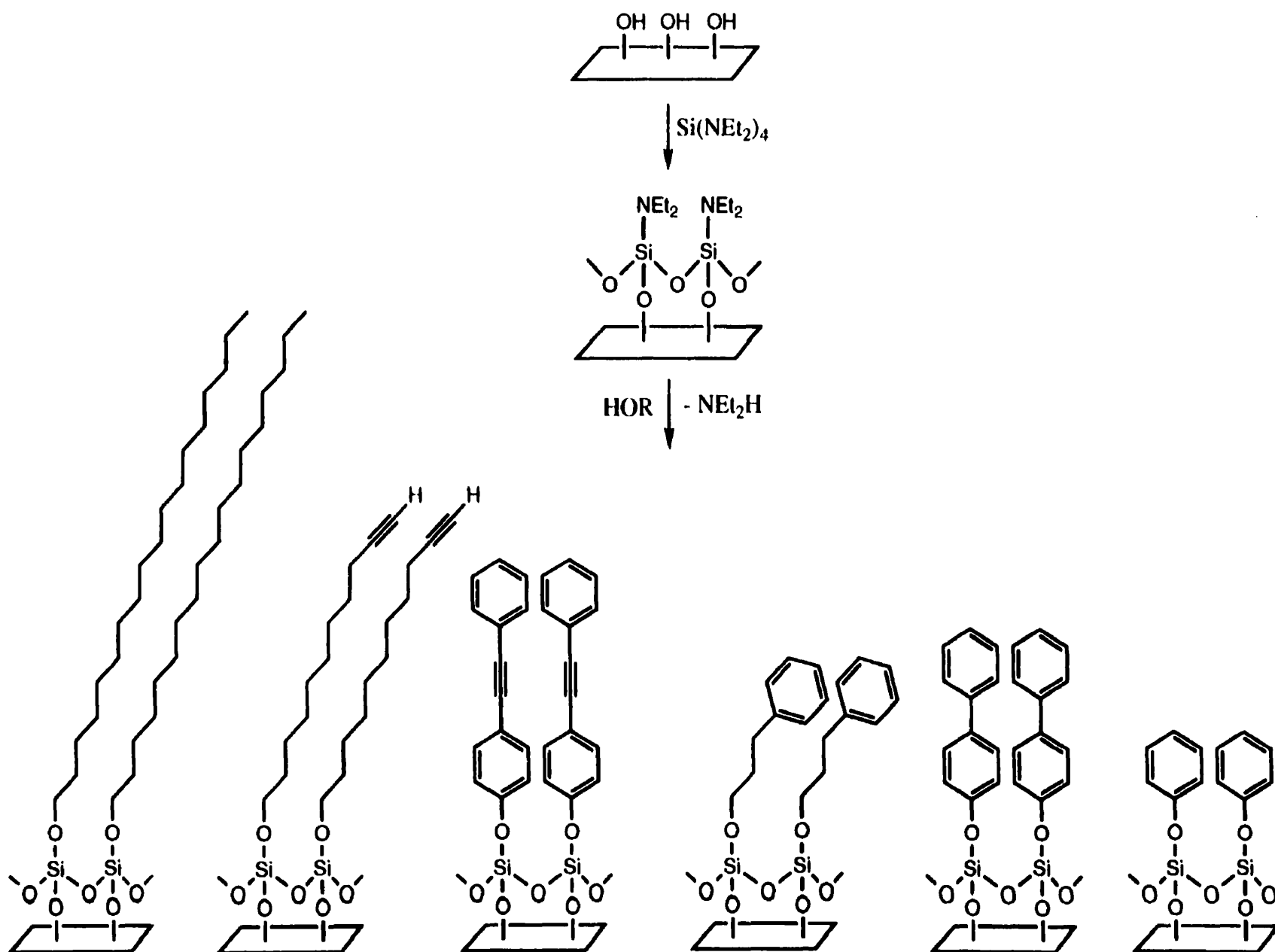
In order to explore the generality of the new acid-base hydrolytic approach to self-assembly, a series of thin films containing short-to-long chain length alcohols terminated with alkyl, phenyl and acetylene groups were self-assembled on glass, quartz and single crystal silicon (Scheme 5.2). The evolution of thin film structures was routinely monitored

by surface wettability measurements, FT-IR, ellipsometry and X-ray photoelectron spectroscopy. This multi-technique approach probes the structure of the newly formed thin films by different physical processes, and can provide complementary and definitive information.¹⁷⁻²⁰

X-ray photoelectron spectroscopy is a useful technique in determining the surface composition of the anchored species in the molecularly self-assembled thin films. We employed this technique for the analytical evaluation of the various organic thin films on silicon wafers, and the survey spectra for these monolayers showed the presence of three elements: silicon (2p, 99 eV, 2p, 103-104 eV), carbon (1s, 285 eV), and oxygen (1s, 532-533 eV). The molecules containing conjugated backbones showed a peak at 291 eV for C_{1s}, corresponding to, for example, aromatic carbon. The data confirms the identity of the molecules in the thin film structures, and is consistent with the one obtained from OTS films.²¹

The presence of a close-packed methyl-terminated monolayer is often indicated by characteristic advancing contact angles of water and hexadecane, and asymmetric and symmetric CH₂ stretching frequencies in their FTIR-ATR spectra.²² Although contact angles do not provide any structural information about the monolayers, they are useful indicators of their quality.²² The contact angles of water, film thicknesses, symmetric and asymmetric stretching frequencies of the methylene groups of well characterized thin films prepared from octadecyltrichlorosilane on silica, are 110°, 23-28 Å and 2850, 2918 cm⁻¹ respectively.²³ As the chain length decreases from -(CH₂)₁₇-CH₃ to -(CH₂)₇-CH₃, the contact angle drops from 110 to 90°, and there is a definite trend towards higher peak frequencies of $\nu_a(\text{CH}_2)$ and $\nu_s(\text{CH}_2)$ stretches.²³

Scheme 5.2 Molecular self-assembly of a series of short-to-long chain length alcohols terminated with alkyl, phenyl and acetylene groups on glass, quartz and single crystal silicon



The data obtained from surface wettability measurements, ellipsometry, and FTIR-ATR for thin films of alcohols prepared using the two-step process (Scheme 5.1) on Si(100) substrates are presented in Table 5.1. Upon comparing this data with that from SAMs prepared using other well-known methods,²³ it is apparent that the new acid-base hydrolytic approach is capable of producing thin films of high quality and order. For example, the static contact angle of water for a thin film of octadecanol is similar in value (110°) to that for the SAMs prepared from OTS on silica based surfaces and thiols on gold, and is well in accord with densely packed and oriented SAMs. However, the advancing contact angle with hexadecane (CA_{HD}) was found to be about 5-10° lower for the octadecanol SAM (30°) on Si(100) than those reported for the monolayers prepared from OTS on silica based surfaces (35-40°). This may be due to a number of factors including (i) the higher hydrophilicity of [Si]-O-R in our SAMs than [Si]-CH₂-R in OTS, and (ii) the Si(100) surface employed in our studies. It has been reported that CA_{HD} of the thin films of CH₃-(CH₂)_n-COO on Si(100) are 10° lower as compared to those on Si(111) surface, although both gave similar contact angles with H₂O (110°).²⁴ In order to confirm this hypothesis, we prepared a SAM of OTS on a Si(100) surface, and a similar lowering of the CA_{HD} angle to 30° was observed.

As the chain length of the alkylalcohol decreases from -(CH₂)₁₇-CH₃ to -(CH₂)₅-CH₃, CA_{H_2O} drops from 110° to 95° (Figure 5.1). It may be due to the sensitivity of the probe liquid to the underlying substrate,⁷ as well as the structures becoming increasingly disordered with lower packing density and coverages in small chain length molecules.^{6,11} For shorter chains, the film is less ordered and dense for lack of cohesive interactions. As the chain length increases, the cohesive forces become strong enough to pull up the molecular chains into 'normal' orientation, for optimal interaction energy.¹¹ Studies of

long-chain alkanethiols adsorbed on gold and silver surfaces showed similar results,⁷⁻⁸ and the same arguments apply to the lowering of CA_{H_2O} of alkynyols from undecynol to propynol (Table 5.1).

Table 5.1. Static contact angles of water (CA_{H_2O}), theoretical (T_t) and ellipsometric thicknesses (T_e), and FTIR-ATR data of alcohol thin films self-assembled on Si(100) substrates by the two-step process

Thin Film on Si(100) {Si}	CA_{H_2O} ($\pm 2^\circ$)	T_t , Å	T_e , Å (± 2 Å)	FTIR-ATR $\nu_a(CH_2)$, $\nu_s(CH_2)$ cm^{-1}	FTIR-ATR $\nu_{C\equiv C-H}$, $\nu_{C\equiv C}$ cm^{-1}	FTIR-ATR $\nu(C_6H_5)$ cm^{-1}
OTS	110	26	24	2920, 2850		
-O(CH ₂) ₁₇ CH ₃	110	27	25	2918, 2849		
-O(CH ₂) ₁₅ CH ₃	105	25	22	2921, 2851		
-O(CH ₂) ₁₃ CH ₃	105	22	19	2922, 2853		
-O(CH ₂) ₉ CH ₃	100	17	15	2922, 2854		
-O(CH ₂) ₅ CH ₃	95	12	10	2924, 2856		
-OC ₆ H ₅	85	9	7			1514
-O(CH ₂) ₃ C ₆ H ₅	90	13	11	2922, 2852		3064, 3027, 1480
-O-C ₆ H ₄ C ₆ H ₅	90	13	11			3068, 3027, 1480
-OC ₆ H ₄ C \equiv CC ₆ H ₅	70	16	14		2240	3066, 3025, 1531
-OCH ₂ C \equiv CH	60	9	7	2920, 2852	3361, 2124	
-O(CH ₂) ₂ C \equiv CH	70	10	8	2921, 2853	3350, 2122	
-O(CH ₂) ₃ C \equiv CH	85	11	9	2921, 2853	3320, 2120	
-O(CH ₂) ₄ C \equiv CH	90	13	10	2920, 2853	3328, 2120	
-O(CH ₂) ₉ C \equiv CH	90	19	17	2921, 2850	3280, 2086	
clean Si wafer	10		20			

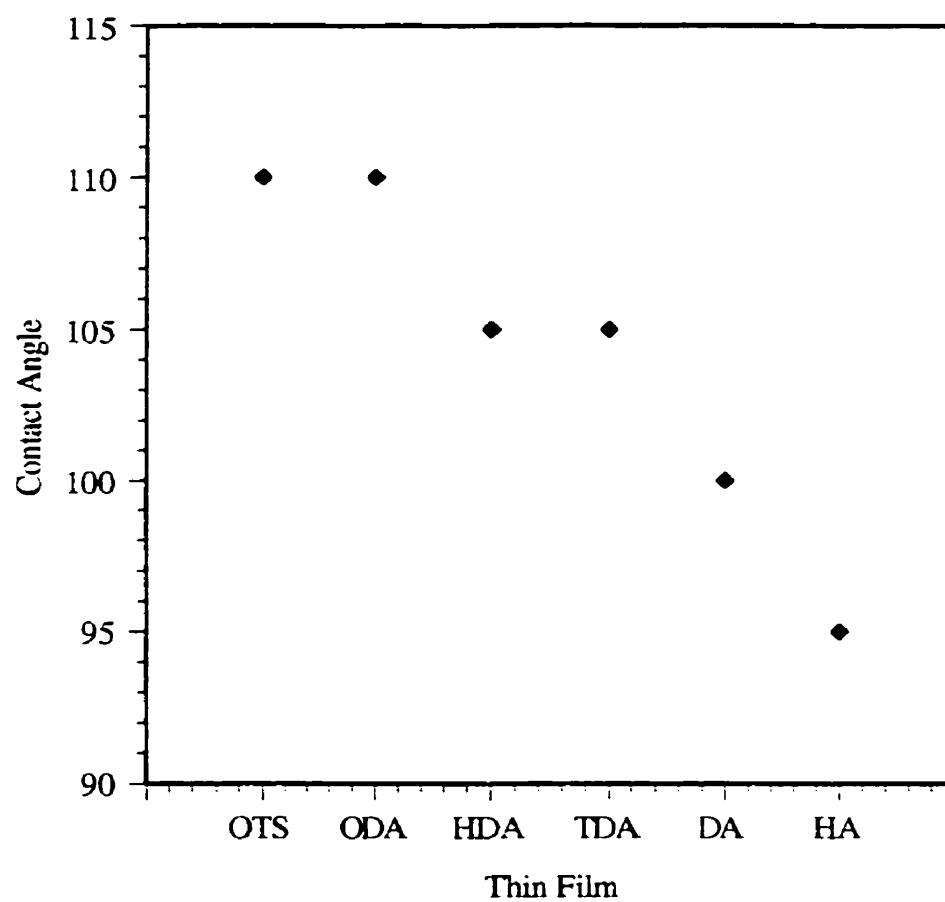


Figure 5.1. Static contact angles of water for monolayers of octadecyltrichlorosilane (OTS), octadecanol (ODA), hexadecanol (HDA), tetradecanol (TDA), decanol (DA), and hexanol (HA) on Si(100) substrates.

The contact angles of water and hexadecane from our thin films terminated with phenyl and acetylene groups are comparable to those obtained from thio-alkynyl and thio-aromatic thin films on gold,^{20,25} but lower than the molecularly self-assembled long chain alkanes. The lower contact angles of water (70-90°) and hexadecane (~15°) on the phenyl or acetylene terminated surfaces than the corresponding long alkyl chains (paraffins, ca. 110° (water) and 35-40° (hexadecane)) may be due to a number of factors including the fact that the $\text{-C}\equiv\text{C-H}$ (sp hybridization) or $\text{-C}_6\text{H}_5$ (sp^2 hybridization) groups adhere more strongly to water than CH_3 (sp^3) groups,¹⁴ and the introduction of any surface functionality into the alkane chain reduces monolayer order.²⁶ It has also been suggested that in paraffin films, the hydrogen atoms form a protective coating preventing attractive forces in a highly polar inorganic oxide surface from contributing to the spread of water drops.²⁷ As in the case of alkane thin films, the contact angle with water for the monolayers terminated with alkynyl groups increases as the chain length increases (Figure 5.2), and this suggests that the thin films become increasingly ordered and tightly packed as the chain length is increased.

Ellipsometry is a commonly employed technique to measure thickness of the newly developed thin films. A detailed evaluation of this technique has been discussed elsewhere.^{28,29} However, to calculate the thickness of an interface, one needs to compare data from the same substrate before and after functionalization. The thickness of the SiO_2 layer introduced from the reaction of aminosilane with surface hydroxyl groups and physisorbed molecular amounts of water was measured for background subtraction, and an assumption was made for the refractive index of the organic phase. For long chain alkanes, a typical value of the refractive index employed for calculating thickness is in the range of 1.45 - 1.50.³⁰ For the self-assembled organic thin films reported in this study, we used a value of 1.46. The typical values of bond lengths between elements projected on the surface were used to obtain theoretical thicknesses of such molecules.³¹ For a trans-extended

chain, the projection of the C-C bond onto the surface normal (z axis) is 1.26 Å, and for the C-Si and Si-O bonds, the projections are 1.52 and 1.33 Å, respectively. Including an additional 1.92 Å for the terminal methyl group, we expect a monolayer prepared from octadecanol to have a thickness of ~26 Å. As shown in Table 5.1, the ellipsometric thicknesses for our monolayers provide strong evidence for the formation of a film one molecular layer in thickness. Upon comparing these values with the calculated thicknesses, the data points to the presence of a densely packed array of chains with a tilt. The ellipsometry data here probably at best provide a qualitative indication that monolayers of alcohols with different terminating groups are being self-assembled on Si/SiO₂ with a certain orientation, similar to those of thiols on gold and alkyltrichlorosilanes on Si/SiO₂.

The peak positions of the frequencies for $\nu_a(\text{CH}_2)$ and $\nu_s(\text{CH}_2)$ modes in the FTIR-ATR spectra provide insight into the intermolecular environment of the alkyl chains in thin film assemblies.⁶ They are also ideal for the alkynyl and phenyl terminated thin films due to the minimal overlap of their absorption bands with those of other modes. Previous FT-IR studies have shown that the location of these peaks are sensitive indicators of the extent of the lateral interactions between long n-alkyl chains.³² A typical spectral pattern observed for an ordered hydrocarbon assembly is that of the peak positions for asymmetric and symmetric CH₂ stretching frequencies at ~2920 and ~2850 cm⁻¹. The latter are characteristic of a closely packed hydrocarbon environment,²¹ and occur at ~2926 and ~2856 cm⁻¹ in liquid-like disordered chains.³² The $\nu_a(\text{CH}_2)$ and $\nu_s(\text{CH}_2)$ stretching frequencies of the octadecanol SAM on the Si(100) surface were observed at 2918 and 2849 cm⁻¹. These are consistent with previously published results for octadecyltrichlorosilane on silica based surfaces,²³ and octadecanethiol on gold.²⁴ In addition, the monolayer of octadecanol showed film thickness and static contact angle of water (Table 5.1) reasonably in accord with previously published results for those well characterized OTS films.²³ These results suggest that the octadecanol SAM is tightly packed and relatively well-ordered.

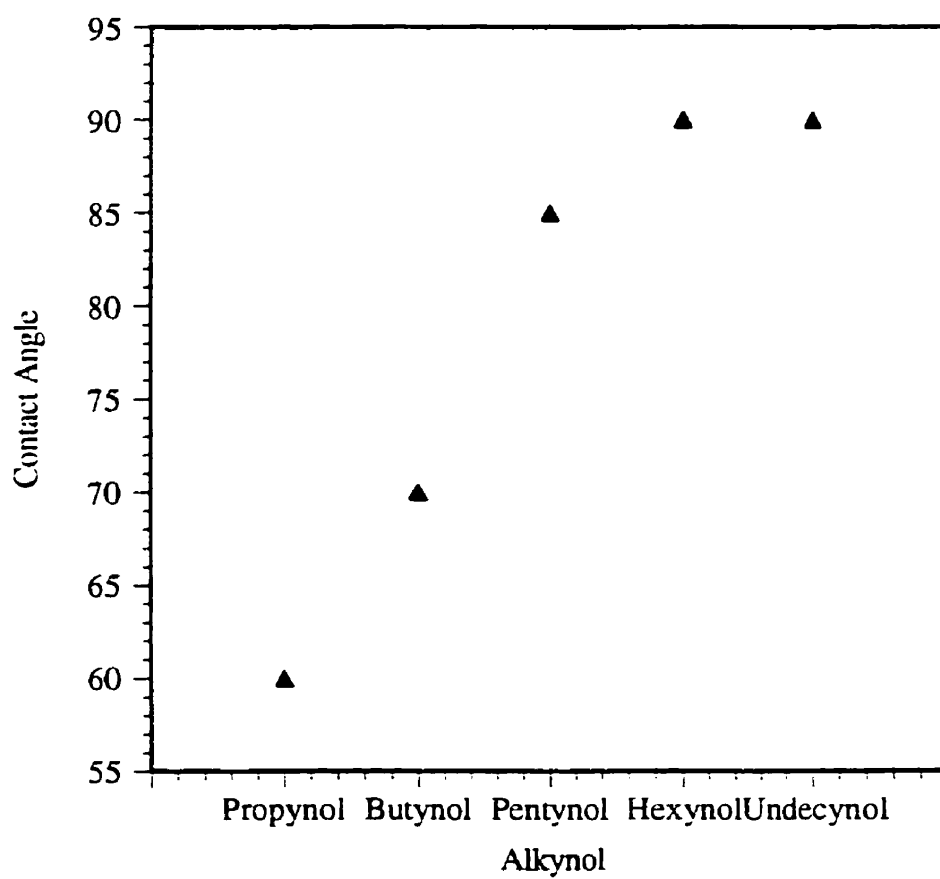


Figure 5.2. Static contact angles of water for monolayers of propynol, butynol, pentynol, hexynol, and undecynol on Si(100) substrates.

As the chain length decreases from $-(\text{CH}_2)_{17}\text{-CH}_3$ to $-(\text{CH}_2)_5\text{-CH}_3$, the $\nu_s(\text{CH}_2)$ and $\nu_a(\text{CH}_2)$ stretching frequencies in the FTIR-ATR spectra of these thin films move to higher wave numbers (from 2918, 2849 cm^{-1} for $-(\text{CH}_2)_{17}\text{-CH}_3$ to 2924, 2856 cm^{-1} for $-(\text{CH}_2)_5\text{-CH}_3$). A similar trend was observed for hydrocarbon thin films prepared from trichlorosilanes on silica and thiols on gold,²³ and suggests that the structure of the monolayers becomes increasingly disordered and liquid like as the chain length decreases, possibly due to lower packing density and chromophore coverage.

The peak positions in the FTIR-ATR spectra of the phenyl and acetylene terminated SAMs (Table 5.1) were observed at ca. 3300, 3000 (1500), 2100, 2920 (2850) cm^{-1} , and can be assigned to acetylene hydrogen, phenyl, acetylene and methylene groups, respectively.³¹ The peak positions of phenyl and acetylene groups in the monolayers on substrates are slightly shifted from the reference spectra obtained from a KBr pellet of the pure compound; however, they are similar to those recently reported for thio-aromatic and thio-alkynyl films on gold.^{20,25} The slight shifts in peak positions on the surface can be attributed to orientation effects in the SAMs.³³ A broad band in the 1000-1150 cm^{-1} region is assigned to vibrations of the siloxane ($-\text{Si-O-Si}-$) bridge and of Si-O- surface bonds.³⁴ The $\nu_s(\text{CH}_2)$ and $\nu_a(\text{CH}_2)$ stretching frequencies for the alkyne terminated alcohols are shown in Figure 5.3, and fall in the region 2920-2921 and 2850-2853 cm^{-1} , respectively.

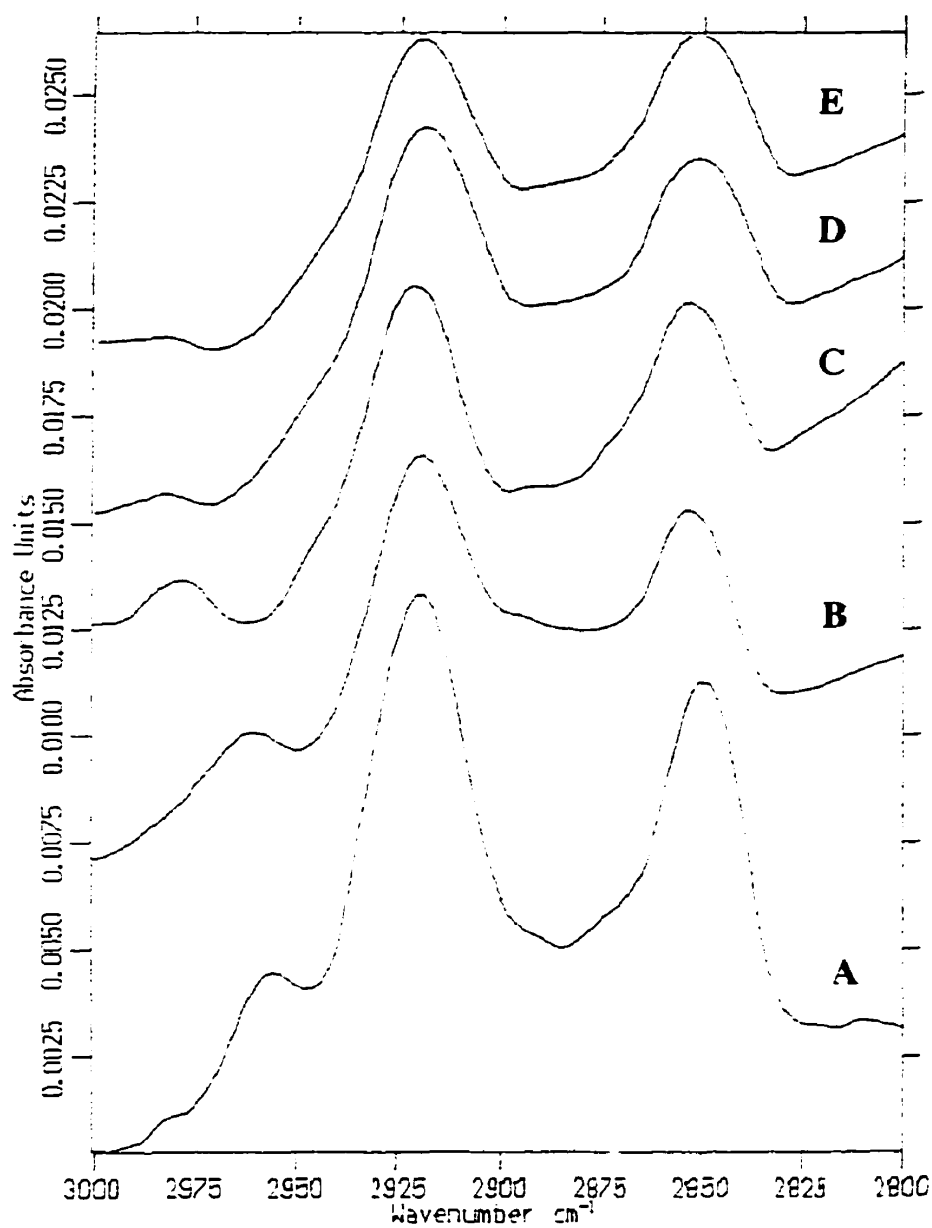


Figure 5.3. FTIR-ATR (nonpolarized) spectra for monolayers of undecynol (A), hexynol (B), pentynol (C), butynol (D) and propynol (E) on Si(100) substrates in the region 2800-3000 cm^{-1} .

5.4 Three-Step vs Two-Step Deposition Process

The wetting characteristics, ellipsometric thicknesses and $\nu_a(\text{CH}_2)$ and $\nu_s(\text{CH}_2)$ frequencies of the thin films prepared from alkanols by a three step process are shown in Table 5.2. A similar trend of decreasing contact angles of water and increasing CH_2 frequencies as in the thin films prepared using the two-step process, is observed as the chain length decreases. The contact angle with water from an octadecanol SAM prepared using the three step process (Scheme 5.1) is lower (105°) than the one prepared using the two step process (110°) as well as that from OTS SAMs on silica surfaces (110°). The ellipsometric thickness for the octadecanol monolayer prepared from the three-step process is approximately 2\AA smaller than the one from the two-step process. Similarly, the asymmetric and symmetric stretching frequencies of the methylene groups at 2920 and 2851 cm^{-1} are slightly higher than the SAM prepared using the two-step process. These results suggest that the film is not as densely packed as that from the two-step process, and there may be some disorder in the structure. The latter may have been introduced during the multistep deposition process (Scheme 5.1). The reaction of SiCl_4 with surface hydroxyl groups may lead to poor surface coverage, and there may be incomplete conversion of the resultant $[\text{Si}]\text{-Cl}$ moieties to $[\text{Si}]\text{-NEt}_2$ upon reacting with NEt_2H . It is evident then that the quality of the thin films can be substantially enhanced by using the two-step process which eliminates the treatment first with SiCl_4 followed by NEt_2H to produce surface anchored amino groups, and employs $\text{Si}(\text{NEt}_2)_4$ directly. As a whole, the two-step process produces more ordered SAMs than the three-step process.

Table 5.2. Static contact angles of water (CA_{H_2O}), theoretical (T_t) and ellipsometric thicknesses (T_e), and FTIR-ATR data of alcohol thin films self-assembled on Si(100) substrates by the three-step process

Thin Film on Si(100) {Si}	CA_{H_2O} , ° ($\pm 2^\circ$)	T_t , Å	T_e , Å ($\pm 2^\circ$)	FTIR-ATR $\nu_a(CH_2)$, $\nu_s(CH_2)$, cm^{-1}
$-O(CH_2)_{17}CH_3$	105	27	23	2920, 2851
$-O(CH_2)_{15}CH_3$	100	25	20	2923, 2853
$-O(CH_2)_{13}CH_3$	95	22	16	2926, 2854
$-O(CH_2)_{11}CH_3$	95	20	19	2926, 2857
$-O(CH_2)_9CH_3$	95	17	15	2927, 2856
$-O(CH_2)_7CH_3$	90	15	15	2928, 2854

5.5 Stability of SAMs

The stabilities of the thin films prepared by our new acid-base hydrolytic approach were tested under a variety of conditions including temperature, organic solvents, acid, base and water. The experiments were monitored by contact angle goniometry, ellipsometry and FTIR-ATR, and the results are presented in Table 5.3 and Figure 5.4.

Upon repeated washing with water at room temperature and wiping off the moisture with a Kimwipe, the contact angle of a monolayer of octadecanol with water was lowered by about 5° , but remained stable from thereon. The ellipsometric thickness did not change much (24 Å), and the asymmetric and symmetric methylene stretches were only slightly shifted to higher frequencies (2920, 2850 cm^{-1}). When the thin film was placed in boiling water, the contact angle with water decreased to 55° , the thickness reduced to 13 Å, and the $\nu_s(CH_2)$ and $\nu_a(CH_2)$ frequencies were increased to broad peaks at 2923 and 2850 cm^{-1} . These results suggest that the thin film has been hydrolyzed. The hydrolysis of the thin film

under these conditions can be understood by considering the nature of Si-to-element bond at the interfaces, and the Si-OR bond is expected to be more sensitive to hydrolysis than the Si-CH₂R bond in the monolayers of octadecyltrichlorosilane (OTS). The treatment¹² of a monolayer of OTS on glass with boiling water for 1 h, led to a decrease in ellipsometric thickness to 23 Å from an initial value of 25 Å, as well as an increase in the $\nu_a(\text{CH}_2)$ stretching frequency to 2919.1 cm⁻¹ (initially at 2917.6 cm⁻¹).

Table 5.3. Results of the stability tests on the octadecanol thin film on a Si(100) substrate

Experiment	CA _{H₂O} , ° (±2)	T _c , Å (±2)	FTIR-ATR $\nu_a(\text{CH}_2)$, $\nu_s(\text{CH}_2)$, cm ⁻¹
-O-(CH ₂) ₁₇ -CH ₃ (before any treatment)	110	25	2918, 2849
Heat, 150°C, 1h	100	21	2921, 2850
Aq.10% 2.5M H ₂ SO ₄ /90% dioxane, 25 °C, 1h, sonicate	55	14	2922, 2852
CHCl ₃ 25 °C, 1h, sonicate	110	24	2923, 2851
Boiling CHCl ₃ , 2h	70	13	
CH ₃ OH 25 °C, 1h, sonicate	105	15	2923, 2852
Boiling CH ₃ OH, 2h	105	10	
Aq.10% 1M NH ₄ OH/90% dioxane, 25 °C, 1h, sonicate	30	5	2925, 2855

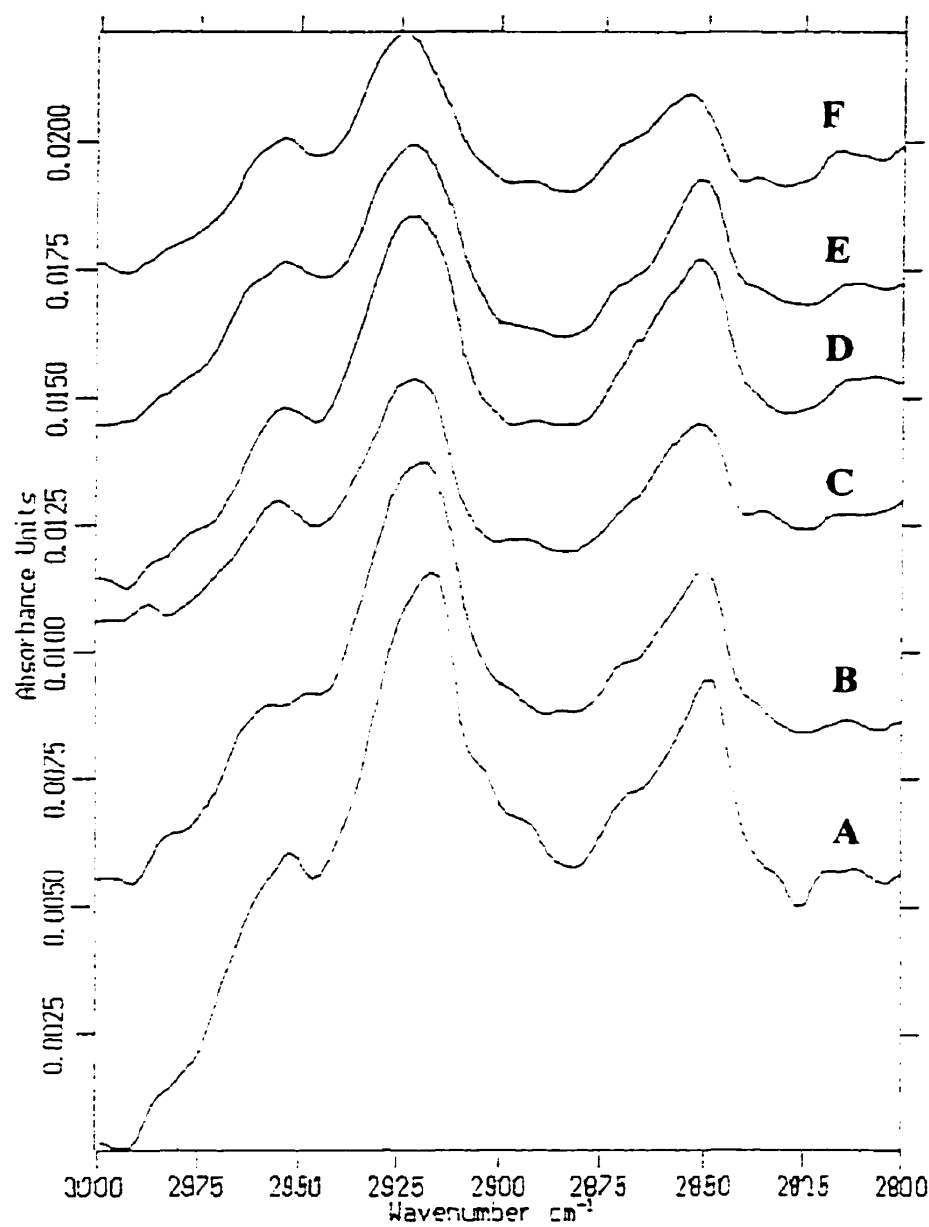


Figure 5.4. FTIR-ATR (nonpolarized) spectra for monolayers of $-\text{O}-(\text{CH}_2)_{17}-\text{CH}_3$ on Si(100) substrates in the region $2800\text{--}3000\text{ cm}^{-1}$: A. before any treatment; B, after heating at $150\text{ }^\circ\text{C}$ for 1 h; C, treatment with aqueous $2.5\text{ M H}_2\text{SO}_4$, $25\text{ }^\circ\text{C}$, 1 h; D, boiling CHCl_3 , 2 h; E, boiling methanol, 2 h; F, aqueous $1\text{ M NH}_4\text{OH}$, $25\text{ }^\circ\text{C}$, 1h.

The octadecanol SAM was found to be stable at room temperature for long periods of time. However, when it was heated to 150 °C for 1 h, the contact angle decreased to 100°, the thickness to 21 Å, and the $\nu_a(\text{CH}_2)$ and $\nu_s(\text{CH}_2)$ stretching frequencies were increased to 2921 and 2850 cm^{-1} (Figure 5.4 B). When an octadecanol SAM was sonicated in methanol for 1 h, the contact angle with water was found to be still relatively high at 105°, but the thickness was reduced to 15 Å. Similarly, when it was placed in boiling methanol for 2 h, the contact angle decreased only to 105°, but the thickness was reduced to 10 Å, and the $\nu_a(\text{CH}_2)$ and $\nu_s(\text{CH}_2)$ stretching frequencies increased to 2923 and 2852 cm^{-1} (Figure 5.4 E). These results suggest that the octadecanol thin film is solvolysed in methanol. The larger contact angles upon hydrolysis in methanol could possibly be explained by considering the conversion of some of the $[\text{Si}]\text{-O}(\text{CH}_2)_{17}\text{-CH}_3$ to $[\text{Si}]\text{-O-CH}_3$ on the surface. The monolayers exposing methyl groups to the surface, $[\text{SiO}]_2\text{-Si}(\text{CH}_3)_2$ and $[\text{Si}]\text{-O-Si}(\text{CH}_3)_3$ give contact angles with water of $\sim 100^\circ$.

In a similar experiment, an octadecanol SAM was placed in boiling chloroform for 2 h, and the contact angle with water was reduced to 70°, the thickness to 13 Å, and the $\nu_a(\text{CH}_2)$ and $\nu_s(\text{CH}_2)$ stretching frequencies were increased to 2923, 2851 cm^{-1} (broad peaks, Figure 5.4 D). A similar behavior for the monolayers prepared using long chain thiols on gold and carboxylic acids on silver, has been observed previously.^{11b,12} For example, a monolayer of octadecanethiol on gold gives a thickness of 28 Å, and $\nu_a(\text{CH}_2)$ stretching frequency at 2917.9 cm^{-1} . Upon treatment with boiling chloroform for 0.5 h, the thickness decreases to 20 Å, and the $\nu_a(\text{CH}_2)$ frequency increases to 2920.8.¹²

The octadecanol monolayers were found to be highly unstable in 10% aqueous 2.5 M H_2SO_4 or 1M NH_4OH in a 90% dioxane by volume. The films were significantly damaged

after 30-60 min in boiling chloroform, and 1 h in boiling acid or base. The surfaces on these films were found to be visibly etched by boiling in 90% dioxane/10% aqueous 1M NH_4OH . Under these conditions, the stability of the octadecanol thin film is similar to that of SAMs prepared using traditional self-assembly routes.¹² It has been reported that the monolayers of OTS on glass and octadecanethiol on gold are also badly damaged, and the surfaces pitted in boiling 90% dioxane/10% aqueous 1M NH_4OH mixture.¹²

5.6 Conclusion

Self-assembled monolayers of a variety of organic chromophores terminated with OH groups on Si(100) (Si/SiO₂) surfaces have been successfully prepared by a simple acid-base hydrolytic chemistry route. The two-step process involving the reaction of surface hydroxyl groups first with $\text{Si}(\text{NEt}_2)_4$ followed by ROH, is more efficient than the three-step process involving the reaction of SiCl_4 , NEt_2H and ROH in sequence, and produces closely-packed and well ordered thin films. The new simple acid-base hydrolytic chemistry two-step route, is able to produce monolayers of similar quality as the traditional self-assembly routes such as deposition of thiols on gold and alkyltrichlorosilanes on inorganic oxides. When placed in hot water and organic solvents, these films are more susceptible to hydrolysis than the corresponding OTS monolayers on silica, as expected; however, they show comparable stabilities at ambient and high temperatures, and upon treatment with acid and base.

5.7 Experimental Section

5.7.1 Materials

Octadecyltrichlorosilane (OTS), $\text{HO}(\text{CH}_2)_x\text{CH}_3$ ($x = 5, 7, 9, 11, 13, 15$ and 17), HOC_6H_5 , $\text{HOC}_6\text{H}_4\text{C}_6\text{H}_5$, $\text{HOCH}_2\text{C}\equiv\text{CH}$, $\text{HO}(\text{CH}_2)_2\text{C}\equiv\text{CH}$ and $\text{HO}(\text{CH}_2)_4\text{C}\equiv\text{CH}$ were purchased in high purity from Aldrich, and used as received. $\text{HO}(\text{CH}_2)_3\text{C}_6\text{H}_5$,

$\text{HO}(\text{CH}_2)_3\text{C}\equiv\text{CH}$ and $\text{HO}(\text{CH}_2)_9\text{C}\equiv\text{CH}$ were purchased from ChemSamp Co. Inc. $\text{HOC}_6\text{H}_4\text{C}\equiv\text{CC}_6\text{H}_5$ was synthesized by modifications of published procedures.³⁵ Its purity was verified by routine characterization methods. Solvents were dried and distilled from appropriate reagents: toluene over sodium; diethylamine over potassium hydroxide. Single side polished Si(100) substrates were purchased from Nova Electronic Materials.

$\text{HOC}_6\text{H}_4\text{C}\equiv\text{CC}_6\text{H}_5$ 1.8 g (8.1 mmol) of $\text{HOC}_6\text{H}_4\text{I}$ was dissolved in 50 ml of dry NEt_3H , and 1 ml of $\text{HC}\equiv\text{CC}_6\text{H}_5$ (8.9 mmol), 0.1 g of $\text{Pd}(\text{PPh}_3)_2\text{Cl}_2$ and 0.03 g of CuI were added. The reaction mixture was stirred at room temperature under nitrogen overnight. Solvent was removed under vacuum, and yellow crystals were obtained by extraction with hot hexane. After recrystallization from hexane, 0.5 g of the compound was obtained in 32% yield; Mass Spec (EI): 194. IR (KBr) ν (OH): 3419 cm^{-1} , ν (C_6H_5): 3076 , 3053 , 3018 , 1512 cm^{-1} , ν ($\text{C}\equiv\text{C}$): 2221 cm^{-1} ; ^1H NMR (200 MHz, CDCl_3) δ ppm 6.82, 7.34, 7.44, 7.51 (m, 9H, Ph), 1.90 (s, 1H, OH).

5.7.2 Substrate Preparation

Glass, quartz and single crystal silicon substrates were first cleaned (i) by soaking in soap solution and sonocating for 1 h; (ii) repeated washing with deionized water; (iii) treatment with a solution mixture containing 70% conc. H_2SO_4 and 30% H_2O_2 (piranha solution) at $100\text{ }^\circ\text{C}$ for 1 h. *Caution:* Piranha solution is highly explosive, and care should be taken while using this mixture; (iv) repeated washings with deionized water; and (v) finally heating in oven at $150\text{ }^\circ\text{C}$ for 5 min and vacuum drying for 5 min.

5.7.3 Two-step Deposition Process

The clean silicon wafers were treated with (i) 0.5 % solution by volume of $\text{Si}(\text{NEt}_2)_4$, which can be conveniently prepared¹⁶ by the reaction of SiCl_4 and excess dry NEt_2H , in dry toluene for 8 h at room temperature; followed by (ii) ROH in dry toluene at 50 °C for 24 h.

5.7.4 Three-step Deposition Process

The general synthetic strategy involved the treatment of clean substrates with (i) 0.5 % solution by volume of SiCl_4 in dry toluene for 18 hr at room temperature, (ii) 0.5 % solution by volume of dry NEt_2H in dry toluene for 18 h at 70 °C, followed by (iii) ROH in dry toluene at 50 °C for upto 24 h.

5.7.5 Contact-Angle (CA) Measurements

The static and advancing contact angles were measured with a Rame-Hart NRL 100 goniometer. On average, 6 drops of water and hexadecane were measured on different areas of the polished side of a silicon wafer for each sample, and the values reported are the mean values with a maximum range of $\pm 2^\circ$. The advancing contact angles of captive drops were found to be roughly 5° above the static values of sessile (free-standing) drops. If the drop was allowed to fall from the needle of the syringe to the surface, smaller contact angles were usually obtained because of the mechanical vibrations.²⁹

5.7.6 Fourier Transform Infrared Spectroscopy in the Attenuated Total Reflection Mode (FTIR-ATR)

The organic thin films were grown on the $\langle 100 \rangle$ surfaces of the single side polished silicon wafers. A KRS crystal was sandwiched between the reflective faces of two silicon wafers (1.2 x 4.0 cm), and the angle of incident light was set at 45° . All spectra were run

for 4000 scans at a resolution of 4 cm^{-1} , using a Bruker IFS-48 spectrometer. A spectrum of two clean silicon wafers with a sandwiched KRS crystal was measured as a background correction.

5.7.7 Ellipsometry

A Gaertner Scientific ellipsometer equipped with a 633 nm He-Ne laser ($\lambda = 6328\text{ Å}$) was employed. The angle of incidence was set at 70.0° , and the compensator angle at 45.0° . All reported values with a maximum range of $\pm 2\text{ Å}$ are the average of at least six measurements taken at different locations on the sample. The thickness was calculated by comparing data from the same substrate before and after functionalization and using a value of 1.46 for the refractive index. This value is based on the assumption that the monolayer is similar to bulk paraffins with a refractive index of 1.45.³⁰ If the monolayer is more crystalline-like, similar to polyethylene, the refractive index thus should be within 1.49-1.55.²⁹ It was found that an increase of 0.1 in the refractive index from 1.45 to 1.55 resulted in a decrease in the measured thickness by $\sim 2\text{ Å}$.

5.7.8 X-ray Photoelectron Spectroscopy (XPS)

The XPS spectra were obtained by using a VG Escalab MKII spectrometer with monochromatized MgK_α X-ray source to produce the photoemission of electrons from the core levels of the surface atoms. About 50 Å of depth was probed for a detector perpendicular to the surface. The analyzed surface was $2 \times 3\text{ mm}$. All peak positions were corrected for carbon at 285.0 eV in binding energy to adjust for charging effects. The power of the source was 300 watts and a pressure of 10^{-9} mbar .

Binding Energies (eV): Octadecyltrichlorosilane: C, 1s 285.0; O, 1s 532.0; Si_{2p} 98.6, 102.6. {Si}-O-(CH₂)₁₇CH₃: C, 1s 285.0; O, 1s 533.1; Si_{2p} 99.0, 104.0; {Si}-O-(CH₂)₅CH₃: C, 1s 285.0; O, 1s 533.2; Si_{2p} 99.1, 103.8; {Si}-O-C₆H₅: C, 1s 285.0, 291.0; O, 1s 533.9; Si_{2p} 98.8, 103.5; {Si}-O-(CH₂)₃-C₆H₅: C, 1s 285.0, 291.1; O, 1s 532.9; Si_{2p} 99.2, 103.7; {Si}-O-C₆H₄-C₆H₅: C, 1s 285.0, 291.1; O, 1s 533.2; Si_{2p} 99.3, 104.1; {Si}-O-C₆H₄-C≡C-C₆H₅: C, 1s 285.0, 291.1; O, 1s 532.9; Si_{2p} 98.7, 103.6; {Si}-O-CH₂-C≡C-H: C, 1s 285.0; O, 1s 532.5; Si_{2p} 98.2, 103.2; {Si}-O-(CH₂)₂-C≡C-H: C, 1s 285.0; O, 1s 532.9; Si_{2p} 98.7, 103.2; {Si}-O-(CH₂)₃-C≡C-H: C, 1s 285.0; O, 1s 533.1; Si_{2p} 99.3, 103.8; {Si}-O-(CH₂)₄-C≡C-H: C, 1s 285.0; O, 1s 532.7; Si_{2p} 99.2, 103.5; {Si}-O-(CH₂)₉-C≡C-H: C, 1s 285.0; O, 1s 531.1; Si_{2p} 99.2, 104.0.

5.8 References

- (1) Wu, C. G.; Chen, J. Y. *Chem. Mater.* **1997**, 9, 399.
- (2) Nuzzo, R. G.; Allara, D. L. *J. Am. Chem. Soc.* **1983**, 105, 4481.
- (3) (a) Jackman, R. J.; Wilbur, J. L.; Whitesides, G. M. *Science* **1995**, 269, 664. (b) Chidsey, C. E. D. *Science* **1991**, 251, 919.
- (4) Sagiv, J. *J. Am. Chem. Soc.* **1980**, 102, 92.
- (5) Bain, C. D.; Troughton, E. B.; Tao, Y.; Evall, J.; Whitesides, G. M.; Nuzzo, R. G. *J. Am. Chem. Soc.* **1989**, 111, 321.
- (6) Porter, M. D.; Bright, T. B.; Allara, D. L.; Chidsey, C. E. D. *J. Am. Chem. Soc.* **1987**, 109, 3559.
- (7) Walczak, M. M.; Chung, C.; Stole, S. M.; Widrig, C. A.; Porter, M. D. *J. Am. Chem. Soc.* **1991**, 113, 2370.
- (8) Laibinis, P. E.; Whitesides, G. M.; Allara, D. L.; Tao, Y.; Parikh, A. N.; Nuzzo, R. G. *J. Am. Chem. Soc.* **1991**, 113, 7152.

- (9) Troughton, E. B.; Bain, C. D.; Whitesides, G. M.; Nuzzo, R. G.; Allara, D. L.; Porter, M. D. *Langmuir* **1988**, *4*, 365.
- (10) Nuzzo, R. G.; Fusco, F. A.; Allara, D. L. *J. Am. Chem. Soc.* **1987**, *109*, 2358.
- (11) (a) Tao, Y. *J. Am. Chem. Soc.* **1993**, *115*, 4350. (b) Schlotter, N. E.; Porter, M. D.; Bright, T. B.; Allara, D. L. *Chem. Phys. Letts.* **1986**, *132*, 93.
- (12) Linford, M. R.; Fenter, P.; Eisenberger, P. M.; Chidsey, C. E. D. *J. Am. Chem. Soc.* **1995**, *117*, 3145.
- (13) Silberzan, P.; Leger, L.; Ausserre, D.; Benattar, J. *Langmuir* **1991**, *7*, 1647.
- (14) (a) Yam, C. M.; Kakkar, A. K. *J. Chem. Soc., Chem. Commun.* **1995**, 907. (b) Yam, C. M.; Dickie, A.; Malkhasian, A.; Kakkar, A. K.; Whitehead, M. A. *Can. J. Chem.* **1998**, *76*, 1766.
- (15) Fessenden, R.; Fessenden, J. S. *Chem. Rev.* **1961**, *61*, 361
- (16) Anderson, H. H. *J. Am. Chem. Soc.* **1952**, *74*, 1421.
- (17) Wasserman, S. R.; Tao, Y.; Whitesides, G. M. *Langmuir* **1989**, *5*, 1074.
- (18) Evans, S. D.; Sharma, R.; Ulman, A. *Langmuir* **1991**, *7*, 156.
- (19) Tao, Y.; Chang, S.; Ma, L. *J. Chin. Chem. Soc.* **1995**, *42*, 659.
- (20) Dhirani, A. A.; Zehner, R. W.; Hsung, R. P.; Sionnest, P. G.; Sita, L. R. *J. Am. Chem. Soc.* **1996**, *118*, 3319.
- (21) Frydman, E.; Cohen, H.; Maoz, R.; Sagiv, J. *Langmuir* **1997**, *13*, 5089.
- (22) Folkers, J. P.; Gorman, C. B.; Laibinis, P. E.; Buchholz, S.; Whitesides G. M.; Nuzzo, R. G. *Langmuir* **1995**, *11*, 813.
- (23) Tillman, N.; Ulman, A.; Schildkraut, J. S.; Penner, T. L. *J. Am. Chem. Soc.* **1988**, *110*, 6136.
- (24) Linford, M. R.; Chidsey, C. E. D. *J. Am. Chem. Soc.* **1993**, *115*, 12631.
- (25) Sabatini, E.; Moulakia, J. C.; Bruening, M.; Rubinstein, I. *Langmuir* **1993**, *9*, 2974.
- (26) Ulman, A. *Chem. Rev.* **1996**, *96*, 1533.

- (27) Adam, N.K. *Contact Angle, Wettability and Adhesion, Advances in Chemistry Series*; ACS: 1964, Vol. 43, p.52.
- (28) Azzam, R.M.A.; Bashara N.M. *Ellipsometry and Polarized Light*; North-Holland Publishing Company: Amsterdam, 1977.
- (29) Ulman, A. *An Introduction to Ultrathin Films from Langmuir-Blodgett to Self-Assembly*, Academic Press: Boston, 1991.
- (30) Wasserman, S. R.; Whitesides, G. M.; Tidswell, I. M.; Ocko, B. M.; Pershan, P. S.; Axe, J. D. *J. Am. Chem. Soc.* **1989**, *111*, 5852.
- (31) Dean, J.A. *Lange's Handbook of Chemistry*; McGraw-Hill: New York, 1992.
- (32) (a) Synder, R. G.; Strauss, H. L.; Elliger, C. A. *J. Phys. Chem.* **1982**, *86*, 5145.
(b) Synder, R. G.; Maroncelli, M.; Strauss, H. L.; Hallmark, V. M. *J. Phys. Chem.* **1986**, *90*, 5623.
- (33) Tour, J. M.; Jones, L., II; Pearson, D. L.; Lamba, J. J. S.; Burgin, T. P.; Whitesides, G. M.; Allara D. L.; Parikh, A. N.; Atre, S. V. *J. Am. Chem. Soc.* **1995**, *117*, 9529.
- (34) Maoz, R.; Sagiv J. *J. Colloid Interface Sci.* **1984**, *100*, 465.
- (35) Wityak, J.; Chan, J. B. *Synthetic Commun.* **1991**, *21*, 977.

Chapter Six

Molecular Self-Assembly of Dihydroxy Terminated Molecules via Acid-Base Hydrolytic Chemistry on Inorganic Oxide Surfaces: Step-by-Step Multilayered Thin Film Construction

6.1 Introduction

Self-organization of molecules on interfaces is an intriguing and highly promising approach to construct ordered and structurally stable thin films, and offers tremendous opportunities in the fabrication of advanced materials for a variety of applications.¹ Much effort has been devoted to the deposition and full characterization of monolayers of organosilicon compounds on hydroxylated surfaces² such as silica, alumina etc., alkanethiols on gold,³⁻⁴ silver,⁵ and copper,⁶ dialkyl sulfides on gold,⁷ dialkyl disulfides on gold,⁸ carboxylic acids on silver and aluminum oxide,⁹ and 1-alkenes on hydrogen terminated Si(111).¹⁰ It has been demonstrated that due to strong intermolecular van der Waals forces of attraction, such monolayers are densely packed and highly ordered.¹¹⁻¹² However, thin film based technology requires the construction of multilayered interfaces with molecules that contain useful moieties in the backbone. To prepare multilayered supramolecular structures, the surface of a monolayer must be modified so that another layer could be adsorbed on top. In silica based chemistry, the terminal group must be converted to a hydroxyl group, and the latter can be achieved by the reduction of a surface ester group,¹³ and hydroboration-oxidation of the terminal double bond.¹⁴ Once a subsequent monolayer is adsorbed on the "activated" monolayer, multilayered films may be built by repetition of this process.

The preparation methodologies for building multilayered structures have limitations associated with controlling film thickness and individual layer compositions of the resulting thin film assemblies. The design requirements for the construction of covalently bound multilayer assemblies on inorganic oxide surfaces, require that an effective synthetic methodology be developed for the quantitative creation of the hydroxylated self-assembled monolayer (SAM) surface using bifunctional molecules, and an efficient reaction sequence of the surface with bifunctional molecules under mild reaction conditions.¹⁵

We have discussed a new synthetic route to molecular self-assembly based on the hydrolysis of surface anchored aminosilanes with molecules containing terminal OH groups in Chapter 4. Using this methodology,¹⁶ silica surfaces can be modified with a variety of SAMs. We were intrigued by the possibility of building multilayered assemblies in a layer-by-layer fashion using bifunctional chromophores. In this chapter, we discuss a two-step thin film construction process involving the reaction of $\text{Si}(\text{NEt}_2)_4$ with hydroxyl groups of the inorganic oxides surfaces, followed by the reaction with dihydroxy chromophores incorporating acetylene, diacetylene and aromatic moieties in the backbone. Upon repetitive reactions with $\text{Si}(\text{NEt}_2)_4$ followed by $\text{R}(\text{OH})_2$, multilayered thin film assemblies were fabricated on glass, quartz, and single crystal Si. The characterization of the mono- and multilayered thin films was carried out using surface wettability measurements, ellipsometry, FT-IR, UV-Vis and X-ray photoelectronic spectroscopies. It has been suggested that the quality of the monolayers obtained from trichlorosilanes, or derivatives thereof, rapidly degrades as the thickness of the film increases. Our results indicate that thin films of appropriate thicknesses can be adsorbed using acid-base hydrolytic chemistry and dihydroxy terminated chromophores, for considerably more than a few layers, without losing order.

An understanding of the factors governing stability of self-assembled supramolecular structures is just beginning to emerge. In Chapter 5, we have observed that SAMs prepared using our acid-base hydrolytic approach may be susceptible to hydrolysis in boiling water

due to the higher sensitivity of the Si-OR bond to water than the Si-C bond in SAMs prepared from trichlorosilanes. From a detailed stability study under varied conditions, our results suggest that the multilayer thin film construction enhances stability of the thin films. We have also investigated topochemical polymerization of the diacetylenic moieties in the mono- and multilayered assemblies. Upon exposure of the diacetylenic thin films to UV-light, the formation of a blue film was observed.

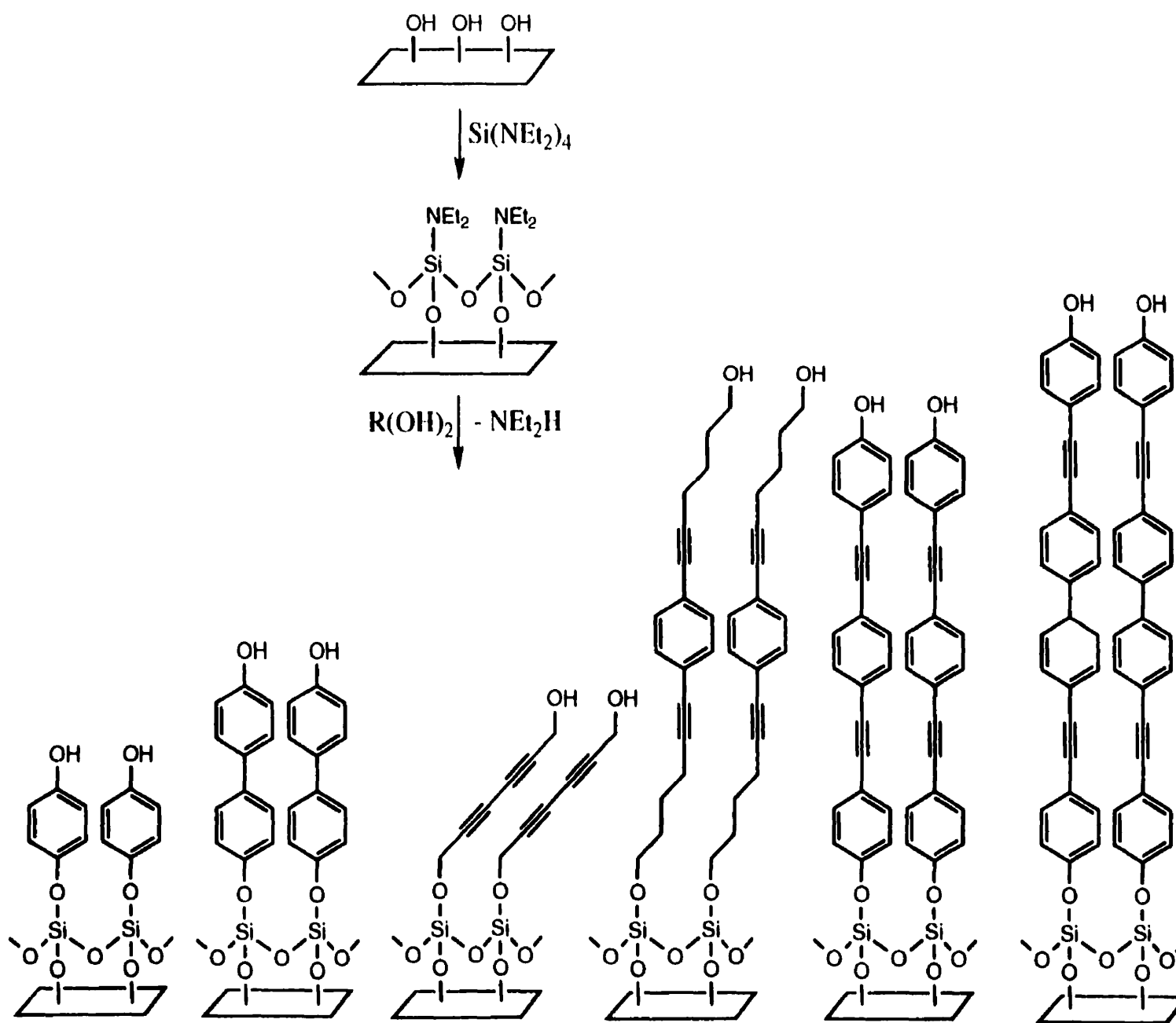
6.2 Acid-Base Hydrolysis

Aminosilanes ($\text{Me}_3\text{Si-NR}_2$, $\text{R} = \text{Me, Et}$), which can be easily prepared from their corresponding chlorosilanes and amines in quantitative yields, undergo acid-base hydrolysis with molecules containing a terminal OH group, to yield the silylated alcohols.¹⁷ We have recently demonstrated a similar behavior of the surface-immobilized Si-NEt_2 groups towards molecules containing terminal OH groups and varied backbones, leading to well ordered thin films based on simple acid-base hydrolytic chemistry.^{16a} The surfaces of glass, quartz and single crystal $\text{Si}(\text{SiO}_2)$ contain hydroxyl groups. The aminosilanes, which are much more basic than alkoxysilanes, undergo a facile acid-base hydrolytic reaction with silica based surfaces and molecules containing terminal OH groups. The simplicity and versatility of this approach prompted us to construct mono- and multilayered supramolecular structures using bifunctional chromophores (HO-R-OH) with desired chemical framework; and $\text{Si}(\text{NEt}_2)_4$, in a two-step reaction methodology.

6.3 Monolayers of Diols

The tetra(diethylamino)silane, $\text{Si}(\text{NEt}_2)_4$ was prepared¹⁸ and isolated in excellent yields by reacting SiCl_4 with excess NEt_2H . It was reacted with clean single crystal silicon (SiO_2) substrates to yield surface anchored Si-NEt_2 moieties, followed by their reaction with a series of dihydroxy chromophores of rigid-rod type, flexible or a mixture thereof, backbones (Scheme 6.1). 5,7-Dodecadiyne-1,12-diol was prepared via CuCl/O_2 catalyzed

Scheme 6.1 Molecular self-assembly of a series of dihydroxy chromophores on glass, quartz and single crystal silicon



coupling of terminal alkyne.¹⁹ Other dihydroxy chromophores were synthesized via palladium/copper catalyzed coupling of hydroxyaryl halides with terminal alkynes.²⁰

The monolayers were characterized by surface wettability measurements, ellipsometry, XPS, and FTIR-ATR spectroscopy. These are commonly used thin film characterization techniques,²¹⁻²³ and provide information about the evolution of the structure at interfaces. The data obtained from the thin films on Si(100) substrates are presented in Tables 6.1 and 6.2. The contact angles of water for the thin films from the dihydroxy chromophores were found to be in the range of 15-60°, and are similar to those for the SAMs from $\text{HOC}_{23}\text{Si/Si}$ ¹³ and $\text{HOC}_{11}\text{SH/Au}$.²⁴ The contact angles of water from the thin films prepared from dihydroxy molecules containing only phenyl, biphenyl and phenylacetylene type backbones (15-35°) suggest that there is no looping of the terminal hydroxy groups toward the surface due to rigidity of their structures, since the thin films will then become more hydrophobic by exposing phenyl or acetylene groups to the surface.

The molecules containing CH_2 groups in the backbone gave contact angles with water (50-60°) that were higher than those obtained from thin films containing purely rigid-rod backbones. It is possible that surface reorganization happens more easily in these films, and the monolayers restructure and minimize free energy of the system by burying the hydroxyl groups as much as possible, given the restrictions imposed by covalent bonding to the surface, and thus expose CH_2 groups to the surface.^{13,22} Such "surface reconstruction" has also been postulated for the oxidized polyethylene thin films, the surfaces of which consist largely of exposed carboxylic acid groups with small amounts of ketones and possibly aldehyde groups.²⁵

Table 6.1. Static contact angles of water (CA_{H_2O}), theoretical (T_t) and ellipsometric (T_e) thicknesses, and XPS data for SAMs prepared from dihydroxy terminated molecules on Si(100) substrates.

Thin Film {Si}	CA_{H_2O} $\pm 2^\circ$	T_t , Å	T_e , Å ± 2	XPS (C 1s, O 1s, Si-Si 2p, Si-O 2p)
OTS	110	26	24	285.0, 532.0, 98.6, 102.6
-O(<i>p</i> -C ₆ H ₄)OH	15	10	8	285.0, 291.1, 533.5, 98.8, 104.2
-O(<i>p</i> -C ₆ H ₄ -C ₆ H ₄)OH	25	15	12	285.0, 291.2, 532.9, 99.1, 103.9
-OCH ₂ C≡C-C≡CCH ₂ OH	30	14	12	285.0, 533.2, 99.0, 103.7
-O(CH ₂) ₄ C≡C-C≡C(CH ₂) ₄ OH	60	22	20	285.0, 533.2, 98.9, 103.3
-O(CH ₂) ₄ C≡C(<i>p</i> -C ₆ H ₄)-C≡C(CH ₂) ₄ OH	50	26	24	285.0, 291.2, 533.2, 99.0, 104.0
-O(CH ₂) ₄ C≡C(<i>p</i> -C ₆ H ₄ -C ₆ H ₄)C≡C(CH ₂) ₄ OH	55	30	28	285.0, 291.2, 533.0, 99.3, 103.6
-O(CH ₂) ₄ C≡C(<i>p</i> -C ₁₄ H ₈)-C≡C(CH ₂) ₄ OH	50	26	24	285.0, 291.2, 532.5, 98.8, 103.1
-O(<i>p</i> -C ₆ H ₄)C≡C(<i>p</i> -C ₆ H ₄)-C≡C(<i>p</i> -C ₆ H ₄)OH	35	24	22	285.0, 291.3, 533.0, 98.9, 103.7
-O(<i>p</i> -C ₆ H ₄)C≡C(<i>p</i> -C ₆ H ₄ -C ₆ H ₄)C≡C(<i>p</i> -C ₆ H ₄)OH	35	28	26	285.0, 291.4, 533.1, 99.3, 103.5
clean Si	10		20	285.0, 532.0, 98.6, 102.6

Table 6.2. FTIR-ATR data for SAMs prepared from dihydroxy terminated molecules on Si(100) substrates

Thin Film {Si}	ν_{OH} , cm^{-1}	$\nu_a(\text{CH}_2)$, $\nu_s(\text{CH}_2)$, cm^{-1}	$\nu(\text{C}_6\text{H}_5)$, cm^{-1}	$\nu_{\text{C}\equiv\text{C}}$, cm^{-1}	ν_{SiO} , cm^{-1}
OTS		2918, 2849			1089
-O(<i>p</i> -C ₆ H ₄)OH	3356		3030, 1522, 1475		1097
-O(<i>p</i> -C ₆ H ₄ -C ₆ H ₄)OH	3358		3028, 1487		1105
-OCH ₂ C \equiv C-C \equiv CCH ₂ OH	3379	2929, 2859		2187, 2134	1095
-O(CH ₂) ₄ C \equiv C-C \equiv C(CH ₂) ₄ OH	3381	2926, 2856		2172	1104
-O(CH ₂) ₄ C \equiv C(<i>p</i> -C ₆ H ₄)C \equiv C(CH ₂) ₄ OH	3370	2920, 2850	3027, 1518, 1579	2188	1104
-O(CH ₂) ₄ C \equiv C(<i>p</i> -C ₆ H ₄ -C ₆ H ₄)C \equiv C(CH ₂) ₄ OH	3394	2920, 2850	3088, 3010, 1483	2165	1080
-O(CH ₂) ₄ C \equiv C(<i>p</i> -C ₁₄ H ₈)C \equiv C(CH ₂) ₄ OH	3284	2920, 2850	3051, 1519	2168	1097
-O(<i>p</i> -C ₆ H ₄)C \equiv C(<i>p</i> -C ₆ H ₄)C \equiv C(<i>p</i> -C ₆ H ₄)OH	3334		3080, 1513	2147	1107
-O(<i>p</i> -C ₆ H ₄)C \equiv C(<i>p</i> -C ₆ H ₄ -C ₆ H ₄)C \equiv C(<i>p</i> -C ₆ H ₄)OH	3356		3025, 1485	2182	1094

Ellipsometry^{26,27} is commonly used to measure thickness of the newly developed thin films, and in general, one compares data from the same substrate before and after functionalization. The thickness of the SiO₂ layer is measured for background subtraction, and an assumption is made for the refractive index of the organic phase. For long chain alkanes, a typical value of the refractive index employed for calculating thickness is 1.45 - 1.50,²⁸ and we used a similar value of 1.46. The typical values of bond length between elements projected on the surface were used for obtaining theoretical thicknesses of such molecules.²⁹ For a trans-extended chain, the projection of the C-C bond onto the surface normal (z axis) is 1.26 Å. For the Si-O and C-O bonds, the projections are 1.33, and 1.17 Å, respectively. For the CH₂-C≡C, C≡C-C≡C and C≡C bonds, the projections are 1.46, 1.38 and 1.18 Å, respectively. Including an additional 0.97 Å for the terminal -OH group, we expect a monolayer prepared from 2,4-hexadiyne-1,6-diol and 5,7-dodecadiyne-1,12-diol to have a thickness of 14 and 22 Å. As shown in Table 6.1, the ellipsometric thicknesses provide strong evidence for the formation of a film one molecular layer in thickness, and suggest a densely packed array of chains with a slight tilt. The ellipsometry data gives a qualitative indication that monolayers of dihydroxy alcohols with different backbones are being self-assembled on Si/SiO₂, similar to those of HOC₂₃Si/Si¹³ and HOC₁₁SH/Au.²⁴

X-ray photoelectron spectroscopy is a well known technique to determine the surface composition of the anchored species in the molecularly self-assembled thin film.²⁶ We employed this technique for the analytical evaluation of the various dihydroxy organic thin films on silicon wafers, and the data presented in Table 6.1 confirms the composition of the thin film structures. The survey spectra for these monolayers show only three elements: silicon (2p, 99 eV, 2p, 103 eV), carbon (1s, 285 eV), and oxygen (1s, 533 eV). The molecules containing conjugated backbones showed a peak at 291 eV for C_{1s} corresponding to, for example, aromatic carbon. These values are comparable to those obtained from thin

films prepared using other methodologies, and serve to confirm the identity of the materials.^{21,30}

The peak positions of the frequencies for asymmetric and symmetric stretching of methylene groups in the FTIR-ATR spectra can provide insight into the intermolecular environment of the backbone chains in these assemblies.⁴ They were selected for structural interpretation owing to the minimal overlap of their absorption bands with those of other modes. A typical spectral pattern for an ordered hydrocarbon assembly has peak frequencies for asymmetric and symmetric CH_2 stretching at ~ 2918 and ~ 2849 cm^{-1} . The latter are characteristic of a closely packed hydrocarbon environment, and at ~ 2928 and ~ 2856 cm^{-1} for liquid-like disordered chains.³¹⁻³² The $\nu_a(\text{CH}_2)$ and $\nu_s(\text{CH}_2)$ stretching frequencies of the dihydroxy SAMs with CH_2 groups in the rigid-rod backbones were observed at ~ 2920 and ~ 2850 cm^{-1} . These are consistent with previously published results for $\text{HOC}_{23}\text{Si/Si}^{13}$ and $\text{HOC}_{11}\text{SH/Au}^{24}$ and suggests that these thin films are relatively well packed.

The peak positions in the FTIR-ATR spectra for the hydroxy, phenyl, and acetylene groups of the dihydroxy SAMs (Table 6.1) were observed at ca. 3300, 3000 (1500), and 2100 cm^{-1} respectively. The peak positions for the phenyl and acetylene groups in the monolayers are slightly shifted from the reference spectra obtained from a KBr pellet of the pure compound, but are similar to those recently reported for the thio-aromatic and thio-alkynyl films on gold.³³ These changes are attributed to orientational effects in SAMs.³⁴ A broad band in the 1050-1150 cm^{-1} region is attributable to vibrations of the siloxane ($-\text{Si-O-Si}-$) bridge and of Si-O- surface bonds.³⁵

6.4 Multilayered Thin Film Assemblies of 2,4-Hexadiyne-1,6-diol and 5,7-Dodecadiyne-1,12-diol

As discussed above, the dihydroxy compounds form SAMs exposing hydroxyl groups to the surface, and by reacting these OH groups with $\text{Si}(\text{NEt}_2)_4$, followed by the

reaction with the dihydroxy chromophores, the process can be continued indefinitely, in principle, to form multilayered structures. The potential of our new acid-base hydrolytic technique in the fabrication of multilayered thin films, was explored using bifunctional chromophores, 2,4-hexadiyne-1,6-diol (**1**) and 5,7-dodecadiyne-1,12-diol (**2**). After one layer of **1** or **2** was self-assembled on the substrate, it was cleaned by sonicating in THF for 5 min, followed by drying in an oven at 120 °C for 5 min. A step-by-step reaction methodology (Scheme 6.2) of reacting the latter monolayer with $\text{Si}(\text{NEt}_2)_4$, followed by the reaction with molecules **1** or **2** led to thin film assemblies of up to 10-layers.

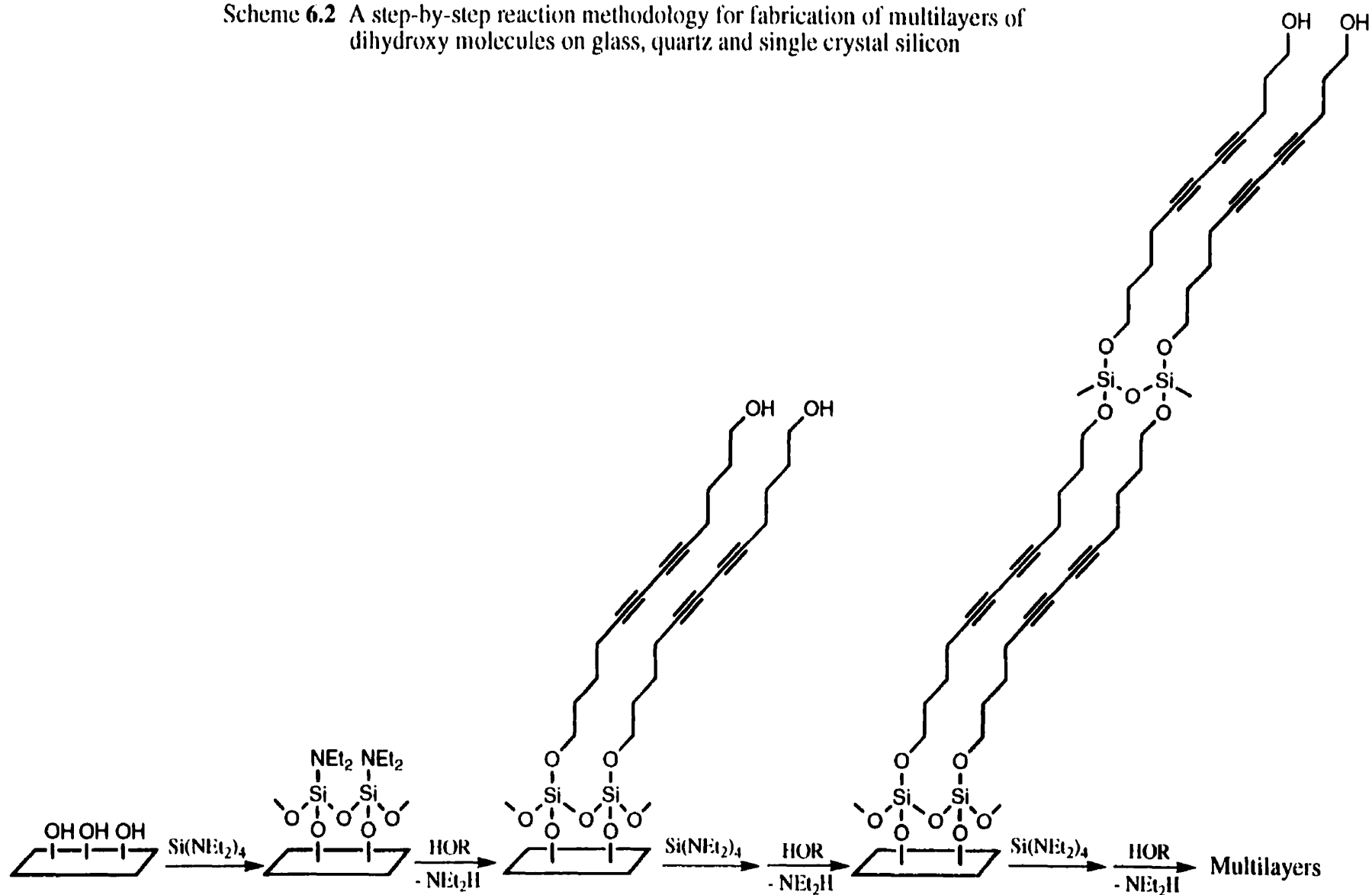
The evolution of the multilayered structures was monitored by contact angle goniometry, ellipsometry, FT-IR, XPS, etc. The thin film assemblies on silicon wafers show a linear relationship between the film thickness and the number of layers (Figures 6.1 and 6.2). The linear regression line through the first five data points shows a slope of 12.5 Å/layer and 21 Å/layer for **1** and **2**, respectively, and the latter are comparable to the monolayer thicknesses. The ellipsometric thickness of multilayered thin films were found to be in the range of ± 2 Å to ± 6 Å of the calculated thickness (Tables 6.3 and 6.4). There was an increase in thickness/layer from 1-layer sample (12 Å) to the 10-layer sample (15 Å) for **1**, and an increase in thickness/layer from 1-layer sample (20 Å) to 10-layer sample (24 Å) for **2**. This may be largely due to a more effective cleaning process which is employed for the monolayers on silicon substrates than is possible for the multilayer samples.¹³ It is probable that in the process of multilayer formation with $\text{Si}(\text{NEt}_2)_4$ or chromophore reaction, a small amount of loosely held material, either by adsorption on top of the monolayer surfaces or inclusion in the monolayer bulk, is introduced.¹³ The peak for the Si-O stretching frequency at $\sim 1100\text{ cm}^{-1}$ in the FT-IR spectrum was found to increase in intensity upon multilayer deposition. It should be noted, however, that 15 and 24 Å are certainly very reasonable thickness values for films with surface groups of **1** and **2**, respectively. Precision of thickness measurements also tends to decrease with increasing number of layers. The uncertainty on the readings of film thickness at various positions

across the face of the sample increases from ca. ± 2 Å for 1-layer samples to ca. ± 6 Å for 10-layer samples of both **1** and **2**. These results are similar to the multilayers of $\text{HOC}_{23}\text{Si/Si}$ prepared by continuing the adsorption-reduction sequence for monolayers of $\text{MeO}_2\text{CC}_{22}\text{Si/Si}$ and $\text{HOC}_{23}\text{Si/Si}$.¹³

For the thin films prepared from **1**, there is a gradual decrease in the static contact angle of water from $\sim 35^\circ$ for a monolayer to $\sim 20^\circ$ for a 10 layered film. Similarly, the asymmetric and symmetric stretching frequencies of methylene groups on the 7th layer decreased to 2922 and 2852 cm^{-1} from the initial values of 2929 and 2859 cm^{-1} respectively, in the 1st layer (Table 6.3 and Figure 6.3). The contact angles of water and FTIR-ATR CH_2 stretching frequencies reflect a general tendency to increasing order in the monolayers with increasing layer number. This may be due to (i) the increasing π - π interactions of the diacetylene groups and (ii) the formation of an effective Si-O-Si cross-linking network within each layer that results in better alignment of the chromophore on the surface.

For the thin films with the surface group of **2**, the asymmetric and symmetric stretching frequencies of methylene groups on the 10th layer also decreased to 2922 and 2852 cm^{-1} from 2926 and 2856 cm^{-1} , respectively, in the 1st layer (Table 6.4 and Figure 6.4). The FT-IR data, once again, points to increasing order in the thin films with increasing layer number. To substantiate these results, we decided to cap the monolayer and multilayered assemblies with monolayers of OTS or C_{18}OH . The contact angles of water from these capped thin films (Tables 6.3-6.4) were found to be in the range $110 - 115^\circ$, and the asymmetric and symmetric methylene stretching frequencies were found to be 2918 and 2850 cm^{-1} , respectively. The terminal OTS/ C_{18}OH monolayers gave the expected thickness of 24 - 26 Å. These results suggest that $\text{Si}(\text{NEt}_2)_4$ is highly efficient in creating a siloxane network that leads to close-packed multilayered thin films.

Scheme 6.2 A step-by-step reaction methodology for fabrication of multilayers of dihydroxy molecules on glass, quartz and single crystal silicon



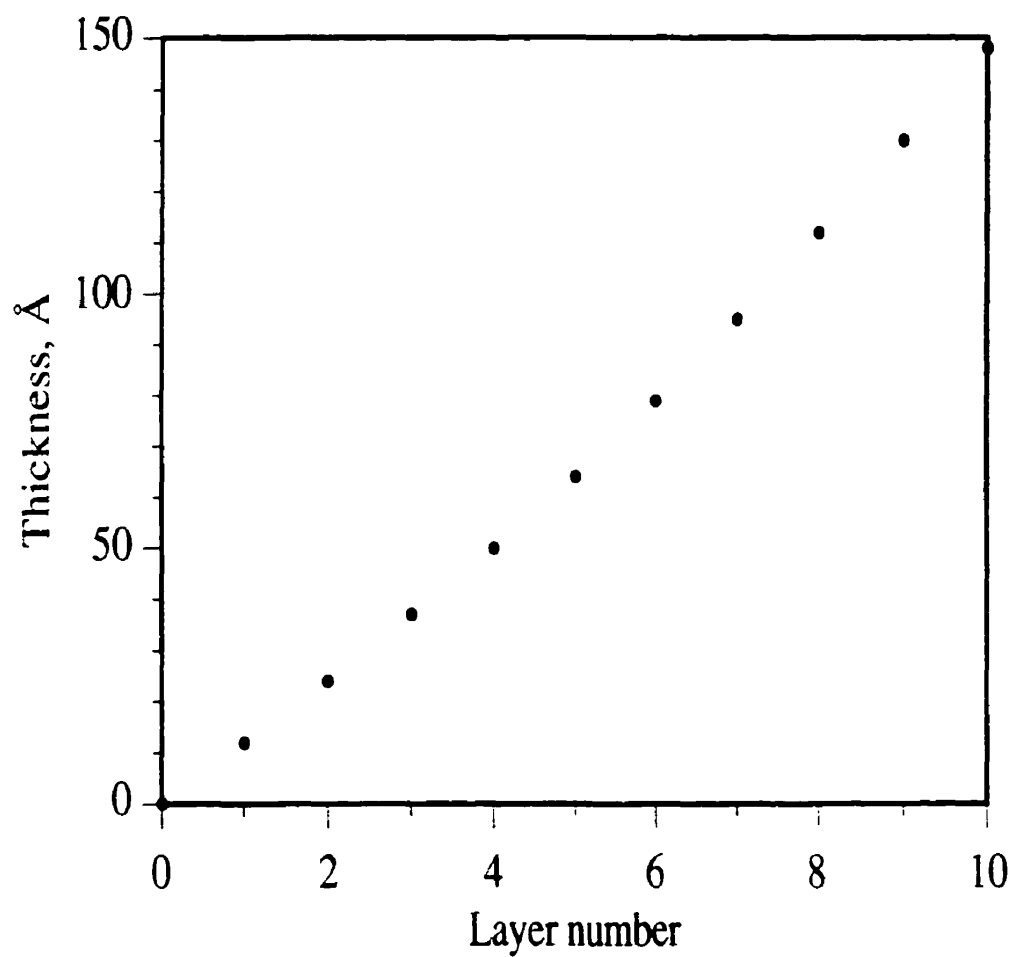


Figure 6.1. Ellipsometric thickness of the 1 to 10 layered thin films of 2,4-hexadiyne-1,6-diol (**1**).

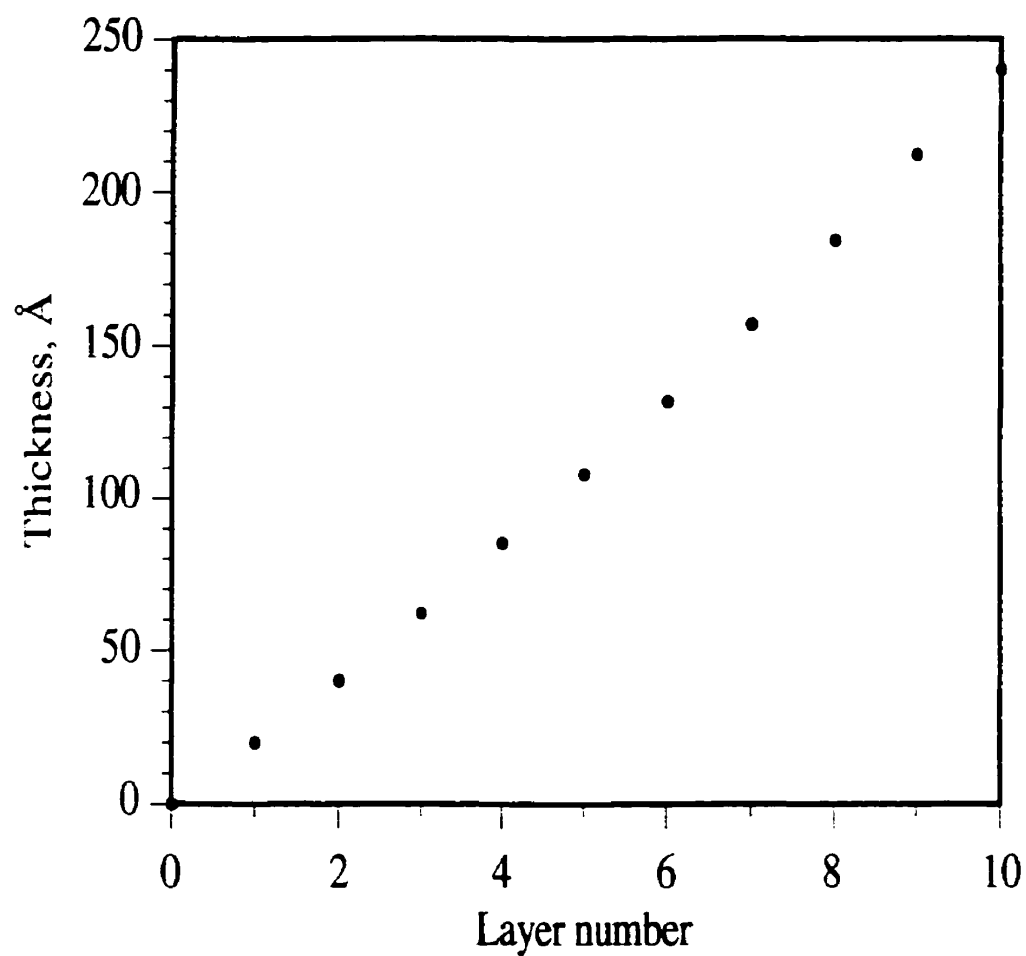


Figure 6.2. Ellipsometric thickness of the 1 to 10 layered thin films of 5,7- dodecadiyne-1,12-diol (**2**).

Table 6.3. Static contact angles of water (CA_{H_2O}), ellipsometric thicknesses (T_e) and FTIR-ATR data for the multilayers prepared from 2,4-hexadiyne-1,6-diol (**1**) on Si(100) substrates

Number of layers of 1	$CA_{H_2O}, \pm 2^\circ$	$T_e, \text{\AA}$	$\nu_a(\text{CH}_2), \nu_s(\text{CH}_2), \nu(\text{C}\equiv\text{C}), \text{cm}^{-1}$
1	35	12 ± 2	2929 (br), 2859 (br), 2187, 2134
1 + OTS	110	36 ± 2	2918, 2849
2	30	24 ± 2	2926 (br), 2864 (br), 2156, 2125
3	25	37 ± 2	2925, 2860, 2176, 2125
4	25	50 ± 2	2924, 2858, 2176, 2125
5	25	64 ± 4	2924, 2854, 2177, 2135
6	20	79 ± 4	2923, 2854, 2190, 2165
7	20	95 ± 4	2922, 2852, 2175, 2128
7 + OTS	115	120 ± 4	2918, 2850
8	20	112 ± 6	2923, 2853, 2176, 2144
9	20	130 ± 6	2923, 2853, 2181, 2133
10	20	148 ± 6	2923, 2854, 2170, 2120
10 + OTS	115	172 ± 6	2918, 2850

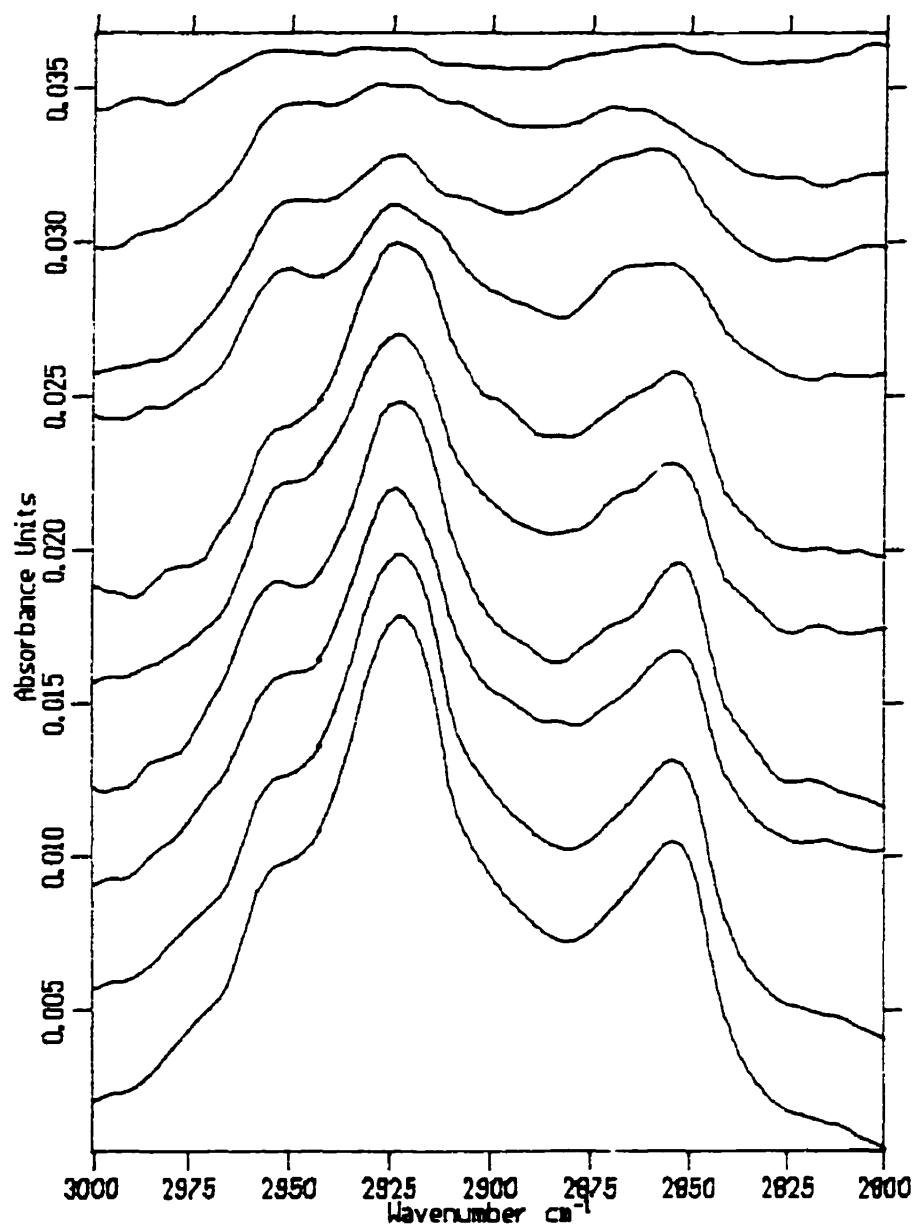


Figure 6.3. FTIR-ATR (nonpolarized) spectra for the 1 to 10 layered (top to bottom) thin films of 2,4-hexadiyne-1,6-diol (1) on Si(100) substrates in the region 2800-3000 cm^{-1} .

Table 6.4. Static contact angles of water (CA_{H_2O}), ellipsometric thicknesses (T_e) and FTIR-ATR data for the multilayers prepared from 5,7-dodecadiyne-1,12-diol (**2**) on Si(100) Substrates

Number of layers of 2	$CA_{H_2O} \pm 2^\circ$	$T_e, \text{\AA}$	$\nu_a(CH_2), \nu_s(CH_2), \nu(C\equiv C), \text{cm}^{-1}$
1	60	20 ± 2	2926 (br), 2856 (br), 2172 (br)
1 + $C_{18}OH$	110	44 ± 2	2918, 2850
2	60	40 ± 2	2924, 2854, 2194, 2123
2 + OTS	115	65 ± 2	2918, 2850
3	55	62 ± 2	2924, 2853, 2184, 2130
4	60	85 ± 2	2923, 2853, 2130
4 + OTS	115	110 ± 2	2918, 2850
5	50	108 ± 4	2924, 2853, 2170, 2140
6	60	132 ± 4	2923, 2852, 2174, 2137
6 + OTS	115	158 ± 4	2918, 2850
7	50	157 ± 4	2923, 2852, 2176, 2142
8	55	184 ± 6	2922, 2852, 2135
8 + OTS	115	210 ± 6	2918, 2850
9	55	212 ± 6	2922, 2822, 2174, 2135
10	60	240 ± 6	2922, 2852, 2168, 2129
10 + OTS	115	265 ± 6	2918, 2850

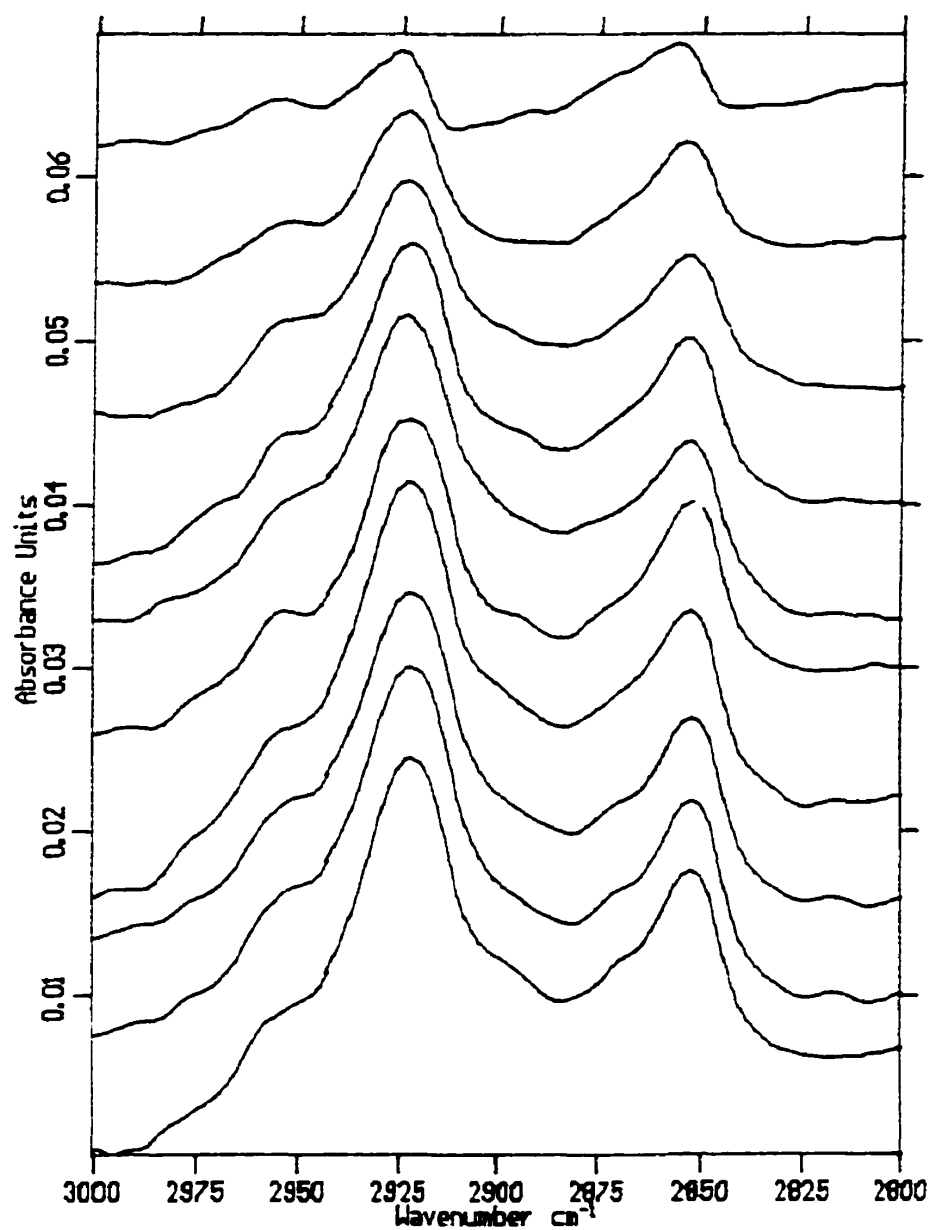


Figure 6.4. FTIR-ATR (nonpolarized) spectra for the 1 to 10 layered (top to bottom) thin films of 5,7-dodecadiyne-1,12-diol (**2**) on Si(100) substrates in the region 2800-3000 cm^{-1} .

6.5 Stability of Mono- and Multilayers

We have recently reported^{16a} detailed studies of the stability of monolayers prepared from monofunctional hydroxyl-terminated chromophores using acid-base hydrolytic chemistry under a variety of conditions. These monolayers were found to be susceptible to hydrolysis in boiling water and chloroform, acids and bases. We would like to look into the possibility that the construction of multilayered structures via a step-by-step deposition methodology might enhance the stability of the thin films. Hence, we examined the behavior of mono- and multilayered thin films of 2,4-hexadiyne-1,6-diol (**1**) and 5,7-dodecadiyne-1,12-diol (**2**) on Si(100) substrates, in hot organic solvents, water, acid, base, and at high temperatures. As shown in Table 6.5a, monolayers of **1** and **2** are hydrolyzed upon treatment with boiling chloroform, methanol and water. Aqueous acids and bases completely etch the films. The behavior of these SAMs are similar to those reported earlier in the literature for long alkane chain assemblies.¹¹

The contact angles of water on hydrophobic surfaces of long hydrocarbon chains and CH_2 symmetric and asymmetric frequencies in the FTIR-ATR spectra can be used to distinguish ordered and disordered interfaces. For example, a densely packed SAM of octadecyltrichlorosilane on glass shows a contact angle of $\sim 110^\circ$ with water, and a liquid-like disordered film has a contact angle of $90\text{--}100^\circ$. It is difficult to notice such sharp changes in the thin films of small chromophores (**1** and **2**) exposing OH groups to surface. Thus, to compare thin film characteristics using contact angles of water and FTIR-ATR, the mono- and multilayered thin films of the dihydroxy chromophores were capped with a SAM of octadecyltrichlorosilane (OTS). The results of these studies are summarized in Table 6.5b-d. The results of stability tests done on a SAM of octadecanol are also included. As discussed earlier,¹⁶ upon treating a SAM of octadecanol with boiling water, chloroform and methanol, the thickness and contact angle of water decrease, and the asymmetric and symmetric methylene stretches in the FTIR-ATR spectra move to 2923 and 2850 cm^{-1} from the initial values of 2918 and 2849 cm^{-1} (Table 6.5b). In contrast, a SAM

of **1** capped with OTS is affected by these solvents to a lesser extent. The thickness and contact angle of water decrease only by 5 Å and 10° respectively, after boiling solvent treatment, and remain unchanged upon heating at 150 °C in an oven for 1 h. These results are similar to the stability tests on a SAM of OTS on oxidized silicon.³⁶ These results suggest that a SAM of OTS acts as a protective coating for the dihydroxy monolayer.

Table 6.5a. Results of the stability studies on SAMs of 2,4-hexadiyne-1,6-diol (**1**) and 5,7-dodecadiyne-1,12-diol (**2**)

Stability Test	-O-CH ₂ -C≡C-C≡C-CH ₂ OH			-O-(CH ₂) ₄ -C≡C-C≡C-(CH ₂) ₄ OH		
	T _c , ±2 Å	ν _a , ν _s , cm ⁻¹	CA _{H₂O} , ±2°	T _c , ±2 Å	ν _a , ν _s , cm ⁻¹	CA _{H₂O} , ±2°
Before any treatment	12	2925, 2856	30	20	2925, 2855	50
Heat, 150 °C, 1 hr	6	2925, 2856 (br)	45	15	2925, 2855 (br)	60
Boiling CHCl ₃ , 1 hr	7	2925, 2856 (br)	50	12	2925, 2855 (br)	50
Boiling MeOH, 1 hr	6	2925, 2856 (br)	45	13	2925, 2855 (br)	70
Boiling water, 1 hr	4	2925, 2856 (br)	45	8	2925, 2855 (br)	45
Boiling Aq.10% 1M NH ₄ OH	etched	---	20	etched	---	25
Boiling Aq.10% 2.5M H ₂ SO ₄	etched	---	20	etched	---	20

Table **6.5b**. Results of the stability studies on a SAM of octadecanol and a thin film of 2,4-hexadiyne-1,6-diol (**1**) capped with OTS

Stability Test	-O-(CH ₂) ₁₇ CH ₃			-O-CH ₂ -C≡C-C≡C-CH ₂ -O-Si-(CH ₂) ₁₇ CH ₃		
	T _e , ±2 Å	ν _a , ν _s , cm ⁻¹	CA _{H₂O} ±2°	T _e , ±2 Å	ν _a , ν _s , cm ⁻¹	CA _{H₂O} ±2°
Before any treatment	25	2918, 2849	110	36	2918, 2849	110
Heat, 150 °C, 1 hr	21	2921, 2850	100	35	2919, 2850	110
Boiling CHCl ₃ , 1 hr	13	2923, 2851	70	32	2919, 2850	100
Boiling MeOH, 1 hr	10	2923, 2852	105	30	2919, 2850	105
Boiling water, 1 hr	13	2923, 2850	55	34	2919, 2850	100
Boiling Aq.10% 1M NH ₄ OH	etched	---	30	etched	---	30
Boiling Aq.10% 2.5M H ₂ SO ₄	14	2922, 2852	55	32	2919, 2850	100

As multilayers of **1** are constructed, their stability towards boiling solvents increases (Table **6.5c**). After the 4th layer, no damage by boiling solvents to the thin films was observed. The thickness and contact angles of water in the multilayers were not affected even after 1 h immersion in the boiling solvents. However, the thin films were very sensitive to hot base, and even a 10 layer assembly was visibly pitted. Similar results were obtained with mono- and multilayers of **2** capped with OTS (Table **6.5d**).

Table 6.5c. Results of the stability studies on multilayers of 2,4-hexadiyne-1,6-diol (**1**) capped with OTS

Thin films of 1 capped with OTS on Si(100)	Before any treatment	Boiling H ₂ O, 1 hr	Boiling H ₂ SO ₄ , 1 hr	Boiling CH ₃ OH, 1 hr	Boiling CHCl ₃ , 1 hr
1-layer + OTS CA _{H₂O} T _c	110° 36Å	100 34	100 32	105 30	100 32
2-layers + OTS CA _{H₂O} T _c	110 50	105 46	105 46	110 48	110 48
3-layers + OTS CA _{H₂O} T _c	110 62	105 60	105 60	110 60	110 60
4-layers + OTS CA _{H₂O} T _c	110 75	110 74	110 74	110 74	110 74
5-layers + OTS CA _{H₂O} T _c	110 90	110 88	110 88	110 88	110 88
6-layers + OTS CA _{H₂O} T _c	110 105	110 104	110 104	110 104	110 104
7-layers + OTS CA _{H₂O} T _c	115 120	115 118	115 118	115 118	115 118
8-layers + OTS CA _{H₂O} T _c	115 138	115 136	115 136	115 136	115 136
9-layers + OTS CA _{H₂O} T _c	115 155	115 154	115 154	115 154	115 154
10-layers + OTS CA _{H₂O} T _c	115 172	115 170	115 170	115 170	115 170

Table 6.5d. Results of the stability studies on multilayers of 5,7-dodecadiyne-1,12-diol (**2**) capped with OTS

2-, 6- and 10-layered thin films of 2 capped with OTS on Si(100)	$CA_{H_2O}, ^\circ$			$T_e, \text{\AA}$		
	2-layers	6-layers	10-layers	2-layers	6-layers	10-layers
Before any treatment	115	115	115	65	158	265
Heat, 150 °C, 1 hr	115	115	115	64	158	265
4 hr	115	115	115	64	156	264
1 day	115	115	115	64	156	264
Water, 25 °C, 1 hr	115	115	115	65	158	265
Boiling Water, 1 hr	105	115	115	60	156	264

6.6 UV-Vis Exposure of Mono- and Multilayers

For the thin films prepared from **1** on quartz, the intensity of absorption at ~315 nm in the UV-Vis absorption spectra increased upon multilayered thin film deposition (Figure 6.5). This is consistent with the increase in density of chromophores and a change in the orientation of the molecules upon multilayer formation.

The thin film assemblies were irradiated with a UV lamp operating at 365 nm for up to 120 min under a nitrogen atmosphere. The intensity of the λ_{max} decreased significantly (Figure 6.6), with the subsequent formation of a blue film that could be observed by a naked eye. This suggests that a structural change has taken place with the $C\equiv C$ bonds becoming parallel to the substrate after UV exposure, as reported previously.³⁷

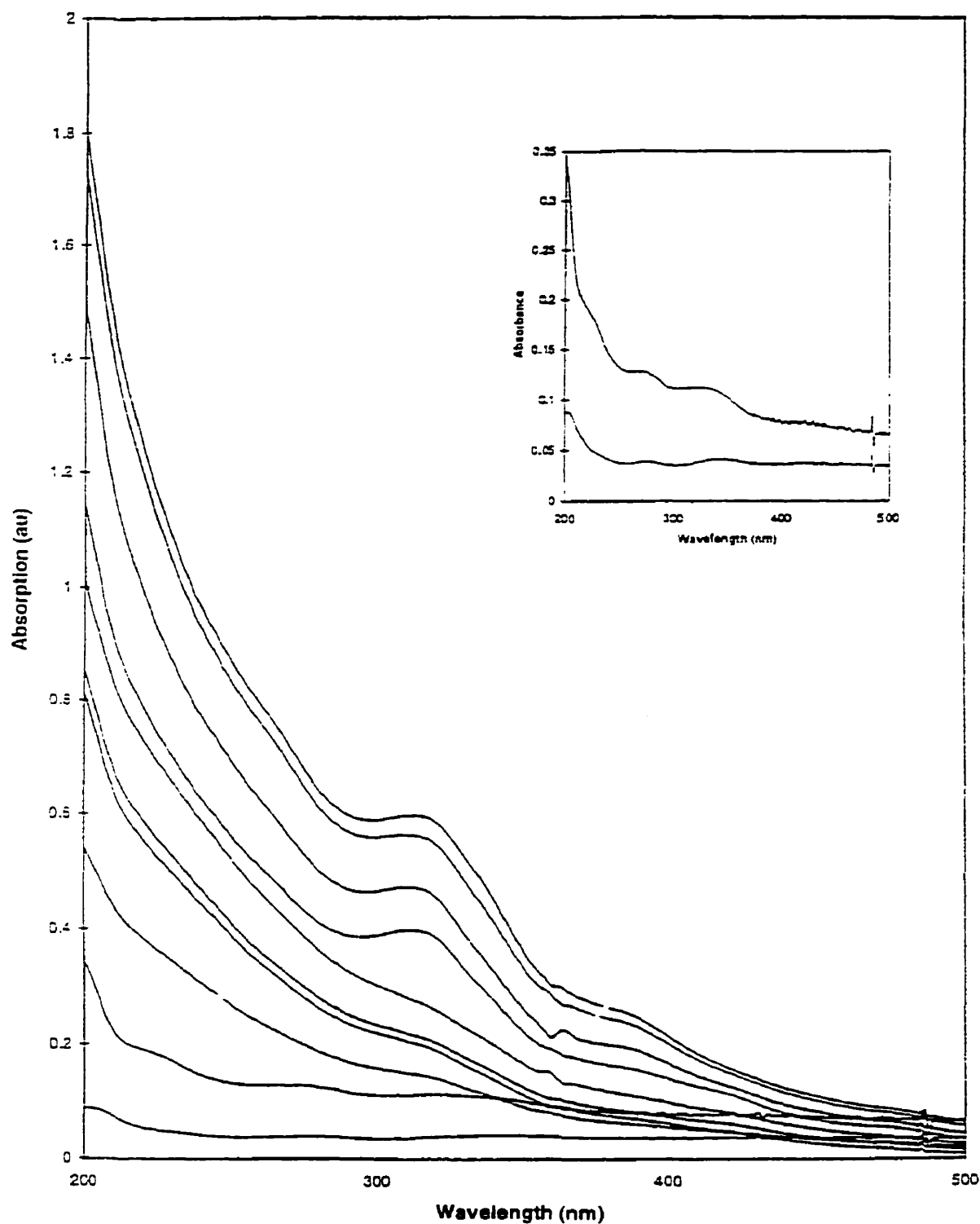


Figure 6.5. UV-Vis spectra of the 1 to 10 layered thin films of 2,4-hexadiyne-1,6-diol (1) on quartz. The inset shows the UV-Vis spectra of the 1 and 2 layered thin films.

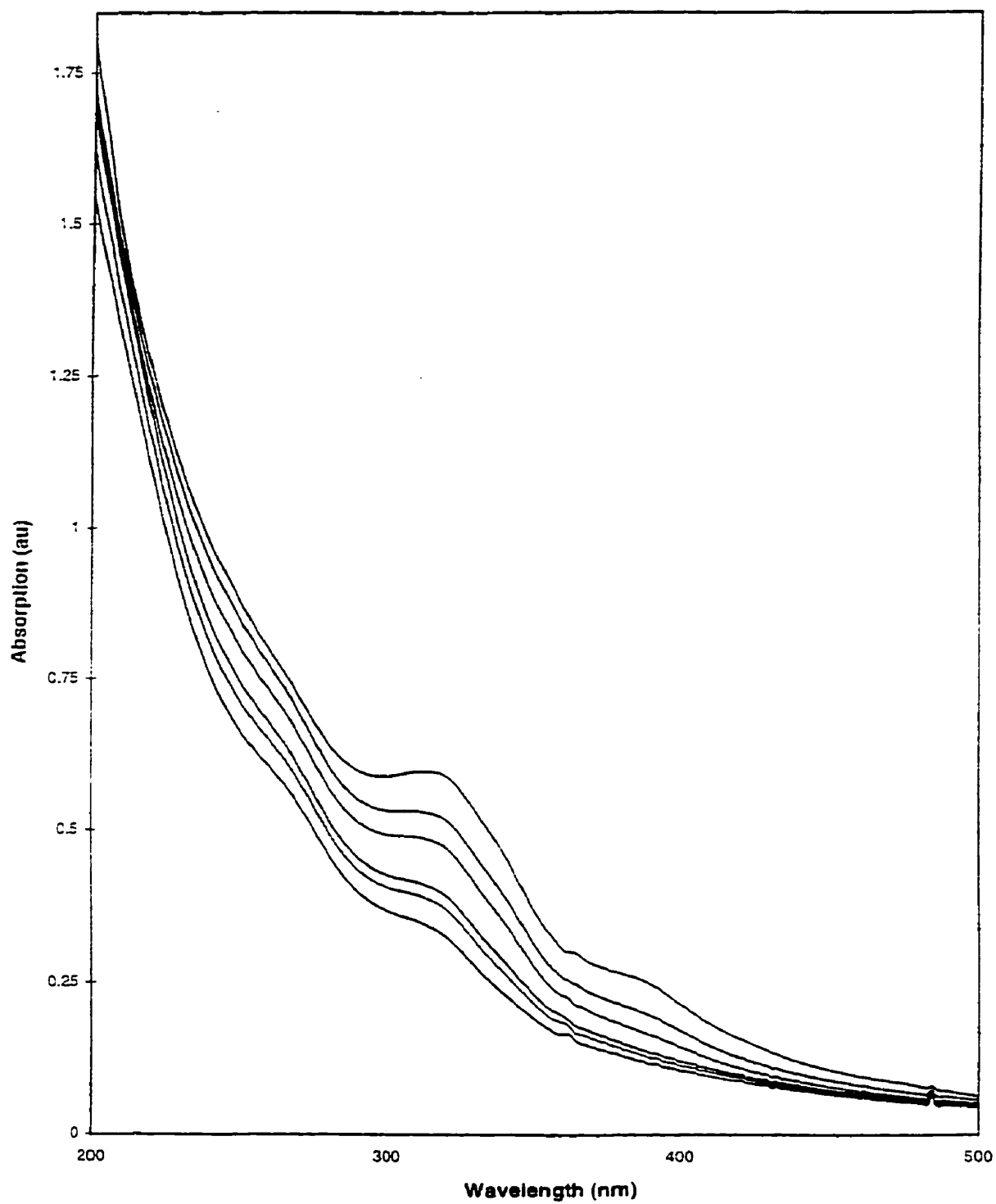


Figure 6.6. UV-Vis spectra of a 10-layered thin film of 2,4-hexadiyne-1,6-diol (1) upon exposure to UV-lamp for a period of 0, 5, 15, 30, 60 and 120 min (top to bottom).

However, only a broad absorption maximum with low intensity between 570 and 610 nm, which might correspond to the formation of the blue polymer after exposure of, for example, carboxylic acid-terminated alkanethiol diacetylene³⁸ to UV light, was observed. A similar formation of a blue film was observed by a naked eye, upon UV exposure of the thin film of **2**, with a weak and broad absorption maximum in the 570-610 nm wavelength region. The low intensity of these bands may be due to the fact that the absorption of C=C bonds, which form upon UV-polymerization, is not strong enough for identification. It is also possible that the topochemical polymerization in these thin films leads to a different polymer backbone structure.^{16b} For a monolayer of 2,4-hexadiyne-1,6-diol, the thickness is calculated to be 14 ± 2 Å, and upon topochemical polymerization, leading to a $\text{--}\equiv\text{--}\equiv\text{--}$ type of structure, it decreases to 12 ± 2 Å. The measured thickness of such a film was found to be 12 ± 2 Å by ellipsometry, and the latter decreased to 11 ± 2 Å upon UV-Vis exposure. Both water contact angle and ellipsometric thickness for the diacetylene films showed only a slight decrease upon UV-Vis exposure, indicating that there has been no gross-deterioration of the film quality on polymerization. A similar behavior has been observed for the diacetylenic dialkyl disulfide thin film on gold.³⁹

6.7 Conclusion

Self-assembled mono- and multilayers of a variety of organic chromophores terminated with OH groups on both ends on Si(100) (Si/SiO₂) surfaces have been successfully prepared by a simple acid-base hydrolytic chemistry route. Multilayers of up to 10 layers were fabricated from the dihydroxy molecules, and there was no increasing disorder upon addition of each successive layer. The stability of the thin films is significantly enhanced upon layer-by-layer deposition of the multilayered thin films. An increase in the intensity of the λ_{max} was observed upon multilayered thin film construction. It suggests that there is an increase in density of chromophores and a change in the

molecular alignment upon multilayer formation. Upon UV exposure, the intensity of the λ_{\max} decreased significantly with the subsequent formation of a blue film, and is accompanied by a structural change where the $\text{C}\equiv\text{C}$ bonds become parallel to the substrate upon topochemical polymerization.

6.8 Experimental Section

6.8.1 Materials

Hydroquinone ($\text{HO}-p\text{-C}_6\text{H}_4\text{-OH}$), biphenol ($\text{HO}-p\text{-C}_6\text{H}_4\text{-C}_6\text{H}_4\text{-OH}$) and 2,4-hexadiyne-1,6-diol ($\text{HOCH}_2\text{C}\equiv\text{CC}\equiv\text{CCH}_2\text{OH}$), were purchased from Aldrich Chemical Company Inc., and used without further purification. 5,7-Dodecadiyne-1,12-diol, 1,4-bis(6-hydroxyhexynyl)benzene, 4,4'-bis(6-hydroxyhexynyl)biphenyl, 9,10-bis(6-hydroxyhexynyl)anthracene, 1,4-bis(*p*-hydroxyphenylethynyl)benzene, 4,4'-bis(*p*-hydroxyphenylethynyl)biphenyl, were prepared by modification of published procedures.¹⁹⁻²⁰ Their purities were verified by routine analytical methods including ^1H NMR, mass spectra and FT-IR spectroscopy. Toluene and THF were dried and distilled over sodium. Single side polished Si(100) substrates were purchased from Nova Electronic Materials.

5,7-Dodecadiyne-1,12-diol, $\text{HO}(\text{CH}_2)_4\text{C}\equiv\text{C}-\text{C}\equiv\text{C}(\text{CH}_2)_4\text{OH}$ To a 100 ml Schlenk flask, charged with 10 ml freshly distilled pyridine, 5-hexyn-1-ol (1.0 ml, 8.7 mmol) and copper(I) chloride (0.1 g) were added. The solution was stirred rigorously at room temperature under oxygen for 4 h. The pyridine was removed in vacuo, and diethylether (10 ml) was added to the dark green liquid that turned pale green. The solvent was removed in vacuo, affording a white solid. It was recrystallized from diethyl ether. Yield: (0.7 g, 82%); Mass Spec (FAB): 194; IR (KBr) ν (OH): 3391, ν (CH_2): 2950, 2931, 2901, 2865 cm^{-1} , ν ($\text{C}\equiv\text{C}$): 2185, 2139 cm^{-1} ; ^1H NMR (270 MHz, CDCl_3) δ ppm

3.66 (t, 4H, $J = 6$ Hz, $-\underline{\text{CH}}_2\text{-OH}$), 2.29 (t, 4H, $J = 6$ Hz, $-\underline{\text{CH}}_2\text{-C}\equiv\text{C}-$), 1.64 (m, 8H, $-\text{CH}_2\text{-CH}_2-$), 1.33 (s, 2H, $-\text{OH}$).

1,4-bis(6-hydroxyhexynyl)benzene, $\text{HO}(\text{CH}_2)_4\text{C}\equiv\text{C}(p\text{-C}_6\text{H}_4)\text{C}\equiv\text{C}(\text{CH}_2)_4\text{OH}$

To a 100 ml Schlenk flask charged with 10 ml freshly distilled diethylamine, 5-hexyn-1-ol (1.5 ml, 0.012 mol), bis(trimethylphosphine)palladium(II) chloride (0.06 g) and copper(I) iodide (0.1 g) were added. To the above solution, *p*-diiodobenzene (2.0 g, 0.006 mol) dissolved in 10 ml diethylamine was added dropwise through an addition funnel. The resulting solution was stirred at room temperature under a nitrogen atmosphere for 18 h. The solvent was removed in vacuo, and the precipitate was extracted into dichloromethane. It was washed 2-3 times with dilute hydrochloric acid and deionized water. The dichloromethane layer was dried over MgSO_4 for 4 h, it was filtered and then the solvent was removed in vacuo. A pale yellow solid was obtained after recrystallization from diethylether. Yield: (0.7 g, 43%); Mass Spec (EI): 270; IR (KBr) ν (OH): 3361 cm^{-1} , ν (C_6H_4): $3076, 3036, 1507, 1483\text{ cm}^{-1}$, ν (CH_2): $2945, 2925, 2895, 2865, 2838\text{ cm}^{-1}$, ν ($\text{C}\equiv\text{C}$): 2231 cm^{-1} ; ^1H NMR (200 MHz, CDCl_3) δ ppm 7.21 (d, 4H, $J = 6$ Hz, C_6H_4), 3.71 (t, 4H, $J = 6$ Hz, $-\underline{\text{CH}}_2\text{-OH}$), 2.45 (t, 4H, $J = 6$ Hz, $-\underline{\text{CH}}_2\text{-C}\equiv\text{C}-$), 1.72 (m, 8H, $-\text{CH}_2\text{-CH}_2-$), 1.42 (s, 2H, $-\text{OH}$).

4,4'-bis(6-hydroxyhexynyl)biphenyl, $\text{HO}(\text{CH}_2)_4\text{C}\equiv\text{C}(p\text{-C}_6\text{H}_4\text{C}_6\text{H}_4)\text{C}\equiv\text{C}(\text{CH}_2)_4\text{OH}$

To a 100 ml Schlenk flask charged with 10 ml freshly distilled diethylamine, 5-hexyn-1-ol (1.5 ml, 0.012 mol), bis(trimethylphosphine)palladium(II) chloride (0.06 g) and copper(I) iodide (0.1 g) were added. To the above pale yellow solution, *p*-diiodobiphenyl (2.4 g, 0.006 mol) dissolved in 10 ml diethylamine was added dropwise using an addition funnel. The resulting solution was stirred at room temperature under an atmosphere of nitrogen for 18 h. The solvent was removed in vacuo and the bright yellow precipitate was extracted into dichloromethane. It was washed 2-3 times with dilute

hydrochloric acid and deionized water. The dichloromethane layer was dried over MgSO_4 for 4 h, it was filtered and the solvent was removed in vacuo. A pale yellow precipitate was obtained after being recrystallized from diethylether. Yield: (0.6 g, 30%); Mass Spec (FAB): 346; IR (KBr) ν (OH): 3378 cm^{-1} , ν (C_{12}H_8): $3089, 3033, 1493\text{ cm}^{-1}$, ν (CH_2): $2945, 2924, 2900, 2859, 2841\text{ cm}^{-1}$, ν ($\text{C}\equiv\text{C}$): $2230, 2210\text{ cm}^{-1}$; ^1H NMR (200 MHz, CDCl_3) δ ppm 7.46 (m, 8H, C_{12}H_8), 3.73 (t, 4H, $J = 6\text{ Hz}$, $-\underline{\text{CH}}_2\text{-OH}$), 2.49 (t, 4H, $J = 6\text{ Hz}$, $-\underline{\text{CH}}_2\text{-C}\equiv\text{C}-$), 1.72 (m, 8H, $-\text{CH}_2\text{-CH}_2-$), 1.20 (s, 2H, $-\text{OH}$).

9,10-bis(6-hydroxyhexynyl)anthracene, $\text{HO}(\text{CH}_2)_4\text{C}\equiv\text{C}(p\text{-C}_{14}\text{H}_8)\text{C}\equiv\text{C}(\text{CH}_2)_4$

OH To a 100 ml Schlenk flask, charged with 15 ml freshly distilled diethylamine, 5-hexyn-1-ol (1.5 ml, 0.012 mol), bis(trimethylphosphine)palladium(II) chloride (0.06 g) and copper(I) iodide (0.1 g) were added in that order. To the above solution, a solution of *p*-dibromoanthracene (2.02 g, 0.006 mol) dissolved in 10 ml diethylamine was added dropwise through an addition funnel. The resulting solution mixture was refluxed for 1 day under an atmosphere of nitrogen. The solvent was removed in vacuo and the green precipitate was extracted into dichloromethane. It was washed 2-3 times with dilute hydrochloric acid and deionized water. The dichloromethane layer was dried over MgSO_4 for 4 h, it was filtered and the solvent was removed in vacuo. A yellow solid was obtained after being recrystallized from diethylether. Yield: (0.72 g, 50%); Mass Spec (EI): 370. IR (KBr) ν (OH): 3300 cm^{-1} , ν (C_{14}H_8): $3059, 1619\text{ cm}^{-1}$, ν (CH_2): $2944, 2864, 2825\text{ cm}^{-1}$, ν ($\text{C}\equiv\text{C}$): 2207 cm^{-1} ; ^1H NMR (200 MHz, CDCl_3) δ ppm 8.54, 7.55 (d, 8H, $J = 4\text{ Hz}$, C_{14}H_8), 3.79 (t, 4H, $J = 4\text{ Hz}$, $-\underline{\text{CH}}_2\text{-OH}$), 2.82 (t, 2H, $J = 4\text{ Hz}$, $-\underline{\text{CH}}_2\text{-C}\equiv\text{C}-$), 1.92 (m, 8H, $-\text{CH}_2\text{-CH}_2-$), 1.35 (s, 2H, $-\text{OH}$).

1,4-bis(*p*-hydroxyphenylethynyl)benzene, $\text{HO}(p\text{-C}_6\text{H}_4)\text{C}\equiv\text{C}(p\text{-C}_6\text{H}_4)\text{C}\equiv\text{C}(p\text{-C}_6\text{H}_4)\text{OH}$

To a 100 ml Schlenk flask, charged with 10 ml freshly distilled diethylamine, *p*-iodophenol (1.1 g, 0.005 mol), bis(trimethylphosphine)palladium(II) chloride (0.02 g) and

copper(I) iodide (0.03 g) were added. To the above solution, *p*-diethynylbenzene (0.25 g, 0.002 mol) dissolved in 10 ml diethylamine was added dropwise through an additional funnel. The resulting solution mixture was stirred overnight at room temperature under an atmosphere of nitrogen. The diethylamine was then removed in vacuo and dichloromethane was added. The yellow precipitate obtained which was insoluble in dichloromethane was filtered, washed 2-3 times with dilute hydrochloric acid and deionized water, and recrystallized from methanol. Yield: (0.36 g, 50%); Mass Spec (EI): 310. IR (KBr) ν (OH): 3329 cm^{-1} , ν (C_6H_4): 3065, 3041, 1519 cm^{-1} , ν ($\text{C}\equiv\text{C}$): 2216 cm^{-1} ; ^1H NMR (200 MHz, CD_3OD) δ ppm 7.44, 7.35, 6.79 (d, 12H, $J = 8$ Hz, C_6H_4), 3.35 (s, 2H, -OH).

4,4'-bis(*p*-hydroxyphenylethynyl)biphenyl, $\text{HO}(p\text{-C}_6\text{H}_4)\text{C}\equiv\text{C}(p\text{-C}_6\text{H}_4\text{-C}_6\text{H}_4)\text{C}\equiv\text{C}(p\text{-C}_6\text{H}_4)\text{OH}$ To a 100 ml Schlenk flask, charged with 15 ml freshly distilled diethylamine, *p*-iodophenol (0.82 g, 0.003 mol), bis(trimethylphosphine)palladium(II) chloride (0.01 g) and copper(I) iodide (0.02 g) were added in that order. To the above solution, we added dropwise the solution of *p*-diethynylbiphenyl (0.3 g, 0.001 mol) dissolved in 10 ml diethylamine through additional funnel. The resulting solution mixture was stirred overnight at room temperature under an atmosphere of nitrogen. The diethylamine was then removed in vacuo and dichloromethane was added. The yellow precipitate which was insoluble in dichloromethane was filtered, washed 2-3 times with dilute hydrochloric acid and deionized water, and recrystallized from methanol. Yield: (0.3 g, 50%); Mass Spec (EI): 386. IR (KBr) ν (OH): 3384, 3277 cm^{-1} , ν (C_6H_4): 3065, 3038, 1512, 1488 cm^{-1} , ν ($\text{C}\equiv\text{C}$): 2215 cm^{-1} ; ^1H NMR (200 MHz, *d*-DMSO) δ ppm 7.78, 7.61, 7.42, 6.83 (d, 16H, $J = 8$ Hz, C_6H_4), 1.14 (s, 2H, -OH).

6.8.2 Substrate Preparation

The glass, quartz or single crystal Si wafers were first cleaned i) by soaking in soap solution and sonocating for 1 h; ii) repeated washings with deionized water; iii) treatment

with a solution mixture containing 70% conc. H_2SO_4 and 30% H_2O_2 (piranha solution) at 100 °C for 1 h. *Caution:* Piranha solution is highly explosive, and care should be taken while using this mixture; iv) repeated washing with deionized water; and v) finally heating in oven at 150 °C for 5 min and vacuum drying for 5 min to remove physisorbed water.

6.8.3 Preparation of SAMs

The surface functionalization involved a two-step process of i) reaction with 0.5 % solution by volume of $\text{Si}(\text{NEt}_2)_4$, which can be conveniently prepared¹⁸ by the reaction of SiCl_4 and excess dry NEt_2H , in dry toluene at room temperature for 8 h; followed by ii) treatment with 0.1 % by weight of the organic chromophore in dry THF at 40 °C for 1 day after sonicating in dry toluene for 5 min to remove excess $\text{Si}(\text{NEt}_2)_4$ physisorbed on the surface. After thorough washing with anhydrous THF, the substrates were dried at 120 °C for 5 min.

6.8.4 Preparation of Multilayers

The multilayered thin film assemblies of 2,4-hexadiyne-1,6-diol (**1**) or 5,7-dodecadiyne-1,12-diol (**2**) were prepared by immersion of the monolayer substrates into 0.5 % by volume of anhydrous toluene solution of $\text{Si}(\text{NEt}_2)_4$ at room temperature for 8 hr, followed by treatment with 0.1 % by weight of anhydrous THF solution of **1** or **2** at 40 °C for up to 24 h, after sonicating into anhydrous toluene for 5 min. The two-layer substrates thus obtained were thoroughly washed with anhydrous THF and then dried at 120 °C for 5 min. The procedure was repeated to obtain multilayered thin films.

6.8.5 Contact-Angle ($\text{CA}_{\text{H}_2\text{O}}$) Measurements

The static and advancing contact angles were measured with a Rame-Hart NRL 100 goniometer. On average, 6 drops of water were measured on different areas of the polished side of a silicon wafer for each sample, and the values reported are the mean values with a

maximum range of $\pm 2^\circ$. The advancing contact angles of captive drops were found to be roughly 5° above the static values of sessile (free-standing) drops. If the drop was allowed to fall from the needle of the syringe to the surface, smaller contact angles were usually obtained because of the mechanical vibrations.²⁶

6.8.6 Fourier Transform Infrared Spectroscopy in the Attenuated Total Reflection Mode (FTIR-ATR)

The organic thin films were grown on the $\langle 100 \rangle$ surfaces of the single side polished silicon wafers. A KRS crystal was sandwiched between the reflective faces of two silicon wafers (1.2 cm X 4.0 cm), and the angle of non-polarized light was set at an angle of 45° . All spectra were run for 4000 scans at a resolution of 4 cm^{-1} , using a Bruker IFS-48 spectrometer. A spectrum of two clean silicon wafers with a sandwiched KRS crystal was measured as a background correction.

6.8.7 Ellipsometry

A Gaertner Scientific ellipsometer operating at 633 nm He-Ne laser ($\lambda = 6328 \text{ \AA}$) was employed. The angle of incidence was 70.0° , and the compensator was set at 45.0° . All reported values are the average of at least six measurements taken at different locations on the sample. The error bar of the thickness increases from $\pm 2 \text{ \AA}$ for 1 to 4-layer, to $\pm 6 \text{ \AA}$ for 8 to 10-layer. The thickness was calculated by comparing data from the same substrate before and after functionalization and using a value of 1.46 for the refractive index. This value is based on the assumption that the monolayer is similar to bulk paraffins with a refractive index of 1.45.²⁸ If the monolayer is more crystalline-like, similar to polyethylene, the refractive index thus should be within 1.49-1.55.²⁶ It was found that an increase of 0.1 in the refractive index from 1.45 to 1.55 resulted in a decrease in the measured thickness by $\sim 2 \text{ \AA}$.

6.8.8 X-ray Photoelectron Spectroscopy (XPS)

The XPS spectra were obtained by using a VG Escalab MKII spectrometer with monochromatized MgK_α X-ray source to produce the photoemission of electrons from the core levels of the surface atoms. About 50 Å of depth was probed for a detector perpendicular to the surface. The analyzed surface was 2 x 3 mm. All peak positions were corrected for carbon at 285.0 eV in binding energy to adjust for charging effects. The power of the source was 300 watts and a pressure of 10^{-9} mbar.

6.8.9 UV-Polymerization

Topochemical polymerization was carried out by placing the substrates into a container, and irradiating them under a nitrogen purge for up to 120 min with a medium pressure Hg vapor lamp (Ace-Hanovia photochemical lamp, model 7830, 230-430 nm with the main spike at 365 nm), with the sample-to-source distance of approx. 3 cm.

6.9 References

- (1) (a) Jackman, R. J.; Wilbur, J. L.; Whitesides, G. M. *Science* **1995**, 269, 664. (b) Chidsey, C.E.D. *Science* **1991**, 251, 919.
- (2) Sagiv, J. *J. Am. Chem. Soc.* **1980**, 102, 92.
- (3) Bain, C. D.; Troughton, E. B.; Tao, Y.; Whitesides, G. M.; Nuzzo, R. G. *J. Am. Chem. Soc.* **1989**, 111, 321.
- (4) Porter, M. D.; Bright, T. B.; Allara, D. L.; Chidsey, C. E. D. *J. Am. Chem. Soc.* **1987**, 109, 3559.
- (5) Walczak, M. M.; Chung, C.; Stole, S. M.; Widrig, C. A.; Porter, M. D. *J. Am. Chem. Soc.* **1991**, 113, 2370.
- (6) Laibinis, P. E.; Whitesides, G. M.; Allara, D. L.; Tao, Y.; Parikh, A. N.; Nuzzo, R. G. *J. Am. Chem. Soc.* **1991**, 113, 7152.

- (7) Troughton, E. B.; Bain, C. D.; Whitesides, G. M.; Nuzzo, R. G.; Allara, D. L.; Porter, M. D. *Langmuir*, **1988**, 4, 365.
- (8) Nuzzo, R. G.; Fusco, F. A.; Allara, D. L. *J. Am. Chem. Soc.* **1987**, 109, 2358.
- (9) Tao, Y. *J. Am. Chem. Soc.* **1993**, 115, 4350.
- (10) Linford, M. R.; Fenter, P.; Eisenberger, P. M.; Chidsey, C. E. D. *J. Am. Chem. Soc.* **1995**, 117, 3145.
- (11) (a) Ulman, A. *Adv. Mater.* **1990**, 2, 573. (b) Swalen, J. D.; Allara, D. L.; Andrade, J. D.; Chandross, E. A.; Garoff, S.; Israelachvili, J.; McCarthy, T. J.; Murray, R.; Pease, R. F.; Rabolt, J. F.; Wynne, K. J.; Yu, H. *Langmuir* **1987**, 3, 932.
- (12) (a) Finklea, H. O.; Robinson, L. R.; Blackburn, A.; Richter, B.; Allara, D.; Bright, T. *Langmuir* **1986**, 2, 239. (b) Maoz, R.; Sagiv, J. *Langmuir* **1987**, 3, 1045.
- (13) Tilman, N.; Ulman, A.; Penner, T. L. *Langmuir* **1989**, 5, 101.
- (14) Maoz, R.; Sagiv, J. *Langmuir* **1987**, 3, 1045.
- (15) Kato, S.; Pac, C. *Langmuir* **1998**, 14, 2372.
- (16) (a) Yam C. M.; Tong, S. S. Y.; Kakkar A. K. *Langmuir* **1998**, 14, 6941. (b) Yam, C. M.; Dickie, A.; Malkhasian, A.; Kakkar, A. K.; Whitehead, M. A. *Can. J. Chem.* **1998**, 76, 1766. (c) Yam C. M.; Kakkar A. K. *J. Chem. Soc., Chem. Commun.* **1995**, 907.
- (17) Fessenden, R.; Fessenden, J. S. *Chem. Rev.* **1961**, 61, 361
- (18) Anderson, H. H. *J. Am. Chem. Soc.* **1952**, 74, 1421.
- (19) Hay, A. *J. Polym. Sci. Pt. A-1*, **1969**, 7, 1625
- (20) (a) Nguyen, P.; Yuan, Z.; Agocs, L.; Lesley, G.; Marder, T. *Inorg. Chim. Acta* **1994**, 220, 289. (b) Takahashi, S.; Kuroyama, Y.; Sonogashira, K.; Hagihara, N. *Synthesis Commun* **1980**, 627.
- (21) Wasserman S. R., Tao Y.; Whitesides, G. M. *Langmuir* **1989**, 5, 1074.
- (22) Evans S. D.; Sharma R.; Ulman A. *Langmuir* **1991**, 7, 156.
- (23) Tao Y.; Chang S.; Ma, L. *J. Chin. Chem. Soc.* **1995**, 42, 659.

- (24) Ulman, A.; Tillman, N. *Langmuir* **1989**, *5*, 1418.
- (25) Holmes-Farley, S. R.; Whitesides, G. M. *Langmuir* **1987**, *3*, 62.
- (26) Ulman A. *An Introduction to Ultrathin Films from Langmuir-Blodgett to Self-Assembly*; Academic Press: Boston, 1991.
- (27) Azzam R. M. A.; Bashara N. M. *Ellipsometry and Polarized Light* ; North-Holland Publishin Company: Amsterdam, 1977.
- (28) Wasserman S. R.; Whitesides G. M.; Tidswell I. M.; Ocko B. M.; Pershan P. S.; Axe J. D. *J. Am. Chem. Soc.* **1989**, *111*, 5852.
- (29) Dean J. A. *Lange's Handbook of Chemistry*; McGraw-Hill: New York, 1992.
- (30) Frydman E.; Cohen H.; Maoz R.; Sagiv J. *Langmuir* **1997**, *13*, 5089.
- (31) (a) Snyder, R. G.; Strauss, H. L.; Elliger, C. A. *J. Phys. Chem.* **1982**, *86*, 5145.
(b) Snyder, R. G.; Maroncelli, M.; Strauss, H. L.; Hallmark, V. M. *J. Phys. Chem.* **1986**, *90*, 5623.
- (32) Tillman, N.; Ulman, A.; Schildkraut, J. S.; Penner, T. L. *J. Am. Chem. Soc.* **1988**, *110*, 6136.
- (33) (a) Sabatini, E.; Moulakia, J.; Bruening, M.; Rubinstein, I. *Langmuir* **1993**, *9*, 2974. (b) Dhirani, A. A.; Zehner, R. W.; Hsung, R. P., Sionnest, P. G.; Sita, L. R. *J. Am. Chem. Soc.* **1996**, *118*, 3319.
- (34) Tour, J. M.; Jones, L., II; Pearson, D. L.; Lamba, J. J, S.; Burgin, T. P.; Whitesides, G. M.; Allara, D. L.; Parikh, A. N.; Atre, S. V. *J. Am. Chem. Soc.* **1995**, *117*, 9529.
- (35) Maoz, R; Sagiv, J. *J. Colloid Interface Sci.* **1984**, *100*, 465.
- (36) Pomerantz, M.; Segmuller, A.; Netzer, L.; Sagiv, J. *Thin Solid Films* **1985**, *132*, 153.
- (37) Porter, M. *Anal. Chem.* **1988**, *6*, 1143A.
- (38) Kim, T.; Crooks, R.; Tsen, M.; Sun, L. *J. Am. Chem. Soc.* **1995**, *117*, 3963.

- (39) Batchelder, D. N.; Evans, S. D.; Freeman, T. L.; Haussling, L.; Ringsdorf, H.; Wolf, H. *J. Am. Chem. Soc.* **1994**, *116*, 1050.

Chapter Seven

Molecular Self-Assembly of Alkynyl Terminated Chromophores via Acid-Base Hydrolytic Chemistry on Inorganic Oxide Surfaces: Monolayer and Step-by-Step Multilayered Thin Film Construction

7.1 Introduction

In recent years, organized molecular systems have attracted growing attention because they offer significant potential in technology¹ which includes, for example, protective and patternable materials, surface preparation and modification, chemically modified electrodes, and biological thin films of proteins. The common techniques² for the construction of such systems comprise Langmuir-Blodgett (LB) and molecular self-assembly (SA), resulting in ordered monolayers. Some of the commonly used methodologies for molecular self-assembly are organosilicon derivatives on silica surfaces,³ alkanethiols on gold,^{4,5} silver,⁶ and copper,⁷ dialkyl sulfides on gold,⁸ dialkyl disulfides on gold,⁹ alkanolic acids¹⁰ on silver, copper and aluminum oxide, 1-alkenes on hydrogen terminated Si(111)¹¹, alkanols¹² and alkynes¹³ on Si/SiO₂. They have been shown to form uniform and ordered structures. Thin films with useful aromatic and acetylenic groups have growing prominence in industry because of their optical and electronic uses.¹⁴

In order to transform thin films into practical devices, multilayers of appropriate thickness need to be reproducibly constructed with minimum reduction in order.¹⁵ In general, multilayered thin films on silica based surfaces are fabricated by modifying the monolayer surface to a hydroxylated one, by the reduction of surface ester group¹⁵, the

hydroboration-oxidation of the terminal vinyl group,¹⁶ the photolysis of the nitrate-bearing group,¹⁷ and the hydrolysis of the boronate-protecting group.¹⁸

We have discussed the construction of monolayers and multilayers of alcohols on Si/SiO₂ via acid-base hydrolytic chemistry in Chapters 5 and 6. An elaboration of this approach using aminostannanes can be used to construct multilayers of alkynes on Si/SiO₂. The reactivity of aminostannanes with molecules containing terminal acidic groups has been well studied.¹⁹ Owing to the high basicity of nitrogen in aminostannanes, the Sn-NEt₂ bond can be easily cleaved by a variety of protic species including acetylenes. Using the acid-base hydrolytic chemistry approach, silica surfaces functionalized with Sn-NEt₂ groups can be easily modified with a number of terminal alkyne molecules with varied backbones.¹³ In this chapter, we discuss a two-step thin film construction process involving the reaction of Sn(NEt₂)₄ with hydroxyl groups of the inorganic oxide surfaces, followed by the reaction with a variety of alkyne molecules incorporating alkyl and aromatic moieties in the backbone. By repetitive reactions with Sn(NEt₂)₂ followed by H-C≡C-R-C≡C-H, multilayered thin film assemblies were fabricated on glass, quartz, and single-crystal Si. The mono- and multilayered thin films were characterized using surface wettability measurements, ellipsometry, XPS, FTIR-ATR, and UV-vis spectroscopy. Our results indicate that thin films of appropriate thickness using dialkynyl chromophores could be easily adsorbed using acid-base hydrolytic chemistry. Surface coverage of rigid-rod alkynes, H-C≡C-R-C≡C-H (R = *p*-C₆H₄, *p*-C₆H₄-C₆H₄, *p*-C₁₄H₈, -C≡C-*p*-C₆H₄-C≡C-), was estimated to be 2-7 molecules/100 Å² which is comparable to the surface hydroxyl density for silica, degassed at 100-150 °C. We have also investigated topochemical polymerization of diacetylene moiety in a SAM of H-C≡C-C≡C-*p*-C₆H₄-C≡C-C≡C-H, and upon UV-Vis exposure, the formation of a blue film was observed. The adsorption of Co₂(CO)₈ in the mono- and multilayered alkyne assemblies was found to be feasible under room temperature conditions. These alkynyl surfaces may become potential candidates for

tethering transition metal fragments leading to organometallic surfaces for heterogenized homogeneous catalysis, one-dimensional conductors, and chemically modified electrodes and sensors.^{1,14}

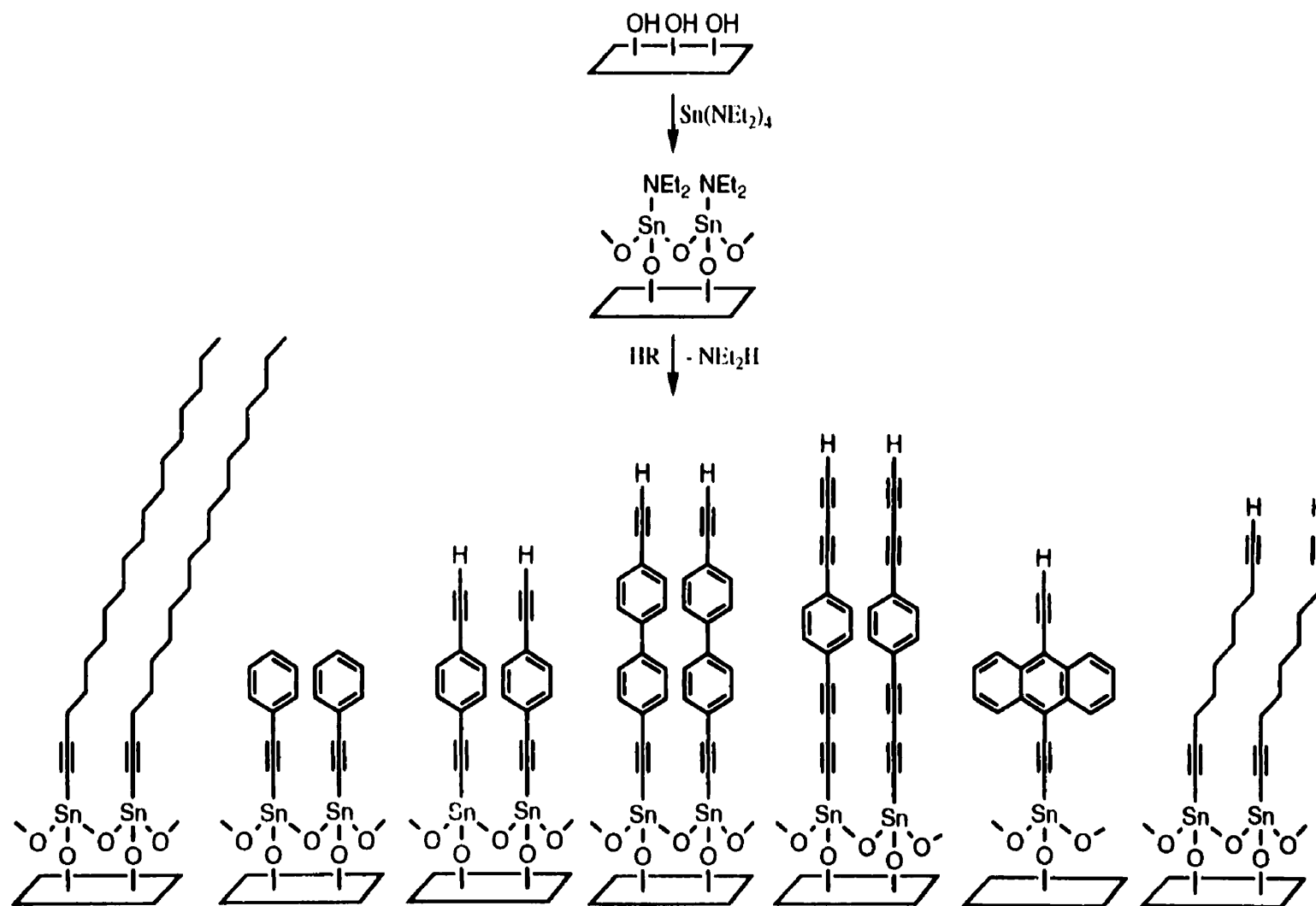
7.2 Acid-Base Hydrolysis

When chlorostannanes react with LiNR_2 ($\text{R} = \text{Me, Et}$), the corresponding aminostannanes ($\text{Me}_3\text{Sn-NR}_2$, $\text{R} = \text{Me, Et}$) are produced in very good yields.¹⁹ Aminostannanes then undergo acid-base hydrolysis with molecules containing terminal acetylene groups to yield stannyl-alkynes.¹⁹ Since the surfaces of inorganic oxides such as silica, glass and quartz contain hydroxyl groups, the acid-base hydrolytic chemistry can be easily applied to these surfaces to give a versatile chemisorption method for a variety of organic microstructures. The hydroxyl groups on the surface of silica were first treated with $\text{Sn}(\text{NEt}_2)_4$ to produce the surface-anchored Sn-NEt_2 groups, which further react with terminal alkyne molecules with varied backbones, leading to ordered thin films based on simple acid-base hydrolytic chemistry (Scheme 7.1).¹³ By repeating this two-step process and using bifunctional chromophores ($\text{H-C}\equiv\text{C-R-C}\equiv\text{C-H}$), multilayers of alkynes with desired backbones were constructed (Scheme 7.2).

7.3 Monolayers of Alkynes

The SAMs of alkynes with varied chain-lengths were characterized by surface wettability measurements, ellipsometry, XPS and FTIR-ATR, and the data are presented in Tables 7.1 and 7.2.

Scheme 7.1 Molecular self-assembly of a series of alkynyl chromophores on glass, quartz and single crystal silicon



Scheme 7.2 A step-by-step reaction methodology for fabrication of multilayers of dialkynes on glass, quartz and single crystal silicon

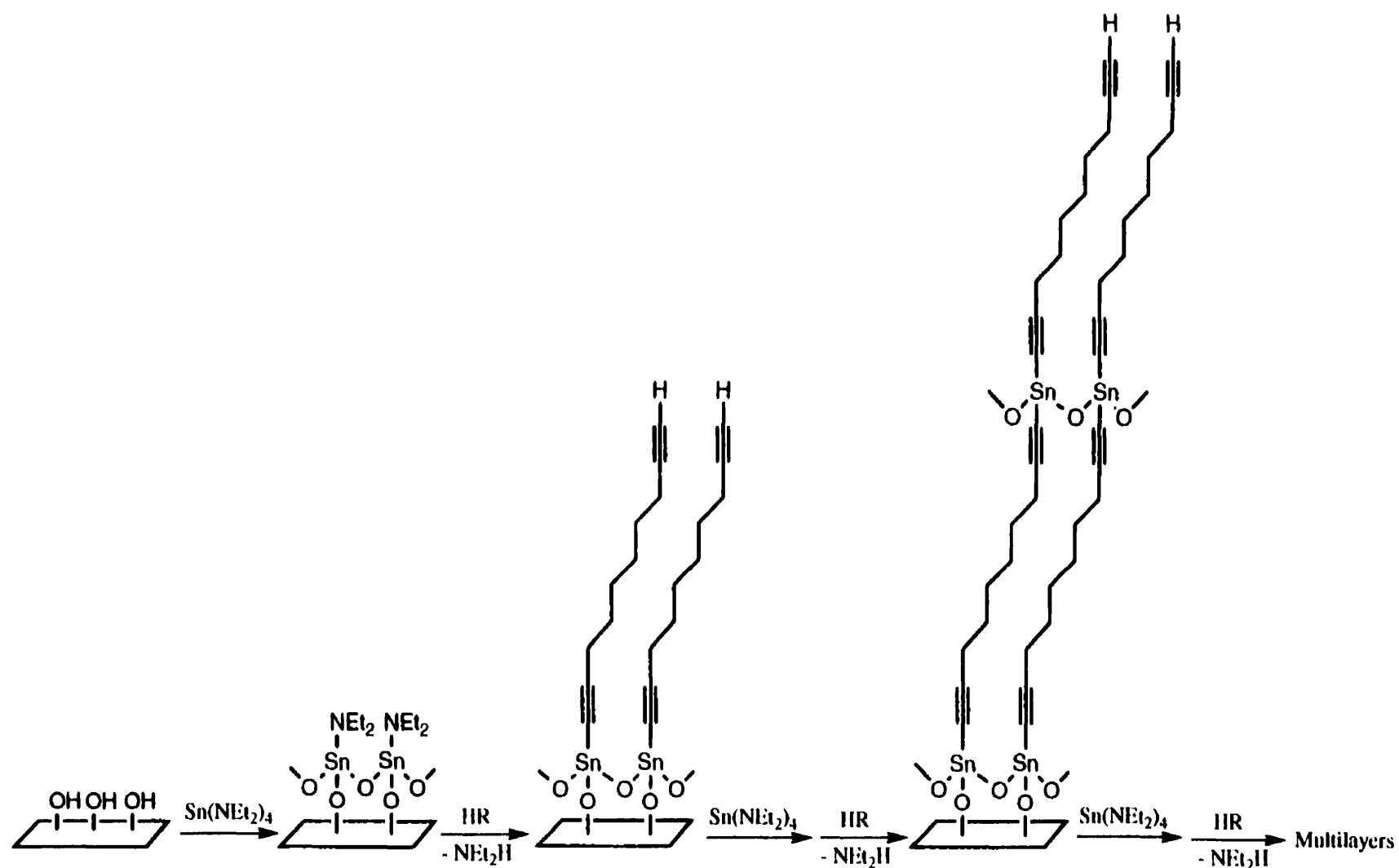


Table 7.1. Static contact angles of water and HD, theoretical (T_t) and ellipsometric thicknesses (T_e), and XPS data for SAMs of alkynes on Si(100) substrates

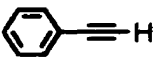

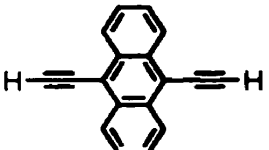
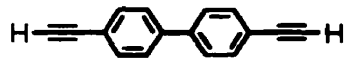

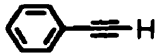

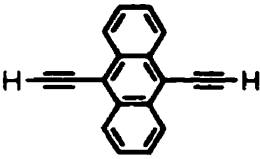


Alkyne	Contact Angle H_2O (HD), °	T_t , Å	T_e , Å	XPS Data (eV) C(1s), O(1s), Si-Si(2p), Si-O(2p), Sn(3d ₃ , 3d ₅)
$CH_3-(CH_2)_{15}-\equiv H$	110 (25)	27	25	285.0, 532.3, 99.0, 103.0, 495.4, 486.9
	80 (12)	11	10	285.0, 291.1, 532.3, 495.8, 487.3
	80 (12)	13	12	285.0, 291.1, 532.0, 99.1, 102.9, 495.5, 487.0
	80 (12)	13	13	285.0, 291.2, 532.2, 99.1, 102.5, 495.2, 486.7
	82 (15)	18	17	285.0, 291.2, 532.5, 98.8, 102.7, 495.4, 487.1
	82 (15)	18	17	285.0, 291.2, 532.4, 99.1, 103.0, 495.5, 487.1
$H-\equiv-(CH_2)_2-\equiv H$	75 (12)	13	10	285.0, 532.1, 99.0, 102.5, 495.4, 487.0
$H-\equiv-(CH_2)_4-\equiv H$	75 (12)	15	12	285.0, 532.6, 99.4, 103.2, 495.9, 487.5
$H-\equiv-(CH_2)_5-\equiv H$	80 (15)	17	14	285.0, 532.4, 99.1, 103.0, 495.6, 487.2
$H-\equiv-(CH_2)_6-\equiv H$	80 (15)	18	16	285.0, 532.5, 99.3, 103.1, 495.8, 487.3

Table 7.2. FTIR-ATR data for SAMs of alkynes on Si(100) substrates

Alkyne	$\nu_{\text{C}\equiv\text{C-H}}, \nu_{\text{C}\equiv\text{C}}$ cm^{-1}	$\nu_{\text{a}}(\text{CH}_2), \nu_{\text{s}}(\text{CH}_2)$ cm^{-1}	$\nu(\text{C}_6\text{H}_5)$ cm^{-1}
$\text{CH}_3-(\text{CH}_2)_{15}-\text{C}\equiv\text{H}$	2077	2918, 2850	
	2106		3066, 1485
	3275, 2103		3082, 1500
	3350, 2066		3124, 1593
	3260, 2097		3033, 1498
	3252, 2165		3094, 1484
$\text{H}-\text{C}\equiv\text{C}-(\text{CH}_2)_2-\text{C}\equiv\text{C}-\text{H}$	3290, 2145	2918 (br), 2848 (br)	
$\text{H}-\text{C}\equiv\text{C}-(\text{CH}_2)_4-\text{C}\equiv\text{C}-\text{H}$	3379, 2118	2921, 2851	
$\text{H}-\text{C}\equiv\text{C}-(\text{CH}_2)_5-\text{C}\equiv\text{C}-\text{H}$	3350, 2064	2919, 2850	
$\text{H}-\text{C}\equiv\text{C}-(\text{CH}_2)_6-\text{C}\equiv\text{C}-\text{H}$	3250, 2097	2920, 2850	

Contact angle goniometry has been routinely used to determine the wetting behavior of thin film assemblies.² Upon comparing the water contact angle of a SAM of octadecyne (110°) with that from SAMs of OTS on silica²⁴ and octadecanethiol on gold,⁴ it is apparent that the new acid-base hydrolytic approach is capable of producing thin films of comparable quality and order. However, the contact angle with hexadecane (CA_{HD}) was found to be about 10° lower for the octadecyne SAM (25°) on Si(100) than those reported for the OTS SAMs on silica-based surfaces (35-40°). This may be due to (i) the higher hydrophilicity of $[Si]-O-Sn-C\equiv C-R$ in our SAM than $[Si]-CH_2-R$ in OTS, and (ii) the Si(100) surface employed in our studies, which have been discussed in Chapter 5.

The lower contact angle of water (75-82°) and hexadecane (12-15°) on the acetylene- or phenyl-terminated surfaces than the corresponding long alkyl chains (paraffins, ca. 110° (water) and 35-40° (hexadecane)) may be the result of the stronger interactions between $-C\equiv C-H$ (sp hybridization) or $-C_6H_5$ (sp^2 hybridization) groups and water than CH_3 (sp^3) groups,¹³ as well as the introduction of disorder into the assemblies by surface functionality.^{12a} The wetting nature of alkynyl surfaces terminated with acetylene or phenyl groups is comparable to that obtained from thio-alkynyl thin films on gold.²⁰

As the chain-length of the alkyne decreases from $-C\equiv C-(CH_2)_6-C\equiv C-H$ to $-C\equiv C-(CH_2)_2-C\equiv C-H$, CA_{H_2O} and CA_{HD} drop from 80° to 75°, and 15° to 12°, respectively (Figure 7.1). It may be due to the sensitivity of the probe liquid to the underlying substrate,^{4,6} as well as the structures becoming increasingly disordered.^{5,10} For shorter chains, the film is less ordered and dense owing to the lack of cohesive interactions. As the chain length increases, the cohesive forces become strong enough to pull the molecular chains into 'normal' orientation for optimal interaction energy.⁵ Studies of alkanethiols adsorbed on gold and silver surfaces,^{6,7} and alkynyl on Si/SiO₂^{12a} showed similar results.

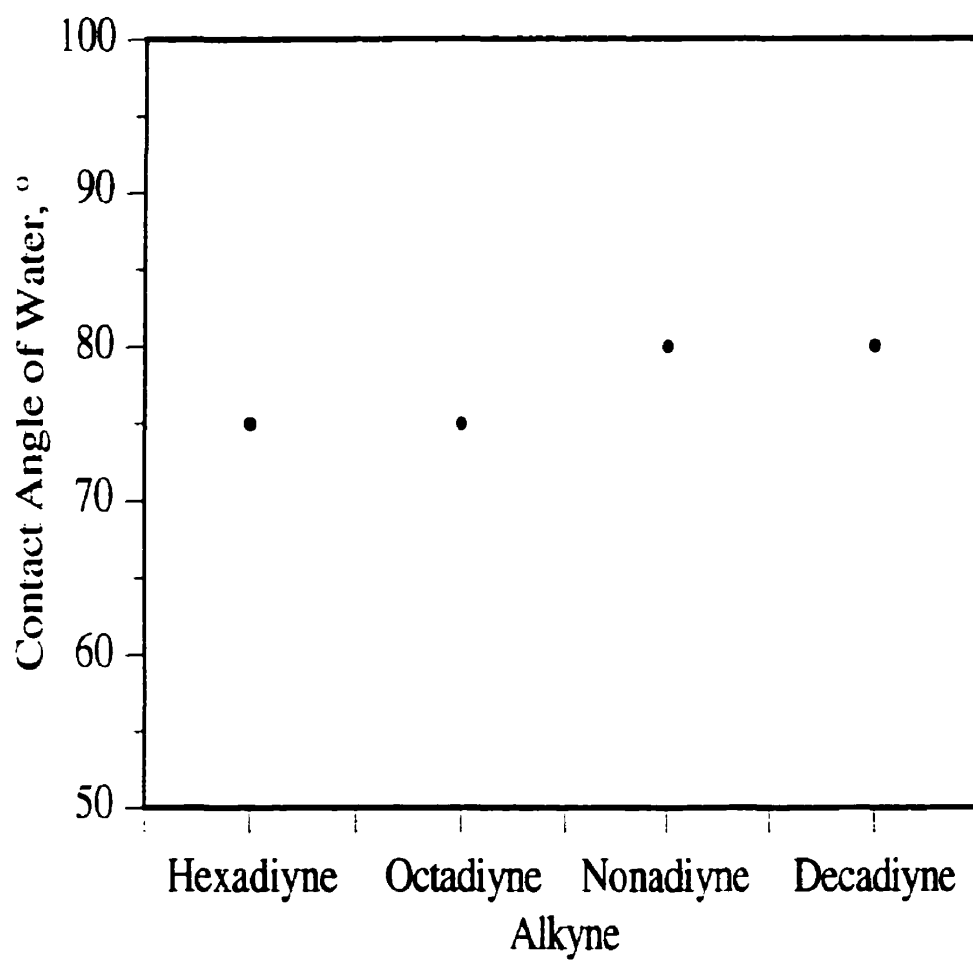


Figure 7.1 Static contact angles of water for monolayers of hexadiyne, octadiyne, nonadiyne and decadiyne on Si(100) substrate.

The thicknesses of the newly self-assembled thin films were measured using ellipsometry. The refractive index for the alkynyl films was assumed to be 1.46^{13a} for calculations. This is comparable to the literature values for the refractive index of hydrocarbon thin film on Si/SiO₂ of 1.45-1.50.²¹ The film thickness was calculated on the basis of data comparison from the same substrate before and after functionalization. A detailed discussion of the ellipsometric technique for the characterization of thin films has been reported elsewhere.²¹⁻²² Table 7.1 shows the ellipsometric thicknesses obtained for the alkynyl films. Theoretical thicknesses were calculated based on typical values²³ of bond lengths between elements projected on the surface. For example, for a trans-extended chain, the projections of the Si-O, Sn-O, Sn-C≡C, C≡C, C≡C-CH₂, CH₂-CH₂ and C≡C-H bonds onto the surface normal (z-axis) are 1.33, 1.58, 2.18, 1.18, 1.46, 1.26 and 1.06 Å, respectively. Hence, a monolayer prepared from 1,9-decadiyne is expected to have a thickness of 18 Å. As shown in Figure 7.2, the ellipsometric thicknesses are in good agreement with theoretical value, and suggest the formation of relatively close-packed monolayers with a slight tilt to normal.

X-ray photoelectron spectroscopy provides a qualitative evidence of the surface composition of thin films. According to Table 7.1, various alkynyl thin films on Si(100) were found to consist of silicon: 2p, 99 eV, 2p, 103 eV; carbon: 1s, 285 eV; oxygen: 1s, 532-533 eV; and tin: 3d_{3/2}, 495-496 eV, 3d_{5/2}, 487 eV, confirming the surface composition of the thin films. The molecules containing conjugated backbones showed a peak at 291 eV for C_{1s}, corresponding to, for example, aromatic carbon.

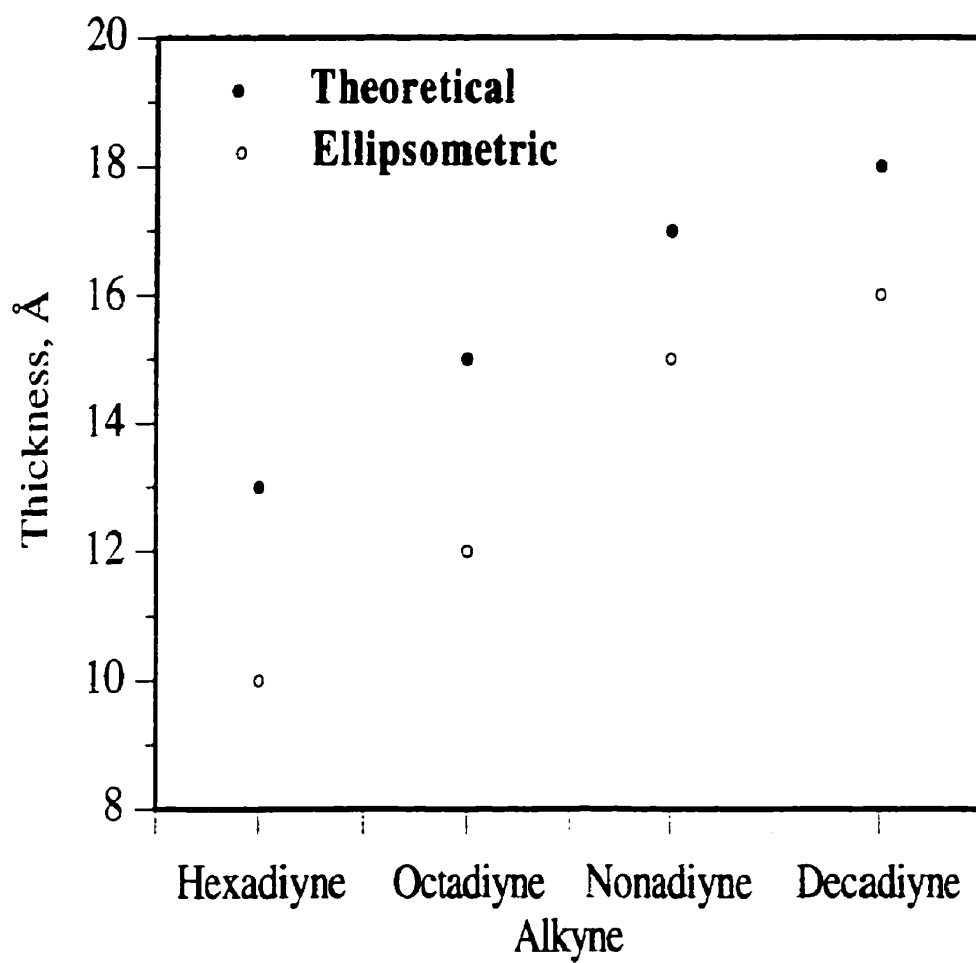


Figure 7.2 Ellipsometric thickness for monolayers of hexadiyne, octadiyne, nonadiyne and decadiyne on Si(100) substrate.

Fourier transform infrared spectroscopy in the attenuated total reflection mode (FTIR-ATR) has been extensively used for the identification of the newly developed thin films.² For the alkyne SAMs containing varied alkyl chain-lengths in the backbone $-(\text{CH}_2)_n-$, $n = 2, 4, 5, 6$, the $\nu_a(\text{CH}_2)$ and $\nu_s(\text{CH}_2)$ stretching frequencies were observed at ~ 2920 and $\sim 2850 \text{ cm}^{-1}$, respectively, with the peaks becoming broader and less intense as the chain-length decreased (Figure 7.3). These observations are consistent with the results on alkyltrichlorosilanes²⁴ and alkynyl^{12a} on glass and thiols⁵ on gold, demonstrating that the structure of these SAMs with shorter chain-length is less ordered and more liquid-like. The positions for asymmetric and symmetric methylene stretches at ~ 2920 and $\sim 2850 \text{ cm}^{-1}$ for longer alkyl chains indicate that π - π interactions of $\text{C}\equiv\text{C}$ groups may complement the order of the systems. A typical spectral pattern for an ordered hydrocarbon assembly gives the peak positions for asymmetric and symmetric methylene stretching frequencies at 2918 and 2849 cm^{-1} , respectively.^{5,24} The $\nu_a(\text{CH}_2)$ and $\nu_s(\text{CH}_2)$ stretching frequencies of octadecyne SAM on the Si(100) surfaces were observed at 2918 and 2850 cm^{-1} . These are consistent with previous published results for OTS on silica based surfaces²⁴ and octadecanethiol on gold,⁵ suggesting that they are highly ordered.

The peaks at ca. 2100 ($\nu_{\text{C}\equiv\text{C}}$), 3300 ($\nu_{\text{C}\equiv\text{C-H}}$), 3050 and 1500 cm^{-1} ($\nu(\text{C}_6\text{H}_5)$) correspond to the acetylene and phenyl groups of the alkyne SAMs. As compared to the spectra from a KBr pellet (or nujol) of the pure compound, the frequencies of the acetylene and phenyl groups on surface are shifted slightly because of the orientation effects in the SAMs,²⁵ as reported similarly for thio-alkynyl films on gold²⁰ and alkynyl on Si/SiO₂.^{12a}

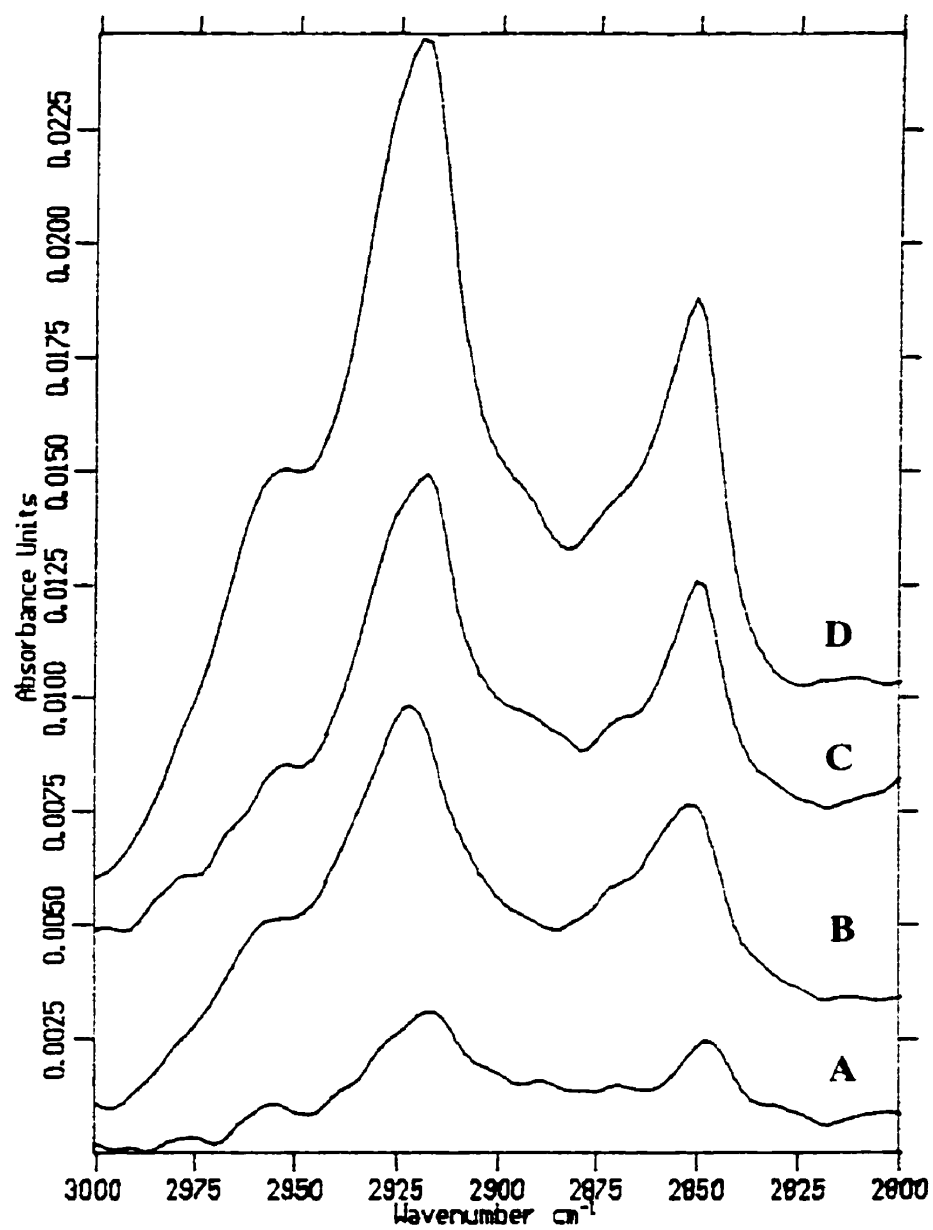



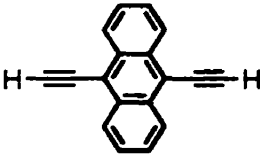
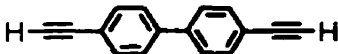

Figure 7.3 FTIR-ATR (nonpolarized) spectra for monolayers of hexadiyne (A), octadiyne (B), nonadiyne (C) and decadiyne (D) on Si(100) substrates in the region 2800-3000 cm^{-1} .

7.4 Estimation of Surface Coverage of Rigid-Rod Alkyne Chromophores

The UV-Vis data for the rigid-rod alkyne chromophores, including *p*-diethynylbenzene, *p*-diethynylbiphenyl, *p*-bis(butadiynyl)benzene and *p*-diethynylanthracene, on quartz are shown in Table 7.3. A typical UV-Vis spectrum for a thin film of *p*-diethynylanthracene on quartz is shown in Figure 7.4, and the spectral absorption at 398 nm is comparable to the solution absorption at 401 nm. The peaks became broad on the surface, and in the case of *p*-diethynylbenzene, λ_{max} shifted to ~30 nm lower than that of the solution spectra. Similar observations have been reported earlier for other chromophores self-assembled on surfaces.²⁶ Using the Beer-Lambert law and assuming the value of extinction coefficient on the surface as that for solution, an estimation of the surface coverage of the chromophores can be obtained. The spectra were collected from a quartz slide functionalized on both sides. Therefore, for calculating surface coverage, absorbance was divided by 2 to obtain the value of each individual monolayer. The surface coverage in the thin films of ~2-7 molecules/100 Å² is reasonable, since the hydroxyl group density for silica degassed at 100-150 °C has been reported to be ~3-8 OH/100 Å².²⁷ This value is also close to the reported surface coverage for other chromophores, for example, pyridine,²⁸ porphyrin²⁹ and NLO-active based SAMs,³⁰ suggesting that the SAMs of the rigid-rod dialkynyl chromophores on Si/SiO₂ are relatively close-packed.

As a result, a combination of contact angles, ellipsometry, XPS, FT-IR and UV-Vis data suggests that the SAMs of dialkynyl chromophores on Si/SiO₂ are relatively ordered and densely packed. The water contact angles of the dialkynyl monolayers with varied alkyl chain-length were found to be lower (75-80°) than the corresponding long alkyl chains (~110°) but were comparable to the SAMs of alkynylol on Si/SiO₂ reported previously.^{12a}

Table 7.3. λ_{\max} (nm), absorbance (A), absorption Coefficient (ϵ), and surface coverage (θ) of rigid-rod alkyne thin films on quartz

Alkyne Film on Quartz	λ_{\max} , nm	A, au	ϵ , 10^7 $\text{cm}^2 \text{mol}^{-1}$	θ , 10^{-10} , mol cm^{-2}	θ , molecule/ 100 \AA^2
	234	0.021	3.28	3.2	1.9
	398	0.10	4.25	12	7.1
	289	0.015	1.26	6.0	3.6
	296	0.085	5.48	7.8	4.7

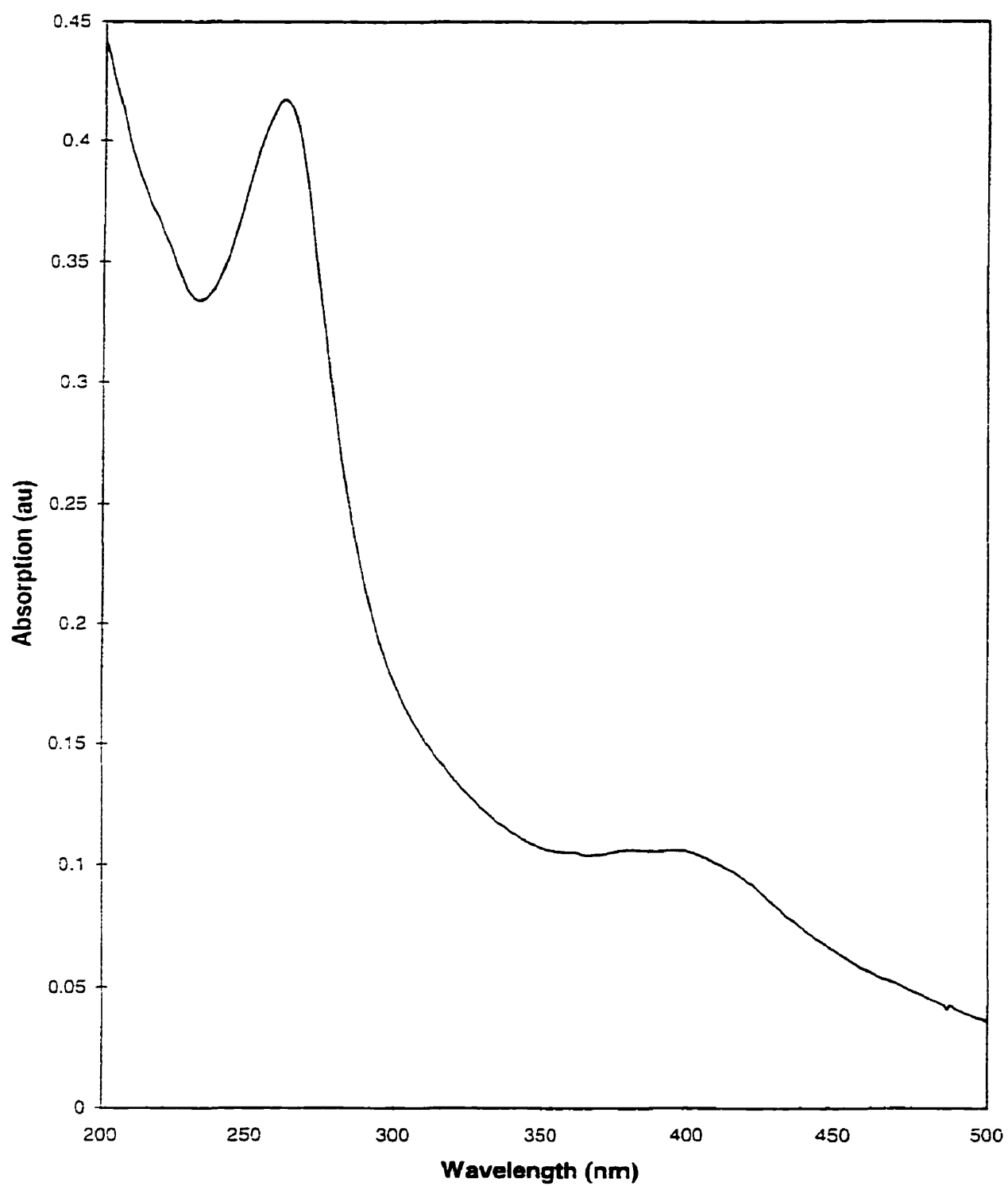


Figure 7.4 UV-Vis spectrum of a monolayer of *p*-diethynylanthracene on quartz.

7.5 UV-Vis Exposure of a SAM of *p*-Bis(butadiynyl)benzene

The thin film assembly of *p*-bis(butadiynyl)benzene was exposed to UV light operating at 365 nm for up to 60 min under a nitrogen atmosphere (Figure 7.5). After a 5-min irradiation, the intensity of λ_{max} at 296 nm in the monolayer decreased significantly and a blue film was observed by a naked eye. Exposure of the film to UV light for times beyond 60 min revealed no further change in intensity at 296 nm. The decrease in intensity may be attributed to a structural change as the $\text{C}\equiv\text{C}$ bonds become parallel to the substrate upon UV-exposure, as reported previously.³¹ A broad peak with weak intensity at 580-620 nm, corresponding to the formation of the blue polymer,³² was observed. It may be due to the fact that (i) the intensity of $\text{C}=\text{C}$ bonds are too weak for identification,^{12b} and (ii) the topochemical merization in these thin films may lead to a different polymer backbone structure.^{13a} The water contact angle and ellipsometric thickness (Table 7.4) for the diacetylene film were found to decrease slightly on exposure to UV for 30 min, indicating that there has been no great deterioration of the film quality on polymerization, as reported previously.³³ Together with a decrease in $\nu_{\text{C}\equiv\text{C}}$, from 2165 to 2115 cm^{-1} , due to extensive electronic delocalization in the backbone of the polymerized diacetylene groups,³⁴ these results support the UV-polymerization of the diacetylenic chromophore, similar to those reported for UV-polymerization of SAMs of carboxylic acid-terminated alkanethiol diacetylene³² and dialkyl disulfide diacetylene.³³

Table 7.4. Static contact angle of water (CA_{H_2O}), ellipsometric thickness (T_e) and FTIR-ATR data of a SAM of *p*-bis(butadiynyl)benzene on a Si(100) substrate upon exposure to UV-lamp for 30 min

$\text{H} \equiv \equiv \text{C} - \text{C}_6\text{H}_4 - \text{C} \equiv \equiv \text{H}$ Film on Si(100)	$CA_{H_2O}, \pm 2^\circ$	$T_e, \pm 2 \text{ \AA}$	$\nu_{C \equiv C}, \text{cm}^{-1}$
before UV-exposure	80	17	2165
after UV-exposure	78	16	2115

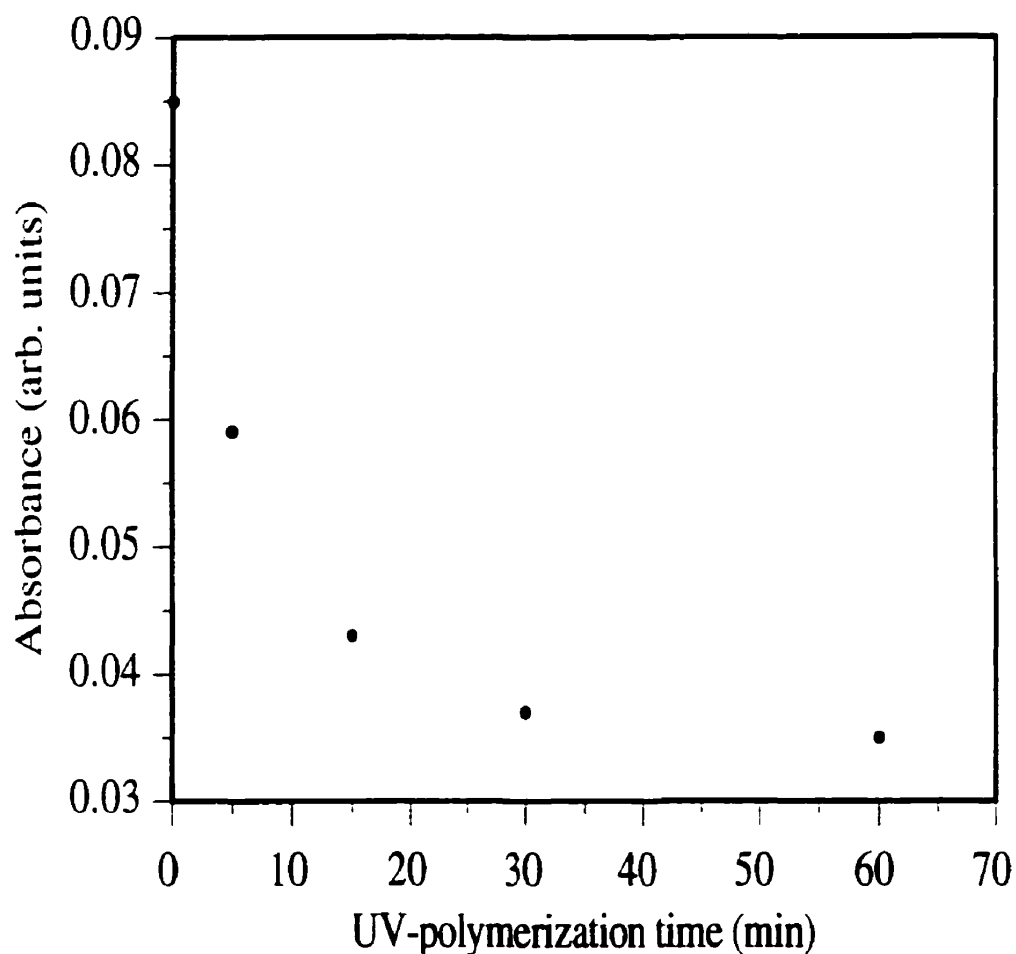


Figure 7.5 UV-Vis absorption ($\lambda_{\text{max}} = 296 \text{ nm}$) of a monolayer of *p*-bis(butadiynyl)-benzene upon exposure to UV-lamp for a period of 0, 5, 15, 30 and 60 min.

7.6 Multilayer Thin Film Assemblies of 1,9-Decadiyne and *p*-Diethynylbenzene

As discussed earlier, SAMs of dialkynyl chromophores exposing terminal $\text{C}\equiv\text{C}-\text{H}$ groups to surface can react further with $\text{Sn}(\text{NEt}_2)_4$. Following the reaction with additional dialkynyl moieties, 2-layered thin film can be fabricated. Repetition of this process can lead to multilayered assemblies. Using this approach, we have successfully prepared multilayered thin films of up to 5 layers of 1,9-decadiyne (**1**) and *p*-diethynylbenzene (**2**) (Scheme 7.2). Before the deposition of each successive layer, the original layer was cleaned by sonicating in toluene for 5 min, followed by drying in an oven at $\sim 100^\circ\text{C}$ for 5 min. A temperature of 70°C was required for the reaction of terminal alkynes with surface-anchored aminostannane (and vice versa) resulting in a closely packed thin films.

The multilayered thin films were characterized by contact angle goniometry, ellipsometry, FT-IR, and UV-Vis spectroscopy. As shown in Figures 7.6 and 7.7, the film thickness increases as the number of layers increases from 1 to 5 for both **1** and **2**. The measured thicknesses match the theoretical values from 1- to 3-layered films for both **1** and **2**. However, they become less close to each other beyond 3-layered films: from 18 Å/layer in 3-layer sample to 22 Å/layer in 5-layer sample for **1** (theoretical monolayer thickness = 18 Å) and from 13 Å/layer in 3-layer sample to 18 Å/layer in 5-layer sample for **2** (theoretical monolayer thickness = 13 Å). This may be due to the fact that (i) the monolayers can be cleaned more effectively than the multilayers, similar to the multilayers of dihydroxy terminated molecules on aminosilane-anchored surface^{12b} and those of $\text{HOC}_{23}\text{Si}/\text{Si}$ prepared from $\text{MeO}_2\text{CC}_{22}\text{Si}/\text{Si}$;¹⁵ and (ii) there is an increase in thickness of tin-oxide layer from monolayer to multilayer due to polymerization of aminostannane at higher temperature (70°C) during multilayer deposition.

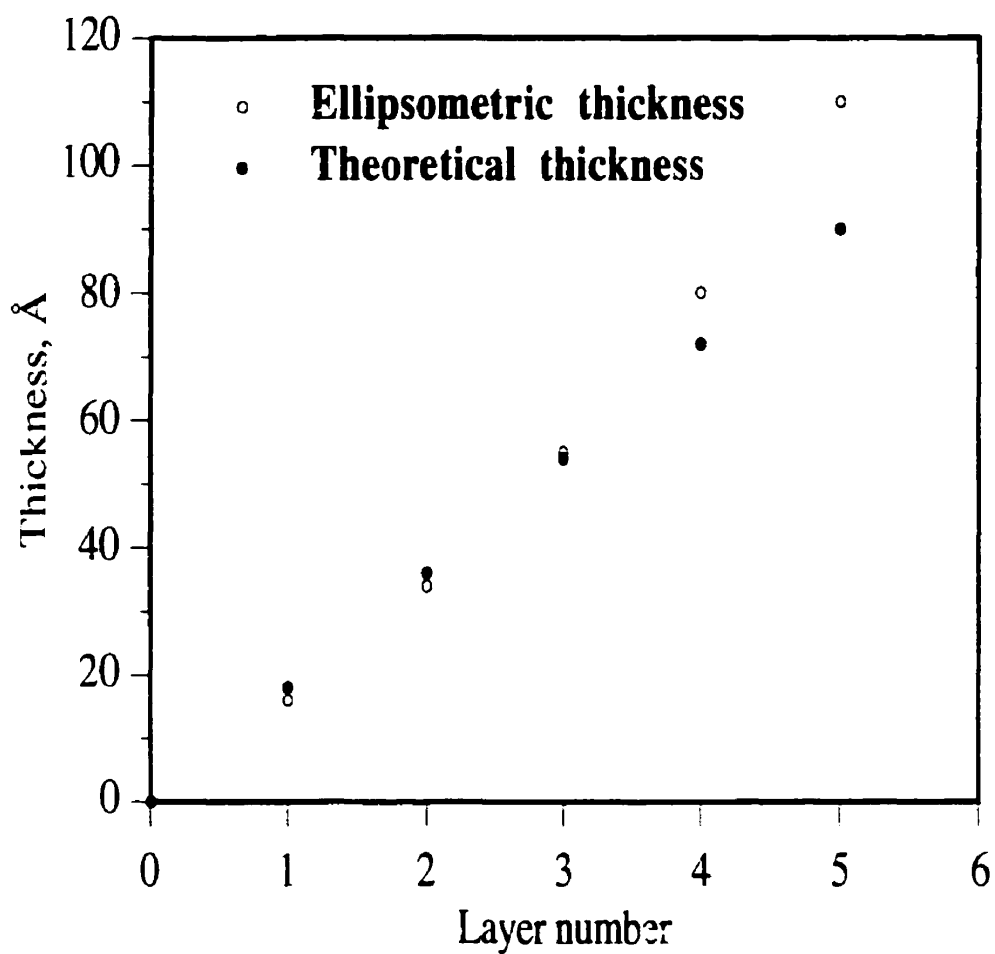


Figure 7.6 Ellipsometric thickness of the 1 to 5 layered thin films of 1,9-decadiyne.

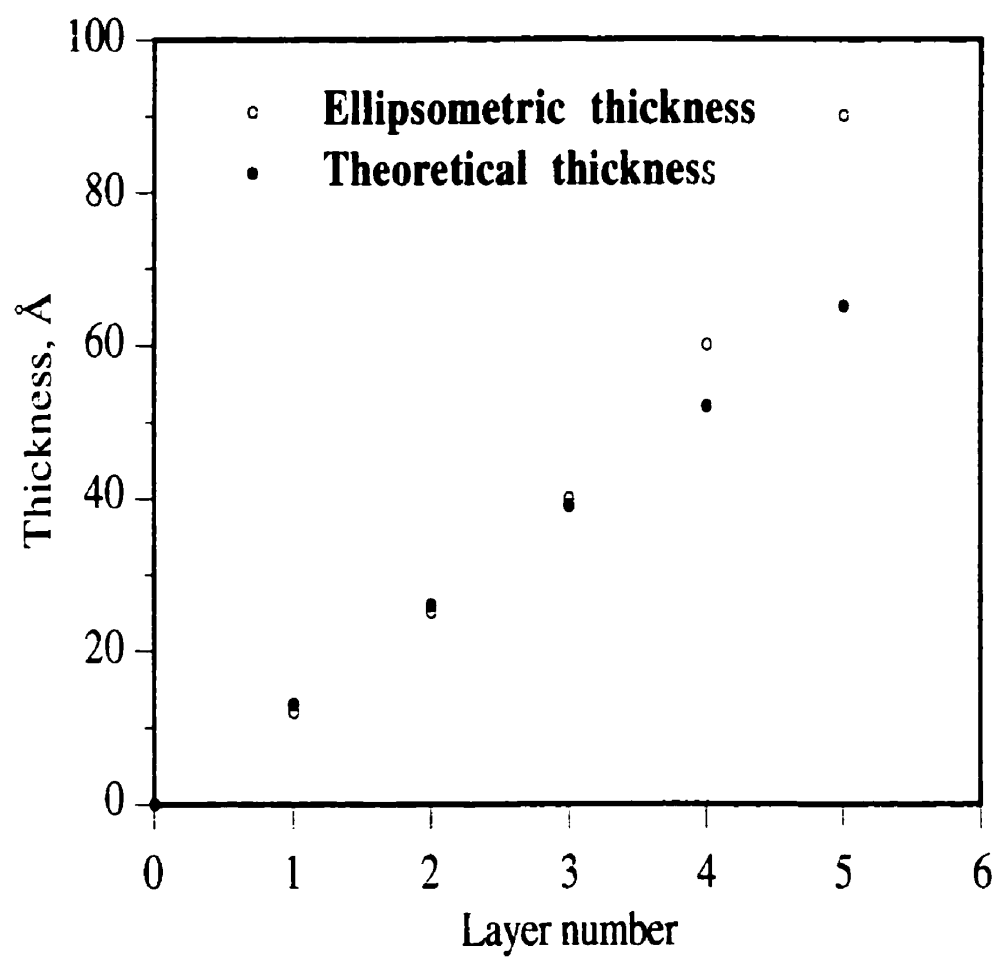


Figure 7.7 Ellipsometric thickness of the 1 to 5 layered thin films of *p*-diethynylbenzene.

Furthermore, the precision of thickness measurements decreases as the number of layers increases, for example, from ca. ± 2 Å for 1-layer samples to ca. ± 5 -6 Å for 5-layer samples of both **1** and **2**. This may also be explained by the small amount of loosely held material being adsorbed on top of the multilayer surfaces or accumulating in the multilayer bulk, during the process of multilayer formation.¹⁵

From the UV-Vis data (Figure 7.8) for thin films of **1** from 1-layer to 5-layer, it was shown that the absorption at ~ 220 nm increased with the increase in the number of layers. This is consistent with an increase in chromophore density upon multilayer formation.

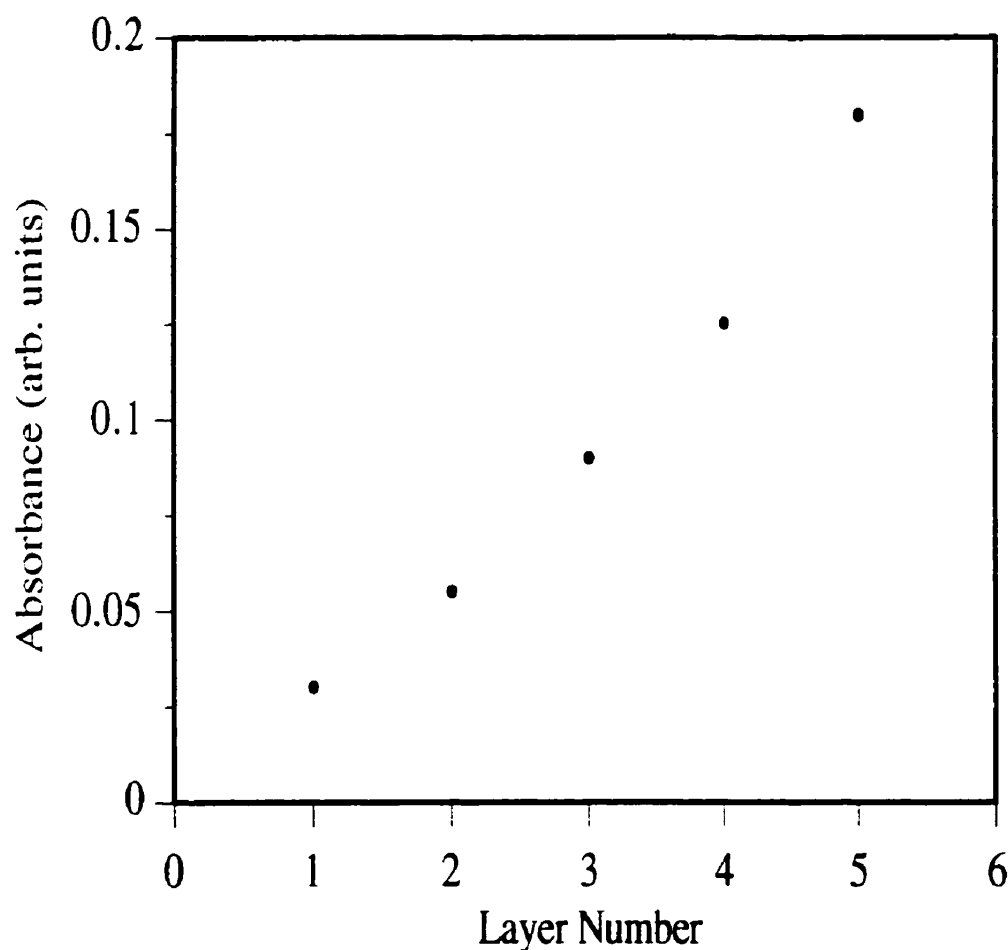


Figure 7.8 UV-Vis absorption of the 1 to 5 layered thin films of 1,9-decadiyne.

The static contact angle of water for the thin film prepared from **1** increases from 80° for a monolayer to 90° for a 5-layer film. Similarly, the static contact angle of hexadecane (HD) increases from 12° to 15° from a monolayer to a 5-layer film (Table 7.5). The data suggest that the thin films become densely packed in the multilayer. It is probably due to effective Sn-O-Sn cross-linking network within each layer which results in better alignment of the chromophores on the surface, increasing π - π interaction of the acetylene groups. A similar behavior has been observed for the thin film prepared from **2** (Table 7.6).

Table 7.5. Static contact angles of water (CA_{H_2O}) and HD (CA_{HD}), ellipsometric thicknesses (T_e), and FTIR-ATR data for the multilayers of 1,9-decadiyne on Si(100) substrates

Decadiyne film on Si(100)	CA_{H_2O} (CA_{HD}) $\pm 2^\circ$	T_e , Å	$\nu_{C\equiv C}$, cm^{-1}
1-layer	80 (12)	16 ± 2	2130, 2097
2-layers	80 (12)	34 ± 2	2126, 2105
3-layers	85 (15)	55 ± 3	2134, 2099
4-layers	85 (15)	80 ± 4	2132, 2108
5-layers	90 (15)	110 ± 6	2139, 2100

In the FTIR-ATR spectrum of a thin film of **1**, there are two peaks corresponding to the stretching frequencies, $\nu_{C\equiv C}$, one for the terminal $C\equiv C-H$ ($\sim 2100\text{ cm}^{-1}$) and the other for the $C\equiv C$ bonded to $-Sn$ ($\sim 2130\text{ cm}^{-1}$). The peaks became more intense on multilayered thin film construction. Similarly, FTIR-ATR spectrum of a thin film of **2** (Table 7.6) showed two peaks (~ 2100 and $\sim 2130\text{ cm}^{-1}$) which are comparable in position to that in the powder

of $\text{HC}\equiv\text{C}-\text{C}_6\text{H}_4-\text{C}\equiv\text{CH}$ (2103 cm^{-1}) and $(\text{CH}_3)_3\text{Sn}-\text{C}\equiv\text{C}-\text{C}_6\text{H}_4-\text{C}\equiv\text{C}-\text{Sn}(\text{CH}_3)_3$ (2130 cm^{-1}). These peaks also show an increase in intensity with multilayer formation.

Table 7.6. Static contact angles of water ($\text{CA}_{\text{H}_2\text{O}}$) and HD (CA_{HD}), ellipsometric thicknesses (T_e), and FTIR-ATR data for the multilayers of *p*-diethynylbenzene on Si(100) substrates

<i>p</i> -Diethynylbenzene film on Si(100)	$\text{CA}_{\text{H}_2\text{O}}$ (CA_{HD}) $\pm 2^\circ$	T_e , Å	$\nu_{\text{C}\equiv\text{C}}$, cm^{-1}
1-layer	80 (12)	12 ± 2	2103
2-layers	85 (13)	25 ± 2	2129, 2105
3-layers	85 (15)	40 ± 3	2130, 2100
4-layers	90 (20)	60 ± 3	2133, 2097
5-layers	90 (20)	90 ± 5	2125, 2100

7.7 Cobalt Carbonyl Adsorption on Monolayers and Multilayers of 1,9-Decadiyne and *p*-Diethynylbenzene

Cobalt carbonyl is of considerable interest because of its catalytic activity toward such reactions as rearrangement of epoxides, reduction of aldehydes and olefin carboxylation.³⁵ In contrast to most other metals, cobalt carbonyl forms very stable complexes with alkynes.³⁶ The selective coordination of cobalt carbonyl with the acetylene groups makes it a useful acetylene protecting group.³⁵ The reaction of acetylene with cobalt carbonyl in solution at room temperature is well-known, and has been studied by many investigators.³⁷ We were interested in finding out the possibility of the adsorption of cobalt carbonyl on thin films of **1** and **2** under similar conditions. Adsorption of cobalt carbonyl on the dialkynyl thin films was found to proceed feasibly under room temperature. After 24 h deposition,

the cobalt carbonyl was successfully adsorbed onto the dialkynyl thin films (**1** and **2**), supported by the ellipsometry, contact angles, FT-IR and UV-Vis data.

The ellipsometric data (Table 7.7) for the thin film assemblies (monolayers or multilayers) of both **1** and **2** show an increase in thickness after adsorption of cobalt carbonyl. This extra thickness may be the consequence of the adsorbed cobalt carbonyl on top of the films, reacting with the terminal alkyne group (resultant bond length of Co-C=O is $\sim 3 \text{ \AA}$ ³⁸). The adsorption of cobalt carbonyl on alkyne film surfaces of **1** and **2** is further supported by a decrease in the static contact angles of water and HD to 65-70° and $\leq 10^\circ$, respectively. These results are similar to thiol monolayers with terminal nitrile, ester, aldehyde and ketone groups adsorbed on gold.⁴

From the FT-IR data for the thin films containing adsorbed cobalt carbonyl on **1** (Co-DY) and **2** (Co-DEB), the peak positions for the acetylene and carbonyl groups (Table 7.7) were observed at ca. 2105 and 2060 (2025) cm^{-1} , respectively. The peak positions for the carbonyl groups in the films are only slightly shifted from the reference spectrum obtained from a KBr pellet of $\text{Co}_2(\text{CO})_8$ (ν_{CO} , terminal = 2054, 2024). It should be noted that the peak at 1849 cm^{-1} in pure $\text{Co}_2(\text{CO})_8$, attributable to its bridging carbonyl group, is absent in both films of Co-DY and Co-DEB, similar to that reported for the acetylenic dicobalt hexacarbonyl compounds.³⁹ Cobalt carbonyl adsorption on alkyne films is further corroborated by the observation of λ_{max} at 277 nm (Figure 7.9), which is comparable to that obtained from $\text{Co}_2(\text{CO})_8$ in methylene chloride (λ_{max} at 276 nm). These results suggest that cobalt carbonyl have been adsorbed onto the dialkynyl mono- and multilayered assemblies via coordination through the acetylene groups with no deterioration of the film quality.

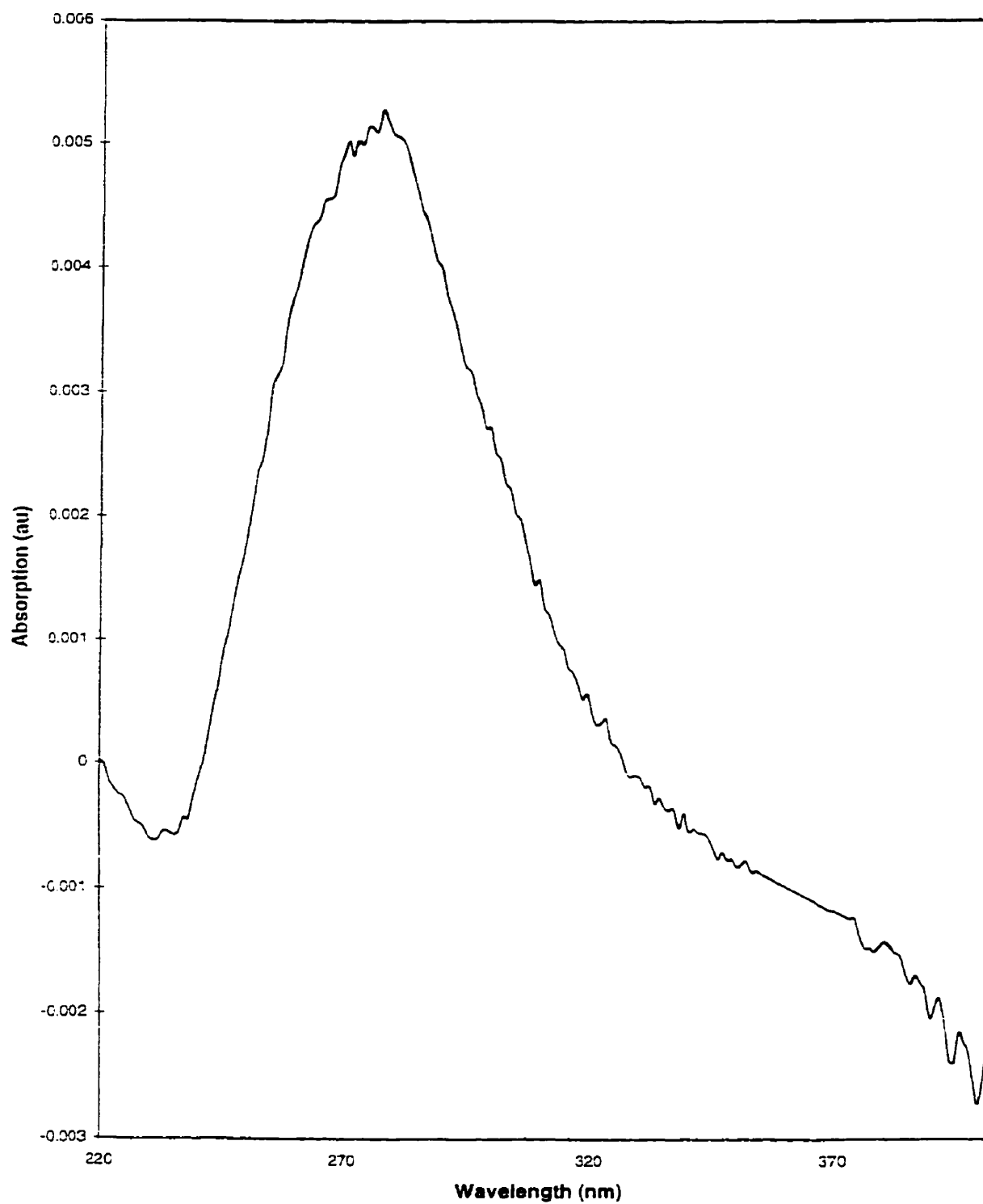


Figure 7.9 UV-Vis spectrum of a thin film on quartz of *p*-diethynylbenzene with adsorbed cobalt carbonyl.

Table 7.7. Static contact angles of water (CA_{H_2O}), ellipsometric thicknesses (T_e), and FTIR-ATR data for the thin films of *p*-diethynylbenzene (Co-DEB) and 1,9-decadiyne (Co-DY) on Si(100) substrates after reaction with cobalt carbonyl

Co-DEB	$CA_{H_2O} \pm 2^\circ$	$T_e, \text{\AA}$	$\nu_{C\equiv C}, \nu_{CO}, \text{cm}^{-1}$
1-layer	65	14 ± 2	2108, 2060, 2027
2-layers	65	28 ± 2	2107, 2056, 2024
3-layers	70	42 ± 3	2108, 2062, 2019
Co-DY, 1-layer	65	18 ± 2	2102, 2067, 2023

7.8 Conclusion

Self-assembled mono- and multilayers of a variety of dialkyne molecules terminated with acetylene groups on Si(100) (Si/SiO₂) surfaces containing anchored aminostannanes have been successfully prepared by a simple acid-base hydrolytic chemistry route. The surface coverage of chromophores was found to be 2-7 molecules/100 Å², comparable to the density of surface hydroxyl groups on silica degassed at 100-150 °C. Upon UV exposure of a SAM of *p*-bis(butadiynyl)benzene, the intensity of the λ_{max} decreased significantly with the formation of a blue film, suggesting a structural change, accompanied by C≡C bonds becoming more parallel to the substrate upon topochemical polymerization. Multilayers of 1,9-decadiyne and *p*-diethynylbenzene of up to 5 layers were fabricated using a step-by-step thin film construction methodology. The results presented here have shown that simple acid-base hydrolytic chemistry of aminostannanes with dialkyne chromophores can be successfully employed for the construction of mono- and multilayer thin film assemblies. Finally, cobalt carbonyl was found to adsorb in the thin film assemblies by reacting with the acetylene groups.

7.9 Experimental Section

7.9.1 Materials

1,8-Nonadiyne and $\text{Sn}(\text{NEt}_2)_4$ were purchased from Aldrich. 1,5-Hexadiyne, 1,7-octadiyne and 1,9-decadiyne were purchased from ChemSamp. Cobalt carbonyl was purchased from Strem Chemicals and used as received. Other rigid-rod alkynes, including *p*-diethynylbenzene, *p*-diethynylbiphenyl, *p*-diethynylanthracene and *p*-bis(butadiynyl)benzene, employed in this study were conveniently prepared using literature procedures.⁴⁰ Toluene was dried and distilled over sodium.

7.9.2 Substrate Preparation

The glass, quartz or single crystal Si wafers were first cleaned (i) by soaking in soap solution and sonocating for 1 h, (ii) repeated washing with deionized water, (iii) treatment with a solution mixture containing 70% conc. H_2SO_4 and 30% H_2O_2 (piranha solution) at 100 °C for 1 h. *Caution:* Piranha solution is highly explosive, and care should be taken while using this mixture, (iv) repeated washing with deionized water, and (v) finally heating in a oven at ~150 °C for 5 min and vacuum drying for 5 min to remove physisorbed water.

7.9.3 Preparation of SAMs

The surface functionalization involved a two-step process: the clean substrates were treated with (i) 0.5 % solution by volume of $\text{Sn}(\text{NEt}_2)_4$ in dry toluene for 8 h at room temperature, followed by (ii) 0.1 % by weight of the alkyne chromophore in dry toluene at 70 °C for 24 h, after sonicating in dry toluene for 5 min to remove excess $\text{Sn}(\text{NEt}_2)_4$ physisorbed on the surface. After thorough washing with dry toluene, the substrates were dried at ~120 °C for 5 min.

7.9.4 Preparation of Multilayers

The multilayered thin film assemblies of 1,9-decadiyne (**1**) or *p*-diethynylbenzene (**2**) were prepared by immersion of the monolayer substrates into 0.5 % by volume of dry toluene solution of $\text{Sn}(\text{NEt}_2)_4$ at 70 °C for 8 h, followed by treatment with 0.1 % by weight of dry toluene solution of **1** or **2** at 70 °C for 24 h, after sonicating into dry toluene for 5 min. The two-layer substrates thus obtained were thoroughly washed with dry toluene and then dried at ~120 °C for 5 min. The procedure was repeated to obtain multilayered thin films.

7.9.5 Cobalt Carbonyl Adsorption

The mono- and multilayered thin film assemblies of (**1**) and (**2**) were immersed into 0.1 % by weight of anhydrous toluene solution of $\text{Co}_2(\text{CO})_8$ at room temperature for 24 h, followed by thorough washing with anhydrous toluene and drying at ~120 °C for 5 min.

7.9.6 Contact-Angle (CA) Measurements

The static and advancing contact angles were measured with a Rame-Hart NRL 100 goniometer. On average, 6 drops of water and hexadecane (HD) were measured on different areas of the polished side of a silicon wafer for each sample, and mean values with a maximum range of $\pm 2^\circ$ are reported. The advancing contact angles of captive drops were found to be roughly 5° above the static values of sessile (free-standing) drops. If the drop was allowed to fall from the needle of the syringe to the surface, smaller contact angles were usually obtained due to mechanical vibrations.²

7.9.7 Fourier Transform Infrared Spectroscopy in the Attenuated Total Reflection Mode (FTIR-ATR)

The organic thin films were grown on the <100> surfaces of the single side polished silicon wafers. A KRS crystal was sandwiched between the reflective faces of two silicon

wafers (1.2 cm X 4.0 cm), and the angle of non-polarized light was set at 45°. All spectra were run for 4000 scans at a resolution of 4 cm⁻¹, using a Bruker IFS-48 spectrometer. A spectrum of two clean silicon wafers with a sandwiched KRS crystal was measured as a background correction.

7.9.8 Ellipsometry

A Gaertner Scientific ellipsometer operating at 633 nm He-Ne laser ($\lambda = 6328 \text{ \AA}$) was employed. The angle of incidence was 70.0°, and the compensator was set at 45.0°. All reported values with a maximum range of $\pm 2 \text{ \AA}$ are the average of at least six measurements taken at different locations on the sample. The thickness was calculated by comparing data from the same substrate before and after functionalization and using a value of 1.46 for the refractive index. This value is based on the assumption that the monolayer is similar to bulk paraffins with a refractive index of 1.45.²¹ If the monolayer is more crystalline-like, similar to polyethylene, the refractive index thus should be within 1.49-1.55.² It was found that an increase of 0.1 in the refractive index from 1.45 to 1.55 resulted in a decrease in the measured thickness by $\sim 2 \text{ \AA}$.

7.9.9 X-ray Photoelectron Spectroscopy (XPS)

The XPS spectra were obtained by using a VG Escalab MKII spectrometer with monochromatized MgK α X-ray source to produce the photoemission of electrons from the core levels of the surface atoms. About 50 \AA of depth was probed for a detector perpendicular to the surface. The analyzed surface was 2 x 3 mm. All peak positions were corrected for carbon at 285.0 eV in binding energy to adjust for charging effects. The power of the source was 300 watts and a pressure of 10⁻⁹ mbar.

7.9.10 UV-Polymerization

Topochemical polymerization was carried out by placing the substrates into a container and irradiating them under a nitrogen purge for up to 60 min with a medium pressure Hg vapor lamp (Ace-Hanovia photochemical lamp, model 7830, 230-430 nm with the main spike at 365 nm), with the sample-source distance of approximately 3 cm.

7.10 References

- (1) Swalen, J. D.; Allara, D. L.; Andrade, J. D.; Chandross, E. A.; Garoff, S.; Israelachvili, J.; McCarthy, T. J.; Murray, R.; Pease, R. F.; Rabolt, J. F.; Wynne, K. J.; Yu, H. *Langmuir* **1987**, *3*, 932.
- (2) Ulman, A. *An Introduction to Ultrathin Organic Films from Langmuir Blodgett to Self-Assembly*; Academic Press: Boston, 1991.
- (3) Sagiv, J. *J. Am. Chem. Soc.* **1980**, *102*, 92.
- (4) Bain, C. D.; Troughton, E. B.; Tao, Y-T.; Evall, J.; Whitesides, G. M.; Nuzzo, R. G. *J. Am. Chem. Soc.* **1989**, *111*, 321.
- (5) Porter, M. D.; Bright, T. B.; Allara, D. L.; Chidsey, C. E. D. *J. Am. Chem. Soc.* **1987**, *109*, 3559.
- (6) Walczak, M. M.; Chung, C.; Stole, S. M.; Widrig, C. A.; Porter, M. D. *J. Am. Chem. Soc.* **1991**, *113*, 2370.
- (7) Laibins, P. E.; Whitesides, G. M.; Allara, D. L.; Tao, Y-T.; Parikh, A. N.; Nuzzo, R. G. *J. Am. Chem. Soc.* **1991**, *113*, 7152.
- (8) Troughton, E. B.; Bain, C. D.; Whitesides, G. M.; Nuzzo, R. G.; Allara, D. L.; Porter, M. D. *Langmuir* **1988**, *4*, 365.
- (9) Nuzzo, R. G.; Fusco, F. A.; Allara, D. L. *J. Am. Chem. Soc.* **1987**, *109*, 2358.
- (10) Tao, Y. T. *J. Am. Chem. Soc.* **1993**, *115*, 4350.
- (11) Linford, M. R.; Fenter, P.; Eisenberger, P. M.; Chidsey, C. E. D. *J. Am. Chem. Soc.* **1995**, *117*, 3145.

- (12) (a) Yam, C. M.; Tong, S. S. Y.; Kakkar, A. K. *Langmuir* **1998**, *14*, 6941. (b) Yam, C. M.; Kakkar, A. K. *Langmuir* **1999**, in press.
- (13) (a) Yam, C. M.; Dickie, A.; Malkhasian, A.; Kakkar, A. K.; Whitehead, M. A. *Can. J. Chem.* **1998**, *76*, 1766. (b) Yam, C. M.; Kakkar, A. K. *J. Chem. Soc., Chem. Commun.* **1995**, 907.
- (14) Khan, M. S.; Kakkar, A. K.; Long, N. J.; Lewis, J.; Raithby, P.; Nguyen, P.; Marder, T. B.; Wittmann, F.; Friend, R. H. *J. Mater. Chem.* **1994**, *4*, 1227.
- (15) Tillman, N.; Ulman, A.; Penner, T. L. *Langmuir* **1989**, *5*, 101.
- (16) Maoz, R.; Sagiv, J. *Langmuir* **1987**, *3*, 1045.
- (17) Collins, R. J.; Bae, I. T.; Sxherson, D. A.; Sukenik, C. N. *Langmuir* **1996**, *12*, 5509.
- (18) Kato, S.; Pac, C. *Langmuir* **1998**, *14*, 2372.
- (19) (a) Jones, K.; Lappert, M. F. In *Organotin Compounds Vol. 2*. Edited by Sawyer, A. K.; Marcell Dekker, Inc.: New York, 1977. (b) Jones, K.; Lappert, M. F. *J. Organomet. Chem.* **1965**, *3*, 295. (3) Thomas, I. M. *Can. J. Chem.* **1961**, *39*, 1386.
- (20) Dhirani, A. A.; Zehner, R. W.; Hsung, R. P.; Guyot-Sionnest, P.; Sita, L. R. *J. Am. Chem. Soc.* **1996**, *118*, 3319.
- (21) Wasserman, S. R.; Whitesides, G. M.; Tidswell, I. M.; Ocko, B. M.; Pershan, P. S.; Axe, J. D. *J. Am. Chem. Soc.* **1989**, *111*, 5852.
- (22) Azzam, R. M. A.; Bashara, N. M. *Ellipsometry and Polarized Light*; North-Holland: Amsterdam, 1977.
- (23) Dean, J. A. *Lange's Handbook of Chemistry*; McGraw-Hill: New York, 1992.
- (24) Tillman, N.; Ulman, A.; Schildkraut, J. S.; Penner, T. L. *J. Am. Chem. Soc.* **1988**, *110*, 6136.

- (25) Tour, J. M.; Jones, L. II; Pearson, D. L.; Lamba, J. J. S.; Burgin, T. P.; Whitesides, G. M.; Allara, D. L.; Parikh, A. N.; Atre, S. V. *J. Am. Chem. Soc.* **1995**, *117*, 9529.
- (26) (a) Liang, Y.; Schmehl, R. H. *J. Chem. Soc., Chem. Commun.* **1995**, 1007. (b) Butterworth, A. J.; Clark, J. H.; Walton, P. H.; Barlow, S. J. *J. Chem. Soc., Chem. Commun.* **1996**, 1859.
- (27) (a) Morrow, B. A.; McFarlan, A. J. *Langmuir* **1991**, *7*, 1695. (b) Iler, R. K. *The Chemistry of Silica*; Wiley: New York, 1979.
- (28) Paulson, S.; Morris, K.; Sullivan, B. P. *J. Chem. Soc., Chem. Commun.* **1992**, 1615.
- (29) Li, D.; Swanson, B. I.; Robinson, J. M.; Hoffbauer, M. A. *J. Am. Chem. Soc.* **1993**, *115*, 6975.
- (30) Roscoe, S. B.; Yitzchaik, S.; Kakkar, A. K.; Marks, T. J.; Xu, Z.; Zhang, T.; Lin, W.; Wong, G. K. *Langmuir* **1996**, *12*, 5338.
- (31) Porter, M. *Anal. Chem.* **1988**, *6*, 1143A.
- (32) Kim, T.; Crooks, R.; Tsen, M.; Sun, L. *J. Am. Chem. Soc.* **1995**, *117*, 3963.
- (33) Batchelder, D. N.; Evans, S. D.; Freeman, T. L.; Haussling, L.; Ringsdorf, H.; Wolf, H. *J. Am. Chem. Soc.* **1994**, *116*, 1050.
- (34) (a) Baughman, R. H.; Witt, J.D.; Yee, K. C. *J. Chem. Phys.* **1974**, *60*, 4755. (b) Angkacw, S.; Wang, H.; Lando, J. B. *Chem. Mater.* **1994**, *6*, 1444.
- (35) (a) Heck, R. F. *Organotransition Metal Chemistry*; Academic Press: New York, 1974. (b) Davies, S. G. *Organotransition Metal Chemistry: Applications to Organic Synthesis*; Pergamon Press: New York, 1982.
- (36) Dickson, R. S.; Fraser, P. J. *Adv. Organomet. Chem.* **1974**, *12*, 323.
- (37) Markby, R.; Wender, I.; Friedel, R. A.; Cotton, F. A.; Sternberg, H. W. *J. Am. Chem. Soc.* **1958**, *80*, 6529.
- (38) Sumner, G. G.; Klug, H. P.; Alexander, L. E. *Acta Cryst.* **1964**, *17*, 732.

- (39) Greenfield, H.; Sternberg, H. W.; Friedel, R. A.; Wotiz, J. H.; Markby, R.; Wender, I. *J. Am. Chem. Soc.* **1956**, 78, 120.
- (40) (a) Lewis, J.; Khan, M. S.; Kakkar, A. K.; Johnson, B. F. G.; Marder, T. B.; Fyfe, H. B.; Wittmann, F.; Friend, R. H.; Dray, A. E. *J. Organomet. Chem.* **1992**, 425, 195. (b) Jiang, J.; Kobayashi, E.; Aoshima, S. *Polym. J.* **1990**, 22, 274. (c) Takahashi, S.; Kuroyama, Y.; Sonogashira, K.; Hagihara, N. *Synthesis Commun.* **1980**, 627.

Chapter Eight

Conclusions, Contributions to Original Knowledge and Suggestions for Future Work

8.1 Conclusions

In conclusion, we have developed a new, simple and versatile approach to molecular self-assembly. Treatment of surface hydroxyl groups on inorganic oxides, such as glass, quartz and single-crystal silicon, with commercially available or easily synthesized reagents, such as $\text{Si}(\text{NEt}_2)_4$ and $\text{Sn}(\text{NEt}_2)_4$, yields surface-anchored- NEt_2 moieties, which can react with several organic molecules containing terminal acidic protons, such as alcohols, thiols, carboxylic acids, cyclopentadiene, indene, phosphines and alkynes, via acid-base hydrolysis, leading to molecularly self-assembled monolayers. After optimizing the deposition conditions, ordered and densely packed mono- and multilayers have been produced. By means of this simple acid-base hydrolytic chemistry approach, self-assembled monolayers of a variety of long chain alcohols containing terminal alkyl, phenyl and acetylene groups on inorganic oxide surfaces have been successfully prepared.

The two-step process involving the reaction of surface hydroxyl groups first with $\text{Si}(\text{NEt}_2)_4$ followed by ROH , is more efficient than the three-step process involving the reaction of SiCl_4 , NEt_2H and ROH in sequence, and produces closely-packed and well-ordered thin films. The two-step route is able to produce monolayers of similar quality as the traditional self-assembly routes such as deposition of thiols on gold and alkyltrichlorosilanes on inorganic oxides. When placed in hot water and organic solvents, these films are more susceptible to hydrolysis than the corresponding OTS monolayers on

silica, as expected, but show comparable stabilities at ambient and high temperatures, and upon treatment with acid and base.

In addition, acid-base hydrolytic chemistry of aminosilanes with dihydroxy terminated molecules containing rigid-rod type and alkyldiacetylene backbones, has been used to construct self-assembled mono- and multilayers on inorganic oxide surfaces. Multilayers of up to 10 layers with good quality and relatively close-packing were fabricated from the dihydroxy molecules, and there was no increasing disorder upon addition of each successive layer. The stability of the thin films is significantly enhanced upon layer-by-layer deposition of the multilayered thin films. An increase in the intensity of the λ_{max} was observed upon multilayered thin film construction. Upon UV exposure, the intensity of the λ_{max} decreased significantly with the subsequent formation of a blue film, and is accompanied by a structural change where the $\text{C}\equiv\text{C}$ bonds become parallel to the substrate upon topochemical polymerization.

The hydrolysis of surface bound basic tin-amide moieties with acidic protons of alkynyl chromophores leads to molecular self-assembly of a variety rigid-rod alkynes on inorganic oxide surfaces. The π - π interactions in the molecules lead to ordered and densely packed thin film structures. The surface coverage of chromophores in these thin films on quartz was found to be 2-7 molecules/100 Å², comparable to the density of surface hydroxyl groups on silica degassed at 100-150 °C. Upon UV-Vis exposure of SAMs of alkynyl chromophores containing rigid-rod type diacetylene backbones, the intensity of the λ_{max} decreased significantly with the formation of a blue film, suggesting a structural change accompanied by $\text{C}\equiv\text{C}$ bonds becoming more parallel to the substrate upon topochemical polymerization.

Furthermore, self-assembled mono- and multilayers of a variety of organic chromophores terminated with acetylene groups on both ends, on inorganic oxide surfaces,

have been successfully prepared by the acid-base hydrolytic chemistry route. Multilayers of dialkynes of up to 5 layers were fabricated and there was no increasing disorder upon addition of each successive layer. It is inferred that simple acid-base hydrolytic chemistry of aminostannanes with dialkyne chromophores can be successfully employed for the construction of relatively close-packed mono- and multilayer thin film assemblies.

Finally, cobalt carbonyl was found to adsorb in the thin film assemblies by reacting with the acetylene groups. These cobalt-adsorbed alkyne films may become potential candidates as heterogenized homogeneous catalysts, one-dimensional conductors and chemically modified electrodes and sensors.

8.2 Contributions to Original Knowledge

Molecular self-assembly has recently become an important area of research due to its potential applications in thin film technology. We have developed a new, general and convenient approach to molecular self-assembly based on acid-base hydrolysis. The advantage of using acid-base hydrolytic chemistry is the ability to incorporate a variety of functionalities on inorganic oxide surfaces. These functionalities are organic compounds with terminal acidic protons having $pK_a \leq 25$ including acids, thiols, alcohols, phosphines, cyclopentadiene, indene and alkynes. The hydroxylated silica based surfaces such as glass, quartz and single-crystal silicon can be easily modified by the reaction of surface-anchored aminosilanes or aminostannanes with these protic species.

We have constructed SAMs of a variety of alcohols containing terminal alkyl, phenyl and acetylene groups on Si(100) (Si/SiO₂) surfaces for the first time via the acid-base hydrolytic chemistry route. The two-step process involves the reaction of surface hydroxyl groups first with Si(NEt₂)₄ followed by ROH. It is more efficient than the three-step process involving the reaction of SiCl₄, NEt₂H and ROH in sequence. The new simple acid-base hydrolytic chemistry two-step route is able to produce relatively close-packed and well ordered thin films of similar quality as alkyltrichlorosilanes on silica and alkanethiols

on gold except that these films are more susceptible to hydrolysis than the corresponding OTS monolayers on silica as expected.

A layer-by-layer construction of multilayers of dihydroxy terminated compounds containing rigid-rod type and alkyldiacetylene backbones on Si(100) (Si/SiO₂) via acid-base hydrolytic chemistry route has been successfully achieved. The diol terminated chromophores form good quality and relatively close-packed thin films on silicon (silica) surfaces, and there is no increasing disorder in the thin films with increasing number of layers. Capping thin films of diol with OTS helps to increase the stability of the films under varied conditions, suggesting that a SAM of OTS acts as a protective coating for the diol films. Multilayer formation enhances the stability of the thin films under varied conditions too. The thin film assemblies can be subjected to topochemical polymerization to produce a blue film upon UV-Vis exposure.

Molecular self-assembly of rigid-rod alkynes with extended π -conjugation on Si(100) (Si/SiO₂) via acid-base hydrolysis of surface bound basic tin-amide moieties has been reported. The π - π interactions in the molecules can lead to relatively highly ordered and densely packed thin film assemblies with a comparatively high surface coverage. In addition, the thin film assembly with diacetylene backbone can be subjected to topochemical polymerization with the formation of a blue film upon UV-Vis exposure.

A layer-by-layer construction methodology using Sn(NEt₂)₄ and dialkyne terminated chromophores containing alkyl or aromatic type backbone can lead to multilayered supramolecular structures with good quality and relatively close-packing on Si(100) (Si/SiO₂); there is no increasing disorder in the thin film assemblies with increasing number of layers. Cobalt carbonyl can successfully adsorb on these thin films under room temperature conditions. These cobalt-adsorbed alkyne films may become potential candidates as heterogenized homogeneous catalysts, one-dimensional conductors and chemically modified electrodes and sensors.

8.3 Suggestions for Future Work

In order to construct good quality, close-packed and highly stable monolayers and multilayers of alcohol and alkynyl chromophores on amino-silane and -stannane functionalized substrates, a complete mechanism of the two-step process involving the reaction of surface hydroxyl groups first with $\text{Si}(\text{NEt}_2)_4/\text{Sn}(\text{NEt}_2)_4$, followed by alcohol/alkyne chromophores should be known. Therefore, a detailed kinetic study of the two-step process should be investigated.

A detailed understanding of the interactions between alkynyl molecules and the role of the substrate in molecular self-assembly is essential in building densely packed thin film materials. Alkynyl moieties in supramolecular structures can be polymerized topochemically to give one-dimensional conductors and third-order nonlinear optical materials.¹ An important requirement for surface polymerization is the orientation of the alkynyl chromophores on the surface. Therefore, molecular modeling and semiempirical calculations are useful in achieving an understanding of molecular self-assembly of rigid-rod alkynes on solid substrates.

Since closely packed and ordered monolayers of alcohols or alkynes can be formed on glass, quartz and $\text{Si}(100)$ (Si/SiO_2), a detailed study of these thin film assemblies on other inorganic oxides such as mica, aluminum oxide and germanium oxide is important to get a complete understanding of the molecular self-assembly of alcohols and alkynes on inorganic oxide surfaces.

Although ellipsometry and contact angle measurements provide information on the surface properties and packing of monolayers and multilayers of alcohol and alkyne chromophores on $\text{Si}(100)$ (Si/SiO_2), this information only indirectly reflects the possible orientation of alkyl chains and of substituents contained in the bulk of the film.² To examine the order in these thin film assemblies, the use of polarized ATR measurements is required. Furthermore, by means of X-ray reflectivity, the determination of the electron distribution

in films ostensibly having variations in electron density along the z axis would provide one direct measure of order in these systems.³

It was reported^{4,5} that the conjugated, rigid-rod chromophores with a phenylene ethynylene/diacetylene backbone have significant third-order nonlinear optical properties, and may act as one-dimensional conductors after subjecting to topochemical polymerization; we can further study these properties for these alcohol and alkyne films possessing rigid-rod phenylene ethynylenediacetylene backbones on Si(100) (Si/SiO₂). In addition, those alcohol and alkyne chromophores with longer phenylene ethynylene/diacetylene backbones processing higher third-order nonlinear optical properties may be constructed for characterization.

Besides cobalt, other transition metals may also adsorb on the alkyne films.⁴ Further study of adsorption of other transition metals on the alkyne assemblies may be necessary to explore their potential uses as chemically modified electrodes and sensors.

Since the reactivity⁶ of Ge(NEt₂)₄ towards protic species and their stability to hydrolysis are in between those of Si(NEt₂)₄ and Sn(NEt₂)₄, it is useful to study the acid-base hydrolytic chemistry approach to molecular self-assembly by the treatment of surface hydroxyl groups on inorganic oxides with Ge(NEt₂)₄ in order to yield the corresponding surface-anchored-NEt₂ moieties followed by reacting with a variety of protic species.

8.4 References

- (1) Ulman, A. *An Introduction to Ultrathin Organic Films from Langmuir-Blodgett to Self-Assembly*; Academic Press: Boston, 1991
- (2) Tillman, N.; Ulman, A.; Schildkraut, J. S.; Penner, T. L. *J. Am. Chem. Soc.* **1988**, *110*, 6136.
- (3) Wasserman, S. R.; Whitesides, G. M.; Tidswell, I. M.; Ocko, B. M.; Pershan, P. S.; Axe, J. D. *J. Am. Chem. Soc.* **1989**, *111*, 5852.
- (4) Khan, M. S.; Kakkar, A. K.; Long, N. L.; Lewis, J.; Raithby, P.; Nguyen, P.;

Marder, T. B.; Wittmann, F.; Friend, R. H. *J. Mater. Chem.* **1994**, *4*, 1227.

- (5) Cygan, M. T.; Dunbar, T. D.; Arnold, J. J.; Bumm, L. A.; Shedlock, N. F.; Burgin, T. P.; Jones II, L.; Allara, D. L.; Tour, J. M.; Weiss, P. S. *J. Am. Chem. Soc.* **1998**, *120*, 2721.
- (6) Lesbre, M.; Mazerolles, P.; Satgé, J. *The Organic Compounds of Germanium*; Wiley: London, 1971.